UNIVERSITY OF LIVERPOOL

Role of the Fanconi anaemia proteins FANCG, FANCA and FANCD2 in the maintenance of chromosomal stability

Thesis submitted in accordance with the requirements of the University of Liverpool for the degree of Doctor in Philosophy

Abdulaziz M. Aladwani

December 2011

ABSTRACT

Fanconi anaemia (FA) is a hereditary, heterogeneous disease that is characterized by chromosomal instability, hypersensitivity to DNA cross-linking agents and cancer. Fifteen FA genes are identified, mutations in any of which are known to cause FA: FANCA, B, C, D1, D2, E, F, G, I, J, L, M, N, O, and P. Cell lines defective for any FA gene show cellular and cytogenetic hypersensitivity to DNA inter-strand cross-linking agents such as mitomycin C (MMC). The FA proteins function through several complexes in a poorly defined, intricate phosphorylation–ubiquitination DNA repair network (the FA-BRCA pathway) that mediates the removal of inter-strand cross-links (ICL). ICL removal requires the action several different repair activities including cross-link unhooking, translesion synthesis and subsequent repair of the double-strand break (DSB) formed by homologous recombination. Critical for ICL repair is the FA core complex (comprising A, B, C, E, F, G, L and M proteins) that is essential for the mono-ubiquitination of FANCD2 and FANCI and formation of the ID complex. FANCG, one component of the FA core complex, is involved in at least two further distinct protein complexes that likely have independent functional roles to the core complex. The G-ERCC-XPF complex (FANCG-XPF-ERCC1) is required for inter-strand cross link (ICL) unhooking. The G-BRCA2 complex (FANCD1/BRCA2-FANCD2-FANCG-XRCC3) is hypothesised to be involved in modulating some aspect of homologous recombination repair (HRR). The aim of this study is to characterise the roles of FANCG and the G-BRCA2 complex in ICL and DSB repair. MMC and phleomycin, that induces DNA strand breaks, were utilized to evaluate the efficiency of the HRR pathway in Chinese hamster ovary *FANCG* mutant cells (NM3) and human *FANCA* (GM6914) and *FANCD2* (PD20) fibroblasts. Drug hypersensitivity, chromosomal instability and HRR were evaluated using growth inhibition and clonal survival assays, metaphase analysis and a plasmid based HRR reporter assay respectively. Cell lines unable to form the G-BRCA2 complex are hypersensitive to phleomycin (in addition to MMC) and exhibit elevated chromosomal aberrations and reduced levels of HRR. This implicates the G-BRCA2 complex in the repair of both indirectly and directly induced DSB. Cell lines able to form the G-BRCA2 complex (such as *FANCA*-deficient cells) exhibit little or no hypersensitivity to phleomycin. The study also provides evidence that FANCD2 that is not mono-ubiquitinated has biological activity, specifically in the G-BRCA2 protein complex. The study provides important new insights into the molecular defects associated with FA and the role of the FA proteins in ICL and DSB repair.

ACKNOWLEDGEMENT

I am extremely grateful to my supervisor, Dr. Nigel Jones, who has been the driving force behind my project. I wish to extend my sincere gratitude to him for his guidance; valuable advice and continuing support throughout the study. This project would also have not been complete without the continuous support of Dr. Jamie Wilson. I extend my deepest gratitude for his immense help, advice and technical assistance. My sincere thanks go also to my assessors Dr. Steve Hill and Dr. Bill Greenhalf for their effort and guidance through annual assessments.

I would like to extend my appreciation to the Jones lab members, Dr. Ryan Cunningham, Dr. Yuxuan Xiao, Dr. Andrew Marriott, Vijayashree Mysore, Jessica Lingley and all my fellow colleagues in the Institute of Integrative Biology/School of Life Sciences who have offered assistance and kind support throughout the period of this project.

The study would have not been possibly done without the scholarship I received from Kuwait Ministry of Health. I would like to sincerely thank the head of the Kuwait Medical Genetic Center Dr. Sadiqa Al-awadi for her encouragement, guidance and care. I wish to extend my gratitude also to the head of Molecular and Cytogenetic Laboratory Dr. Sawsan Abulhasan for her rigorous training, guidance and care. Thanks also to all members of KMGC for their support and encouragement.

Finally, I would like to sincerely thank my parents; Mohammed Aladwani and Nada Alathami, my wife Hessa Almejbel, daughter Monira Aladwani, family members and friends who have stood by me and continually supported me in completing my PhD.

ABBREVIATIONS

5-BU : 5-bromouracil
AA8 : Chinese hamster parental cell line (wild type)
AML : Acute myelogenous leukaemia
APH : Aphidicolin (DNA synthesis inhibitor)
AT : Ataxia telangiectasia
AT-LD: AT like disorder
ATM : Ataxia telangiectasia mutated
ATR: Ataxia telangiecasia and RAD3 related
ATRIP : ATR interacting protein (the binding partner of ATR)
AZT : azydothymidine
BACH1: BRCA1-associated C-terminal helicase 1
BER : Base excision repair
BFB : breakage-fusion-bridge
BRCA : Breast cancer susceptibility
BRCA1: Breast cancer susceptibility gene 1
BRCA2: Breast cancer susceptibility gene 2
BRIP1 : BRCA1-interacting protein 1
BS: Bloom syndrome
c DNA : Complementery DNA
C.G.H : Comparative genomic hybridization
CA : Chromosome aberration
CAs : chromosomal aberrations
Chk1 : Checkpoint Kinase
CHK1 : S-phase checkpoint kinase (checkpoint kinase 1)
CHK1: Kinase checkpoint kinase 1
CHO : Chineese hamster ovary
chro break : Chromosome break
chro exch : Chromosome exchange
CPDs : Cyclobutane pyrimidine dimers
Cr : chromate
ctid break : Chromatid break
ctid exch : Chromatid exchange
Cyto-B : Cytochalasian-B
D37 value : The dose of agent that allows 37% of the cells to survive
DEB : Diepoxybutane
DMSO : Dimethylsulfoxide
DNA: Deoxyribonucleic acid
DNA-PKcs : DNA-dependent protein kinase

dRP : deoxyribose-phosphate
ds : Double strand
DSBs: Double strand breaks
dsDNA : Double strand DNA
EDTA: Ethylene di-amino-tetra-acetic-acid
EMS : Ethyle methane sulphonate
ERCC: Excision Repair Cross Complementing
ERCC1: Excision repair protein that in humans is encoded by the ERCC1 gene
ERCC4 : is a DNA repair endonuclease XPF enzyme that in humans is encoded by the ERCC4 gene
ESTs : Expressed Sequence Tags
F.I.S.H : Fluorescent in situ hybridization
FA: Fanconi anaemia
FAAP : FA-associated protein; or FANC associated polypeptides
FA-ID : FANCI –FANCD2 complex
FANC J: Fanconi anaemia , complementation group J, (BRIP1) or (BACH1)
FANCA : Fanconi anaemia , complementation group A
FANCB : Fanconi anaemia , complementation group B, FAAP95
FANCC : Fanconi anaemia , complementation group C
FANCD1 : Fanconi anaemia , complementation group D1, BRCA2
FANCD2 : Fanconi anaemia , complementation group D2
FANCD2-L : FANCD2 Long isoform, monoubiquitinated FANCD2, (PHF9) or (FAAP43)
FANCD2-S : FANCD2 Short isoform, non-monoubiquitinated FANCD2
FANCE : Fanconi anaemia , complementation group E
FANCF : Fanconi anaemia , complementation group F
FANCG : Fanconi anaemia , complementation group G, XRCC9
FANCI : Fanconi anaemia , complementation group I
FANCL : Fanconi anaemia , complementation group L
FANCM : Fanconi anaemia , complementation group M, FAAP250
FANCN : Fanconi anaemia , complementation group N, PALB2
FANCO : Fanconi anaemia , complementation group O, RAD51C
FANCP : Fanconi anaemia , complementation group P,SLX4
G1 phase : Growth 1 phase, a period in the cell cycle during interphase, before the S phase
G2 phase: Growth 2 phase, is the final subphase of interphase in the cell cycle directly preceding mitosis
GI : Growth inhibition
GI-50 : The dose of agent that allows 50% of the cells to grow
HCLK : a biological clock gene (*clk-2*)
HJs : Holliday junctions
HR: Homologous recombination
HRR: Homologous recombination repair
hygR : Hygromycin resistant gene

ICL : Inter-strand cross-link
ICLs : Interstrand cross-links
IKK2 : Inhibitor of nuclear factor kappa-B kinase subunit beta, (IKK-β)
IR: Ionizing radiation
irs1SF : Ionizing radiation sensitive cells 1 San Francisco
KCL : Potassium chloride
KU70 : is a protein that, in humans, is encoded by the XRCC6 gene
KU80 : Ku80 is a protein that, in humans, is encoded by the XRCC5 gene
LOH : loss of heterozygosity
MHF : FANCM-associated histone-fold MHF heterodimer (MHF1-MHF2)
MI : Mitotic index
Mlh1 : human gene on chromosome 3 commonly associated with hereditary nonpolyposis colorectal canc
MMC: Mitomycin C
MMR: Mismatch repair
MN: Micronucleus
M-R-N complex: MreII-Rad50-NbsI
mRNA : Messenger RNA
NBS : Nijmegen breakage syndrome
neoR : G418 resistant gene
NER : Nucleotide excision repair
NHEJ: Non-homologous end joining
NiSO4 : Nickel sulfate
NLS : nuclear localization signal
NM : Nitrogen mustard
NM3 : Chinese hamster cell line, a nitrogen mustered hypersensitive mutant to DNA damaging agents
OH : Hydroxyl group
P : Phosphorylation
PALB2: Partner and localizer of BRCA2
PCR: Polymerase chain reaction
PHF9 : PHD finger protein 9
PolN : Human DNA polymerase N
PTM: Post translational modifications
RACE : Rapid Amplification of cDNA Ends
RAD51 : a member of the RAD51 protein family that assist in repair of DNA double strand breaks
RF : Recombination frequency
RIISp : Non-erythroid R spectrin (structural protein)
RNA : Ribonucleic acid
RPA : Replication protein A
SCEs : Sister chromatid exchanges
SDS : Sodium dodecyl sulphate
siRNAs : Small interfering RNA, or short interfering RNA or silencing RNA

SNX5 : Sorting nexin-5 is a protein that in humans is encoded by the SNX5 gene
S-phase : synthesis phase whhen DNA is replicated, occurring between G1 phase and G2 phase
SSA : Single strand annealing
ssDNA : Single strand DNA
STDEV : Standard deviation
SV40 : Human fibroblasts immortalized by Simian Virus 40
TAE: Tris-Acetic acid-EDTA
TBS : Tris buffer saline
TLS : Translesion DNA synthesis
TPR : Tetra-trico-peptide repeat motifs
Tris : tris (hydroxymethyl) methylamine
Ub : Ubiquitin
UBE2T : ubiquitin-conjugating enzyme E2T
USP1 : Ubiquitin specific protease 1
UV: Ultraviolet radiation
V(D) J : Variable, Diverse, and Joining
VO : Vector only
WD40: Repeat motif found in b-transducin and other proteins.
WS: Werner's syndrome
WT : Wild type
XP : Xeroderma pigmentosum
XPA : is a protein that in humans is encoded by the XPA gene (Xeroderma pigmentosum-A)
XPF : xeroderma pigmentosum group F
XRCC: X-ray Repair Cross Complementing
XRCC3 : X-ray complementation FANC group, (RAD51 paralog)
XRCC9 : X-ray repair complementing defective repair 9
αSpIIΣ : The structural protein nonerythroid α spectrin (alphaSpIISigma)

LIST OF CONTENTS

ABSTRACT II
ACKNOWLEDGEMENT III
ABBREVIATIONS IV
LIST OF CONTENTS VIII
LIST OF FIGURES XVIII
LIST OF TABLES XXI

Chapter-1 1
Introduction 1
1.1 DNA integrity and DNA damage 1
1.1.1 Spontaneous DNA damage 2
1.1.2 DNA lesions 2
1.1.3 Spontaneous Lesion Mechanisms 3
1.1.3.1 Deamination 3
1.1.3.2 Tautomeric shift 4
1.1.3.3 Streisinger slipped mis-pairing 5
1.1.4 Induced Mutations 5
1.1.4.1 Chemical mutagens 5
1.1.4.1.1 Base analogs 6
1.1.4.1.2 5-bromouracil (5-BU) 6
1.1.4.1.3 Ethylmethane Sulfonate (C3H8O3) 7
1.1.4.1.4 Intercalating Agents 7
1.1.4.1.5 Radiomimetic agents 8
1.1.4.1.6 Cross-linking agents 10
1.1.4.1.6.1 Psoralens 10
1.1.4.1.6.2 Platinum compounds 10
1.1.4.1.6.3 Nitrogen mustards 10

1.1.4.1.6.4 Nitrosoureas 11
1.1.4.1.6.5 Diepoxybutane (DEB) 12
1.1.4.1.6.6 Mitomycin C (MMC) 12
1.1.4.2 Radiation Mutagens 16
1.1.4.2.1 Ultraviolet (UV) radiation 16
1.1.4.2.2 Pyrimidine dimerization 16
1.1.4.2.3 X-rays 17
1.2 DNA repair pathways 18
1.2.1 DNA repair mechanisms 18
1.2.2 Base excision repair (BER) 18
1.2.3 Nucleotide excision repair (NER) 18
1.2.4 Mismatch repair (MMR) 19
1.2.5 Translesion synthesis (TLS) 19
1.2.6 DNA DSBs Repair 20
1.2.6.1 DNA repair through Homologous recombination repair (HRR) 21
1.2.6.2 DNA repair through non-homologous end joining (NHEJ) 24
1.2.7 Causes and repair of Inter-strand cross-links 26
1.2.7.1 Causes of ICLs occurrence in prokaryotes and eukaryotes 26
1.2.7.2 ICL repair 27
1.3 Instability Syndromes 31
1.3.1 Instability syndromes and cancer 31
1.3.2 Centrosome instability and telomere dysfunction 31
1.4 Fanconi anaemia 34
1.4.1 Fanconi anaemia mode of Inheritance 34
1.4.2 Fanconi anaemia clinical manifestations 35
1.4.3 FA diagnosis and hypersensitivity to interstrand crosslinking agents 37
1.4.4 Fanconi anaemia pathway 38
1.4.5 The upstream FA pathway proteins 41
1.4.5.1 Fanconi anaemia core complex 41
1.4.5.1.1 FANCA 41
1.4.5.1.2 FANCB 41

1.4.5.1.3 FANCC 42
1.4.5.1.4 FANCE 42
1.4.5.1.5 FANCF 42
1.4.5.1.6 FANCG 43
1.4.5.1.7 FANCL 43
1.4.5.1.8 FANCM 44
1.4.6 The downstream FA pathway proteins 46
1.4.6.1 FANCD1 46
1.4.6.2 FANCD2 46
1.4.6.3 FANCI 47
1.4.6.4 FANCJ 48
1.4.6.5 FANCN 48
1.4.6.6 FANCO 48
1.4.6.7 FANCP 49
1.4.7 Fanconi anaemia *FANCG* 49
1.4.7.1 FANCG and its role in the FA pathway 49
1.4.7.2 FANCG- tetratricopeptide repeat motifs (TPRs) 53
1.4.7.3 FANCG protein is a phospho-protein phosphorylated at mitosis at two amino acids; S383 and S387 56
1.4.7.4 FANCG is a phospho-protein phosphorylated at serine 7 57
1.4.8 Fanconi anaemia *FANCA* 58
1.4.8.1 FANCA protein 58
1.4.8.2 FANCA is part of the multi-subunit nuclear complex (FA-core complex).. 60
1.4.8.3 FANCA protein interactions with a wide range of other proteins 60
1.4.8.4 FANCA involvement in other complexes 61
1.4.8.5 FANCA protein is phospho-protein phosphorylated at serine-1449 62
1.4.9 Fanconi anaemia *FANCD2* 64
1.4.9.1 FANCD2 protein 64
1.4.9.2 Functional and non functional FANCD2 isoforms 65
1.4.9.3 The mono-ubiquitination of FANCD2 and the FA-core complex 65

1.4.9.4 FANCD2 mono-ubiquitination requirement for functional complementation and foci formation 66

1.4.9.5 FANCD2 phosphorylation by ATM and ATR and the role of CHK1 kinase.. 67

1.4.9.6 Hypersensitivity of FANCD2 mutant cells PD20, PD20-K561R and PD20-S331A to cross linking agent MMC 67

1.4.9.7 FANCD2 phosphorylation at S331 is critical for its *in vivo* interaction with FANCD1/BRCA2 68

1.4.9.8 FANCD2 forms with FANCD1/BRCA2, FANCG and XRCC3 the G-BRCA2 complex 70

1.4.9.9 FANCD2 and FANCI forms the FANCD2-FANCI complex 70

1.4.9.10 FANCD2 and its roles in sustaining chromosomal integrity 71

1.5 Model systems to study Fanconi anaemia 73

1.5.1 Model systems utilized in FA research 73

1.5.2 Use of Chinese hamster cell mutants to study FA and FANCG 73

1.5.2.1 The use of hamster model in cloning homologous recombination repair genes 73

1.5.2.2 Use of a hamster model to express FANCG mutations 74

1.5.3 Use of human FANCA fibroblasts (GM6914) in FA research 75

1.5.3.1 Isolation of GM6914 cells and assigning them to FA complementation group A 75

1.5.3.2 FANCA protein is found in both the cytoplasm and the nucleus 76

1.5.3.3 FANCA protein is a FA-core complex component 76

1.5.3.4 FANCA mutant cells exhibit cellular hypersensitivity to MMC 77

1.5.3.5 Reported cytogenetic profile of GM6914 cell line 78

1.5.4 Use of human FANCD2 fibroblasts (PD20) in FA research 78

1.5.4.1 Pin pointing the FANCD2 gene using PD20 cells and mutation analysis 78

1.5.4.2 PD20 cells are *FANCD2* deficient and *FANCD2* cDNA complemented functionally *FANCD2* deficient cells 79

1.6 Aims 80

Chapter-2 81

Material and methods 81

2.1 Materials and methods 81

2.1.1 Material 81

2.1.1.1 Cell lines used 81

2.1.1.1.1 Chinese hamster (CH) cell lines (*FANCG* lines) 81

2.1.1.1.2 Human fibroblast FA cell lines 82

2.1.1.1.2.1 FANCA cell lines 82

2.1.1.1.2.2 FANCD2 cell lines 83

2.1.1.2 Vectors for HRR assay 85

2.1.1.3 Antibodies for Western blotting 85

2.1.1.3.1 Primary antibodies 85

2.1.1.3.2 Secondary antibodies 85

2.1.1.4 Chemical agents used 86

2.1.1.4.1 Mitomycin C (MMC) 86

2.1.1.4.2 Phleomycin 86

2.1.2 Methods 87

2.1.2.1 Cell culture and maintenance 87

2.1.2.2 Cell storage 87

2.1.2.3 Growing cell lines from frozen stocks 88

2.1.2.4 Cell passage 88

2.1.2.5 Fibroblast cell line growth inhibition assay 88

2.1.2.6 Transfection 89

2.1.2.7 Homologous recombination repair (HRR) assay 90

2.1.2.7.1 Introduction 90

2.1.2.7.2 HRR Protocol 91

2.1.2.8 Survival assays 93

2.1.2.9 Immunoblotting (Western Blot) 93

2.1.2.10 Cytogenetic methods 94

2.1.2.10.1 Cytogenetic methods introduction 94

2.1.2.10.2 Cytogenetic protocols 96
2.1.2.10.2.1 The Micronucleus Assay 96
2.1.2.10.2.2 Metaphase spreads preparation for cytogenetic analysis 97
2.1.2.10.3 Chromosomal aberration scoring 99
2.1.2.10.4 Converting exchanges to chromatid breaks 100

Chapter-3 107
Investigating the role of FANCG protein in the repair of induced inter cross links 107
3.1 Introduction 107
3.1.1 FANCG and the repair of ICLs 107
3.1.2 FANCG is a scaffold phospho-protein central to many repair complexes 108
3.1.3 Cell lines used in this chapter 109
3.1.4 Role of FANCG in HRR and ICL repair 110
3.2 Results 111
3.2.1 Validation and growth inhibition responses of cell lines used for metaphase analysis 111
3.2.1.1 Immunoblotting 111
3.2.1.2 Growth inhibition assays results 114
3.2.2 Chromosomal aberration analysis results 116
3.2.2.1 Chromosome and chromatid aberration rates in control cell cultures 117
3.2.2.2 Chromosome and chromatid aberration rates in treated cell cultures 117
3.2.2.3 Aberration types and predominance 127
3.2.2.4 Classification of cytogenetic aberrations 128
3.2.3 Homologous recombination repair assay results 132
3.3 Discussion 135
3.4 Summary of the chapter 142

Chapter-4 145

Investigating the role of FANCG protein in the repair of induced DNA double strand breaks 145

4.1 Introduction 145

4.1.1 DNA strand breaks 145

4.1.2 NM3 cells hypersensitivity to radiomimetic agents 145

4.1.3 Cell lines used in this chapter 146

4.2 Results 147

4.2.1 Survival assays results 147

4.2.2 Growth inhibition assays results 147

4.2.3 Chromosomal aberration analysis results 151

4.2.3.1 Preliminary metaphase analysis in NM3 and NM3-gWT post exposure to low doses of phleomycin 151

4.2.3.2 The introduction of NM3-S7A cell line to phleomycin cytogenetic structural aberration assays using selected doses 156

4.2.3.3 The introduction of NM3-S387A cell line to phleomycin cytogenetic structural aberration assays using selected doses 156

4.2.3.4 Chromosome and chromatid aberration rates in control cell cultures 157

4.2.3.5 Chromosome and chromatid aberration rates in treated cell cultures 157

4.2.3.6 Average aberrations per cell, percentage aberrant cells and number of total chromatid breaks per cell 158

4.2.3.7 Aberration type and predominance 173

4.2.3.8 Cytogenetic numerical aberration rates in control and treated cell cultures 183

4.2.3.9 Chromatid Gaps in phleomycin-treated cell lines 192

4.2.4 Homologous recombination repair assay results 192

4.2.5 MN assay 196

4.2.5.1 Optimizing the MN assay procedure 196

4.2.5.2 Problems encountered in the MN procedure 198

4.3 Discussion 201

4.3.1 Discussion 201

4.3.2 Survival and growth inhibition data 201

4.3.3 Cytogenetic data 202
4.3.3.1 Chromosomal aberrations rate and type in FANCG cell lines 202
4.3.3.2 Chromatid lesions produced post treatment with DNA strand breakers .. 203
4.3.3.3 Cytogenetic data comparison to other repair deficient mutants 204
4.3.3.4 Numerical instability in response to phleomycin applied to FA cell lines.. 206
4.3.4 Homologous recombination repair assay data 207
4.4 Summary of the chapter 208

Chapter-5 210
Investigating the role of FANCA protein in the repair of induced DNA double strand breaks and (ICLs) 210
5.1 Introduction 210
5.1.1 Cell lines used in this chapter 210
5.1.2 Investigation of the induction of chromosome aberrations in GM6914 fibroblasts 211
5.2 Results 212
5.2.1 GM6914 fibroblasts exposed to phleomycin growth inhibition results 212
5.2.2 GM6914 fibroblasts cytogenetic findings 214
5.2.2.1 GM6914 fibroblasts cytogenetic analysis results after exposure to phleomycin 214
5.2.2.1.1 GM6914 fibroblasts chromosome and chromatid aberration rates in control cell cultures 214
5.2.2.1.2 GM6914 fibroblasts chromosome and chromatid aberration rates in treated cell cultures exposed to phleomycin 215
5.2.2.1.3 The cytogenetic aberration types and predominance in GM6914 fibroblasts exposed to phleomycin 224
5.2.2.2 GM6914 fibroblasts chromosomal aberration analysis results to MMC ... 228
5.2.2.2.1 GM6914 fibroblasts chromosome and chromatid aberration rates in control cell cultures exposed to MMC 228
5.2.2.2.2 GM6914 fibroblasts chromosome and chromatid aberration rates in treated cell cultures to MMC 229
5.2.2.2.3 The cytogenetic aberration types and predominance in GM6914 fibroblasts to MMC 241

5.3 Discussion 246
5.4 Summary of the chapter 250

Chapter-6 252
Investigating the role of the FANCD2 protein in the repair of DNA double strand breaks and inter-strand cross-links 252
6.1 Introduction 252
6.1.1 Introduction 252
6.1.2 Cell lines utilized in this chapter 253
6.2 Results 253
6.2.1 Growth inhibition assays results of PD20 cells exposed to phleomycin 253
6.2.2 Metaphase analysis in PD20 cells 256
6.2.2.1 Phleomycin-induced chromosomal aberration in PD20 cell lines 256
6.2.2.1.1 Spontaneous chromosome and chromatid aberrations 256
6.2.2.1.2 Phleomycin-induced chromosome and chromatid aberrations 257
6.2.2.1.3 Aberrations per cell, percentage aberrant cells and total chromatid breaks per cell 264
6.2.2.1.4 Types of cytogenetic aberrations induced by phleomycin 268
6.2.2.1.5 Phleomycin-PD20 cytogenetic experiments with high variability due to an unidentified technical problem 273
6.2.3 Growth inhibition assays results of PD20 cells exposed to MMC 274
6.2.4 MMC- PD20 cytogenetic experiments that have suffered an unidentified technical problem 274
6.3 Discussion 277
6.3.1 Requirement of post-translational modifications of FANCD2 for efficient DNA repair 277
6.3.2 Functions of S331-phosphorylated FANCD2 and non-ubiquitinated FANCD2. 278
6.3.3 Problems encountered with metaphase analysis of PD20 cell lines 280
6.4 Summary of the chapter 281
6.5 Appendix of Chapter-6 283

Chapter-7 299

General discussion 299

7.1 Discussion 299

7.1.1 Introduction 299

7.1.2 DNA inter-strand cross-link repair 300

7.1.2.1 Unhooking 300

7.1.2.2 Processing of Double Strand Breaks in ICL Repair 304

7.1.2.3 Determining the role of the G-BRCA2 complex (comprising BRCA2-FANCD2-FANCG-XRCC3) in ICL and DSB repair 306

7.1.3 Conclusions 317

References 319

Appendix 350

List of Figures

Chapter-1

Figure (1.1): Phleomycin chemical structure **9**
Figure (1.2): Mitomycin C chemical structure **15**
Figure (1.3): Model illustrating DSBs repair by error free homologous recombination . **23**
Figure (1.4): Schematic representation of DSB repair by error prone NHEJ pathway ... **25**
Figure (1.5): Model of FANCG role in ICL repair via the upstream FA pathway **29**
Figure (1.6): Model for Inter-strand cross-link repair **30**
Figure (1.7): Telomeric dysfunction leading to structural and numerical chromosome instability **33**
Figure (1.8): The FA pathway activation: Upstream FA–BRCA regulation **39**
Figure (1.9): The FA pathway activation: downstream FA–BRCA regulation model **40**
Figure (1.10): FANCG complexes in inter-strand-cross link (ICL) repair **51**
Figure (1.11): Model of αIISp, FANCG, and ERCC1-XPF interactions in ICL repair ... **52**
Figure (1.12): FANCG tetratricopeptide repeat motifs and phosphorylation sites **55**

Chapter-2

Figure (2.1): Assay for homologous recombination repair (HRR) using an integrated vector with a neomycin reporter gene **92**
Figure (2.2): Formation of complex chromatid exchanges **103**
Figure (2.3): Chromosome aberrations formation **104**
Figure (2.4): Triradial formation **105**
Figure (2.5): Quadri-radial formation **106**

Chapter-3

Figure (3.1): Western blot of FANCG protein in NM3 cell lines 112
Figure (3.2): Western blot of FANCG protein in NM3 cell lines 113
Figure (3.3): Growth Inhibition -NM3- MMC 115
Figure (3.4): NM3- MMC Average Aberrations per cell 124
Figure (3.5): NM3- MMC Average % Aberrant cells 125
Figure (3.6): NM3- MMC Average of Total Chromatid Breaks (after converting exchanges) per cell 126
Figure (3.7): HRR-Non-induced Recombination Frequency - MMC 133
Figure (3.8): HRR-Induced Recombination Frequency - MMC 134

Chapter-4

Figure (4.1): NM3-Phleomycin survival 149
Figure (4.2): NM3-Phleomycin- Growth Inhibition 150
Figure (4.3): NM3- phleomycin -Average Aberrations per cell 169
Figure (4.4): NM3- phleomycin --Average % Aberrant cells 170
Figure (4.5): NM3- phleomycin --Average of Total Chromatid Breaks (after converting exchanges) per cell 171
Figure (4.6): NM3- Average Number of chromosomes post phleomycin treatment 191
Figure (4.7): NM3-HRR-Non-induced Recombination Frequency -Phleomycin 194
Figure (4.8): NM3-HRR-Induced Recombination Frequency -Phleomycin 195
Figure (4.9): Micronucleus assay cells 200

Chapter-5

Figure (5.1): Growth Inhibition - 6914 A cells - Phleomycin 213

Figure (5.2): 6914 A cells - phleomycin --Average Aberrations Per cell 219

Figure (5.3): 6914 A cells - phleomycin --Average % Aberrant cells 222

Figure (5.4): 6914 A cells - phleomycin --Average number of Chromatid Breaks (after converting exchanges) per cell 223

Figure (5.5): 6914 A cells - MMC Average Aberrations Per cell 238

Figure (5.6): 6914 A cells - MMC Average % Aberrant cells 239

Figure (5.7): 6914 A cells -MMC Average number of Chromatid Breaks (after converting exchanges) per cell 240

Chapter-6

Figure (6.1): Growth Inhibition - PD20 cells – Phleomycin 255

Figure (6.2): PD20 cells - phleomycin --Average Aberrations Per cell 262

Figure (6.3): PD20 cells - phleomycin --Average % Aberrant cells 263

Figure (6.4): PD20 cells - phleomycin --Average number of Chromatid Breaks (after converting exchanges) per cell 267

Figure (6.5): PD20 cells -Growth Inhibition - MMC 276

Chapter-7

Figure (7.1): The proposed model to repair ICLs and double strand DNA breaks via FANCG complexes 303

List of Tables

Chapter-1

Table (1.1): Fanconi anaemia clinical manifestations 36

Table (1.2): Fanconi anaemia genes/proteins 45

Chapter-2

Table (2.1): Converting chromosome and chromatid exchanges into chromatid breaks 102

Chapter-3

Table 3.1.A: NM3- MMC treated cell lines and aberrations found in experiment..... 119

Table 3.2.A: NM3- MMC treated cell lines and aberrations found in experiment..... 120

Table 3.3.A: NM3- MMC treated cell lines and aberrations found in experiment..... 121

Table 3.4: NM3- MMC - Average / Standard deviation - Table results for (Tables 3.1.A, 3.2.A and 3.3.A) 123

Table 3.1.B: NM3- MMC types of chromatid /chromosome exchanges 129

Table 3.2.B: NM3- MMC types of chromatid /chromosome exchanges 130

Table 3.3.B: NM3- MMC types of chromatid / chromosome exchanges 131

Chapter-4

Table (4.1) NM3- phleomycin treated cell lines and structural aberrations..... 153

Table (4.2) NM3- phleomycin treated cell lines and structural aberrations..... 154

Table (4.3) NM3- phleomycin treated cell lines and structural aberrations..... 155

Table (4.4.A): NM3- phleomycin treated cells and aberrations found in experiment.... 161

Table (4.5.A): NM3- phleomycin treated cells and aberrations found in experiment.... 162

Table (4.6.A): NM3- phleomycin treated cells and aberrations found in experiment.... 163

Table (4.7.A): NM3- phleomycin treated cells and aberrations found in experiment.... 164

Table (4.8.A): NM3- phleomycin treated cells and aberrations found in experiment.... 165

Table (4.9.A): NM3- phleomycin treated cells and aberrations found in experiment.... 166

Table (4.10.A): NM3- phleomycin treated cells and aberrations found in experiment.. 167

Table (4.11.A): NM3- phleomycin treated cells and aberrations found in experiment.. 168

Table (4.12): NM3-phleomycin - Average /Standard deviation (STDEV) - Tables- results for tables- (4.4.A, 4.5.A, 4.6.A, 4.7.A, 4.8.A, 4.9.A, 4.10.A & 4.11.A) 172

Table (4.4.B):NM3-phleomycin types of chromatid and chromosome exchanges 175

Table (4.5.B):NM3-phleomycin types of chromatid and chromosome exchanges 176

Table (4.6.B):NM3-phleomycin types of chromatid and chromosome exchanges 177

Table (4.7.B):NM3-phleomycin types of chromatid and chromosome exchanges 178

Table (4.8.B):NM3-phleomycin types of chromatid and chromosome exchanges 179

Table (4.9.B):NM3-phleomycin types of chromatid and chromosome exchanges 180

Table (4.10.B):NM3-phleomycin types of chromatid / chromosome exchanges 181

Table (4.11.B):NM3-phleomycin types of chromatid / chromosome exchanges 182

Table (4.13): Phleomycin treated NM3 cells - Average chromosome numbers count.... 185

Table (4.14): Phleomycin treated NM3 cells- Average chromosome numbers count..... 186

Table (4.15): Phleomycin treated NM3 cells- Average chromosome numbers count..... 187

Table (4.16): Phleomycin treated NM3 cells- Average chromosome numbers count..... 188

Table (4.17): Phleomycin treated NM3 cells- Average chromosome numbers count..... 189

Table (4.18): Phleomycin treated NM3 -Average Number of chromosome in five experiments as shown in tables (4.13, 4.14, 4.15, 4.16, and 4.17) 190

Chapter-5

Table (5.1-A): 6914-phleomycin treated cells and structural aberrations 216

Table (5.2-A): 6914-phleomycin treated cells and structural aberrations 217

Table (5.3-A): 6914-phleomycin treated cells and structural aberrations 218

Table (5.4): Average /Standard deviation (STDEV) - Tables-Results for Human cells 6914 cells - phleomycin 221

Table (5.1-B): 6914A-phleomycin types of chromatid and chromosome exchanges 225

Table (5.2-B): 6914A-phleomycin types of chromatid and chromosome exchanges 226

Table (5.3-B): 6914A-phleomycin types of chromatid and chromosome exchanges 227

Table (5.5-A): MMC treated 6914 cell lines and aberrations 232

Table (5.6-A): MMC treated 6914 cell lines and aberrations 233

Table (5.7-A): MMC treated 6914 cell lines and aberrations 234

Table (5.8-A): MMC treated 6914 cell lines and aberrations 235

Table (5.9): Average /Standard deviation -Table results for 6914 cells MMC..... 236

Table (5.5-B): 6914A- MMC - types of chromatid and chromosome exchanges 242

Table (5.6-B): 6914A- MMC - types of chromatid and chromosome exchanges 243

Table (5.7-B): 6914A- MMC - types of chromatid and chromosome exchanges 244

Table (5.8-B): 6914A- MMC - types of chromatid and chromosome exchanges 245

Chapter-6

Table (6.1-A): PD20- phleomycin treated cells and structural aberrations found 259

Table (6.2-A): PD20- phleomycin treated cells and structural aberrations found 260

Table (6.3-A): PD20- phleomycin treated cells and structural aberrations found 261

Table (6.4): Average / Standard deviation- Table results for PD20 cells - phleomycin.. 266

Table (6.1-B): PD20- phleomycin types of chromatid and chromosome exchanges 270

Table (6.2-B): PD20- phleomycin types of chromatid and chromosome exchanges 271

Table (6.3-B): PD20- phleomycin types of chromatid and chromosome exchanges 272

Appendix of chapter-6:

Table (6.5-A): PD20- phleomycin treated cells and structural aberrations 283
Table (6.6-A): PD20- phleomycin treated cells and structural aberrations 284
Table (6.7-A): PD20- phleomycin treated cells and structural aberrations 285
Table (6.8-A): PD20- phleomycin treated cells and structural aberrations 286
Table (6.9-A): PD20- phleomycin treated cells and structural aberrations 287
Table (6.5-B): PD20- phleomycin types of chromatid and chromosome exchanges 288
Table (6.6-B): PD20- phleomycin types of chromatid and chromosome exchanges 289
Table (6.7-B): PD20- phleomycin types of chromatid and chromosome exchanges 290
Table (6.8-B): PD20- phleomycin types of chromatid and chromosome exchanges 291
Table (6.9-B): PD20- phleomycin types of chromatid and chromosome exchanges 292
Table (6.10-A): PD20- MMC treated cells and structural aberrations found..... 293
Table (6.11-A): PD20- MMC treated cells and structural aberrations found..... 294
Table (6.12-A): PD20- MMC treated cells and structural aberrations found..... 295
Table (6.10-B): PD20- MMC types of chromatid and chromosome exchanges 296
Table (6.11-B): PD20- MMC types of chromatid and chromosome exchanges 297
Table (6.12-B): PD20- MMC types of chromatid and chromosome exchanges 298

Chapter-7

Table (7.1): FANCG cell lines findings to MMC and phleomycin 310
Table (7.2): FANCA cell lines findings to MMC and phleomycin..... 311
Table (7.3): FANCD2 cell findings to MMC and phleomycin 316

Chapter-1

Introduction

1.1 DNA integrity and DNA damage

The integrity of the genetic material is essential for continuous stable cellular replication, which enables the transfer of deoxyribonucleic acid (DNA) to new daughter cells. An intricate network of systems such as cell cycle arrest, DNA damage recognition and repair collaborate to evade the transfer of damaged DNA during mitosis ensuring accurate functionality of the DNA **(Futaki and Liu, 2001).** However, DNA damage can be encountered spontaneously or it may be induced. Exogenous agents, such as ultraviolet radiation (UV), ionizing radiation (IR) or naturally occurring or manufactured chemicals may cause DNA damage. Chromosomal integrity is dependent upon the proficient repair of these DNA lesions. In the absence of comprehensive DNA repair and surveillance systems, chromosomal aberrations (CA) are allowed to accumulate in cells leading to genome instability which can have devastating consequences for growth and development. Ataxia telangiectasia (AT), Ataxia telangiectasia-like disorder, Bloom syndrome (BS), Fanconi anaemia (FA) and Nijmegen breakage syndrome (NBS) are examples of recessively inherited syndromes that are likely to develop chromosomal aberrations. They arise from specific defects in DNA damage response genes and are classified as chromosomal instability or breakage syndromes **(Futaki and Liu, 2001).** A simplistic 'cytogeneticists' definition of chromosomal instability would be the situation where cells have both numerical and structural chromosomal aberrations as a result of developing continually new chromosomal mutations, at an elevated rate compared to that of normal cells **(Taylor, 2001; Talwar *et al.*, 2004).**

1.1.1 Spontaneous DNA damage

DNA is subjected to damage from several sources. DNA damage is an expression encircling the several chemical alterations that may modify the DNA structure. Damage can occur through reactions disrupting the DNA phosphate groups, the deoxyribose sugar ring, or bonds in the nucleotide-bases or by the addition of chemical groups such as methyl groups, hydroxyl groups, or groups derived from polycyclic molecules. These additions are usually called DNA adducts **(Lange *et al.*, 2011).** Spontaneous DNA lesions may occur due to errors in normal cellular processes such as DNA metabolism, replication and recombination **(Marnett and Plastaras., 2001)**. Inevitable reactions such as water-catalysed reactions and attack by reactive oxygen species (ROS) lead to recurrent damaging alterations in DNA **(Lange *et al.*, 2011).** Normal cellular respiration produces highly-reactive oxygen radicals that can harm the DNA **(Joenje and Oostra, 1983).**

1.1.2 DNA lesions

Damaged to DNA is frequently due to denaturing in weak hydrogen bonds implicated in base pairing. DNA lesions include the presence of an irregular base in the DNA or injured sugar-phosphate backbone. DNA damage can arise in either: the template strand or in the new synthesized strand. A lesion is a physical change in DNA, unlike a mutation, which involves modification of the DNA sequence. DNA lesions can be repaired unlike several mutations **(Pages and Fuchs, 2002).**

1.1.3 Spontaneous Lesion Mechanisms

Spontaneous mutations arise during cell processes. DNA lesions lead ultimately to mutations. DNA lesions are produced via two main ways; transversion or the more common transition. Ionizing radiation and alkylating agents may cause Transversions which are defined as the substitution of a purine for a pyrimidine or vice versa leading to dramatic change in the chemical structure. For instance, longer bonds result and a shift of the bases would occur enabling a (C) to pairs with a (T). Transitions are defined as the substitution of a pyrimidine for a pyrimidine or a purine for a purine **(Golo and Volkov 2003).**

1.1.3.1 Deamination

Deamination is defined as eliminating an amine group facilitated by deaminase. Oxidation, reduction, or hydrolysis causes amino acid deamination **(Frankel *et al,* 1980).** Turning cytosine into uracil via hydrolysis is an example of DNA deamination. A major source of spontaneous mutations is cytosine deamination **(Duncan and Miller, 1980).** When a cytosine in a normal GC pair converts to a uracil, then following replication, an adenine will bind to the uracil. As uracil causes the DNA to be chemically modified then this is termed a lesion. Nevertheless, following the next replication a transition mutation results as the adenine binds to a thymine which illustrates how DNA lesions lead to mutations. Deamination can also be caused via chemical mutagens such as Nitrous acid (HNO2) deaminating cytosine to uracil or deaminating adenine to hypoxanthine **(Frankel *et al,* 1980; Sidorkina *et al,* 1997).**

1.1.3.2 Tautomeric shift

Spontaneous DNA mutations result from tautomeric transitions **(Golo and Volkov 2003).** Normally, cytosine pairs with guanine forming (CG pair) and likewise adenine pairs with thymine forming (AT pair), Nevertheless, these bases occur rarely in tautomeric forms also **(Tsolakidis and Kaxiras 2005).** Guanine and thymine are usually found in their keto-tautomeric form, however, as hydrogen from their NH group reallocates to the double bonded oxygen to construct an OH group; the base is altered to its rare enol form **(Tsolakidis and Kaxiras 2005).** Likewise, cytosine and adenine are usually found in their amino structure, however as a hydrogen (H) from their NH2 group reallocates to the single nitrogen in the ring constructing an NH group, the base is altered to its rare imino structure **(Tsolakidis and Kaxiras 2005).**

Each tautomeric form (tautomer) pairs with the wrong, normal base of the correct (pyrimidine or purine) type. As a result of the hydrogen shifts, these tautomers result in incorrect base pairs, so the enol form of T pairs with the keto form of guanine, forming a TG pair and in the same way, enol guanine pairs with keto thymine , imino adenine with amino cytosine and imino cytosine with amino adenine **(Tsolakidis and Kaxiras 2005).** After the first round of DNA replication, these tautomeric forms result in an irregular DNA sequence in the new synthesised strand. Following the next replication round, the transcription of this irregular DNA sequence leads to a mutation on the newly synthesized strand. This genetic modification is termed a transition mutation **(Golo and Volkov 2003).**

1.1.3.3 Streisinger slipped mis-pairing

Many repetitive sequences in DNA are thought to be a result of a DNA lesion termed Streisinger slipped mis-pairing. This is supported by **Streisinger and Owen, (1985)** who proposed a model supporting the occurrence of high frequencies of frame shift mutations in DNA segments of repeated base sequences. Streisinger model shows frame shifts arising when loops in single-stranded segments are stabilized via the "slipped mis-pairing" of DNA repeated sequences **(Thomas *et al.*, 1998).**

This strand slippage takes place mostly in repetitive non-coding DNA. Nucleotide bases may slip and pair with other bases leading to a bulge consisting of additional bases. This strand slippage is likely to happen in the presence of repetitive sequences **(Levinson and Gutman, 1987)** and probably do not occur in the absence of sequence repeat. Three repeated unpaired bases can generate a loop in the strand **(Lovett, 2004).** Due to the absence of complementary bases in the other strand, the additional nucleotide or nucleotides in either strand becomes conspicuous plugging and sticking out from the rest of the strand **(Streisinger and Owen, 1985).** Gain of additional nucleotides occurs if slippage arises in the newly produced DNA strand as a bulge is formed. Conversely, nucleotide bases are lost or deleted if slippage arises in the template DNA strand **(Streisinger and Owen, 1985).**

1.1.4 Induced Mutations

1.1.4.1 Chemical mutagens

DNA is susceptible to induced chemical damage. Transitions or transversions (point mutations) are induced through the action of chemical mutagens. Chemical mutagens include base analogs,

base modifiers, intercalating agents, intercalating agents, ionizing radiation such as; gamma rays, x-rays, and ultraviolet light. The exposure to environmental chemicals such as some hydrocarbons found in cigarette smoke **(Talwar *et al.*, 2004)** or glycopeptide antibiotics such as DNA strand breaker phleomycin **(Tevethia and Rapp, 1969)** or the application of antitumour agents in chemotherapy such as DNA cross linker mitomycin C (MMC) **(Tomasz, 1995)** will induce DNA damage.

1.1.4.1.1 Base analogs

Base analogs are chemical mutagens that replace normal DNA bases as a result of similarity in their chemical structure. Base analogs are inconsistent in base pairing as they base pair with two different bases, therefore leading to mutations. The inability of DNA polymerase to differentiate between base analogs and normal DNA bases results in the incorporation of base analogs in DNA during DNA replication **(Pierce, 2007).** Examples of base analogs include; 5-bromouracil (5-BU) and azydothymidine (AZT).

1.1.4.1.2 5-bromouracil (5-BU)

Mutation inducer; 5-bromouracil is a base analogs that replaces thymine modifying the chromatin structure through altering DNA and the nuclear matrix interactions **(Ogino *et al.*, 2002).** 5-bromouracil has two tautomeric forms: one as a keto form (imitating T) pairing with (A) and a second enol form (imitating C) pairing with (G), therefore base pairing of A: T shifts to G: C **(Ronen *et al.*, 1976).** DNA and proteins interaction is

altered when 5-bromouracil becomes incorporated into the DNA **(Ogino *et al.*, 2002).**

1.1.4.1.3 Ethylmethane Sulfonate (C3H8O3)

Mutation inducer; ethylmethane sulfonate is an agent that alkylates **(Keightley *et al.*, 2000)** the keto groups at position number 6 of guanine and at position number 4 of thymine to form O-6-ethylguanine and O-4-ethylthymine, respectively.

After the first round of DNA replication, DNA polymerase will pair thymine with O-6-ethylguanine rather than pairing a cytosine with a normal guanine. Following the next replication round, the earlier pervious CG pair will be modified to an AT pair, therefore resulting a mutation. This genetic modification is termed a transition mutation **(Golo and Volkov, 2003; Keightley *et al.*, 2000).** It has been found that ethylmethane sulfonate has mutagenic inclination favoring transitions of GC to AT **(Vidal *et al.*, 1995).**

1.1.4.1.4 Intercalating Agents

Intercalating gents have the ability to insert themselves between successive DNA bases, resulting in DNA deformation preventing its proper functioning. The DNA double helix becomes so stressed that the backbones stretch distorting the helixes. Hydrodynamic DNA modifications also result via intercalation; these alterations are reversible as long as the intercalator elimination does not damage the DNA duplex structure **(Richards and Rodger, 2007).** Reagents ethidium bromide, acridine orange and proflavin are examples of intercalating agents. Consequent to DNA deformation DNA polymerase may insert an additional base opposite the intercalating

agent, or it may also be incapable of inserting a complementary base, thus leading to a deletion. Therefore, an insertion or deletion mutation may result from, the DNA deformation.

Based on the intercalating agents' shape and structure, each agent has a different unwinding and lengthening effect on DNA strands **(Long and Barton, 1990)** which usually prevents proper DNA replication and transcription.

1.1.4.1.5 Radiomimetic agents

Bleomycin and phleomycin are termed radiomimetic as they are DNA damaging agents that mimic functionally the effect of IR. Hydroxyl radicals; which are an example of reactive oxygen species (ROS) can be produced in the presence of metal ions such as Fe^{+2} and Cu^{+2} by radiomimetic agents **(Sugiura, 1979).** The action of the free radicals produced is parallel to the indirect effect of IR which involves the oxidation and breaking of the deoxyribose.

Phleomycin **Fig.1.1;** is a glycopeptide antibiotic related to the bleomycin family that displays similar specificity of DNA base release as bleomycin. Cu (II)-complexes which approximate DNA and induce oxidative DNA degradation are produced by both bleomycin and phleomycin **(Povirk *et al.*, 1981).** Phleomycin which is produced by *Streptomyces verticullus* induces DNA strand breaks and is a strong inhibitor of DNA replication **(Sleigh, 1976; Chen *et al.*, 2008).**

Phleomycin chemical structure

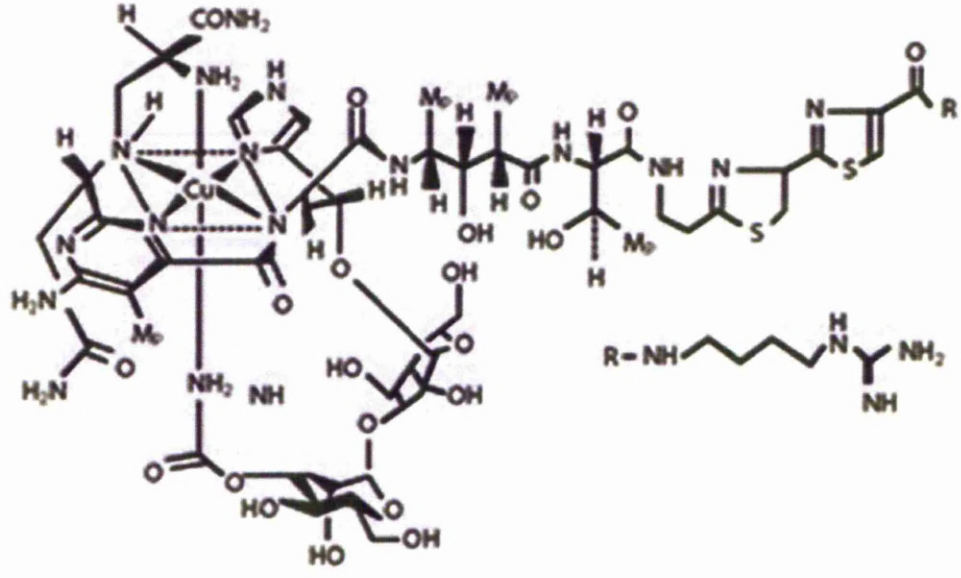

$C_{55}H_{85}O_{21}N_{20}S_2Cu \cdot HCl$

Figure (1.1): Diagram illustrating phleomycin chemical structure with molecular formula ($C_{55}H_{85}O_{21}N_{20}S_2Cu \cdot HCl$) Diagram taken from Bio-world company

1.1.4.1.6 Cross-linking agents

1.1.4.1.6.1 Psoralens

Psoralens belong to a family of natural products known as *furocoumarins* found in plants and cosmetics **(Scott *et al.*, 1976)** and is used therapeutically in several skin diseases. UVA light activates Psoralens to inducing thymine mono-adducts and ICLs between thymines. Both the wavelength and dose of UVA may influence the ratio of ICLs to mono-adducts Thus, up to 40% of adducts conversion to ICLs could take place via altering wavelength and dose of UVA **(Brendel and Ruhland, 1984; Dronkert and Kanaar, 2001).**

1.1.4.1.6.2 Platinum compounds

An example of platinum compounds is *cis*-Diamminedichloroplatinum (II) (cisplatin) which induces DNA damage mainly as intra-strand cross-links, mono-adducts and di-adducts, while ICLs between guanines are a minor product **(Malinge *et al.*, 1999).** Carboplatin is another example of platinum compounds that induces mainly DNA damage as adducts similar to cisplatin adducts, with ICLs as a minor product **(Blommaert *et al.*, 1995).** Another example; is transplatin also called trans-diamminedichloroplatinum (II) induces mainly both intra-strand cross-links and ICLs **(Brabec and Leng, 1993).**

1.1.4.1.6.3 Nitrogen mustards

Nitrogen mustards are bi-functional alkylating agents used widely in cancer chemotherapy. Nitrogen mustards induce inter-strand N7-N7 cross-links involving the two guanines also induce mono-functional guanine-N7 adducts **(Povirk and Shuke, 1994).** Intra-strand cross-links and

DNA-protein cross-links are the major products of the DNA damage induced by nitrogen mustards and its derivatives while ICLs and mono-adducts are a minor product **(Ewig and Kohn, 1977; Balcome *et al.*, 2004).** Nitrogen mustards produce a number of lesions including; DNA–protein cross-links, N-7 guanine ICLs and guanine mono-adducts, **(Dronkert and Kanaar, 2001)**. N-3 adenine adducts are also produced by the aromatic mustards Melphalan and chlorambucil **(Povirk and Shuke, 1994).**

1.1.4.1.6.4 Nitrosoureas

Nitrosourea compounds are DNA alkylating agents that act on several sites within DNA such as N^3 of the cytosine and O^6 and N^7 of the guanine and N^1 of the adenine **(Goth and Rajewsky, 1974; Kramer *et al.*, 1974; Tong and Ludlum, 1979; Bodell *et al.*, 1988).** Bis-chloroethyl-nitrosourea (BCNU or carmustin) is an example of nitrosoureas which post metabolic activation forms guanine–cytosine ICLs, guanine intra-strand cross-links and guanine and cytosine mono-adducts. In addition, BCNU produces DNA–protein cross-links and DNA strand breaks. The BCNU carbamoylating activity attacks proteins as well **(Dronkert and Kanaar, 2001; Ewig and Kohn, 1977).** Thus a range of DNA lesions is produced by nitrosourea compounds such as DNA-protein cross-links, guanine-cytosine ICLs, guanine intra-strand cross-links and guanine and cytosine mono-adducts (**Kramer *et al.*, 1974; Ewig and Kohn, 1978; Bodell *et al.*, 1985; Bodell *et al.*, 1990**).

1.1.4.1.6.5 Diepoxybutane (DEB)

Diepoxybutane (1, 2, 3, 4-diepoxybutane) (DEB) produces a range of DNA lesions, including guanine-guanine, guanine-adenine DNA cross-links and mono-adducts **(Tretyakova *et al.*, 1997a; Tretyakova *et al.*, 1997b; Park *et al.*, 2004),** leading to point mutations and chromosomal aberrations **(Cochrane and Skopek, 1994; Recio *et al.*, 2001).** DEB alkylation activity targets adjacent bases **(Lawley and Brookes, 1967)** and acts on N^3, N^6, N^7, N^1 of the adenine and N^7 of the guanine **(Tretyakova *et al.*, 1997a; Tretyakova *et al.*, 1997b; Park *et al.*, 2004).**

1.1.4.1.6.6 Mitomycin C (MMC)

In the 1950s in the fermentation cultures of *Streptomyces caespitosus* a group of natural product antibiotics were discovered in Japan and were given the family name 'mitomycins' (reviewed by **Champeil *et al.*, 2010).** The significant antitumor properties of these mitomycins were recognized soon following their isolation.

One member of the family 'mitomycins' is Mitomycin C **Fig.1.2;** isolated as blue-violet crystals in 1958, which demonstrates both antibacterial and antineoplastic activity. Mitomycin C is more effective than the previously isolated fractions (mitomycin A and B) (reviewed by **Crooke and Bradner *et al.*, 1976).** Mitomycin C is utilized in clinical cancer chemotherapy owing to its antitumor antibiotic properties **(Champeil and Tomasz, 2006).** It has been shown to cause the formation of covalent DNA mono-adducts, DNA inter-strand and intra-strand cross-links through the mono-functionally and bi-functionally DNA alkylation **(Tomasz and Palom, 1997).**

This covalent linkage is generally irreversible. These DNA lesions, adducts **(Bizanek *et al.*, 1993)** and cross-links **(Fracasso and Sartorelli, 1986;** are assumed to be primarily responsible for MMC observed cytotoxcic biological effect to cancerous cells, especially when the formation rate of ICLs demonstrates correlation with MMC cytotoxicity and that inter-strand cross links (ICLs) are more accountable than mono-adducts **(Palom *et al.*, 2002)** or intra-strand cross links for cellular death (reviewed by **Deans and West, 2011).** In 2011 **Deans and West** reviewed how ICLs may be repaired via complex networks of DNA repair processes.

In the 1960's MMC Japanese clinical trials were reviewed and further experimentation to refine MMC dosage had been conducted until MMC became commercially available in 1974 in America (reviewed by **Crooke and Bradner *et al.*, 1976).**

MMC becomes activated via chemical or enzymatic reduction **(Tomasz and Lipman, 1981)** generating an electrophilic center which interacts with DNA, triggering the formation of a second electrophilic center for a second interaction with DNA **(Tomasz *et al.*, 1987).** The minor and major grooves of DNA at N^2 and N^7 positions of guanine respectively are the sites of MMC action **(Tomasz *et al.*, 1986; Prakash *et al.*, 1993).**

Reports by **(Paz *et al.*, 2008; Champeil and Tomasz, 2006)** point out that despite current knowledge of the six main adducts produced by MMC in the process of alkylating and creating cross-links in DNA strands, further work is required to study these adducts. They propose alternative methods in this cause such as an altered organic synthetic assay **(Champeil and Tomasz, 2006)** or a mass spectrometry assay **(Paz *et al.*, 2008)** in order to achieve better understanding of these adducts. When in aqueous solution mitomycin C becomes inactivated by

direct light hence the precautions one must consider when using MMC solution in laboratory experiments **(Yajima and Mizunoya, 1981).**

Oxidative stress effect is more pronounced in producing chromosomal aberrations in MMC treated FA cells **(Joenje and Oostra, 1983).** If left unrepaired, DNA lesions such as DSBs can lead to cell cycle arrest, apoptosis, or cell death caused by loss of genomic integrity. If repaired incorrectly, they can lead to carcinogenesis through translocations, inversions, or deletions **(Rothkamm *et al.*, 2003).**

Mitomycin C chemical structure

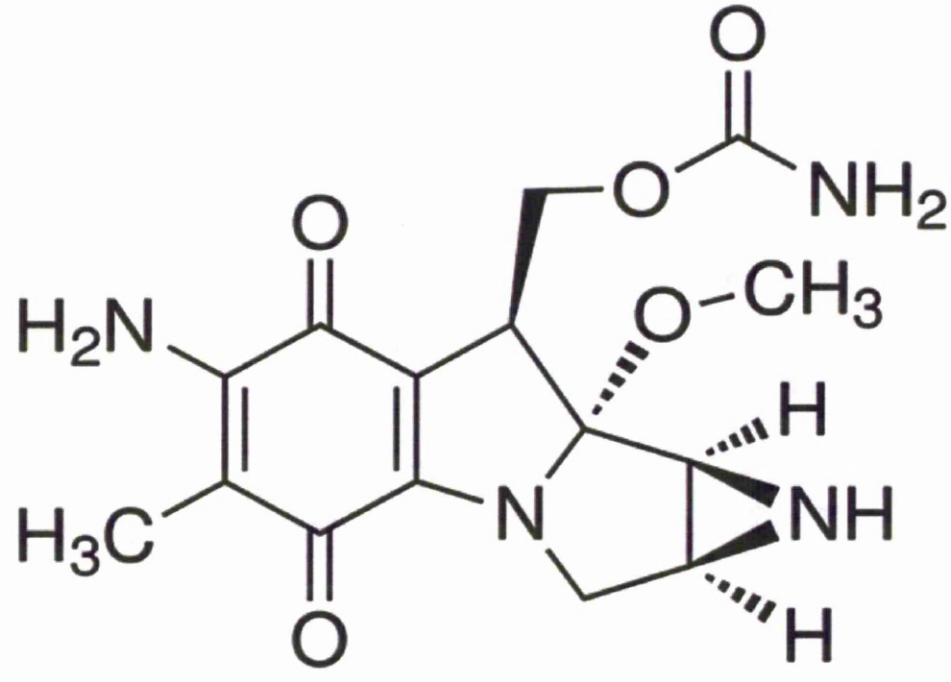

$C_{15}H_{18}N_4O_5$

Figure (1.2): Diagram illustrating Mitomycin C chemical structure with molecular formula ($C_{15}H_{18}N_4O_5$) Diagram taken from Sigma Aldrich Company

1.1.4.2 Radiation Mutagens

Ultraviolet, Gamma rays and X-ray are high energy radiation which results in a variety of DNA lesions.

1.1.4.2.1 Ultraviolet (UV) radiation

Bonds between adjacent pyrimidine bases on the same strand are found in most UV photoproducts. UVB rays directly damage DNA via pyrimidine dimers formation. DNA polymerase misinterprets these dimers as two adenine bases throughout replication, thus inserting two thymine bases in its place.

Squamous cell carcinoma of the skin has been linked to ultraviolet light excessive exposure. **(Brash *et al.*, 1991).** Mutation of tumor suppressor gene (the p53) has been attributed mostly to (UVB) and linked with 58% of squamous cell carcinomas of the skin **(Brash *et al.*, 1991).**

1.1.4.2.2 Pyrimidine dimerization

Pyrimidine dimers are structurally altered DNA bases due to the formation a cyclobutane ring between two successive pyrimidines. These dimers inhibit the action of polymerase III and the replication fork movement. Cytosine or thymine bases in DNA can form pyrimidine dimers, which are molecular lesions formed through photochemical reactions **(Goodsell, 2001).** Ultraviolet light induces the formation of covalent bonds and induces the formation of pyrimidine dimers, **(Goodsell, 2001).** Cyclobutane pyrimidine dimers (CPDs, including thymine dimers) and 6, 4 photoproducts are two common UV products **(Brash *et al.*, 1991).** These premutagenic lesions alter the structure of DNA and consequently inhibit polymerases and arrest

replication. Pyrimidine dimers may be repaired and neutralized by photo-reactivation or nucleotide excision repair **(Whitmore *et al.*, 2001; Goodsell, 2001)** and unrepaired dimers remain mutagenic.

1.1.4.2.3 X-rays

Genetic mutations may arise by direct or indirect exposure of low doses of X-ray radiation. After cellular exposure to radiation, genomic instability may be induced and transmitted to following generation of cells through cellular replication. **(Giovanetti *et al.*, 2008).** It has been reported that phosphorylation of a histone protein, H2AX, occurs in places of DNA double-strand breaks, post exposure to X-ray radiation **(MacPhail *et al.*, 2003).** This phosphorylation event precedes the enzymatic repair action that takes place at these sites of DNA damage.

Free radicals produced by X-ray radiation modify the DNA in living cells **(Ratnapalan *et al.*, 2008).** These extremely reactive free radicals are able to penetrate cells to react with other compounds producing other radicals leading to a chain reaction throughout the organism **(Gordy, 1958).** Lesions are formed when these radicals react with a base pair. As the gene with the lesion undergoes a number of replication cycles, a mutation results from that lesion. These mutations may be germ line or somatic mutations. Germ-line mutations are inherited, while somatic mutations are not, as somatic cells do not produce gametes.

1.2 DNA repair pathways

1.2.1 DNA repair mechanisms

DNA repair involves both the removal of incorrect or damaged bases, and DNA re-synthesis by DNA polymerases utilizing as a template the undamaged strand.

1.2.2 Base excision repair (BER)

The removal and replacement of single base residues is established usually by base excision repair (BER). Substrates comprise damaged DNA bases and uracil residues resulting from methylation, reactive oxygen species and hydrolytic reactions. A particular DNA glycosylase eliminates single damaged bases. An endonuclease (APEX1) incises the resulting apurinic or apyrimidinic abasic site and a deoxyribose-phosphate (dRP) lyase removes the 5′- dRP residue producing a one nucleotide gap which is filled later via the action of DNA polymerase β (Pol β) **(Lange *et al.*, 2011).**

1.2.3 Nucleotide excision repair (NER)

Identification of bulky deformations in the DNA double helix is achieved by nucleotide excision repair enzymes which also remove the deformed short single-stranded DNA segment enclosing the lesion, leaving a single-strand gap in the DNA, which is filled later via the action of DNA polymerase using the undamaged strand as a template.

Once the deformed DNA segment is identified, the damaged DNA adduct is excised via two incisions made on either side. Polymerases; Pol δ or Pol ε and Pol κ fill the resulting 27–29 nucleotide gap. A range of helix-distorting adducts, such as those caused by polycyclic aromatic hydrocarbons, UV radiation and cisplatin and are removed by NER **(Lange *et al.*, 2011).**

1.2.4 Mismatch repair (MMR)

Mismatched bases are repaired by an excision repair process termed Mismatch repair (MMR) which starts via mismatch identification proteins recognizing mismatches. Following DNA segment excision, Pol δ fills the resulting DNA gap **(Lange *et al.*, 2011).**

1.2.5 Translesion synthesis (TLS)

TLS polymerases assist in tolerating DNA damage by bypass DNA lesions resisting the effects of DNA-damaging agents, enabling the reestablishment of stalled replication forks or filling in ssDNA gaps post DNA damage. Nevertheless, elevation in mutation frequency occurs in TLS **(Waters *et al.*, 2009).** In translesion synthesis DNA lesions are bypassed via the incorporation of a nucleotide opposite to the lesion. Many specialized TLS polymerases that belong mostly to the Y family **(Ohmori *et al.*, 2001)** of DNA polymerases are utilized such as; Rev1 **(Baynton *et al.*, 1999),** Pol ι **(Zhang *et al.*, 2000),** Pol η (eta) **(McDonald *et al.*, 1999)** and others. Also other polymerases from the B-family for example; Pol ζ (zeta) **(Nelson *et al.*, 1996)** and polymerase N also called Pol *ν* from the A-family **(Takata *et al.*, 2006)** and others.

1.2.6 DNA DSBs Repair

Many external agents and spontaneous endogenous processes cause DNA damage continuously **(Friedberg *et al.*, 1995).** An array of DNA lesions may be produced by an agent or a process; for instance, free radicals that induce numerous base alterations destroy deoxyribose residues and make single and double strand breaks, are generated by ionizing radiation **(Frimmer *et al.*, 1976).** Ionizing radiation or enzymes that cleave DNA yield DNA ends that require processing or trimming and re-synthesis of bases in order to ligate these strand breaks. Many repair pathways operate to repair the dangerous DNA DSBs, mainly HRR and NHEJ **(Lange *et al.*, 2011; van Gent and van der Burg, 2007).** An essential DNA DSBs repair process is the essentially error-free, precise mode of repair HRR which employs a homologous sequence at a comparable location on a sister chromatid as a template in repairing and restoration of the original sequence of the damaged chromosome **(Jablonovich *et al.*, 1999).** However, HRR may also employ allelic sequences at a comparable location on homologous chromosomes in resolving DSBs. This mode of allelic sequences employment in repair may be associated with loss of heterozygosity (LOH) thus the uncovering of recessive mutations **(Lasko *et al.*, 1991).**

Genomic instability can arise through the accumulation of double stand breaks **(Wyman *et al.*, 2008; O'Driscoll and Jeggo, 2006).**The most severe form of DNA damage is perhaps DSBs due to the consequences that they have on the progress of transcription, replication, and chromosome segregation. Chromosomal instability leading to abnormal gene expression and carcinogenesis may result if DSBs fail to be repaired **(Hoeijmakers, 2001).** HRR and NHEJ are the DNA repair mechanisms standing out in the literature as possible repair pathways for DNA double strand damage **(Rothkamm *et al.*, 2003; van Gent and van der Burg, 2007; Wyman *et al.*, 2008; Wyman and Kanaar, 2006).**

1.2.6.1 DNA repair through Homologous recombination repair (HRR)

It seems that to repair these DSBs, cells have evolved these two distinct pathways: homologous recombination (HR) **Fig.1.3** and non-homologous end joining (NHEJ) **(Jackson, 2002)**. Most HR-based repair occurs at late S- and G2-phases of the cell cycle when an undamaged sister chromatid is accessible and can be used as a repair template. The RAD52 epistasis group of proteins (RAD50, RAD51, RAD52, RAD54, and MRE11) is involved in mediating this process **(Sonoda *et al.*, 2001).** RAD52 protein is probably, the initial sensor of the damaged DNA ends. Processing of the damaged ends produces of a new 3' single-stranded DNA (ssDNA) overhangs which bound by RAD51 to form a nucleoprotein filament. Accessory factors in filament assembly and subsequent RAD51 activities include: RPA, RAD52, RAD54, BRCA1, BRCA2, and several additional RAD51-related proteins **(Jackson, 2002)**. BRCA2 loads RAD51 onto ssDNA then, RAD51 nucleoprotein filament identifies the undamaged DNA on the sister chromatid to use as a template for homologous repair. Following that DNA strand exchange occurs, where the damaged DNA strand invades the undamaged DNA duplex. A DNA polymerase then extends the 3' end of the invading strand and subsequent ligation by DNA Ligase I produces a heteroduplexed DNA structure. By resolving this recombination intermediate, the error-free correction of the DSB completes. Eukaryotic resolvases are still hard to define, despite the recognition of many resolvases with Holliday junctions processing activity in prokaryotes. For example, whether or not RAD51C and XRCC3 are involved in Holliday junction resolution in mammalian cells is controversial **(Sharan and Kuznetsov, 2007).**

The homologous recombination mechanisms and their exact role in rebuilding stalled or broken replication forks are still widely unknown **(Barre *et al.*, 2001). A study by Barlow *et al.*, (2008)**

in budding yeast suggests that the DNA repair machinery is able to differentiate between different types of DNA damage in G1 and by doing so it specifies the most appropriate repair pathway. The path to repair is dependent on the circumstances under which the DSB is generated such as the chemical structure of the DNA ends. This specificity was also suggested earlier by **Wyman and Kanaar, (2006).**

A model illustrating DSBs repair by error free homologous recombination

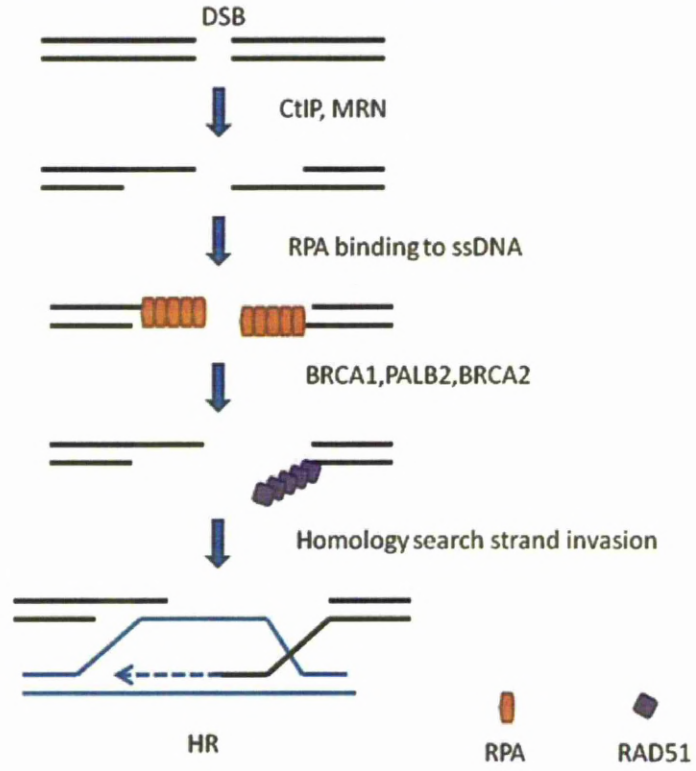

Figure (1.3): A model illustrating DSBs repair by error free homologous recombination: starts by action of CtIP exonuclease on exposed ssDNA 3' overhangs; DSBs are processed to generate 3' single-stranded ends which become later hot spots for RAD51 nucleoprotein microfilament assembly. Then Replication protein (RPA) binds to the ssDNA prior to replacement with Rad51 (a step which requires BRCA1, PALB2, and BRCA2). One of these ssDNA–RAD51 pre-synaptic filaments (ends) invades the homologous DNA by strand displacement leading to the formation of a D-loop. Using the homologous DNA as a template, the invading strand primes DNA synthesis. Also by utilizing the displaced strand as a template, the second single-stranded DNA is also employed for priming DNA synthesis. **Adapted from Kee & D'Andrea, 2010**

1.2.6.2 DNA repair through non-homologous end joining (NHEJ)

Non Homologous End Joining (NHEJ) is the primary DSB repair process in higher eukaryotes. NHEJ involves the ligation of two DNA ends regardless of their homology to one another **(Lewis and Resnick, 2000, Karran, 2000)** and most frequently associated with processing or remodeling of the DNA broken ends before rejoining them. The DSBs presence in the cell can lead to the joining of DNA ends that are located on two different chromosomes through NHEJ mechanism. Therefore, NHEJ is error-prone and is normally coupled with genomic rearrangements such as translocations and or deletions.

Error prone NHEJ **Fig.1.4** requires no sequence homology to rejoin broken ends **(O'Driscoll and Jeggo, 2006).** Essential to the NHEJ pathway is the activity of the Ku70/Ku80 heterodimeric protein **(Featherstone *et al.*, 1999).** NHEJ is initiated through the Ku heterodimer by binding to the free ends of the DNA and recruiting DNA-dependent protein kinase (DNA-PK), XRCC4, and DNA Ligase IV and other NHEJ factors to the site of DNA damage (**Jackson, 2002**). Upon binding to the DNA, DNA-PK is activated. It is thought that the activated DNA-PK then further facilitate the repair process by phosphorylating p53, Ku, and the DNA Ligase IV cofactor XRCC4. Limited processing of the damaged DNA strand ends are needed by nucleases and/or polymerases before NHEJ can proceed. The nucleases responsible for this step are unknown. Ligation is the final step in NHEJ repair involving joining the DNA ends by Ligase IV in a complex that includes XRCC4 and Ku as well.

Schematic representation of DSB repair by error prone NHEJ pathway

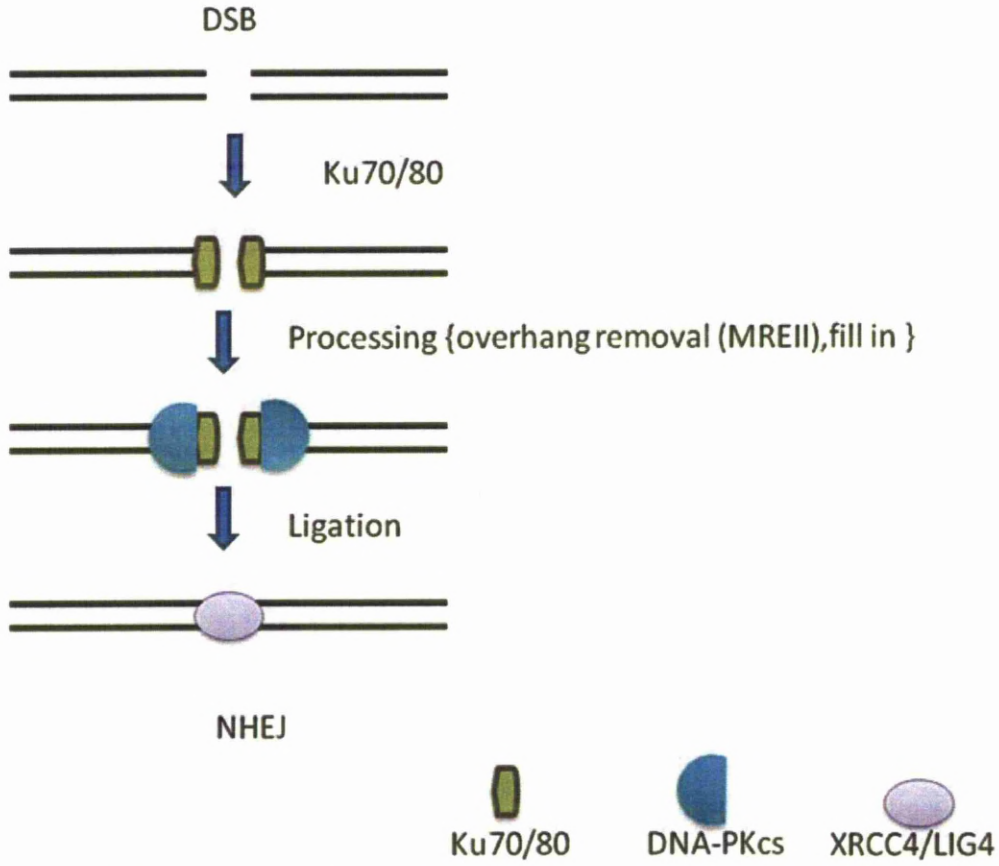

Figure (1.4): DSB repair by error prone NHEJ pathway where the two double strand break ends are directly joined together without the need for a homologous template. The regulatory subunits of DNA-PK (Ku70/80), bind at double strand break ends and recruit DNA-PKcs. Activated DNA-PKcs then recruits DNA ligase IV (LIG4) joining the two broken DNA ends. The removal of DNA overhangs is facilitated via MRE11 exonuclease. **Adapted from Kee & D'Andrea, 2010**

1.2.7 Causes and repair of Inter-strand cross-links

1.2.7.1 Causes of ICLs occurrence in prokaryotes and eukaryotes

Both genomic and cellular integrity are compromised by DNA ICLs as they block replication by forming covalent links between the two DNA strands that form the double helix, thus preventing essential genome maintenance and transcription proteins from translocating along the DNA strands. In bacteria or yeast, cellular death may result from a single, unrepaired ICL **(Lawley and Brookes, 1968; Grossmann *et al.*, 2001).** In mammalian cells which are unable to repair ICLs, 20 or more ICLs per genome are enough to bring about their death **(Lawley and Phillips, 1996).** DNA ICLs may be produced due to exposure to endogenous, exogenous or naturally occurring compounds. One chief source of endogenous stresses that provoke endogenous DNA damage is sugar moieties and base oxidation **(Barnes and Lindahl, 2004).** The endogenous ICL formation is difficult to study due to its rarity, however evidence from *in vitro* studies support their occurrence (reviewed in **Pang and Andreassen, 2009).** Endogenous ICL may form due to malondialdehyde, which is an endogenous metabolic product that forms through lipid peroxidation, **(Niedernhofer *et al.*, 2003).** ICLs may be introduced through toxic, exogenous chemicals such as nitrogen mustard, cisplatin and mitomycin C compounds which are frequently used in certain cancers as chemotherapy (reviewed in **Scharer, 2005).** ICLs may also be produced by the action of psoralen- related furocoumarins or Photoactive furocoumarins which are naturally occurring compounds found in small quantities in numerous plants such as parsley leaves, a Nile Valley weed called *Ammi majus* (Umbelliferae), or *Psoralea corylifolia* **(Manderfeld *et al.*, 1997; Scott *et al.*, 1976).** To survive this ICLs blockade and restore essential DNA maintenance processes, cells have to proficiently identify and eliminate this DNA lesion (ICLs).

1.2.7.2 ICL repair

Replication forks are stalled by ICLs and the FA pathway is activated as shown in **Fig.1.5.** FANCG recruits endonucleases that are involved in the incision step of cross link repair. A double strand break is produced as an intermediate structure of this repair process and this eventually leads to the formation of ssDNA which activates the ATR complex and its binding partners: a biological clock gene (*clk-2*) (HCLK) and ATRIP. FANCM helicase is recruited by HCLK to the site of damage. FANCM helicase binds to and stabilises the replication fork then recruits and loads the FA core complex to chromatin at the lesion site **(Deakyne and Mazin, 2011; Kitao and Takata, 2011).** The FA core complex then recruits the FANCI –FANCD2 (FA-ID) complex to the site of damage by FANCI and FANCD2 mono-ubiquitination permitting FA-ID complex phosphorylation and activation by ATR. The crosslink is then excised by the FA-ID complex and FAN1 **(Liu *et al.*, 2010)** allowing lesion repair via translesion polymerases. FANCG interacts with other downstream proteins including FANCN, FANCD2, FANCJ, BRCA1, BRCA2, RAD51 to initiate DSB repair via HRR and restart the replication fork as shown in **Fig.1.5 (Deakyne and Mazin, 2011).**

The initial, two incision events occur in cross-links repair on the DNA strand flanking the ICL at stalled replication forks catalysed by XPF-ERCC1, MUS81-EME1 or FAN1 nuclease as shown in **Fig.1.6 (Smogorzewska *et al.*, 2010; Kee and D'Andrea, 2010; Kitao and Takata, 2011).** Then bypass synthesis follows the repair of the DNA lesion via the action of a translesion polymerase, probably Rev1 **(Simpson and Sale, 2003; Niedzwiedz *et al.*, 2004; Kitao and Takata, 2011)** and possibly other translesion polymerases such as Rev3, Rev7 and PolN, **(Lehmann *et al.*, 2007; Raschle *et al.*, 2008; Moldovan *et al.*, 2010; Zietlow *et al.*, 2009).** Another two more incisions take place following bypass synthesis, permitting ICL lesion

excision as shown in **Fig.1.6.** The ubiquitinated ID complex is critical for the occurrence of the incision and the bypass polymerase activity **(Raschle *et al.*, 2008; Knipscheer *et al.*, 2009; Kitao and Takata, 2011).** Homologous recombination machinery then repairs the initial cleaved strand **(Section 1.4.7.1** for more details**).** Although the details of the nucleases implicated in ICL repair are still unclear, XPF-ERCC1 and Mus81 complexes have been pointed out as complexes connected to the nuclease activity accountable for the incision and excision action in ICL repair **(Ciccia *et al.*, 2008).** Also recently, *FANCP* also known as *SLX4* has been implicated in the nuclease action in ICL repair. SLX4 interacts with endonuclease complexes, such as MUS81-EME1 and XPF-ERCC1 and combines with SLX1 to form a Holliday junction resolvase **(Kim *et al.*, 2011, Stoepker *et al.*, 2011).** Whether conferring resistance to DNA cross-links is due to SLX4 activity or SLX4 activity is not clear yet **(Fekairi *et al.*, 2009; Munoz *et al.*, 2009; Saito *et al.*, 2009; Svendsen *et al.*, 2009).** Homologous recombination machinery then repairs the double strand breaks generated. Unresolved questions in the FA pathway include questions related to the nature of the role of ubiquitination and the mechanistic role the ID complex in regulating repair. Is it a structural role sustaining the complex at sites of DNA damage, or a role in repair factors recruitment? Also unknown are the enzymatic factors involved in lesion repair and if other ICL repair pathways exist in the absence of FA **(Smogorzewska *et al.*, 2010).**

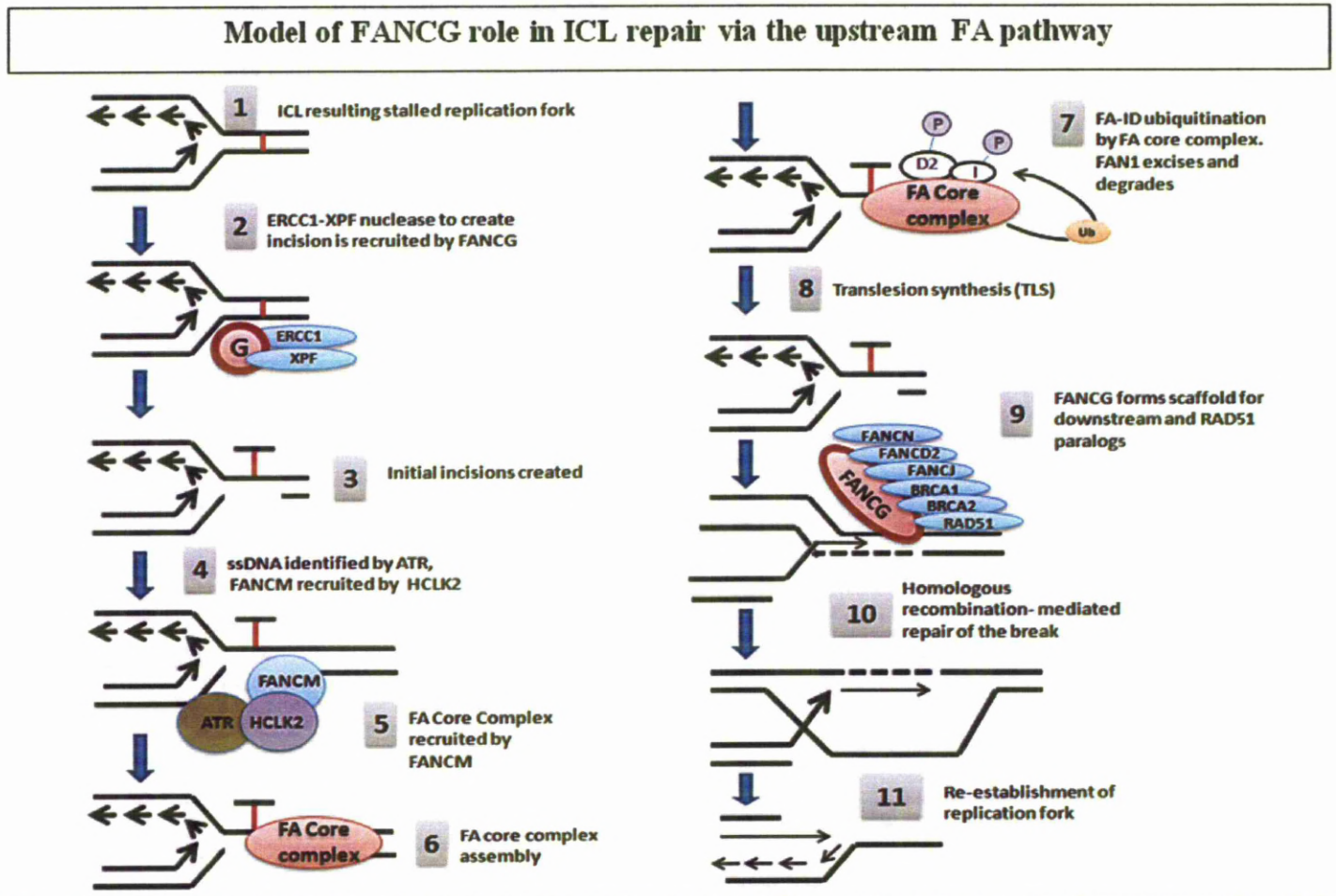

Figure (1.5): (1) Replication forks are stalled by ICLs and the FA pathway is activated. (2)FANCG recruits endonucleases. (3) Incision step of cross link repair. (4) ssDNA activates the ATR complex and its binding partners ATRIP and HCLK which recruits FANCM helicase to the site of damage. (5) FANCM helicase binds to and stabilises the replication fork then loads the FA core complex to the lesion site. (6) FA core complex assembly. (7) The FA core complex then recruits the FA-ID complex to the site of damage by FANCI and FANCD2 mono-ubiquitination permitting FA-ID complex phosphorylation and activation by ATR. (8) TLS, the crosslink is then excised by the FA-ID complex and FAN1 allowing lesion repair via translesion polymerases. (9) FANCG interacts with other downstream proteins FANCN, FANCD2, FANCJ, BRCA1, BRCA2, RAD51 to initiate DSB repair. (10) HRR start. (11) Restart the replication fork

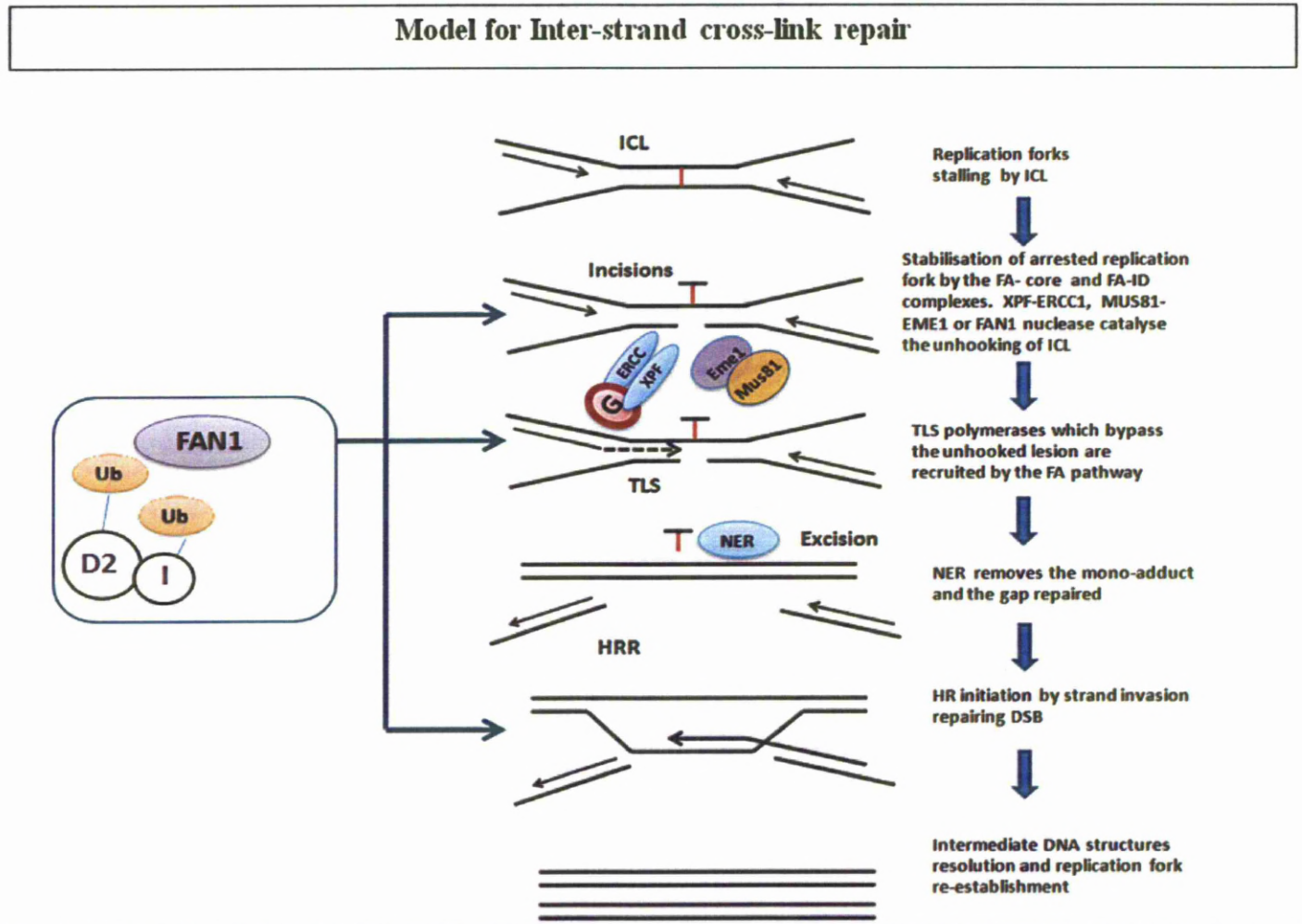

Figure (1.6): Diagram illustrating ICL repair. ICLs block replication fork progression resulting in the stalled fork triggering mono-ubiquitination of the FANCD2-FANCI heterodimer. The ICL is incised by XPF-ERCC1, MUS81-EME1 or FAN1 nuclease. The nucleases cut one side of the DNA, subsequently unhooking the crosslink and exposing a gap which is then bypassed by TLS polymerases allowing NER to remove mono-adducts and repair the gap. DSBs are an intermediate of the ICL repair process and these are repaired by HR. Ub; ubiquitination, I; FANCI, D2; FANCD2, G; FANCG, NER; Nucleotide excision repair Diagram **based on models presented by (Smogorzewska *et al.*, 2010; Kee & D'Andrea, 2010; Kitao and Takata, 2011)**

1.3 Instability Syndromes

1.3.1 Instability syndromes and cancer

Defective genes responsible for chromosome breakage syndromes such as the FA-associated genes, *NBS1, ATM* and *ATR* (ataxia telangiecasia and RAD3 related) work through intricate networks in response to DNA damage sustaining chromosomal stability throughout the cell cycle **(Eyfjord *et al.*, 2005).** Elevated cancer susceptibility is evident in many instability syndromes which show sensitivity to a number of DNA damaging agents **(Eyfjord *et al.*, 2005, Lindh *et al.*, 2006; Van der Heijden *et al.*, 2004).** Cell transformation which is a precursor of cancer may result if genome integrity is lost. The normal functionality of several tumor suppressor genes is connected to the regular DNA repair process **(Eyfjord *et al.*, 2005, Smogorzewska *et al.*, 2007).**

1.3.2 Centrosome instability and telomere dysfunction

It has been suggested that the origins of genetic instability may be related to telomeric dysfunction **(Pathak *et al.*, 2002).** Throughout life, the normal cell-ageing process produces shorter telomeres as age progresses. As cellular DNA repair rate fails to compensate efficiently, the natural DNA damage occurring throughout the aging process, complex chromosomal aberrations, genome instability and cancer may result. Whether this is due to DNA damage accumulating or other molecular or physiological processes is controversial **(DePinho *et al.*, 2000, Maser *et al.*, 2003).**

Telomeric erosions were proposed to be the initial structural aberrations initiating genetic instability **(Maser *et al.*, 2003, Feldser *et al.*, 2003).** As shown in **Figure 1.7;** a cascade of events follows telomeric DNA erosions: starting from secondary structural aberrations such as dicentric or ring chromosomes, followed by endomitosis and centrosomal amplification, chromosomal aneuploidy induction and finally cancerous tissue formation **(Pathak *et al.*, 2002, Lingle *et al.*, 2002, Eyfjord *et al.*, 2005).**

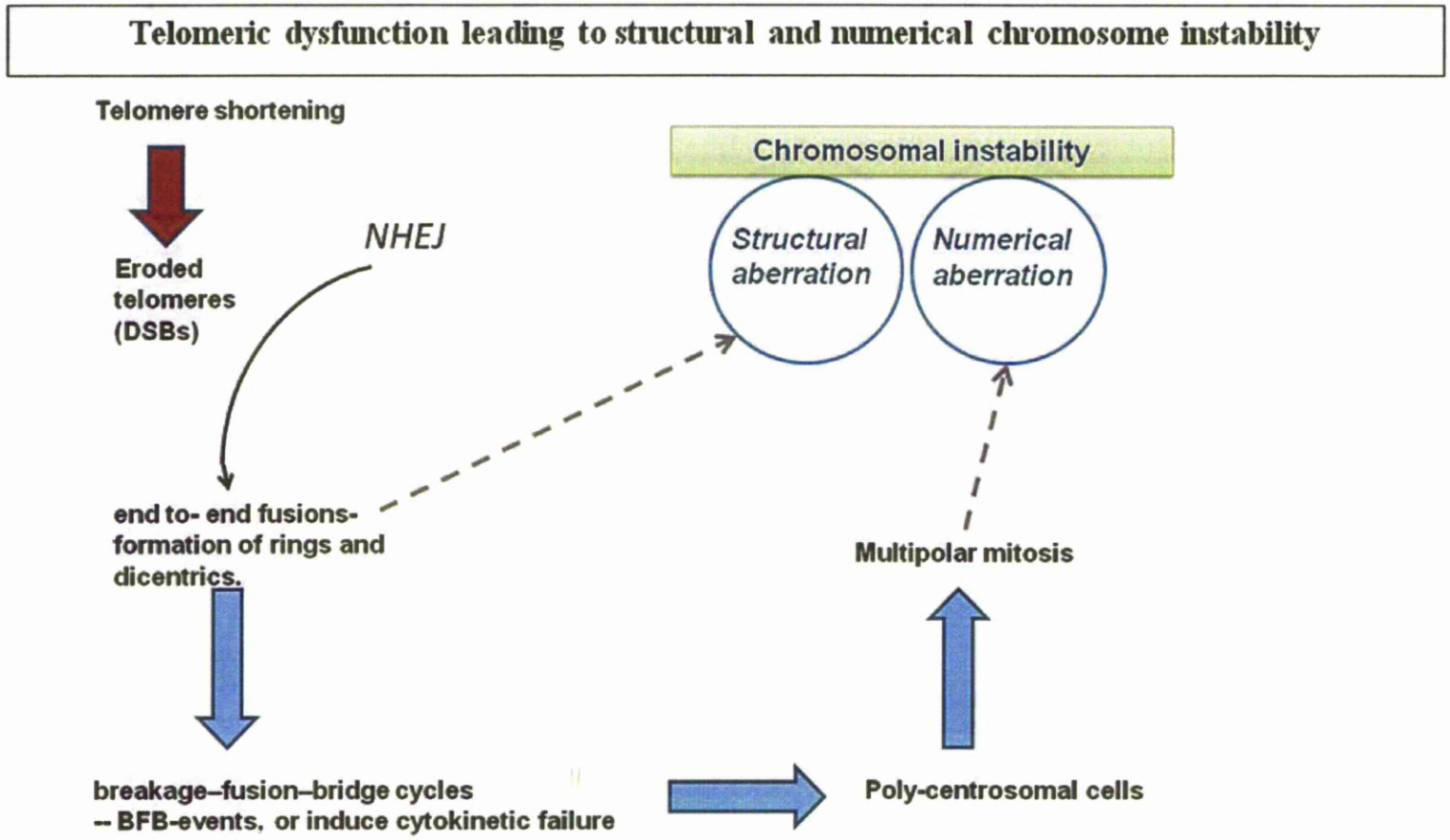

Figure (1.7): Telomeric dysfunction compromise the integrity of chromosome ends leading ultimately to structural and numerical chromosome instability. As error prone NHEJ leads to the formation of complex instable chromosomal arrangements such as rings, dicentrics, triradials, quadric-radials etc. These instable structures may form anaphase bridges, which either breaks and initiate a chain of chromosomal breakage-fusion-bridge (BFB)-events, or provoke cytokinetic failure resulting in the creation of binucleate cells with supernumerary centrosomes. Cells consisting of irregular centrosome number may form multipolar mitoses at the following cellular division.

1.4 Fanconi anaemia

In 1927, a Swiss pediatrician noted the presence of "perniziosiforme anaemia" (macrocytic red cells and pancytopenia) along with several physical anomalies in 3 siblings and described the first cases of Fanconi anaemia **(Shimamura and Alter, 2010).** Fanconi anaemia diagnostic criteria today doesn't simply require the presence of aplastic anaemia and birth defects, but are much more extensive, and requires the illustration of chromosomal aberrations in cells cultured with mitomycin C induced chromosomal breakage test **(Tonnies *et al.*, 2003; Talwar *et al.*, 2004; Ameziane *et al.*, 2008).**

1.4.1 Fanconi anaemia mode of Inheritance

Fanconi pancytopenia, or Fanconi anaemia, is mainly an autosomal recessive chromosomal instability syndrome with an incidence of approximately one to three per 10^5 live births **(Schroeder *et al.*, 1976)** and a heterozygote frequency of about 1 in 300 in Europe and the United States **(Swift, 1971).** The Fanconi anaemia (FA) carrier frequency is remarkably high in the Ashkenazi Jewish population **(Kutler and Auerbach, 2004).** Fanconi anaemia is associated with progressive bone marrow failure and an elevated cancer risk, particularly solid tumors and acute myelogenous leukemia (AML) **(Joenje and Patel, 2001; Tischkowitz and Hodgson, 2003; Van der Heijden *et al.*, 2004; Swift, 1971).**The one exception to FA being autosomal recessive is *FANCB*, as this gene is found to be localized at Xp22.31 on the X chromosome **(Meetei *et al.*, 2004a).** Mutations in *FANCB* are inherited in an X-linked manner making FA

both an autosomal recessive and an X-linked heritable disease. FA carriers are asymptomatic and are not identified by the either DEB or MMC test.

1.4.2 Fanconi anaemia clinical manifestations

FA clinical manifestations include pre- and postnatal developmental retardation, hearing loss, hypogonadism and reduced fertility, kidney, heart and skeleton malformations, absent or abnormal thumbs, a typical 'elfin' facial appearance, caused by microcephaly, small eyes and mouth and cutaneous abnormalities such as hyper-pigmentation or hypo-pigmentation (reviewed by **Joenje and Patel, 2001).** Chromosomal instability and hypersensitivity to DNA cross-linking agents is characteristic of FA cell lines **(Joenje and Patel, 2001).** More FA clinical manifestations are illustrated in **Table 1.1.**

Table (1.1): Fanconi anaemia clinical manifestations

Upper limbs, unilateral or bilateral

Thumbs : Attached by a thread, bifid, duplicated, rudimentary,, triphalangeal, long, low set, absent or hypoplastic

Radii : Absent or weak pulse, absent or hypoplastic (only with abnormal thumbs)

Hands : Absent first metacarpal, clinodactyly, flat thenar eminence, polydactyly

Ulnae : Short, dysplastic

Lower limbs

Feet: abnormal toes, club feet, toe syndactyly

Legs: Congenital hip dislocation

Skeletal

Head : hydrocephaly, microcephaly

Face : Dysmorphic, micrognathia, mid-face hypoplasia, triangular, birdlike

Neck : Short, low hairline, sprengel, Klippel–Feil, web

Spine : Hemivertebrae, abnormal ribs, spina bifida, scoliosis, coccygeal aplasia

Gonads

Males : Micropenis, absent testes, undescended testes, hypospadias, hypogenitalia

Females : Malposition, small ovaries, hypogenitalia, bicornuate uterus

Other symptoms

Developmental delay : Developmental delay, mental retardation

Ears : Abnormal middle ear, dysplastic, atretic, deaf (usually conductive), abnormal shape, narrow ear canal

Cardiopulmonary : Atrial septal defect, ventricular septal defect, truncus arteriosus, congenital heart disease, patent ductus arteriosus, coarctation, situs inversus

Low birth weight

Any physical abnormality

Microsomia : Short stature

Skin : Hypo-pigmented areas, generalized hyperpigmentation; café au lait spots

Gastrointestinal : Annular pancreas, atresia (esophagus, duodenum, jejunum), malrotation, imperforate anus, tracheoesophageal fistula

Central nervous system : absent corpus callosum, cerebellar hypoplasia, hydrocephalus, small pituitary, dilated ventricles, pituitary stalk interruption syndrome

Table (1.1): Illustrating clinical manifestations of FA. Reconstructed from **(Shimamura and Alter, 2010)**

1.4.3 Fanconi anaemia diagnosis and hypersensitivity to inter-strand cross-linking agents

Fanconi anaemia (FA) cells are characterized by their cellular hypersensitivity to DNA inter-strand cross-linking (ICL) agents **(Busch *et al.*, 1996; Wilson *et al.*, 2001;** reviewed by **Joenje and Patel, 2001; Taniguchi and D'Andrea, 2006; Moldovan and D'Andrea, 2009)**. This hypersensitivity is reflected at the level of the chromosome allowing Fanconi Anaemia (FA) to be diagnosed by cytogenetic testing for increased chromosomal breakage or rearrangement in the presence of bi-functional alkylating (inter-strand cross-linking) agents such as mitomycin C (MMC) and diepoxybutane (DEB) **(Sasaki and Tonomura , 1973; Cervenka *et al.*, 1981, Auerbach and Wolman, 1976; Auerbach, 1993; Esmer *et al.*, 2004).**

Typically the induced cytogenetic aberrations are predominantly chromatid exchanges such as triradials and quadri-radials due to inability to repair cross-links produced by these agents **(Kuhn and Therman, 1982; Busch *et al.*, 1996; Joenje and Patel, 2001; Moldovan and D'Andrea, 2009).**

The clinically diverse disorder FA should be confirmed at the cellular level by means of a mitomycin C induced chromosomal breakage test **(Tonnies *et al.*, 2003; Talwar *et al.*, 2004; Ameziane *et al.*, 2008)** which is a cytogenetic test facilitating the diagnostic differentiation between FA and similar disorders such as "idiopathic" Aplastic anaemia. This method is based on the effect of the alkylating agent mitomycin C (MMC) on chromosomes of peripheral lymphocytes in culture. At higher concentrations of MMC, elevated rates of CA are observed along with reduced mitotic activity in FA lymphocytes compared to average values of either healthy control or aplastic anaemia cells **(Cervenka J, *et al;* 1981).** FA clinical and cellular features can result from any disorder within the FA pathway **(Kennedy and D'Andrea, 2005).**

1.4.4 Fanconi anaemia pathway

The FA pathway promotes the repair of crosslink damage and other types of DNA damage. So far, fifteen FA genes have been reported; [A, B, C, D1 (*BRCA2*), D2, E, F, G, I, J (*BRIP1/BACH1*), L, M, N (*PALB2*), O (*RAD51C*), and P (*SLX4*) (reviewed by **Thompson and Hinz, 2009).** however the range of many of their protein functions or the intricacy of their interactions remains to be determined **(Levitus *et al.*, 2006).** Despite FANCD2 lacking any recognizable domains that are found in DNA-repair molecules, its mono-ubiquitination is crucial in the FA–BRCA network. The concentration of mono-ubiquitinated FANCD2 increases when cells are either engaged in DNA replication or exposed to DNA-damaging reagents **(Garcia-Higuera *et al.*, 2001; Taniguchi *et al.*, 2002b).** Various elements in the FA pathway are still unknown **(Kennedy and D'Andrea, 2005).** Schematic illustrations of the FA proteins involved in upstream and downstream interactions are shown in **Fig. 1.8** and **Fig 1.9**.

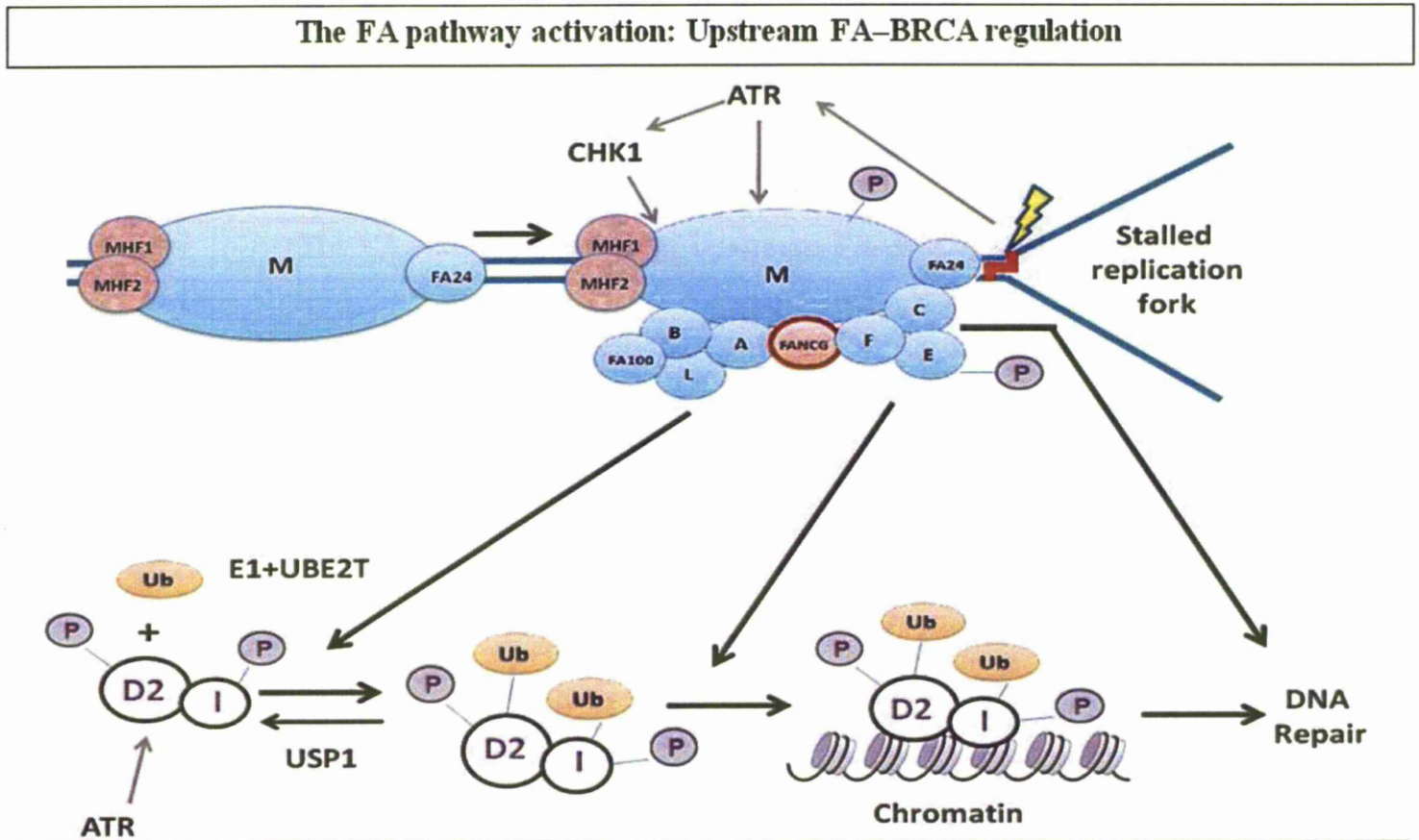

Figure (1.8): The FA pathway activation: Upstream FA–BRCA regulation model

An ICL cause the replication fork to stall. (ATR) is activated by a stalled replication fork along with its downstream kinase checkpoint kinase 1 (CHK1) and they activate the FA core (FA proteins A, B, C, E, F, G and L) and ID complex (FA proteins D2 and I) through phosphorylation. The core complex translocates and is recruited to sites of DNA damage by FANCM, FAAP24, MHF1 and MHF2 where it mono-ubiquitinates the FA–ID complex, and also help to engage the ID complex to chromatin. FANCM and FAAP24 may also be directly involved in processing DNA as part of a DNA-repair reaction. The ubiquitin-activating enzyme (E1) and a conjugating enzyme (UBE2T) work with the FA core complex (E3) in order to mono-ubiquitinate the ID complex. A de-ubiquitination enzyme, USP1, eliminates the mono-ubiquitin from the ID complex to shut down the network after repairs to the lesion have been made. **Diagram reconstructed and modified from (Wang, 2007a & Kitao &Takata, 2011)**

Figure (1.9): The FA pathway activation: downstream FA–BRCA regulation model

ATR phosphorylates the histone H2A variant H2AX (making γH2AX), along with BRCA1 and BRCA2, which may permit different repair complexes to be utilized in repairing the damaged loci by protein–protein interactions. The BRCT domains in BRCA1 recognize phosphorylated ATR or ataxia telangiectasia mutated (ATM) sites, and may be responsible for the repair protein assembly. A complex of BRCA2 and FANCN can promote a homologous recombination dependent restart of the replication fork, whereas FANCJ probably promotes an alternative translesion bypass. The BLM helicase complex may collaborate with the FA core complex to stabilize and re-start the stalled replication forks. P: phosphorylation; Ub: ubiquitination **Diagram adopted from (Wang, 2007a)**

1.4.5 The upstream FA pathway proteins

1.4.5.1 Fanconi anaemia core complex

The FA nuclear core complex is composed of eight FANC proteins (FANCA/B/C/E/F/G/L/M proteins) accompanied by FANC associated polypeptides FAAP24 and FAAP100 **(Ciccia *et al.*, 2007).** This core complex and the presence of FANCI are required for the mono-ubiquitination of FANCD2 through the activity of the E3 ubiquitinase ligase (FANCL) **(Meetei *et al.*, 2004b; Levitus *et al.*, 2006, Sims *et al.*, 2007, Smogorzewska *et al.*, 2007).** The upstream FA proteins are the FA core complex proteins and these are presented below.

1.4.5.1.1 FANCA

FANCA is located at chromosome number 16 on locus 16q24.3 encoding for FANCA protein as shown in **Table 1.2.** FANCA is a phospho-protein and a component of the FA core complex. FANCA is phosphorylated following DNA damage **(Wang, 2007a). Collins *et al.*, (2009)** suggested that ATR kinase may phosphorylate FANCA at serine 1449. *FANCA* pathologic mutations are various and highly variable among different populations **(Levran *et al.*, 1997, Morgan *et al.*, 1999, Wijker *et al.*, 1999) (Section 1.4.8** for more details about FANCA).

1.4.5.1.2 FANCB

FANCB also known as *FAAP95* encodes for FANCB protein. FANCB is located at the X chromosome on locus Xp22.31 as shown in **Table 1.2.** Mutations in *FANCB* are inherited in an X-linked manner **(Meetei *et al.*, 2004a).** FANCB is a component of the FA core complex and contains a putative bipartite nuclear localization sequence (NLS) **(Meetei *et al.*, 2004a; Wang, 2007a).**

1.4.5.1.3 FANCC

FANCC is located at chromosome number 9 on locus 9q22.3 encoding for FANCC protein as shown in **Table 1.2.** FANCC is a component of the FA nuclear core complex, nevertheless it can also be found in the cytoplasm and may have cytoplasmic functions **(Yamashita *et al.*, 1994; Wang, 2007a)**.

1.4.5.1.4 FANCE

FANCE is located at chromosome number 6 on locus 6p22-p21 encoding for FANCE protein which is a component of the FA core complex as shown in **Table 1.2.** FANCE directly binds to FANCD2 and is phosphorylated by CHK1 post DNA damage **(Wang, 2007a)**. Theoretically, FANCE has a phospho-dependent role as a shuttle protein between FANCD2 and the nuclear FA core complex **(Wang, 2007a)**.

1.4.5.1.5 FANCF

FANCF is located at chromosome number 11 on locus 11p15 encoding for FANCF protein which is a component of the FA core complex **(de Winter *et al.*, 2000a; de Winter *et al.*, 2000b; Garcia-Higuera *et al.*, 2001)** as shown in **Table 1.2.** FANCF is regarded as an agile adaptor protein for the FA core complex assembly **(Leveille *et al.*, 2004).** The N-terminus of FANCF has been found to be important for FANCC/FANCE binding also stabilizes FANCA/FANCG interaction. Through its C-terminus, FANCF is able to directly interact with FANCG **(Leveille *et al.*, 2004).**

1.4.5.1.6 FANCG

FANCG is located at chromosome number 9 on locus 9p13 encoding for FANCG protein which is a component of the FA core complex as shown in **Table 1.2.** *FANCG* mutations are various and highly variable among different populations. Some populations may hold specific mutations **(Demuth *et al.*, 2000, Nakanishi *et al.*, 2002).** FANCG consists of seven tetratricopeptide repeat motifs (TPRs) **(Blom *et al.*, 2004).** FANCG is a phospho-protein with phospho-sites at serines 7, 383 and 387. FANCG serines 383 and 387 are essential for FANCG exclusion from chromatin in mitosis and are phosphorylated most likely by cdc2 in the M phase of the cell cycle **(Mi *et al.*, 2004).** FANCG phospho-site (serine 7) is phosphorylated post DNA damage **(Qiao *et al.*, 2004).** FANCG complexes with FANCD1, FANCD2, and XRCC3 forming the G-BRCA2 complex implying that FANCG plays several roles in DNA repair processes as it is found to be part of several complexes such as the FA core complex, the G-BRCA2 complex **(Wang *et al.*, 2007b)** and the G-XPF complex **(Wang and Lambert, 2010) (Section 1.4.7** for more details about FANCG).

1.4.5.1.7 FANCL

FANCL is located at chromosome number 2 on locus 2p16.1 encoding for FANCL protein which is an E3 ubiquitin-protein ligase. This E3 ubiquitin ligase activity is vital for mono-ubiquitination of the FA-ID complex **(Wang, 2007a)**. FANCL is a component of the FA core complex as shown in **Table 1.2 (Meetei *et al.*, 2003)** and is assumed to be the FA core complex catalytic subunit for FANCI and FANCD2. UBE2T (E2 ubiquitin conjugating enzyme) directly interacts with FANCL **(Machida *et al.*, 2006).**

1.4.5.1.8 FANCM

FANCM is located at chromosome number 14 on locus 14q21.3 encoding for FANCM protein which is a component of the FA core complex as shown in **Table 1.2.** FANCM is a phospho-protein that is phosphorylated post DNA damage and participates with, a FANCM binding protein (FAAP24) in a checkpoint regulation in response to DNA damage **(Huang *et al.*, 2010).**

It is arguable whether people with *FANCM* mutations should be assigned in to a formal complementation group as only one reference cell line (family) has been recognized and that cell line had shown biallelic mutations in both *FANCM* and *FANCA.* Nevertheless, FA phenotype is obtained via knocking down *FANCM* in laboratory conditions **(Singh *et al.*, 2009).**

Table (1.2): Fanconi anaemia genes/proteins

Gene Symbol	Complementation Group	Locus	Protein	FANCD2 monoubiquitination	Prevalence percentage	Main function of the protein	Other names	Protien size Kilo-dalton	Mode of inheretance	References
FANCA	FA-A	16q24.3	FA group A protein	(+)	66	FA-CC		163	AR	(Apostolou *et al.*, 1996, Lo Ten Foe *et al.*, 1996)
FANCB	FA-B	Xp22.31	FA group B protein	(+)	~2	FA-CC	FAAP95	95	X-linked	(Meetei *et al.*, 2004a)
FANCC	FA-C	9q22.3	FA group C protein	(+)	10	FA-CC		63	AR	(Strathdee *et al.*, 1992)
FANCD1 (BRCA2)	FA-D1	13q12.3	Breast cancer type 2 susceptibility protein	(-)	~2	RAD51 recruitment	BRCA2	380	AR	(Howlett *et al.*, 2002)
FANCD2	FA-D2	3p25.3	FA group D2 protein	(+)	~2	?		155, 162	AR	(Timmers *et al.*, 2001)
FANCE	FA-E	6p22-p21	FA group E protein	(+)	~2	FA-CC		60	AR	(de Winter *et al.*, 2000)
FANCF	FA-F	11p15	FA group F protein	(+)	~2	FA-CC		42	AR	(de Winter *et al.*, 2000)
FANCG	FA-G	9p13	FA group G protein	(+)	9	FA-CC	XRCC9	68	AR	[de Winter et al., 2000]
FANCI	FA-I	15q25-q26	FA group I protein	(+)	~2	?		?	AR	(Dorsman *et al.*, 2007, Sims *et al.*, 2007, Smogorzewska *et al.*, 2007)
FANCJ (BRIP1)	FA-J	17q22	FA group J protein	(-)	~2	5' > 3' DNA helicase/ATPase	(BRIP1) or (BACH1)	130	AR	(Levitus *et al.*, 2005, Levran *et al.*, 2005b, Litman *et al.*, 2005)
FANCL	FA-L	2p16.1	E3 ubiquitin-protein ligase FANCL	(+)	<0.2	FA-CC, ubiquitin ligase	(PHF9) or (FAAP43)	43	AR	(Meetei *et al.*, 2003)
FANCM	Contraversial	14q21.3	FA group M protein	(+)	<0.2	FA-CC, ATPase/ translocase	FAAP250	250	AR	(Meetei *et al.*, 2005)
FANCN (PALB2)	FA-N	16p12	Partner and localizer of BRCA2		~2		PALB2		AR	(Reid *et al.*, 2007, Xia *et al.*, 2007)
FANCO (RAD51C)	Contraversial	17q22	DNA repair protein RAD51 homolog 3		~2		RAD51C		AR	(Vaz *et al.*, 2010)
FANCP (SLX4)	Contraversial	16p13.3	Structure-specific endonuclease subunit SLX4		~2		SLX4		AR	(Stoepker *et al.*, 2011, Kim *et al.*, 2011)

Table (1.2): illustrating a summary of Fanconi anaemia genes/proteins, their alternative names and their requirement for FANCD2 mono-ubiquitination, FA core complex and their mode of inheritance. FA: Fanconi anaemia; FA-CC: core complex; AR: autosomal recessive; (+): required; (-): not required. References to construct this table are **(Taniguchi and D'Andrea, 2006; Wang, 2007a; Shimamura & Alter, 2010; Kim *et al.*, 2011, Stoepker *et al.*, 2011)**

1.4.6 The downstream FA pathway proteins

1.4.6.1 FANCD1

FANCD1, also known as *BRCA2* is located at chromosome number 13 on locus 13q12.3 encoding for FANCD1 protein as shown in **Table 1.2** Breast cancer type two susceptibility protein (BRCA2) modulates homologous recombination repair (HRR) via RAD51 recombinase activity regulation (**Davies *et al.*, 2001; Moynahan *et al.*, 2001a; Moynahan *et al.*, 2001b; Wang, 2007a**). FANCD1 plays other roles in cytokinesis regulation and stalled replication forks stabilization **(Daniels *et al.*, 2004)**. FANCD1 works with RAD51 in processing DNA double strand break ends, where FANCD1 loads RAD51 onto ssDNA to repair these lesions. FANCD1 is involved in other various sub-complexes with other FA proteins, such as FANCN, FANCG, and FANCD2 **(Wilson *et al.*, 2010; Xia *et al.*, 2007).** FANCD1 complexes with FANCG, FANCD2, and XRCC3 formulating the G-BRCA2 complex **(Wilson *et al.*, 2010).**

1.4.6.2 FANCD2

FANCD2 is located at chromosome number 3 on locus 3p25.3 encoding for FANCD2 protein as shown in **Table 1.2.** FANCD2 has two isoforms; isoform (a) and isoform (b) which give rise to functional and non-functional FANCD2 protein variants **(Montes de Oca *et al.*, 2005).** FANCD2 has shown to have a role in resection of ends surrounding cross-links in DNA lesion repair **(Knipscheer *et al.*, 2009). Huang and D'Andrea (2010)** illustrated that FANCD2 binds to FAN1 nuclease.

FANCD2 is mono-ubiquitinated on lysine 561 via the FA core complex and is transported to chromatin fraction after ubiquitination, to form nuclear foci with RAD51, BRCA1, BRCA2 **(Taniguchi *et al.*, 2002b)** and FANCI where the repair of DNA lesions is thought to takes place.

FANCD2 is a phospho-protein that is phosphorylated and mono-ubiquitinated post DNA damage. FANCD2 interacts with FANCI forming the FA-ID complex which seems to be the heart of the FA pathway. FANCD2 phosphorylation may be performed via ATM **(Ho *et al.*, 2006)** and possibly by ATR **(Andreassen *et al.*, 2004)** post DNA damage. CHK1 phosphorylates FANCD2 at serine 331 to bind BRCA2 **(Zhi *et al.*, 2009) (See Section 1.4.9** for more details about FANCD2**).**

1.4.6.3 FANCI

FANCI is located at chromosome number 15 on locus 15q25-q26 encoding for FANCI protein which is a component of the FANCI-FANCD2 (FA-ID) complex as shown in **Table 1.2.** FANCI is a phospho-protein that is phosphorylated and mono-ubiquitinated post DNA damage and is a partner for FANCD2 in the (FA-ID) complex. FANCI is mono-ubiquitinated on lysine 523 prior translocation to nuclear foci to co-localize with other proteins such as FANCD2, RAD51, BRCA1, and FANCD1. FANCI and FANCD2 function in a similar manner thus can be analyzed in the same way by assays involving cellular survival, mono-ubiquitination or DNA nuclear repair foci **(Ishiai *et al.*, 2008).**

1.4.6.4 FANCJ

FANCJ also known as *BRIP1* (BRCA1 interacting protein C-terminal helicase 1) and has also been called *BACH1* (BRCA1-associated C-terminal helicase 1). *FANCJ* is located at chromosome number 17 on locus 17q22 encoding for FANCJ protein as shown in **Table 1.2.** FANCJ is a phospho-protein that is phosphorylated post DNA damage. FANCJ is a 5'-to-3' DNA helicase (DEAH helicase) and a DNA-dependent ATPase which binds directly to BRCA1 **(Cantor *et al.*, 2001).**

1.4.6.5 FANCN

FANCN is also known as the partner and localizer of BRCA2 protein (*PALB2*). *PALB2* or *FANCN* is located at chromosome number 16 on locus 16p12 encoding for FANCN protein as shown in **Table 1.2.** BRCA2 stability and nuclear localization requires FANCN as a central regulating partner **(Wang, 2007a).** As FANCN regulates FANCD1/BRCA2 stability and nuclear localization, then it plays a role in the HRR pathway **(Xia *et al.*, 2007).**

1.4.6.6 FANCO

FANCO also known as *RAD51C* is located at chromosome number 17 on locus 17q22 encoding for RAD51C protein as shown in **Table 1.2.** RAD51C is a component of several distinct protein complexes involved in HRR. RAD51 C and RAD51 variants work with FANCD1 and bind to single strand overhangs arising post DNA lesion processing **(Somyajit *et al.*, 2010).** It is arguable whether people with *FANCO* mutations should be assigned to a formal

complementation group since only one reference consanguineous cell line (family) has been recognized **(Vaz *et al.*, 2010).**

1.4.6.7 FANCP

FANCP also known as *SLX4* is located at chromosome number 16 on locus 16p13.3 encoding for SLX4 protein as shown in **Table 1.2.** SLX4 is a scaffold for various DNA repair nucleases and seems to interact with endonuclease complexes, such as MUS81-EME1 and XPF-ERCC1 and appear to be connected to the resolution of homologous recombination intermediates, for example; Holliday junctions **(Kim *et al.*, 2011, Stoepker *et al.*, 2011).** It is arguable whether people with *FANCP* mutations should be assigned to a formal complementation group since only few reference families have been recognized **(Kim *et al.*, 2011, Stoepker *et al.*, 2011).**

1.4.7 Fanconi anaemia *FANCG*

1.4.7.1 FANCG and its role in the FA pathway

Fanconi anaemia, complementation group G (*FANCG*) is located on the short arm of chromosome 9 coding for a 68 kDa protein **(Wang, 2007a).** FANCG represents one of fifteen complementation FA groups that have been confirmed to date [A, B, C, D1, D2, E, F, G, I, J, L, M, N, O, and P] (reviewed by **Thompson and Hinz, 2009).** These complementation groups can be recognized through the identification of the cDNA of the FA-related genes **(Pulsipher *et al.*, 1998; Chandra *et al.*, 2005).**

The FA nuclear core complex is composed of eight FANC proteins (FANCA/B/C/E/F/G/L/M proteins) accompanied by FANC associated polypeptides FAAP24 and FAAP100 **(Ciccia *et al.*,**

2007). As shown in **Fig.1.10;** this entire core complex including FANCG and the presence of FANCI are required for the mono-ubiquitination of FANCD2 through the activity of the E3 ubiquitinase ligase (FANCL) **(Levitus *et al.*, 2006, Sims *et al.*, 2007, Smogorzewska *et al.*, 2007).**

In addition to its function as part of the FA core complex, FANCG is thought to be involved in another independent protein complex. Thus it is likely to have functional roles in addition to that associated with the core complex. The G-BRCA2 complex as shown in **Fig.1.10** which encompasses: FANCD1/BRCA2-FANCD2-FANCG-XRCC3 **(Wilson *et al.*, 2008).** It has been suggested that the homologous recombination repair (HRR) stage of the ICL repair process is modulated through a distinct complex G-BRCA2, which if any of its components is defective the promotion of HRR process will be compromised **(Wilson *et al.*, 2008).** In addition FANCG may be present as a third complex **Fig.1.10**. Findings of **Kumaresan *et al.*,** in 2007 supporting the failure of FA cells to proficiently produce incisions at the site of a cross-link combined with findings of **Wang and Lambert** in 2010 which demonstrated that FANCG binds directly to ERCC1-XPF endonuclease establishes the importance of FANCG protein in the unhooking step of the ICL repair pathway **Fig.1.11**. At the site of the ICL a structural protein termed non-erythroid R spectrin (RIISp) binds to the DNA, then FANCG binds to the SH3 domain of RIISp. Following FANCG-RIISp binding, ERCC1-XPF is recruited to the ICL by FANCG. Then the DNA on the 5' side of the ICL is incised by ERCC1-XPF unhooking the cross-link as shown in **Fig.1.11 (Wang and Lambert, 2010).**

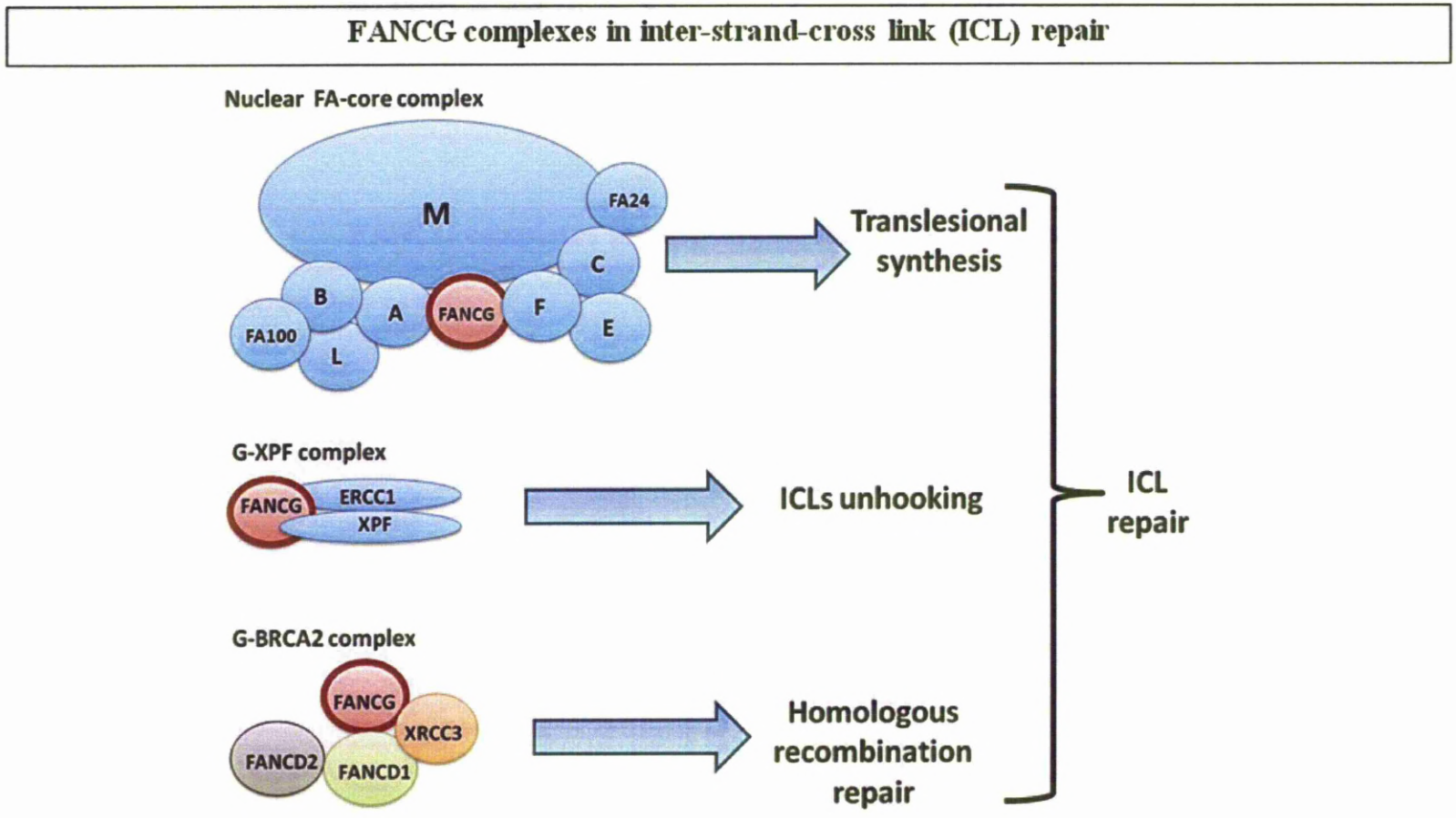

Figure (1.10): illustrating DNA repair protein complexes consisting of FANCG that are involved in inter-strand-cross link (ICL) repair. Each FANCG complex is active in different pathways that are all part of the multifaceted repair of ICLs. FANC(A,B,C,E,F,L,M,G), FAA100 & FAA24 (FA associated proteins) compose the FA complex, whereas, the G-BRCA2 is composed of FANC(G,D1,D2) & XRCC3 and the G-XPF consists of (FANCG,ERCC1 & XPF).

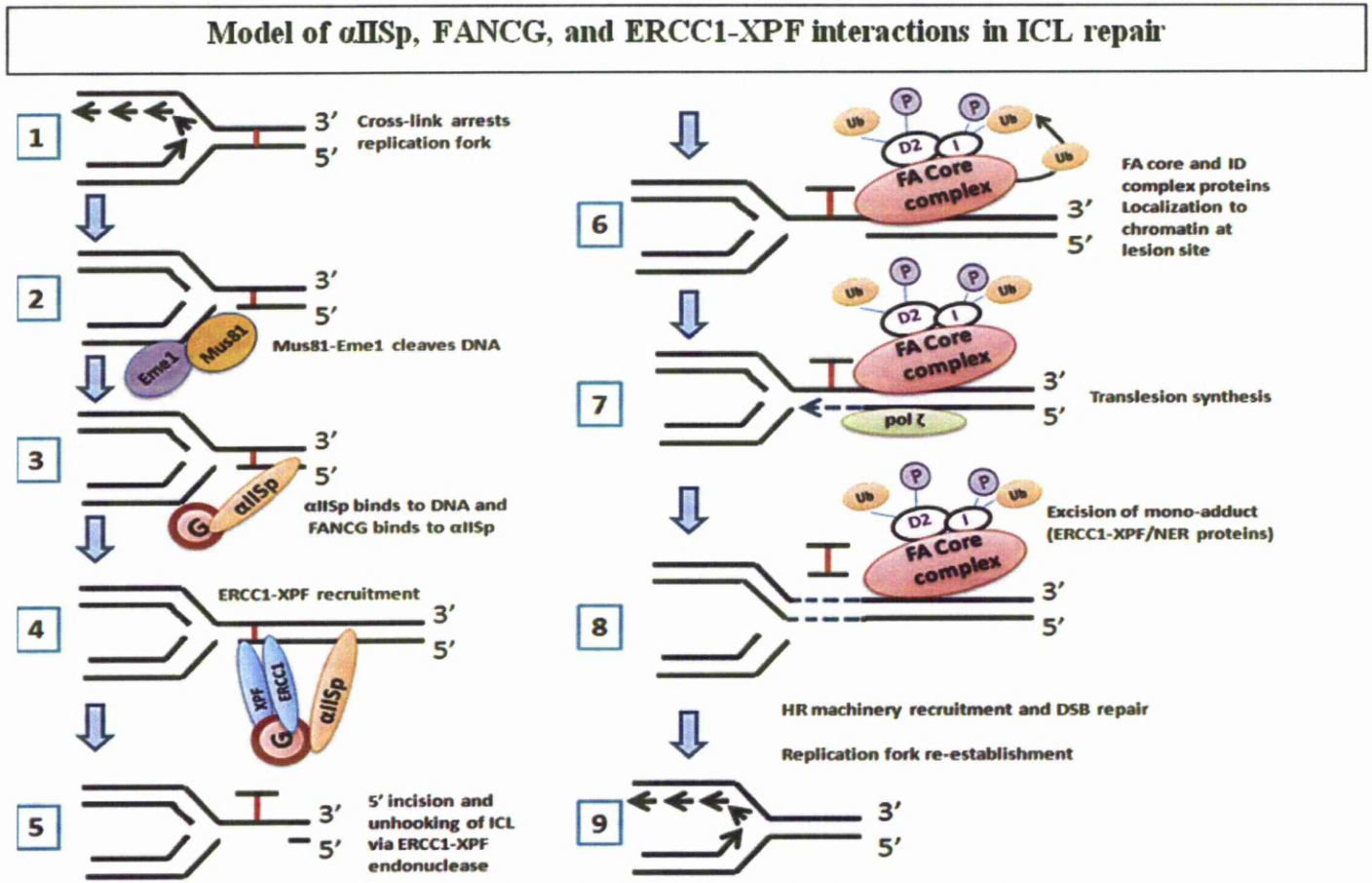

Figure (1.11): Diagram illustrating αIISp, FANCG, and ERCC1-XPF interactions in inter-strand cross-link repair at arrested replication forks. (1) ICL Arrests replication fork. (2) Mus81 and Eme1 incise DNA at the stalled replication fork on the 3′-side of the ICL resulting a DSB. (3) At the site of ICL; αIISp binds to the DNA and binds to FANCG via the SH3 domain of αIISp. (4) The αIISp bound FANCG recruits ERCC1-XPF to the ICL. (5) ERCC1-XPF incises the DNA strand on the 5′ side of the ICL, therefore unhooking the cross-link. (6) FA core and ID complex proteins Localization to chromatin at lesion site post FANCD2 mono-ubiquitination. (7) Polymerases such as pol ζ fill in the gap left post ICL unhooking via translesion synthesis. (8) Mono-adduct excision via nucleotide excision repair (NER) using ERCC1-XPF and other NER proteins. (9) DSB repair via homologous recombination (HR) machinery and replication fork re-established. Diagram based on models presented by **(Wang and Lambert -2010; Bhagwat et al., 2009; Thompson and Hinz, 2009)**

1.4.7.2 FANCG- tetratricopeptide repeat motifs (TPRs)

FANCG protein is thought to play a central role of complex assembly and/or stabilization (**Blom *et al*, 2004**) through the identification of seven tetratricopeptide repeat motifs (TPRs) **Fig. 1.12**. TPRs are degenerate 34-amino acid repeat motifs which function as scaffolds mediating protein–protein interactions, often found in multi-protein complexes. Studies showed that most FANCG TPRs are required for the interaction between FANCG and FANCA, confirming the structural importance of these TPR motifs **(Blom *et al*, 2004).** Further studies showed the requirement of these TPRs in the interaction of FANCG protein with other proteins that are involved in DNA damage repair (**Hussain *et al.*, 2006**). **Hussain *et al.* (2006)** illustrated by yeast-two-hybrid that the interaction of FANCG–FANCA, FANCG-XRCC3, BRCA2 N-terminal–FANCG and FANCG–FANCF required both TPR5 and TPR6. TPR1 and TPR2 were required also for FANCG–FANCF interaction. **Hussain *et al.*, (2006)** suggested that TPR1 and TPR2 most likely bind to BRCA2 C-terminus, thus recruiting XRCC3 and BRCA2 together in a protein complex. Co-immunoprecipitation experiments carried out later by **Wilson *et al.*, (2010)** demonstrated using Chinese hamster *FANCG* mutant NM3 cell lines, that mutating TPR motifs TPR1, TPR2, TPR5 and TPR6 at a conserved consensus residue compromised the FANCG *in vivo* binding activity leading to the inability to bring together the components or formulate either the FA core complex or the G- BRCA2 protein complex. These TPR *FANCG* mutants fail to interact with BRCA2, XRCC3, FANCA or FANCF proteins. **Wilson *et al.*, (2010)** also demonstrated that despite the fact that TPR7 (R563E)-mutated FANCG protein co-precipitating with FANCA, BRCA2 and XRCC3, a mutation at TPR7 (R563E) is associated with reduced FANCG -FANCF interaction and leads to sub-optimal interactions of FANCG in the core complex and the G-BRCA2 complex explaining the encountered MMC and phleomycin hypersensitivity in NM3

cells. **Wilson *et al.*, (2010)** data suggests the importance of FANCG role in mediating interactions linking proteins and hence the formulations of multi-protein complexes such as the FA core complex and the G- BRCA2 protein complex.

Wang and Lambert in 2010 showed by yeast two-hybrid experiments that FANCG had moderate affinity for XPF but great affinity for ERCC1. **Wang and Lambert, (2010)** determined using site-directed mutagenesis the requirement of TPRs 1, 3, 5, and 6 for binding of FANCG directly to ERCC1 which in turn binds to XPF via a different binding region from that of FANCG.

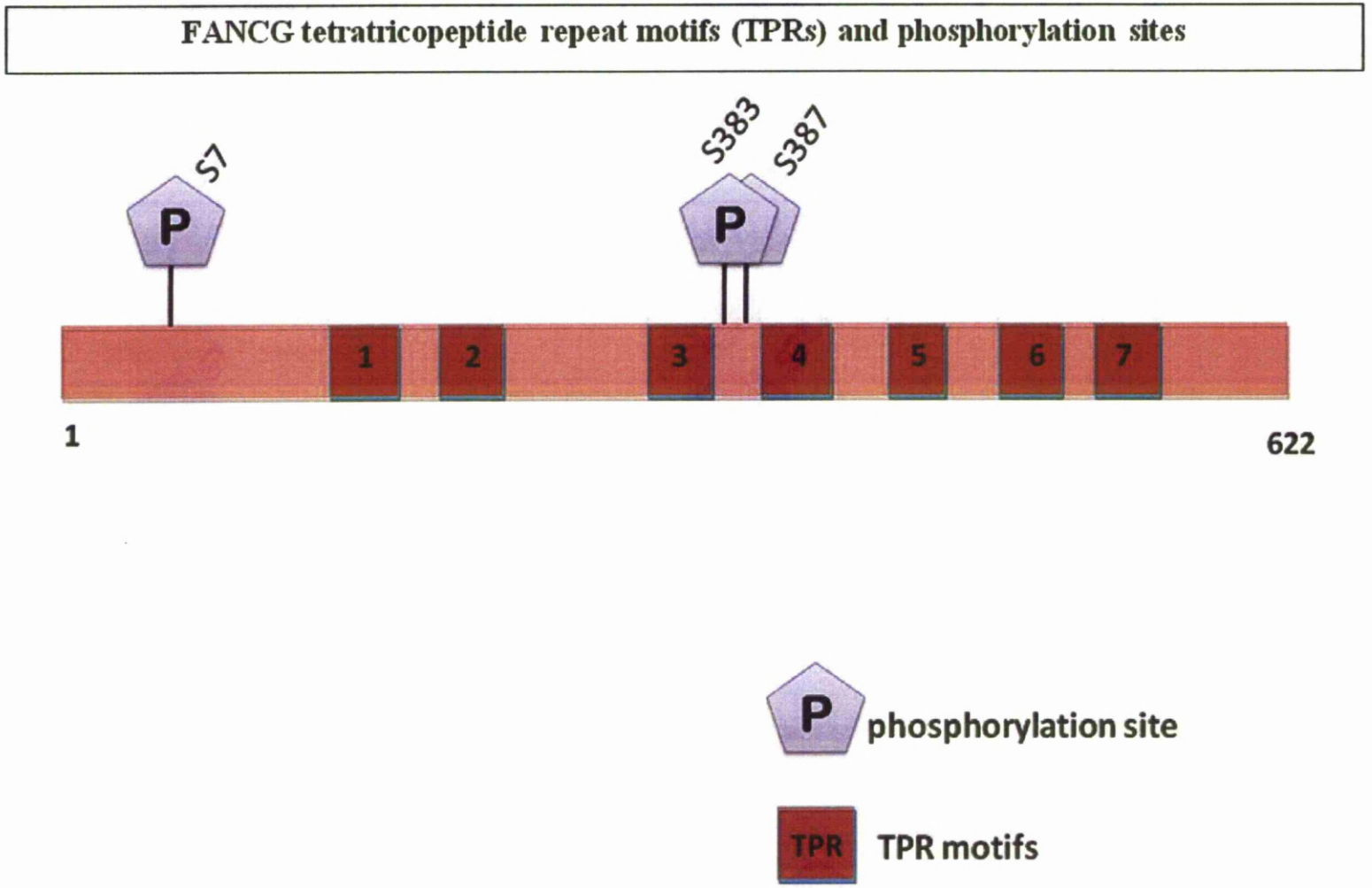

Figure (1.12): a diagram illustrating the seven tetratricopeptide repeat motifs (TPRs) motifs and the FANCG phosphorylation sites at serine positions 7,383 and 387 in full-length FANCG (residues 1-622). The specific phosphorylation event at the FANCG serine at position 7 is thought to be the trigger for the formation of the G-BRCA2 complex while serine 383 and serine 387 are mitotic phospho-sites.

1.4.7.3 FANCG protein is a phospho-protein, phosphorylated at mitosis at two amino acids, S383 and S387

FANCG is phosphorylated at mitosis **(Qiao *et al.*, 2001).** In 2004, through the use of mass spectrometry analysis, kinase motif analysis and PCR-directed in vitro mutagenesis, **Mi *et al.*, (2004)** mapped the phosphorylation sites of *FANCG* at mitosis at two amino acids; S383 and S387 and confirmed their findings through utilizing phospho-specific antibodies **Fig.1.12. Mi *et al.*, (2004)** evaluated the functional value of these phosphorylation sites and concluded that the phosphorylation of FANCG at mitosis is compromised in S383 and S387 mutant cells. Both mutants; S387A and S383A did not affect the binding ability of FANCG to FANCA **(Mi *et al.*, 2004)**, suggesting the FA core complex presence, despite the notion that, in the case of FANCG(S387A) diminished stability of or reduced affinity for FANCA may have occurred **(Garcia-Higuera *et al.*, 2000). Mi *et al.*, (2004)** demonstrated that S387A mutant stopped FANCG phosphorylation by cdc2 and showed how the phosphorylation of FANCG participates in regulating the FA pathway which is tightly controlled through a chain of phosphorylation steps that are essential to its function generally. These *FANCG* mitosis phospho-mutants caused the inability of FANCG to correct *FANCG* mutant cells in either hamster or human cells **(Mi *et al.*, 2004).** FANCG S383 and S387 amino acids are found in human, mouse and hamster. *FANCG* was first cloned from a CHO line hypersensitive to ionizing radiation and MMC **(de Winter *et al.*, 1998; Liu *et al.*, 1997)** therefore; the hamster would be an encouraging model to use in transgenic experiments for the expression of these *FANCG* mutants.

1.4.7.4 FANCG is a phospho-protein phosphorylated at serine 7

FANCG protein is phosphorylated **(Qiao *et al.*, 2004; Qiao *et al.*, 2001; Futaki *et al.*, 2001).** Using mass spectrometry analysis, **Qiao *et al.*,** in 2004 identified a phosphopeptide at FANCG amino acid serine 7 determining that FANCG phosphorylation occurs at phosphoamino acid serine 7 **Fig.1.12.** Via PCR-mediated site-directed *in vitro* mutagenesis, **Qiao *et al.*, (2004)** mutated serine 7 to alanine and employed CHO cells to observe that *FANCG* (S7A) partially correct *FANCG* mutant cells post MMC treatment and only wild-type *FANCG* cDNA fully corrected *FANG* mutant cells. **Qiao *et al.*, (2004)** concluded that FANCG phosphorylation at serine 7 is functionally essential in the FA pathway. Notably, the FANCG (S7A) mutant is itself stable, binds to and stabilizes both FANCA and FANCC proteins via their interaction. As FANCG (S7A) was shown to localize to chromatin at damaged DNA sites **(Qiao *et al.*, 2004),** the observed partial function in FANCG (S7A) could be explained by the stability in FANCG (S7A) interactions despite the fact that FANCG (S7A) like other FANCG mutant cells expresses increased nuclear bridges, especially post MMC treatment **(Qiao *et al.*, 2004).** Inter-nuclear bridging is an event observed in cells exhibiting genomic instability.

Accumulating evidence indicate the involvement of FANCD2, FANCC **(Niedzwiedz *et al.*, 2004),** FANCA **(Yang *et al.*, 2005),** FANCG and other FANC proteins in HRR **(Taniguchi and D'Andrea, 2006).** In 2003, 2004 and 2006, **Hussain *et al.*** demonstrated the occurrence of a direct interaction between the following pairs of proteins: FANCG–BRCA2; FANCD2–BRCA2; FANCG–XRCC3. XRCC3 gene encodes a member of the RecA/Rad51-related protein family, which is involved in HRR **(Thacker, 2005).** In 2008, **Wilson *et al.*** illustrated using human and hamster cells that for BRCA2-FANCD2 co-precipitation, FANCG protein is required unlike the other core complex protein. **Wilson *et al.*, (2008)** also illustrated the requirement of FANCG

serine 7 for the direct interaction of BRCA2–FANCD2 and for FANCG co-precipitation with BRCA2, XRCC3 and FANCD2. These findings in 2008 suggest an independent role of FANCG other than its role in the nuclear FA-core complex. It has been suggested that FANCG-(serine 7) phosphorylation is the signaling event required prior the formation of the G-BRCA2 complex which is suggested to be liable for promoting proficient HRR in DNA crosslink repair **(Wilson *et al.*, 2008)**. A role for G-BRCA2 complex in (HRR) is suggested by the **Wilson *et al.*,** finding, using DT40 chicken cells, in 2008 that *FANCG* and *XRCC3* are epistatic for sensitivity to DNA cross-linking agents.

1.4.8 Fanconi anaemia *FANCA*

1.4.8.1 FANCA protein

The *FANCA* gene has been mapped through linkage analysis to chromosome 16q24.3 **(Pronk *et al.*, 1995; Levran *et al.*, 1997).** About 60-66% of FA cases are caused by *FANCA* mutations **(Buchwald, 1995; Gschwend *et al.*, 1996; Faivre *et al.*, 2000).** Employing linkage and allelic association analysis, **Apostolou *et al.*, (1996)** have isolated *FANCA* gene which encodes a protein that has no striking homology to any other known proteins, and was classified as a new class of genes connected to DNA damage prevention and repair. Through mutation analysis, **Castella *et al.*, (2011)** revealed a wide *FANCA* mutational spectrum and argued that the lack of negative selection for biallelic *FANCA* mutations did not hinder human embryonic development which may partially explain the observed FANCA complementation group predominance among FA patients. The presence of high mutability or hyper-mutable region in *FANCA* may also explain *FANCA* mutations predominance **(Wijker *et al.*, 1999).** Mutations in some FA genes

have been associated with embryonic lethality, such as with *FANCD2* as illustrated by **van de Vrugt *et al.*, (2009)** using mouse model to study the effects of combined mutations in *FANCD2* and mismatch repair (*Mlh1*).

Magdalena *et al.*, (2005), Callén *et al.*, in 2005 and others **(Savino *et al.*, 2003; Tipping *et al.*, 2001; Tamary *et al.*, 2000; Tachibana *et al.*, 1999)** demonstrated that specific *FANCA* mutations may be more predominant in different populations, however *FANCA* gene is highly polymorphic **(Levran *et al.*, 2005a)**, with over a hundred mutations reported, without a specific allele in other populations being outstandingly high, ruling out mutation screening as a conclusive diagnostic method **(Savino *et al.*, 1997; Levran *et al.*, 1997).** Nevertheless, the majority of, FA patients may be diagnosed employing mutation screening for FANCD2 protein mono-ubiquitination as the absence of the mono-ubiquitinated FANCD2 isoform in immunoblots correlates with a positive diagnosis of FA **(Magdalena *et al.*, 2005; Ameziane *et al.*, 2008).**

In order to further characterize the role of FANCA in the repair process of both radiomimetic agent (phleomycin) induced damage (DNA strand breaks) and cross-linking agent (MMC) induced damage (DNA ICLs), the role of FANCA in maintaining chromosome stability in response to ICL was investigated using *FANCA* deficient cells. In doing so, the types of aberrations induced may give an insight into the role of the FANCA containing complex (FA-core complex) in these repair processes and the types of chromosome aberrations that may arise.

1.4.8.2 FANCA is part of the multi-subunit nuclear complex (FA-core complex)

FANCA and FANCC proteins interact forming a cytoplasmic and nuclear complex in normal cells. FANCA and FANCC cooperate in performing a nuclear function through multi-subunit nuclear complex formation that has been illustrated by **(Kupfer *et al.*, 1997; Naf *et al.*, 1998)** who suggested a function for this nuclear complex in chromosomal stability preservation. For binding between FANCA and FANCC to occur FANCG is required **(Garcia-Higuera *et al.*, 1999)** and FANCA, FANCC and FANCG are elements in this nuclear protein complex which is essential in preventing cellular and clinical phenotype seen in most FA complementation groups. The FANCA N-terminal nuclear localization signal is necessary for FANCC binding, FANCG binding, and for complementation of MMC sensitivity in FANCA lymphocytes, as well as for nuclear localization. **Garcia-Higuera *et al.*, (1999)** findings suggested that the binding of FANCC needed both FANCA/FANCG binding and the products of other FA genes, while FANCA/FANCG interaction was constitutive and probably direct without the need to FANCC or any FA genes products for regulation.

1.4.8.3 FANCA protein interactions with a wide range of other proteins

A wide range of proteins interact with FANCA protein such as those mentioned earlier to form the FA core complex FANCG **(Garcia-Higuera *et al.*, 1999; Otsuki, *et al.*, 2002; Taniguchi and D'Andrea, 2002)**, FANCC **(Garcia-Higuera *et al.*, 1999; de Winter *et al.*, 2000a; Otsuki, *et al.*, 2002; Taniguchi and D'Andrea, 2002; Meetei *et al.*, 2003)** , FANCF **(de Winter *et al.*, 2000a; Meetei *et al.*, 2003)**, FANCE **(Taniguchi and D'Andrea, 2002; Meetei *et al.*, 2003)**, BRCA1 **(Folias, *et al.*, 2002)**, or other proteins such as; SNX5 **(Otsuki, *et al.*, 1999)**,

nonerythroid α spectrin(α SpIIΣ) **(McMahon, *et al.*, 2001; Sridharan, *et al.*, 2003)**, IKK2 **(Otsuki, *et al.*, 2002)** and DNA repair endonuclease XPF encoded by (*ERCC4*) **(Sridharan, *et al.*, 2003)**.

1.4.8.4 FANCA involvement in other complexes

Despite evidence implicating the involvement of FA proteins in DNA interstrand cross-links (ICLs) repair, the exact mechanism through which they act is still undetermined **(Niedernhofer *et al.*, 2005; Thompson and Hinz, 2009).** Nevertheless, evidence suggests the interplay of a number of repair pathways such as; NER, HR, and translesion synthesis (TLS) in this repair process **(Dronkert and Kanaar, 2001; Zheng *et al.*, 2003; Thompson *et al.*, 2005; Hanada *et al.*, 2006)**. Studying inter-strand cross-links repair employing immunoprecipitation in 2003, **Sridharan, *et al.*, (2003)** indicated that XPF and FANCA co-immunoprecipitated with αSpIIS. Using anti-FANCA and anti-XPF immunoprecipitation confirmed that αSpIIS, XPF and FANCA bind to one another which led **Sridharan, *et al.*, (2003)** to propose a model for the involvement of FANCA with the structural protein nonerythroid α spectrin (αSpIIΣ) and XPF in the nucleus suggesting a common nuclear functional relationship between these proteins where αSpIIΣ (alpha SpII Sigma), acts as a scaffold recruiting and organizing repair proteins at sites of DNA damage. **Sridharan, *et al.*, (2003)** suggested that FANCA-XPF- αSpIIΣ complex has an important role in DNA inter-strand cross-links repair. The involvement of FANCG had also been suggested in this complex, repairing ICLs as early as 2001 as reported by **McMahon, *et al.* (2001)** in human cells post MMC exposure. In 2010, **Wang and Lambert (2010)** demonstrated that FANCG binds directly to ERCC1-XPF endonuclease which is involved in

ICLs unhooking as shown in **Fig.1.11** and argued that their findings did not support direct binding of FANCA to XPF.

1.4.8.5 FANCA protein is a phospho-protein phosphorylated at serine-1449

ATM (ataxia telangectasia mutated) and ATR (ATM and Rad3-related) regulate through phosphorylation the DNA damage response including the FA pathway which is controlled by ATR. Responding to exposed or naked ssDNA during replication stress, ATR is activated. However, it is not yet determined how ATR manages cell-cycle repair or cell-cycle arrest **(McGowan and Russell, 2004).** The mono-ubiquitination of FANCD2 post DNA damage is dependent on ATR **(Andreassen *et al.*, 2004)** and the phosphorylation FANCD2 is managed by both ATM **(Taniguchi *et al.*, 2002a)** and ATR **(Ho *et al.*, 2006).**

The FA pathway is a heavily phospho-regulated pathway that requires phosphorylation to a number of components of the FA pathway such as phospho-proteins; FANCG **(Qiao *et al.*, 2004; Mi *et al.*, 2004),** FANCM **(Meetei *et al.*, 2005),** FANCE **(Wang *et al.*, 2007b),** FANCD2 **(Taniguchi *et al.*, 2002a),** and FANCI **(Smogorzewska *et al.*, 2007),** FANCA **(Yamashita *et al.*, 1998; Kupfer *et al.*, 1999; Thomashevski *et al.*, 2004).** It was in 2009, when **Collins *et al.*,** identified the amino acid position where phospho-protein FANCA is phosphorylated by possibly, ATR which may act as a FANCA kinase phosphorylating its binding partner, ATR interacting protein (ATRIP) so as to relocate ATR–ATRIP complex **(Itakura *et al.*, 2004)** along with phosphorylated FANCA to chromatin **(Thomashevski *et al.*, 2004; Qiao *et al.*, 2001).** Unlike ATR, neither checkpoint kinase (CHK1) **(Jackson *et al.*, 2000),** nor ATM activation is required for FANCA phosphorylation post DNA damage.

Collins *et al.*, (2009) illustrated the functional significance of FANCA phosphorylation in connection to normal FANCD2 mono-ubiquitination as part of a functional FA pathway. Normal levels of mono-ubiquitinated FANCD2 were diminished when FANCA phosphorylation was defective (**Collins *et al.*, 2009**). Mass spectrometry was used to show that FANCA undergoes phosphorylation at serine amino acid in position 1449 and is localized to chromatin following induction of DNA damage, but not during S phase **(Qiao *et al.*, 2001).** This is unlike other post-translational modifications of FA proteins which take place usually during the S phase (**Collins *et al.*, 2009**).

Collins *et al.*, (2009) findings pointed out that mutating FANCA at serine 1449 to alanine (S1449A) did not compromise FANCG-FANCA association indicating the presence of at least partially intact FA core complex in the phospho-defective cell line FANC-S1449A and FANCA (S1449A) exhibited MMC hypersensitivity. Using a mono-ubiquitinated FANCD2 assay **Collins *et al.*, (2009)** found that post MMC exposure, *FANCA* (S1449A) cells illustrated reduced levels of mono-ubiquitinated FANCD2 compared to wild-type *FANCA* levels, confirming the functional importance of FANCA phosphorylation at S1449 in the FA pathway. This reduction in FANCD2-L was attributed to differences in the distribution of cells between the various cell cycle stages in the wild type and phospho-mutant cells, as FANCD2 is predominantly ubiquitinated in S-phase.

1.4.9 Fanconi anaemia *FANCD2*

1.4.9.1 FANCD2 protein

Extensively utilized for cell and molecular biology model of study are human fibroblasts immortalized by Simian Virus 40 (SV40) **(Wood *et al.*, 1987).** In 1996 through chemical mutagenesis with ethyl methane sulphonate (EMS) of SV40 transformed primary fibroblasts, **Jakobs *et al.* (1996).** reported the generation of four immortalized FA fibroblast cell lines (PD20i, PD220i, PD224i and PD259i) which maintained their FA phenotype **(Wood *et al.*, 1987)** and pointed out their potential to be used in cloning *FANCA, FANCD* genes and in functional studies as well as their practical use as the former (GM6914) isolated fibroblasts.

Timmers *et al.*, (2001) findings illustrates the heterogeneity of Fanconi anaemia group D which include FANCD1 and FANCD2 genes, thus, two distinct genes, BRCA2/FANCD1 and FANCD2 belong to the heterogeneous complementation group D up to this date. FANCD2, like other FA proteins has no recognized functional domains; however, FANCD2 is highly conserved in organisms such as *Drosophila*, *A. thaliana*, and *C. elegans* which can be easily employed for genetic study .While the lack of sequence homologs in FANCA, C, E, in non-vertebrates, made these genetic studies difficult to conduct. BRCA1 co-localizes and interacts with FANCD2 **(Garcia-Higuera *et al.*, 2001).** FANCD2 is part of at least two complexes in the FA pathway; the FA-ID complex comprising both FANCI and FANCD2 proteins and the G-BRCA2 complex comprising (FANCD2, FANCD1, FANCG and XRCC3) proteins. FANCD2 consists of many phosphorylation sites that are thought to control and regulate its activities. In 2009, **Knipscheer *et al.*, (2009)** illustrated FANCD2 resection function of the ends surrounding cross-links in DNA repair. **Huang and D'Andrea *et al.*, (2010),** demonstrated the occurrence of FANCD2-FAN1

binding. These facts, taken together make FANCD2 very interesting to study as it may further clarify the functional roles it plays along with the components of the FA pathway in DNA repair.

1.4.9.2 Functional and non functional FANCD2 isoforms

In 2005, **Montes de Oca *et al.***, identified two *FANCD2* isoforms; [isoform (a) and isoform (b)] producing a functional protein from (*FANCD2* -isoform b with 44 exons) and a non functional protein from (*FANCD2* -isoform (a) with 43 exons). The two FANCD2 proteins variants differ in their carboxy terminal 24 amino acids. The functional protein (*FANCD2*-44), depending on its mono-ubiquitination could be found either in its long form (FANCD2-L) or in its short non ubiquitinated form (FANCD2-S).

1.4.9.3 The mono-ubiquitination of FANCD2 and the FA-core complex

When DNA damage is encountered; FANCD2 is known to relocate to chromatin in a still poorly defined mechanism. Mono-ubiquitination of FANCD2 protein at (lysine 561) requires the FA-core complex, a conjugating enzyme (UBE2T) and FANCI. This FANCD2 mono-ubiquitination requires FANCE and FANCD2 proteins interaction **(Pace *et al.*, 2002; Taniguchi and D'Andrea, 2002)** and this mono-ubiquitination is needed to translocate (FANCD2-L) to chromatin fraction, and form nuclear foci consisting of proteins such as RAD51, BRCA1, FANCD1 **(Taniguchi *et al.*, 2002b)** and FANCI. Knowing the roles of RAD51, BRCA1 **(Moynahan *et al.*, 1999)** and FANCD1 **(Moynahan *et al.*, 2001a; Moynahan *et al.*, 2001b)** play in HRR; these foci are likely to be the sites of HRR in the nucleus. FA characteristic clinical and cellular features, including MMC hypersensitivity result from FA/BRCA pathway

disruption **(Auerbach *et al.*, 1989).** FANCD2 seem to have a critical role in the FA-pathway as the core complex activates FANCD2 by mono-ubiquitination and translocates it to chromatin where it is thought to be involved in supporting DNA damage bypass and repair through TLS and HRR pathways **(Thompson *et al.*, 2005; Wang, 2008).**

1.4.9.4 FANCD2 mono-ubiquitination requirement for functional complementation and foci formation

Garcia-Higuera *et al.*, (2001) utilized PD20, PD20-K561R and PD20-D2WT cells to demonstrate the functional significance of mono-ubiquitination at lysine 561 in regulating the activity of FANCD2 and in FANCD2 foci construction. PD20-D2WT expressed both forms of FANCD2 (FANCD2-S and FANCD2-L), producing FANCD2 foci at DNA lesion sites and restoring cellular resistance to agents MMC and IR, while PD20-K561R cells failed to mono-ubiquitinate FANCD2 expressing only (FANCD2-S), did not produce FANCD2 foci at DNA lesion sites and had cellular hypersensitivity to agents MMC and IR. FANCD2 deficient (PD20) cells failed to express FANCD2 completely. Based on these results **Garcia-Higuera *et al.*, (2001)** concluded the importance of mono-ubiquitination of FANCD2 at lysine 561 in the FA pathway through FANCD2 nuclear foci formation and accumulation.

1.4.9.5 FANCD2 phosphorylation by ATM and ATR and the role of CHK1 kinase

Post DNA damage FANCD2 phosphorylation can be carried by ATM **(Taniguchi *et al.*, 2002a; Ho *et al.*, 2006)** and ATR **(Pichierri and Rosselli, 2004 ; Andreassen *et al.*, 2004)** can phosphorylate FANCD2. FANCD2 serine 717 and threonine 691 are phosphorylated by ATR promoting FANCD2 mono-ubiquitenation **(Ho *et al.*, 2006).** In 2009, **Zhi *et al.*, (2009)** suggested that serine 331 is phosphorylated by the S-phase checkpoint kinase (CHK1) in order for FANCD2- BRCA2 interaction to occur to sustain cellular resistance to mitomycin C. CHK1 also phosphorylates FANCE threonine 346 and serine 374, an event which is vital for FANCD2 mono-ubiquitenation **(Wang *et al.*, 2007b).** **Zhi *et al.*, (2009)** also suggested that S331 can be efficiently phosphorylated independently from either the FA-core complex or FANCD2 mono-ubiquitination and is critical for FANCD2 mono-ubiquitenation and the restoration of normal cellular phenotype post MMC exposure.

1.4.9.6 Hypersensitivity of FANCD2 mutant cells PD20, PD20-K561R and PD20-S331A to cross linking agent MMC

Montes de Oca *et al.*, (2005) illustrated that PD20 and PD20-K561R had MMC hypersensitivity and explained that FANCD2 proteins produced by PD20 and PD20-K561R failed to become mono-ubiquitinated and thus failed to relocate and bind chromatin leading to the inability to correct the ICLs damage induced by MMC and restore the cellular phenotype to that observed in the corrected wild type. **Montes de Oca *et al.*, (2005)** findings suggest that FANCD2 binding to chromatin is regulated through FANCD2 mono-ubiquitination and predicts that the FANCD2

protein produced by FANCD2-isoform (b) has a carboxy terminus which may be important in DNA damage sensing or repair. Testing for *in vivo* phosphorylation of FANCD2 at S331 in 2009, **Zhi *et al.,*** used FANCD2-deficient PD20 cells and their derivative mutants (K561R, S331A) and suggested serine 331 to be a phosphorylation site needed for FANCD2- BRCA2 interaction to sustain cellular resistance to mitomycin C.

1.4.9.7 FANCD2 phosphorylation at S331 is critical for its *in vivo* interaction with FANCD1/BRCA2

Using yeast two-hybrid analysis in 2004, **Hussain *et al.,*** showed that FANCD2 did not interact with RAD51 also illustrated the binding of FANCD2 to a highly conserved carboxy terminus of FANCD1/BRCA2 and their coimmunoprecipitation in mammalian cells. **Wang *et al.,* (2004)** stressed the importance of the FANCD1/BRCA2 conserved carboxy terminus in the interaction between FANCD2 and FANCD1. **Wang *et al.,* (2004)** also showed how FANCD2 mono-ubiquitination followed by its translocation to chromatin promoted FANCD1/BRCA2 loading into chromatin complexes which seems to be essential for HRR. FANCD1 directly interacted with RAD51 and thus has a role in HRR **(Goodsell, 2005; Davies and Pellegrini, 2007; Esashi *et al.,* 2007).** In 2008, **Wilson *et al.,* (2008)** demonstrated that FANCD2 and FANCD1 interact *in vivo* in core complex mutants such as FANCC and FANCA. In 2004, **Hussain *et al.,*** illustrated that for FANCD2 and FANCD1 to interact a sequence of amino acid residues (248-359) encompassing S331 is vital. In 2009, **Zhi *et al.,* (2009)** illustrated through the use of immunoprecipitation-immunoblotting experiments employing FANCD2-mutant PD20 cells (PD20-FANCD2 deficient cells, PD20 phospho-mutant (S331A; S331D) cells that S331 phosphorylation is critical for FANCD2 and FANCD1 interaction. FANCD2 with BRCA2

interaction was absent only in both cell lines PD20 and PD20-S331A while present in corrected wild type and PD20-S331D cells. FANCD2 isoforms (long and short) interact with FANCD1 in corrected wild-type FANCD2 cells (**Wilson *et al.*, 2008**) and in FANCD2-S331D but not in FANCD2-S331A suggesting a critical role of S331 phosphorylation by CHK1 kinase in the interaction between FANCD2 and FANCD1 (**Zhi *et al.*, 2009**). The point mutation in S331A compromised both the FANCD2 mono-ubiquitination and the Fanconi anaemia pathway leading to the observed MMC hypersensitivity in FANCD2-deficient PD20 cells (**Zhi *et al.*, 2009**). **Zhi *et al.*, (2009)**, suggested that FANCD2 mono-ubiquitination is independent of FANCD1 and also suggested the simultaneous requirement of S331 phosphorylation for FANCD2-FANCD1 interaction and FANCD2 mono-ubiquitination promotion.

Zhi *et al.*, (2009) illustrated that unlike PD20-S331A, phospho-mimetic mutation S331D (PD20-S331D) where aspartic acid replaces serine in position 331 did not affect FANCD2 mono-ubiquitination or the MMC cellular resistance and predicted that the failure of PD20-S331A cells to mono-ubiquitinate FANCD2 is possibly due to substantial structural modifications rather than nuclear localization failure as supported by previous fluorescence microscopy imagery showing the co-localization of mutant FANCD2 and wild type FANCD2 at the nuclear foci (**Marte, 2002**).

1.4.9.8 FANCD2 forms with FANCD1/BRCA2, FANCG and XRCC3 the G-BRCA2 complex

FANCD2 and FANCD1 are two components of the (G-BRCA2) protein complex which also encloses FANCG and XRCC3 (RAD51 paralogue) **(Hussain *et al.*, 2006; Wilson *et al.*, 2008).** **Wilson *et al.*, (2008)** illustrated using mammalian cells that FANCG (S7) phosphorylation is also critical for FANCD2 and FANCD1/BRCA2 interaction. The mechanistic coordination between the FANCG-(S7) and the FANCD20 (S331A) is not clear yet.

1.4.9.9 FANCD2 and FANCI form the FANCD2-FANCI complex

Comprising the heart of the FA pathway and ICL repair is the 296 kD FANCI-FANCD2 (ID) complex **(Joo *et al.*, 2011)** whose activation occurs post DNA damage and is controlled via ATR phosphorylation **(Moldovan and D'Andrea, 2009)** and mono-ubiquitination via the ubiquitine ligase activity of the FA core complex **(Timmers *et al.*, 2001; Meetei *et al.*, 2003; Dorsman *et al.*, 2007; Moldovan and D'Andrea, 2009).** FANCI interacts with FANCD2 composing the ID complex **(Smogorzewska *et al.*, 2007).** Post replication fork stress or DNA damage, FANCD2 and FANCI are independently mono-ubiquitinated and translocated to nuclear foci **(Sims *et al.*, 2007)** at DNA damage sites organizing DNA repair through nucleolytic alteration of the DNA near by the DNA lesion followed by bypass synthesis through a still unclear mechanism.

In 2009, **Knipscheer *et al.*,** illustrated FANCD2 resection function of the ends surrounding cross-links in DNA repair. **Huang and D'Andrea *et al.*, (2010),** demonstrated the occurrence of FANCD2-FAN1binding. FAN1 is involved in cleaving branched and nicked structures due to its intrinsic 5′-3′ exonuclease and endonuclease activity **(Kratz *et al.*, 2010; MacKay *et al.*, 2010).**

Smogorzewska *et al.*, (2010) proposed that the ubiquitinated ID complex binds (FAN1) engaging this repair nuclease (FAN1) to sites of DNA crosslink lesions. In addition to (FAN1), **Smogorzewska *et al.*, (2010)** also points out the involvement of another essential nuclease (EXDL2) in the crosslink repair. FANCD2 and FANCI comprise 1451 and 1328 amino acids, respectively. A homology region of about 150–amino acids is shared between FANCD2 and FANCI around their mono-ubiquitination sites **(Joo *et al.*, 2011).**

1.4.9.10 FANCD2 and its roles in sustaining chromosomal integrity

In Fanconi anaemia cells, elevation of chromosome breakage **(Porfirio, *et al.*, 1991; Fundia *et al.*, 1994; Howlett *et al.*, 2005)** and micro-nucleation **(Willingale-Theune *et al.*, 1989; Maluf and Erdtmann, 2001)** have been reported. **Fundia *et al.*, (1994)** findings do not agree with views that adopt randomness in chromosome breakage and suggest very strongly that the occurrence of break points at explicit chromosome points is connected with site fragility and breakpoints related to acute myeloid leukemia. Thus providing supportive explanation of the observed elevated predisposition to leukemia, and also sustaining the hypothesis that carcinogenesis results from the loss of chromosomal integrity or stability.

Valeria and Filippo, (2009) examined FANCD2 localization during cellular mitosis in order to explore a probable function of FANCD2 in chromosomal segregation. **Valeria and Filippo, (2009)** utilized FANC-deficient cells including PD20 (FANCD2 deficient) cells along with the corrected wild type and FANC-proficient human fibroblasts. At anaphase-telophase stage the occurrence of unequal chromosome partitioning, lagging chromosomes, lagging fragments, anaphase bridges, was considerably elevated in FANC-deficient cells compared to both the wild type and to the FANC-proficient human fibroblasts as noted by **Valeria and Filippo, (2009),**

suggesting that chromosome segregation is severely affected in Fanconi anaemia cells. **Valeria and Filippo, (2009)** suggested that although the mitotic progression in Fanconi anaemia cells was not hindered, elevation in chromosomal aberrations resulting from segregation defects implicates the involvement of FANC pathway in maintaining chromosome stability. This is done through chromosome instability and aneuploidy prevention throughout mitosis, especially post replication stress. This role is in addition to the role that FA pathway plays in sustaining chromosome stability through its DNA damage response **(Wang, 2007a).**

In 2009, **Valeria and Filippo** found that FANCD2 targets discrete spots on mitotic chromosomes and hypothesized that these sites may be replication fork stalling sites. **Chan *et al.*, (2009)** and **Valeria and Filippo, (2009),** have shown that in response to replicative stress, FANCD2 protein translocates to chromosomes during mitosis and is exclusively found at aphidicolin (APH)-induced chromatid gaps and breaks, which indicates its targeting to chromatid fragile sites. **(Howlett *et al.*, (2005)** findings are consistent with and support findings of **Chan *et al.*, (2009)** and **Valeria and Filippo, (2009). Chan *et al.*, (2009)** suggested that the unresolved replication figures are a more critical source of bridges compared to end-to-end fusions between chromosomes and suggested that these observed aberrant bridges lead to non-programmed DNA breakage that consequently brings about the illegitimate DNA repair resulting in the observed chromosomal and chromatid exchanges.

1.5 Model systems to study Fanconi anaemia

1.5.1 Model systems utilized in FA research

Various model systems are utilized in the research of FA. The model systems include cell lines that have been derived from the transparent roundworm called nematode, *Caenorhabditis elegans* **(Collis *et al.*, 2006; Youds *et al.*, 2009),** fruit fly, *Drosophila melanogaster* **(Marek and Bale, 2006),** zebrafish, *Danio rerio* **(Titus *et al.*, 2006; Titus *et al.*, 2009),** chicken, *Gallus gallus* **(Matsushita *et al.*, 2005; Takata *et al.*, 2007),** the African clawed frog , *Xenopus lavis* **(Stone *et al.*, 2007),** mouse, *Mus musculus* **(Houghtaling *et al.*, 2003)** and Chinese hamster, *Cricetulus griseus* **(Busch *et al.*, 1996,; Lamerdin *et al.*, 2004; Tebbs *et al.*, 2005; Wilson *et al.*, 2001).**

1.5.2 Use of Chinese hamster cell mutants to study FA and FANCG

1.5.2.1 The use of hamster model in cloning homologous recombination repair genes

The availability of naturally occurring cell mutants or mutants isolated in the laboratory through chemical mutagenesis has bridged the progress made in DNA damage response and DNA repair understanding **(Hickson and Harris, 1988).** Chinese hamster mutant cell lines that are hypersensitive to clastogens have become primary models utilized in genetic analysis of DNA repair pathways and recombination processes **(Thompson, 1998; Zdzienicka, 1996; Lee *et al.*, 1995).**

The molecular cloning of human repair *ERCC* (*E*xcision *R*epair *C*ross *C*omplementing) or *XRCC* (*X*-ray *R*epair *C*ross *C*omplementing) genes that are involved in maintaining genome stability has been made possible through the use of (CH) mutants that are hypersensitive to UV or ionizing radiation. These genes which are required for nucleotide excision repair (NER) include *ERCC2/XPD, ERCC3/XPB, ERCC4/XPF* and *ERCC5/XP* **(Thompson, 1998).** Using CH mutants termed *irs1 and irs1SF*; other genes which are involved in homologous recombination repair such as *XRCC2 and XRCC3*, RAD51-family members were cloned **(Tebbs *et al.*, 1995; Liu *et al.*, 1998).**

1.5.2.2 Use of a hamster model to express FANCG mutations

Human *FANCG* and *XRCC9* proved to be the same gene **(de Winter *et al.*, 1998).** The human *FANCG/XRCC9* gene was first cloned by genetic complementation of the MMC sensitivity of CHO mutant UV40 **(Liu *et al.*, 1997).** UV40 mutant cells exhibits extreme sensitivity to mitomycin C (11 fold) and is about 2-fold sensitive to ionizing radiations and UV **(Lamerdin *et al.*, 2004; Busch *et al.*, 1996).** By introducing CHO *FANCG* gene into mutant NM3 it had been illustrated that hamster *FANCG* fully corrects the 10- fold hypersensitivity to MMC **(Lamerdin *et al.*, 2004; Wilson *et al.*, 2001)**. Based on a 7-fold hypersensitivity to the crosslinking agent nitrogen mustard, **Meyn *et al.*** isolated NM3 from the CHO cell line AA8 **(Meyn *et al.*, 1991).** NM3 is hypersensitive to MMC and is around 3-fold hypersensitive to UV and gamma-rays **(Meyn *et al.*, 1991).** NM3 and UV40 have been allocated to the same complementation group due to similar but not identical patterns of hypersensitivity to various DNA damaging agents. For example: NM3 and UV40 are both about 3-fold hypersensitive to ionizing radiation and UV and

are both hypersensitive to MMC, nevertheless, NM3 displays normal levels of spontaneous sister chromatid exchanges (SCEs) **(Wilson *et al.*, 2001)** compared to (3- to 4-fold) of SCEs of UV40 cells **(Meyn *et al.*, 1991; Busch *et al.*, 1996).**

FANCG was originally cloned from a Chinese Hamster Ovary cell line hypersensitive to MMC and ionizing radiation, **(Liu *et al.*, 1997; de Winter *et al.*, 1998).** Hence the preference to use the hamster model in performing these transgenic tests to express FANCG mutations. Fibroblast Chinese Hamster cell lines readily form colonies, thus making clonal forming assays such as clonal survival assays or clonal HRR assays suitable to use. The findings of the clonal forming assays utilized were added to those of growth inhibition assays which are also capable of determining the hypersensitivity of the selected cell lines. Human lymphoblastic *FANCG* cell lines were avoided as it was unfeasible to implement the clonal forming assays used on slow growing, non-clonal forming lymphoblastic cells. In Chapters 3 and 4, *FANCG* Chinese hamster ovary (CHO) mutant NM3 cell lines were utilized.

1.5.3 Use of human FANCA fibroblasts (GM6914) in FA research

1.5.3.1 Isolation of GM6914 cells and assigning them to FA complementation group A

Extensively utilized for cell and molecular biology model of study are human fibroblasts immortalized by Simian Virus 40 (SV40) **(Wood *et al.*, 1987). Duckworth-Rysiecki *et al.*, (1986)** characterized and isolated a SV40-transformed human fibroblast cell line (GM6914) derived from an FA patient in 1986. Similar to FA cells, GM6914 cells expressed cellular hypersensitivity to MMC and elevated chromosomal instability. The growth rate of both

GM6914 and SV40 human fibroblasts is similar and both cell lines are immortalized human fibroblasts. GM6914 cells are classed in to FA complementation group A, according to complementation analysis studies performed by **Duckworth-Rysiecki *et al.*, (1986)** utilizing lymphoblasts derived from two affected brothers of the FA patient from which GM6914 cells were obtained.

1.5.3.2 FANCA protein is found in both the cytoplasm and the nucleus

In 1997, GM6914 cells were employed by **Kupfer *et al.*, (1997)** after correcting with retroviral FAA cDNA to test for FANCA and FANCC interactions. **Kupfer *et al.*, (1997)** found that protein binding correlated with the functional activity of FANCA and FANCC, as mutant FANCC protein, (Leucine 554 to Proline), did not bind FANCA protein. **Kupfer *et al.* (1997)** concluded that FANCA interacts with FANCC forming a FAA-FAC complex. Taken together, that both proteins FANCA and FANCC are abundant in the cytoplasm, and FAA-FAC complex found in similar levels in cytoplasm and nucleus, this leads to the suggestion that this FAA-FAC complex has a nuclear function.

1.5.3.3 FANCA protein is a FA-core complex component

FANCA protein is part of the multi-protein nuclear FA core complex which also include proteins FANCC, FANCE, FANCF, FANCG, FANCL (reviewed by **Soulier *et al.*, 2005)** and FANCM **(Meetei *et al.*, 2005).** This nuclear FA core complex is required to activate FANCD2 protein mono-ubiquitination during the S phase of the cell cycle and post exposure to DNA cross-linking

agents **(Garcia-Higuera *et al.*, 2001)**. **Meetei *et al.*** suggested in 2003 that FANCL is likely to be the crucial catalytic subunit in the FA core complex and considered the other components functioning as regulatory subunits.

1.5.3.4 FANCA mutant cells exhibit cellular hypersensitivity to MMC

In 1999, **Kupfer *et al.*,** employed GM6914 fibroblasts to test the effect of a homozygous mutation in the *FANCA* gene (3329A>C) on FANCA function, using retroviral-mediated transduction to express FANCA(H1110P) and wild type FANCA protein. Unlike wild-type FANCA, FANCA (H1110P) did not correct cellular hypersensitivity the mitomycin C, nor did it succeed in nuclear accumulation in the transduced cells, emphasizing the impact of the phosphorylation of FANCA, its binding to FANCC, and the FANCA /FANCC nuclear accumulation on the FA pathway.

Utilizing GM6914 fibroblasts in response to DNA damage, **Adachi *et al.*, (2002)** findings indicate that no activation of FA-pathway occurred in FANCA-null cells, while altered FANCA proteins activated the FA pathway to variable degrees, as assessed by FANCD2 mono-ubiquitination. **Adachi *et al.*, (2002)** used various FANCA point-mutations (19 mutations) some of which were disease-associated and other mutations were mis-sense variants presenting wild type (WT-FANCA) behaviour. **Adachi *et al.*, (2002)** suggested that the various FANCA point-mutations affected the tertiary structure of FANCA which leads to compromised FANCA proteins phosphorylation and interaction with FANCC and FANCF affecting FANCA interaction with other proteins. **Adachi *et al.*, (2002)** concluded that various FANCA patient-derived mutants have variable degrees of influence on FANCA functions.

1.5.3.5 Reported cytogenetic profile of GM6914 cell line

GM6914 cells show elevated rates of spontaneous CA and are hypersensitive to DNA-cross-linking agents such as MMC or nitrogen mustard **(Duckworth-Rysiecki *et al.*, 1986).** Characteristically similar to all FA cell types examined, elevated rates of CA are observed in GM6914 cells post exposure to cross linking agents such as MMC compared to spontaneous levels of aberrations in control cells **(Sasaki and Tonomura, 1973; Weksberg *et al.*, 1979; Cervenka *et al.*, 1981; Duckworth-Rysiecki *et al.*, 1984).**

1.5.4 Use of human FANCD2 fibroblasts (PD20) in FA research

1.5.4.1 Pin pointing the FANCD2 gene using PD20 cells and mutation analysis

Employing microcell-mediated chromosome transfer into PD20 cell line **(Whitney *et al.*, 1995)** reported that the gene mutated in PD20 is located in the short arm (p) of chromosome number 3. The candidate region for the FANCD2 gene was narrowed down to about 200 kb via further detailed analysis to five overlapping micro-deletions surrounding the locus in five microcell hybrids **(Hejna *et al.*, 2000).** Three candidate expressed sequence tags (ESTs) were identified as present in or near FANCD2 critical region **(Hejna *et al.*, 2000).**

Full-length cDNAs were obtained by employing 5′ and 3′ rapid amplification of cDNA ends (RACE), then followed by genes sequencing and expression pattern analysis via Northern blot. Like earlier cloned FA genes, EST (SGC34603) had reduced ubiquitous mRNA expression levels **(de Winter *et al.*, 1998; Timmers *et al.*, 2001).**

The open reading frames for EST TIGR-A004X28, AA609512, and SGC34603 were in length (234, 531, and 4413 bp respectively) **Timmers *et al.*, (2001)**. Through sequencing cloned RT–PCR products, the three were analyzed to detect mutations in PD20 cells. SGC34603 had five sequence changes, while TIGR-A004X28 and AA609512 had no sequence changes **Timmers *et al.*, (2001)**. Further analysis to the five sequence changes revealed three alleles to be polymorphic variations; while the other two represented maternally and paternally inherited mutations. In determining SGC34603 gene structure **Timmers *et al.*, (2001)** discovered forty-four exons with exon 2 enclosing the start codon. **Timmers *et al.*, (2001)** findings led them to suggest that SGC34603 is the FANCD2 gene.

1.5.4.2 PD20 cells are *FANCD2* deficient and *FANCD2* cDNA complemented functionally *FANCD2* deficient cells

Using immunoblotting, survival assays and cytogenetic analysis, **Timmers *et al.*, (2001)** findings illustrated that the cloned FANCD2 cDNA encoded the non-mono-ubiquitinated form of FANCD2 protein, which was post translationally modified into the mono-ubiquitinated FANCD2 protein correcting the MMC hypersensitivity of PD20-FANCD2 deficient cells. **Timmers *et al.*, (2001)** using a specific (SGC34603) antibody in Western blots confirmed SGC34603 gene as *FANCD2* and illustrated the expression of both mono-ubiquitinated and non-mono-ubiquitinated FANCD2 in wild-type cells and the diminished FANCD2 levels in all PD20 cells.

1.6 Aims

- To characterize the role of the FANCG protein and its two phosphorylation sites, located at serine-7 and serine-387, in the repair of inter-cross links (ICLs) and the homologous recombination repair (HRR) of double-strand breaks. *FANCG* mutant cell lines have been utilized to investigate the precise roles of the FANCG protein in the FA-BRCA pathway and specifically in ICL repair and HRR.
- To characterize the function of the G-BRCA2 protein complex (comprising BRCA2/FANCD1-FANCD2-FANCG-XRCC3) in homologous recombination repair of DSB that either: 1) arise indirectly in ICL repair or 2) are directly induced by a radio-mimetic agent (phleomycin). Mitomycin C was used to induce interstrand cross-links and phleomycin was used to induce DNA strand breaks.
- In order to achieve these aims I characterized mammalian *FANCG, FANCA* and *FANCD2* mutant cell lines by establishing their cellular and cytogenetic responses to the cross-linking agent MMC and radiomimetic strand-breaker phleomycin. A plasmid-based reporter assay was used to measure homologous recombination repair (HRR) in selected cell lines.

Chapter-2

Material and methods

2.1 Materials and methods

2.1.1 Materials

2.1.1.1 Cell lines used

2.1.1.1.1 Chinese hamster (CH) cell lines (*FANCG* lines)

AA8: Wild type (parental) Chinese hamster ovary fibroblast cell line **(Thompson *et al.*, 1980; Meyn *et al.*, 1991; Wilson *et al.*, 2001)**

NM3: is an AA8 derivative *fancg* mutant fibroblastic cell line which is sensitive to nitrogen mustard. It contains a point mutation which leads to a premature stop codon in exon 3 resulting in a highly unstable truncated protein **(Meyn *et al.*, 1991; Wilson *et al.*, 2001; Lamerdin *et al.*, 2004).**

NM3-(gWT): Human full length *fancg* cDNA in the pCEP4 hygromycin resistant vector was transduced into NM3 and a cell line established.

NM3-TPR6: Human *fancg* cDNA mutated at TPR6:G521Q in the pCEP4 hygromycin resistant vector was transduced into NM3 and a cell line established.

NM3 SCneo2 pMMP-gWT: NM3 cell line transfected with the SCneo2 construct and transduced with pMMP vector containing the human full length *fancg* cDNA **(Dr. N.J. Jones and Dr. J.B. Wilson personal communication).** It will be referred to as **NM3–gWT**

NM3 SCneo2 pMMP-VO: NM3 cell line transfected with the SCneo2 construct and transduced with pMMP vector. It will be referred to as **NM3–VO (Dr. N.J. Jones and Dr. J.B. Wilson personal communication).**

NM3 SCneo2 pMMP-S7A: NM3 cell line transfected with the SCneo2 construct and transduced with pMMP vector containing the human *fancg* cDNA mutated at phosphorylation site (S7) serine to alanine substitution. It will be referred to as **NM3–S7A.**

NM3 SCneo2 pMMP-S387A: NM3 cell line transfected with the SCneo2 construct and transduced with pMMP vector containing the human *fancg* cDNA mutated at phosphorylation site (S387) serine to alanine substitution. It will be referred to as **NM3–S387A.**

2.1.1.1.2 Human fibroblast FA cell lines

2.1.1.1.2.1 FANCA cell lines

GM6914 (FA-A) SCneo: Immortalized FA-A complementation group human fibroblast cell line transfected with the SCneo construct and transduced with pMMP vector **(Duckworth-Rysiecki *et al.*, 1986; Collins *et al.*, 2009).**

GM6914 + FANCA SCneo: Immortalized FA-A complementation group human fibroblast cell line transfected with the SCneo construct and transduced with full length human FANCA cDNA tagged with Flag in the pMMP vector **(Collins *et al.*, 2009).**

GM6914-S1449A SCneo: is a *FANCA* mutant immortalized human fibroblast cell line transfected with the SCneo construct and transduced with human FANCA cDNA that has been mutated via site-directed mutagenesis in *FANCA* at serine 1449 to alanine (S1449A) **(Collins *et al.*, 2009).**

2.1.1.1.2.2 FANCD2 cell lines

PD20: is a FA-D2 complementation group human fibroblast cell line, (FANCD2-deficient) **(Whitney *et al.*, 1995; Jakobs *et al.*, 1996; Zhi *et al.*, 2009).**

PD20 SCneo: is a PD20 cell line transfected with the SCneo construct and transduced with an empty vector. The cell line produced at the Jones' laboratory **(Dr. N.J. Jones and Dr. J.B. Wilson personal communication).** It will be referred to as **PD20.**

PD20 K561R SCneo: is a PD20 cell line transfected with the SCneo construct, then retrovirally transduced with pMMP vector containing site-directed mutagenesis mutated human cDNA of FANCD2 so that arginine replaces lysine in position 561 produced at the Jones' laboratory **(Garcia-Higuera *et al.*, 2001).** It will be referred to as **PD20-K561R.**

PD20 S331D SCneo: is a PD20 cell line transfected with the SCneo construct, then retrovirally transduced with pMMP vector containing site-directed mutagenesis mutated human cDNA of

FANCD2 so that aspartic acid replaces serine in position 331 and tagged with FLAG produced at the Jones' laboratory **(Zhi *et al.*, 2009; Dr. Gary M Kupfer personal communication).** It will be referred to as **PD20-S331D.**

PD20 S331A SCneo: is a PD20 cell line transfected with the SCneo construct, then retrovirally transduced with pMMP vector containing site-directed mutagenesis mutated human cDNA of FANCD2 so that alanine replaces serine in position 331 **(Zhi *et al.*, 2009; Dr. Gary M Kupfer personal communication).** It will be referred to as **PD20-S331A.**

PD20 + FANCD2 SCneo: is a PD20 cell line transfected with the SCneo construct, then retrovirally transduced with pMMP vector containing FANCD2 full length human cDNA **(Zhi *et al.*, 2009; Dr. Gary M Kupfer personal communication).** It will be referred to as **PD20-D2WT.**

PD20 -3-15 SCneo: is a PD20 cell line transfected with the SCneo construct, then corrected by microcell mediated transfer of human chromosome fragment enclosing FANCD2 gene produced at the Jones' laboratory **(Whitney *et al.*, 1995; Naim and Rosselli, 2009).** It will be referred to as **PD20-315.**

Cell lines (GM6914, PD20 S331A, PD20 S331D, and PD20 + FANCD2) were a kind gift from Dr. Gary Kupfer, Yale University School of Medicine, USA. Cell lines (PD20, PD20 K561R and PD20 -3-15) were a kind gift from Dr. Alan D'Andrea, Dana-Farber Cancer Institute, Harvard Medical School, USA.

2.1.1.2 Vectors for HRR assay

SCneo: is a direct recombination reporter substrate construct SCneo inserted into pUC9 plasmid **(Johnson *et al.*, 1999)** as shown in **Fig. 2.1**.

2.1.1.3 Antibodies for Western blotting

2.1.1.3.1 Primary antibodies

Antibody to FANCG (H: 83-622, R#2924-2944) (anti-FANCG) is a kind gift from Dr. Maureen Hoatlin of Oregon Health and Science University, Portland **(Waisfisz *et al.*, 1999).**

Beta (β)-actin (ab6276) (anti-β-actin) were obtained from Abcam Limited, UK.

2.1.1.3.2 Secondary antibodies

Anti-rabbit and anti-mouse hourse radish peroxide (HRP) labeled antibodies were obtained from GE Health-care (RPN2108), UK.

2.1.1.4 Chemical agents used

2.1.1.4.1 Mitomycin C (MMC)

Mitomycin C (MMC) (Sigma-Aldrich, UK) was prepared to obtain a 1mM stock solution by dissolving 2mg of MMC powder into 5.89 ml of Hanks balanced salt solution without calcium and magnesium and with phenol red (HBSS) (Lonza, Belgium). The preparation was filter sterilized and stored at -18°C into 130 µl aliquots. During preparation direct light was avoided as MMC is light sensitive.

2.1.1.4.2 Phleomycin

Phleomycin (Sigma-Aldrich, UK) was prepared to obtain a 1mg/ml stock solution by dissolving 5mg of Phleomycin powder into 5 ml of PCR distilled water (BDH, UK). The preparation was filter sterilized and stored at -18°C into 130 µl aliquots.

2.1.2 Methods

2.1.2.1 Cell culture and maintenance

CH and human fibroblast cell lines were cultured and sub-cultured routinely and maintained in a state of exponential growing phase utilizing Dulbecco's Modified Eagle's medium with Ultra glutamine and 4.5 g/L glucose (Lonza, Belgium), supplemented with 10% (v/v) foetal calf serum (Autogene Bioclear, UK), 100 µl/ml penicillin and streptomycin sulphate (Lonza, Belgium) and 1% (v/v) non-essential amino acids (100X concentration) (Lonza, Belgium) **(Wilson *et al.*, 2001).**

2.1.2.2 Cell storage

Cell lines stocks have been stored in liquid nitrogen at -196°C. To safely freeze down cell lines cryovials containing about (1×10^6 cells) re-suspended in 1ml of complete medium containing 10% DMSO (Sigma-Aldrich, UK) was placed in a isopropanol freezing-down vessel in order to gradually reduce the cellular temperature overnight at the -80°C freezer before transfer to liquid nitrogen.

2.1.2.3 Growing cell lines from frozen stocks

Cell lines (in cryovials) retrieved from liquid nitrogen have been thawed before transferring and diluting into 10ml culture medium followed by centrifugation at 2000 rpm for five minutes at room temperature. Then the cell pellets were re-suspended in 5ml of complete medium and transferred into a 75 cm^2 culture flask (Greiner bio-one, Germany) containing 10ml culture medium followed by incubation at 37°C, 5% and CO_2 until approaching 70% confluence.

2.1.2.4 Cell passage

In order to obtain cells growing at the exponential growing phase to be utilized, cells have been passaged only when they approached confluence (about 70% confluence). Cell passage was carried out by removing growth medium from the culture flask followed by washing the cells with HBSS. Then the cells were detached from the flask's surface by the addition of a trypsin solution [0.12% (v/v) trypsin with 0.008% (w/v) ethylene diaminotetraacetic acid (EDTA) (Lonza, Belgium)].

2.1.2.5 Fibroblast cell line growth inhibition assay

$1x10^6$ cells in culture medium suspension were seeded in to $75cm^2$ culture flasks and then the appropriate clastogen doses were added to culture flasks before incubating them into 37°C, and

5% CO_2. The incubation period was until the untreated flasks (controls) approached 70% cellular confluence. Then, cell cultures were trypsinised and cell pellets were collected by centrifugation at 2000 rpm for five minutes at room temperature. Then the cell pellets were re-suspended in 2ml of medium and cellular densities determined through a haemocytometer count, and then these cellular densities were compared to that of the control cultures.

2.1.2.6 Transfection

Following lipofectamine transfection, the SCneo vector transfection into selected cell lines was performed. Lipofectamine reagent (50µl) and plasmid DNA (100 ng) (Invitrogen, UK) were mixed individually each with 1.5 ml of OPTI-MEM I (Invitrogen, UK) and kept for fifteen minutes (15 min) at room temperature. The two mixtures were then mixed together and further incubated for another thirty minutes (30 min) before adding three mls of 37°C pre-warmed OPTI-MEM I giving the six mls transfection mixture. This transfection mixture was added to the 70% confluent cells which were seeded in to 75cm^2 culture flasks (after washing them twice with HBSS). These culture flasks were then incubated for five hours at 37°C, and 5% CO_2 before replacing the transfection mixture with fresh culture medium and incubated again at 37°C, and 5% CO_2 overnight. The transfected cell lines in the culture flasks were trypsinised and pellet collected, then seeded into tissue culture dishes with cellular numbers of (200, 500, 5000 and 10000). Five tissue culture dishes were used for each plating number. All tissue culture dishes were then incubated at 37°C, and 5% CO_2 overnight. Finally, a selecting agent (500 µg/ml hygromycin B) was added to these tissue culture dishes.

2.1.2.7 Homologous recombination repair (HRR) assay

2.1.2.7.1 Introduction

HRR assay is used to evaluate the rate of homologous recombination repair occurring within cell lines after induction of DNA damage especially DSBs and stalled or collapsed replication forks **(Saleh-Gohari *et al.*, 2005).** The SCneo construct is a DNA recombination reporter segment comprising two non-functional copies of the neomycin phosphotransferase (*neo*) gene; (3`*neo*) and (*S2neo*) joined by a functional hygromycin resistant gene (hyg^R) **(Johnson *et al.*, 1999).** This SCneo construct is introduced via a pMMP vector to trasfect NM3 cell line for future testing in the HRR assay. Successfully transfected cells consisting of the SCneo construct have been isolated through hygromycin selection and the cells were allowed to grow in culture medium normally before use in HRR assays. Cell lines consisting of the SCneo2 construct were further transduced with various pMMP vectors to produce other cell lines for the HHR assay.

In principle as shown in **Fig. 2.1,** when DSBs are induced in these cell lines containing SCneo construct, the error-free HRR process will join the two non-functional genes producing a functional G418 resistant gene (neo^R) **(Saleh-Gohari and Helleday, 2004).** Isolating cells with successful HRR events can be achieved through G418 selection by exposing the cells to geneticin (G418) antibiotic. Only cells which have successful HHR event will form colonies. Calculating HRR frequency in a specific cell line is possible through calculating the successful HRR events represented by the average rate of G418 resistant colony count over the total cell population with plating efficiency corrected. Recombination frequency fold increase can be

calculated through comparison of recombination frequency of damage induced (treated cells) with spontaneous recombination frequency of (untreated cells). Exposing cell lines to clastogens such as phleomycin and MMC is carried out in HRR assays to determine the rate of HRR occurring in each cell line and hence evaluating the requirement of the proteins in question and their phosphorylation at specific sites for proficient HRR.

2.1.2.7.2 HRR Protocol

For each cell line, two culture flasks were set up and cells were seeded in to: untreated (control) culture flask and a drug treated culture flask with the clastogen added for a period of 24 hours. Then the cells in the culture flasks were trypsinised and pellet collected and seeded into 10 ml tissue culture dishes which contained either 1 normal culture medium (control) or (1mg/ml G418) culture medium. The control culture dishes (6 plates with 200 cells per plate) used to determine plating (cloning) efficiency and the G418 culture dishes (10 plates with 3×10^5 cells per plate). All the culture dishes were incubated for ten days at 37°C, and 5% CO_2. The colonies produced were stained and fixed by 10% methylene blue. Colonies produced in the culture dishes were counted and in order to calculate the level of HRR (recombination frequency) the following formula was applied;

$$\text{Recombination Frequency} = \frac{\text{Average colony number in G418 selective medium}}{(3 \times 10^5) \times \frac{\text{Average colony number in nonselective medium}}{200}}$$

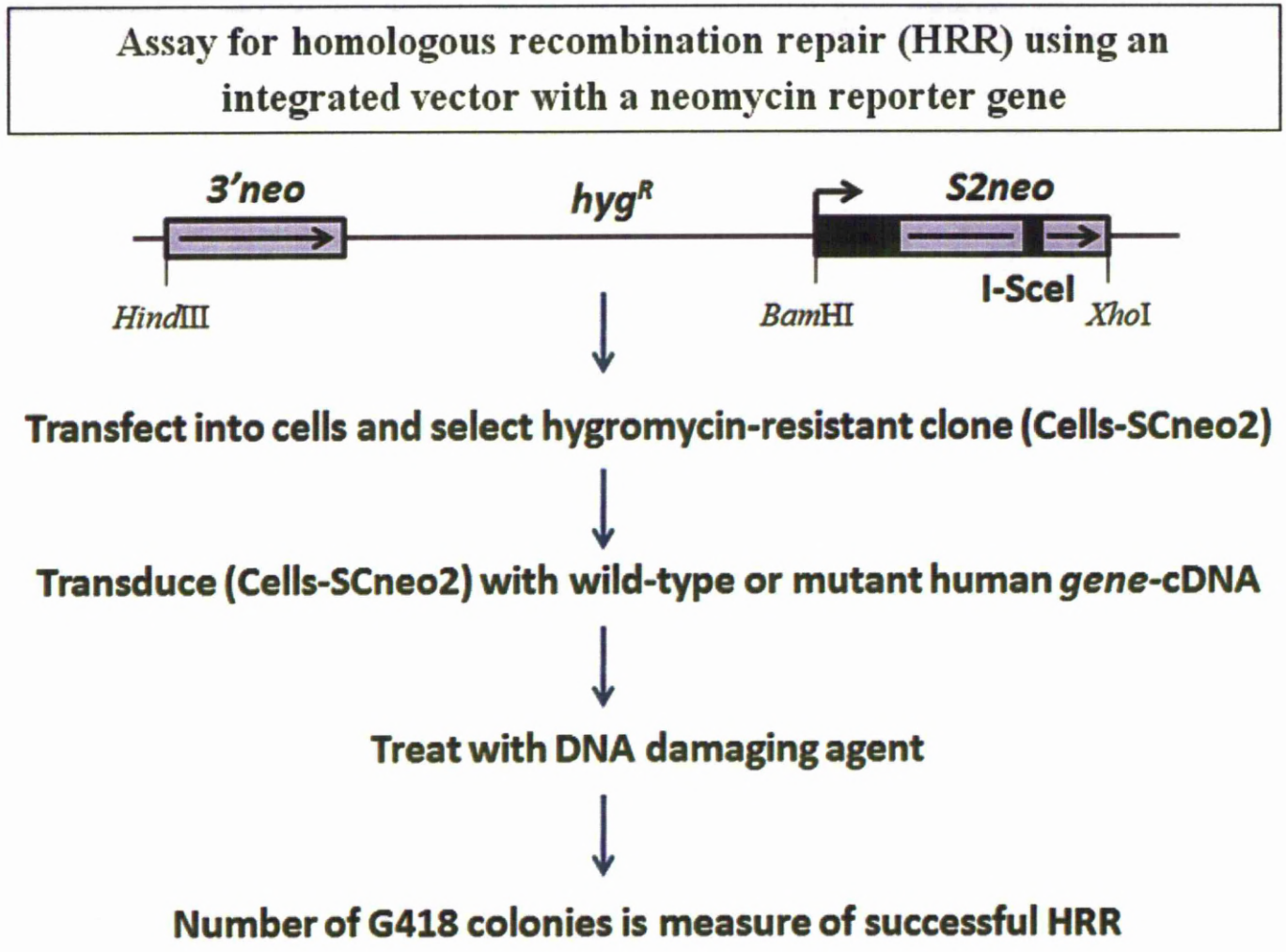

Figure: (2.1) Showing the cellular transfection with a hygromicin resistant construct that consist of two non-functional copies of the neomycin phosphotransferase (*neo*) gene. The selection of hygromicin resistant colonies isolates successful cellular transfection with the construct. The transfected cells then are subjected to DNA damage followed by selection with another drug (G418) which isolates successful recombination events by isolating colonies resistant to G418 as a result of reuniting the two non-functional copies of the (*neo*) gene producing the functional (neo^R) gene which is G418 resistant.

2.1.2.8 Survival assays

Exponentially growing cells were trypsinised and plated into tissue culture petri dishes. Diluted clastogens (MMC or phleomycin) were added in gradually increasing doses to the culture medium. The dishes were placed in a 37°C incubator for 10 days permitting colony formation. Five control dishes with no clastogen were set at 200 cells/dish, those containing the drug were set in triplicate with increasing cell numbers used at higher doses. Uninterrupted clastogen exposure was applied for 10 days. Following the 10 day period culture media was removed and dishes were stained with methylene blue for 1 hour, then water rinsed and air-dried. Only colonies greater than 50 cells/colony were considered and counted. Survival data presented after correction by comparison to untreated cell cloning efficiencies. Graphs of dose–response sensitivity represent the mean of the experiments performed. Numbers were drawn on a semi-log plot and the dose required to reduce survival to 37% was determined for each cell line (D_{37}). Once established this D_{37} value has been a starting point in determining the cytotoxicity of the selected clastogens, which allowed a selection of the suitable doses required for other assays including the CA assay.

2.1.2.9 Immunoblotting (Western Blot)

Western blotting was performed as described by **Wilson *et al.*** in 2001. Antibodies to beta actin (ab6276) which is a mono-clonal antibody raised in mouse and FANCG (a kind gift from Hoatlin) which is a poly-clonal antibody raised in rabbit were obtained from Abcam Limited

(Cambridge, UK). Cells were grown to near-confluence in 75 cm^2 peel-back flasks (Greiner, UK) followed by washing extensively with HBSS. Protein extraction buffer was used to lyse cells (50 mM Tris–HCl, pH 6.8, 1% sodium dodecyl sulphate (SDS), 1% EDTA, 0.25% glycerol, 0.25% ß-mercaptoethanol) followed by lysate boiling for 10 min. Then 10 minutes centrifugation followed by subjecting the supernatant to polyacrylamide SDS gel electrophoresis. Using a submerged transfer apparatus (Wolf laboratories) the proteins were transferred to nitrocellulose filled with 25 mM Tris base, 192 mM glycine and 20% methanol. Following blocking with 5% non-fat dried milk in TBS-T (50 mM Tris–HCl, pH 8.0, 150 mM NaCl, 1% Tween 20) the membranes were incubated with the anti-beta actin (ab6276) and anti FANCG polyclonal antibody diluted in a TBS-T solution (1:1000 dilution). Following extensive wash of the membrane, it was incubated with anti-rabbit horseradish peroxidase-linked secondary antibody and chemiluminescence used for detection (Amersham, Little Chalfont, UK).

2.1.2.10 Cytogenetic methods

2.1.2.10.1 Cytogenetic methods introduction

Classical cytogenetic analysis has been implemented in this investigation (using Giemsa stain). Structural chromosomal aberrations were determined, classified and analyzed through metaphase spread analysis. Selected cell lines are cultured in the presence and absence of the cross-linking agent. Metaphase spreads were scored and analyzed for chromosomal breakage as well as for the formation of complex chromosomal arrangements. Findings for FANC mutant cell lines are

compared with findings from corrected control cells. Cellular cultures without the DNA clastogenic agent were used to measure the spontaneous breakage rate. Results are reported as the number of aberrations per cell, the percentage of aberrant cells and the total number of chromatid breaks per cell.

The aberrations are categorized into two main types which are chromosome and chromatid aberrations. Further classification of these aberrations is made into breaks and exchanges. Chromatid exchanges are further classified in to three sub-sections which include the radial forms triradials, quadri-radials and complex exchanges (see **Table 2.1**). The complex chromatid exchanges are classified based on the number of chromosomes that are involved in each complex. FA cell lines after treatment with MMC illustrated elevated rates of chromosomal breakage and radial formation a mark of chromosomal breakage syndromes.

Elevated chromosome alterations constitute most of the spontaneous or induced mutations found in somatic mammalian cells linked to cancer. Post exposure to carcinogenic agents and the occurrence of initial molecular damage represented by specific chromosomal aberrations are likely to lead to a sequence of events preceding the formation of a cancerous tissue. In principle the type of chromosomal aberrations presented, and their breakpoints, may highlight the influence of structural or functional features that chromatin may have on processes of DNA repair or mis-repair after encountering DNA damage. Also the analysis of this type of information can point out the genes and controlling dynamics whose expression or suppression set the molecular grounds from which malignant transformations stem. Therefore, cytogenetic data may provide valuable means for more detailed studies on the dynamics of repair.

Given the accessibility to repair deficient mutant cell lines or knockdown strategies, protein immunecytochemical detection apparatus combined with cytogenetics in addition to the

advanced molecular cytogenetics such as (F.I.S.H.) or (C.G.H), it can be seen that cytogenetics can provide valuable data about the DNA repair process and its associated protein interactions that can be logically interpreted to further clarify the details of the dynamic bigger picture of DNA repair processes. In this thesis classical cytogenetic analysis has been utilized.

2.1.2.10.2 Cytogenetic protocols

2.1.2.10.2.1 The Micronucleus Assay

The micronucleus (MN) assay determines the frequency of micronuclei formation, structures that may result from either chromosome breakage or chromosome loss. The MN assay is used to evaluate spontaneous and drug induced numerical and structural instability. Exponentially growing CHO cells (5 x10^5) were plated in 25-cm^2 tissue culture flask with 5ml culture medium. The cells were allowed to attach and were left to grow for 48 hours at 37°C, 5% CO_2. Duplicate cultures were prepared for each treatment group and negative controls were included. Cytochalasian-B (Cyto-B) and MMC were added 48 hours after culture initiation. Based on earlier reports **(Fenech and Morley, 1985; Krishna *et al.*, 1989)** the optimum Cyto-B concentration has been used (3µg/ml) and the final concentration of dimethyl sulfoxide (DMSO) did not exceed 0.3% **(Ellard *et al.*, 1991).** Selected MMC doses used were 300nM and 600nM **(Krishna *et al.*, 1989; Lynch *et al.*, 1993; Gabriele *et al.*, 1995).** Cyto-B (Sigma Chemical Company) was dissolved in DMSO and stored at -80°C.

The flasks were re-incubated and cells were allowed to grow for further 20 hours at 37°C and 5% CO_2 before harvesting. Harvesting began with removing the culture medium by aspiration followed by washing the flasks twice with phosphate buffer solution (PBS), then trypsinising using 5ml trypsine solution (0.12% trypsin and 0.008% EDTA) and removing the cells from the culture flasks into centrifuge tubes containing 5ml medium. Tubes were centrifuged at 1700 RPM for 5 minutes followed by removal of most of the supernatant keeping the pellet in 0.5 ml supernatant. The pellet was re-suspended by flicking or pipetting, then fixed by adding cool, fresh fixation solution (acetic acid-methanol solution, 1:25) drop by drop (5mls) and leaving tubes for 15 minutes in fixative at room temperature. Tubes were spun again, supernatant removed, new fixation solution is added and the pellet is dropped on slides. Three slides were prepared for each treatment group by the dropping method and after air drying the slides were stained before scoring in accordance to the recommended criteria **(Fenech, 2000).**

2.1.2.10.2.2 Metaphase spreads preparation for cytogenetic analysis

Experimentation was performed on exponentially growing cells. Routinely cells were re-suspended in culture medium (DMEM, BioWhittaker, Cambrex Corp., Nottingham, UK supplemented with 10% foetal calf serum, penicillin and streptomycin antibiotics) and were allowed to grow in a 37°C with 5% CO2 incubator until cells were about 70% confluent enough to be utilized (usually 48 hours for either CHO or human cells). The cells were harvested by trypsinization from culture flasks. CHO cell numbers of (0.5×10^5, 1×10^5 and 2×10^5cells) then were allowed to firmly attach on glass slides for 3 hours before adding further culture medium and allowing a growth period of (24 hours). Clastogens such as MMC or phleomycin were added

to the CHO cells for 24, 18 hours respectively after cell-slide attachment. Human fibroblast cell numbers of (0.3×10^5, 0.5×10^5 and 1×10^5cells) were allowed to firmly attach on glass slides for 3 hours before adding further culture medium and allowing a growth period of 30 hours. Clastogens such as MMC or phleomycin were added to the human fibroblasts for 40 hours.

By adding 100 µl demecolcine solution (10 µg/ml in Hanks Buffered Saline Solution (HBSS) (CAS No. 477-30-5) cellular growth arrested at the metaphase stage at a final concentration of 1 µg/ml to cell cultures in10 ml of culture medium. The cells remained in demecolcine concentration of 1 µg/ml for three hours. The cells were then treated with 37°C pre-warmed 0.075 M KC1 for 15 minutes at room temperature, then fixed with cold methanol: glacial acetic acid (3:1, v/v) for about 30 minutes, the slides were air dried and stained with 5% Giemsa for 5-10 min, followed by scoring 100 cells for chromosomal aberrations from controls and treated cells when possible, or 50 cells for each treated cell line. The slides were coded to ensure unbiased judgment of any possible aberrations.

Solutions were freshly prepared each time for each experiment. The exposure time for both MMC and phleomycin in all experiments was 24, 18 hours respectively. MMC (CAS No. 50-07-7) and phleomycin (CAS No.11006-33-0) were purchased from Sigma. Stock solutions of MMC and phleomycin were prepared in HBSS and water respectively and stored at (- 20°C). Metaphase chromosome spreads were prepared as described above. All slides were coded, and then scored for chromatid and chromosome aberrations. Chromatid and chromosome gaps were scored and presented separately in the data tables.

2.1.2.10.3 Chromosomal aberration scoring

It is possible to identify certain chromosomal aberrations (CA) in metaphase chromosomes through light microscopy using specific chromosomal preparation and staining procedures (**Appendix-1**). CA that could be recognized in this project until this stage include; chromosome exchanges such as; di-centrics (**Appendix-2**), rings (**Appendix-3**), or chromatid exchanges such as; tri-radials (**Appendix-4**), quad-radials (**Appendix-5**) or complex structures (**Appendix-6**) or chromosome or chromatid breaks (**Appendix-7**), or gaps (**Appendix-8**) **(Passarge, 1995; Verma and, Babu 1994).** Advantages of Giemsa staining technique include its cost effectiveness and the simplicity with which it is performed **(Sra *et al.*, 2005)**. However, the procedure requires dividing cells which can be time consuming and may fail to detect cryptic translocations, deletions, insertions or duplications **(Sra *et al.*, 2005)**. CA such as, isochromosomes, reciprocal translocations or other micro-rearrangements have not been addressed as they are beyond the cytogenetic scope of this part of the project. The gaps observed in stained chromosomes may reflect problems in DNA replication such as stalled replication forks or may result sometimes from staining variation. In order to overcome this problem in interpretation of the results, gaps were scored as a separate type of aberration and placed separately in the scoring tables. A simplistic definition of a break can be: an achromatic area more than a chromatid in width **(Auerbach *et al.*, 1979).** In this project the aberrations were classified into chromosome or chromatid aberrations as described by **(Kirkland, 1990; Savage, 1976). Appendix (9-A and 9-B)** illustrates some of the main aberrations and their classification (adopted from **Kirkland, 1990**). Similar to Chinese hamster cells, these aberrations can also be found in human cells 6914 FANCA and PD20. **Appendix-11** and **Appendix-12** illustrate normal

metaphase spreads of 6914 FANCA cells. These can be compared to 6914 FANCA cells with aberrations (**Appendix-13** and **Appendix-14).** Normal metaphase spreads of PD20 cells are shown in **Appendix-15** and **Appendix-16** and can be compared to **PD20** cells with aberrations **(Appendix-17** and **Appendix-18).** Human cells 6914 FANCA and PD20 lines are immortalized cell lines with chromosomal counts ranging between 50-70 chromosomes per metaphase as observed in untreated culture conditions.

2.1.2.10.4 Converting exchanges to chromatid breaks

In order to calculate the total number of chromatid break, firstly, chromsome breaks, chromosome exchanges and chromatid exchanges including triradials, quadri-radials and complex arrangements were converted to the minimal number of chromatid breaks required for the formation of each specific type of aberration. Then this minimal number of chromatid breaks required for the formation of those aberrations was added to the observed number of chromatid breaks. Then this total number of chromatid breaks has been presented as total chromatid breaks per cell. The conversion was made according to **Table: 2.1** showing the minimal number of chromatid breaks required to form the complex arrangement and explained in **Figs. 2.2, 2.3, 2.3 and 2.4**. From **Table: 2.1** and **Figs. 2.2, 2.3, 2.3 and 2.4** it can be seen that for example; a chromosome break is equivalent to two chromatid breaks and that for rings or dicentrics to form a minimal number of four chromatid (telomeric) breaks are required to form the chromosomal arrangement. Likewise, for a complex chromatid exchange involving four chromosomes (or four centromeres) will require a minimum of six chromatid breaks. For a dicentric triradial a minimum of three chromatid breaks are needed for this figure to form; one chromatid break

along the length of a chromatid arm and two chromatid (telomeric) breaks. In the same way, for a quadri-centric quadri-radial to form a minimum of eight chromatid (telomeric) breaks is required. Clearly other numbers of chromatid breaks are possible to have the same chromosome or chromatid arrangements, however our calculation takes into consideration the minimal possible number required of chromatid breaks to form these structures.

Converting chromosome and chromatid exchanges into chromatid breaks		
Aberration type		**Minimal number of chromatid breaks**
Chromosome type aberrations	Chromosome break	2
	Chromosome exchange (Dicentrics and Rings)	4
Complex chromatid arrangements involving	Two chromosomes	2
	Three chromosomes	4
	Four chromosomes	6
	Five chromosomes	8
Triradials	Monocentric	3
	Dicentric	3
	Tricentric	6
Quadriradials	Monocentric	4
	Dicentric	2
	Tricentric	6
	Quadricentric	8

Table 2.1: Showing the minimum number of chromatid breaks required to have the chromosome or chromatid various complex figures described.

Figure (2.2): Complex chromatid arrangements involving two, three, four or five chromosomes. Chromatid exchanges involving two chromosomes are considered simple exchanges, but was included here to show the progression from simple to complex and to simplify the classification method. Chromatid exchanges involving three or more chromosomes are considered complex arrangements.

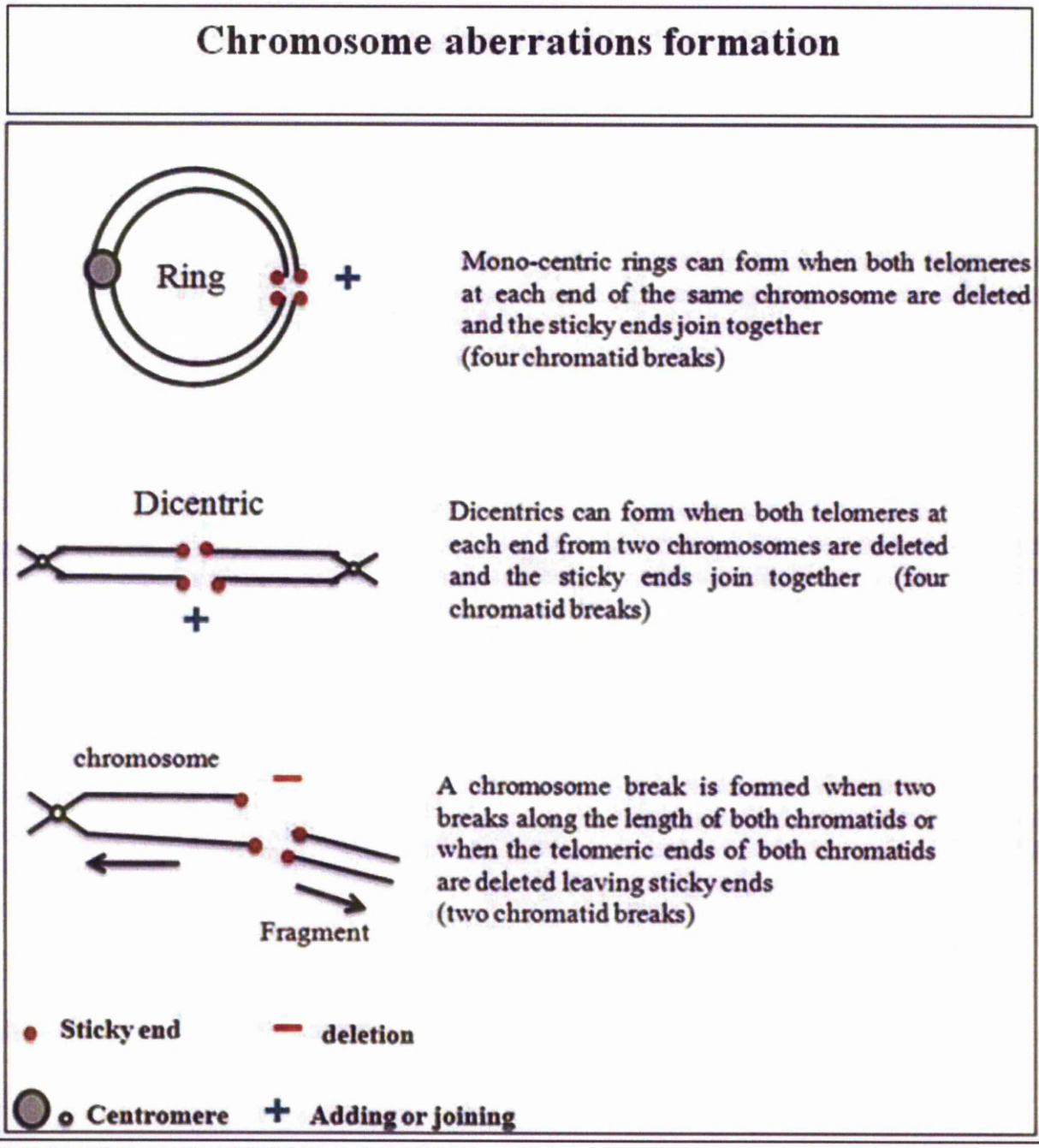

Figure (2.3): Chromosome breaks produce two chromatid breaks, on the other hand chromosome exchange such as dicentrics and rings require a minimum of four chromatid breaks.

Figure (2.4): Triradial formation requires a minimal of two chromosomes; acentric chromosome plus centric chromosome to form a mono-centric triradial (not shown in diagram) and a minimum of three chromatid breaks. A dicentric triradial requires a minimum of three chromatid breaks as shown in the diagram. Tricentric triradials requires a minimal of three chromosomes and a minimum of six chromatid (telomeric) breaks as extra centromeres indicate other chromosomes involvement, thus the involvement of other chromatid breaks. The minimal number to form these structures was considered here despite the presence of other possibilities involving more chromatid breaks.

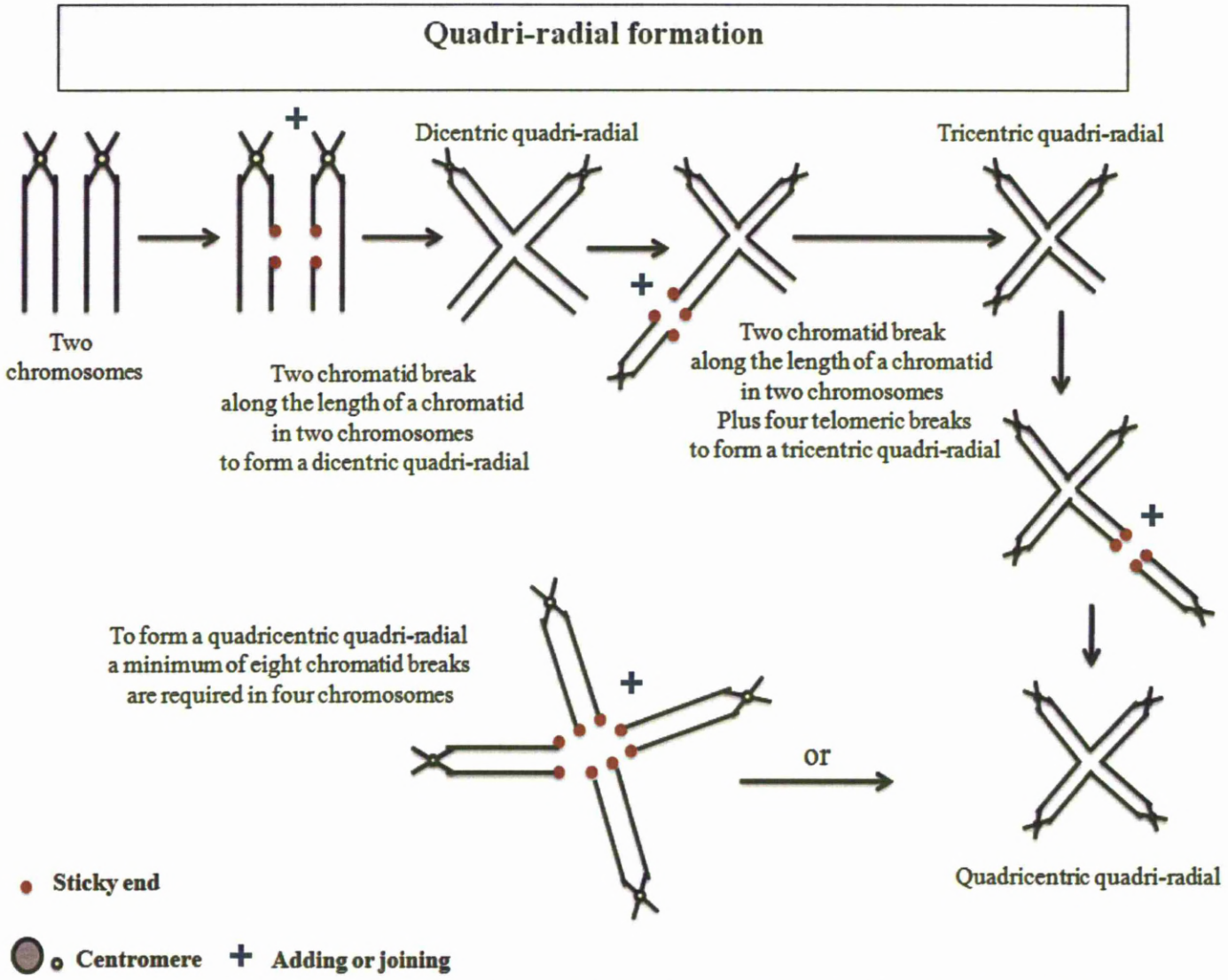

Figure (2.5): Quadri-radial formation requires a minimal of two chromosomes (two centromeres) and a minimum of two chromatid breaks along the length of two chromatid strands in two chromosomes. The presence of extra centromeres suggests the involvement of other chromosomes in the quadric-radial, thus the involvement of other chromatid breaks. The minimal number to form these structures was considered here despite the presence of other possibilities involving more chromatid breaks

Chapter-3

Investigating the role of FANCG protein in the repair of induced inter cross links (ICLs)

3.1 Introduction

FANCG is a phospho-protein with phosphorylation sites identified at serine 7 **(Qiao *et al.*, 2004)**, serine 387 and serine 383 **(Mi *et al.*, 2004)**; it also contains seven tetratricopeptide repeat (TPR) motifs **(Blom *et al.*, 2004, and Mi *et al.*, 2004)**. FANCG protein is known to be involved in at least three protein complexes, each of which are thought to be involved in the repair of DNA lesions through the FA-BRCA pathway. This is supported by recent evidence suggesting the involvement of FANCG protein in the unhooking of DNA inter cross links **(Wang and Lambert, 2010)**. These three FANCG multiple protein complexes are termed the FA-core complex **(Kupfer *et al.*, 1997; de Winter *et al.*, 2000a; Medhurst *et al.*, 2001)**, the G-BRCA2 complex **(Wilson *et al.*, 2008)** and the G-XPF-ERCC1 complex **(Wang and Lambert, 2010)**.

3.1.1 FANCG and the repair of ICLs

ICL repair at stalled replication forks is a multi-stage complex process that is proposed to comprise several DNA repair mechanisms. These include lesion unhooking, lesion bypass or translesion synthesis, excision of unhooked crosslink by nucleotide excision repair (NER), the

production of a double-strand break at stalled replication fork sites and subsequent homologous recombination repair (reviewed by **Niedernhofer *et al.*, 2005; Patel and Joenje, 2007; Thompson and Hinz, 2009).** However, the order in which these events take place is unclear and the subject of much discussion in the literature (reviewed by **Deans and West, 2011).** There is evidence that FANCG is involved in several of these stages. Post-treatment with DNA cross-linking agents, FANCG has been shown to co-localize with the HRR proteins, BRCA2 and RAD51 **(Hussain *et al.*, 2004).** This suggests that FANCG is directly linked with HRR, which is involved in ICL repair after the unhooking of the ICL by the ERCC1/XPF endonuclease and the generation of a double-strand break **(Thompson *et al.*, 2005; Bhagwat *et al.*, 2009).** The main role of FANCG in the FA core complex appears to be in stabilizing replication forks that encounter gaps, nicks, or replication-blocking lesions, thereby promoting a number of repair pathways such as translesion synthesis of blocking lesions, HRR and possibly non-homologous end joining of broken replication forks **(Tebbs *et al.*, 2005; Hinz *et al.*, 2006).** In addition, FANCG was recently shown to directly interact with the ERCC1/XPF endonuclease **(Wang and Lambert, 2010).**

3.1.2 FANCG is a scaffold phospho-protein central to many repair complexes

The tetratricopeptide repeat (TPR) motifs and phosphorylation sites of FANCG have been shown to play a role in its protein interactions and the formation of the various FANCG complexes such as the FA nuclear core, G-BRCA2 and the G-XPF-ERCC1 complexes **(Wang *et al.*, 2007b; Wilson *et al.*, 2008; Wang and Lambert, 2010).** In an attempt to further characterize the role of

FANCG in the repair of DNA ICLs investigations were carried out to determine how FANCG is involved in maintaining chromosome stability in response to ICLs. To do this a *FANCG* deficient Chinese hamster cell line was used **(Meyn *et al.*, 1991; Wilson *et al.*, 2001)** and chromosomal aberrations induced after MMC treatment were assayed using metaphase analysis **(Wiegant *et al.*, 2006; Auerbach *et al.*, 1979; Rosendorff and Bernstein, 1988; Savage, 1976; Marx *et al.*, 1983)**. Concurrent to these experiments the role of FANCG in homologous recombination repair (HRR) of ICL adducts was analysed using an integrated vector based system in the same *FANCG* deficient cell line.

3.1.3 Cell lines used in this chapter

The cell lines used in this chapter were all derived from Chinese hamster ovary (CHO) cell line AA8 **(Meyn *et al.*, 1991).** The cell lines used are either wild type or corrected to wild type compared to *FANCG* defective cell lines. For full details of NM3 cells see sections **1.5.1.1** and **1.5.1.2.**

Cell lines used include **NM3, NM3–VO, NM3–S7A, and NM3–S387A and NM3–gWT. NM3** is a *FANCG* mutant cell line containing a point mutation resulting in a highly unstable truncated protein. Based on its seven fold hypersensitivity to cross linking agent (nitrogen mustard), **Meyn *et al.*** isolated NM3 in 1991 from the CHO cell line AA8. **NM3–VO** is an NM3 cell line transfected with the SCneo2 recombination reporter construct **(Johnson *et al.*, 1999; Saleh-Gohari and Helleday, 2004),** and then transduced with an empty pMMP vector **(Qiao *et al.*, 2001; Qiao *et al.*, 2004; Mi *et al.*, 2004). NM3-gWT** is an NM3 cell line transfected with the SCneo2 recombination reporter construct and transduced with the wild type *fancg* cDNA to

restore its phenotype to that of the wild type cell line (AA8). **NM3–S7A** is an NM3 cell line transfected with the SCneo2 recombination reporter construct and transduced with pMMP vector containing the human *fancg* cDNA mutated at phosphorylation site (S7) serine to alanine substitution. **NM3–S387A** is an NM3 cell line transfected with the SCneo2 recombination reporter construct and transduced with pMMP vector containing the human *fancg* cDNA mutated at phosphorylation site (S387) serine to alanine substitution and transfected with the SCneo2 construct as explained in Methods (**Sections 2.1.1.1.1, 2.1.2.7** and **Fig. 2.1.**

3.1.4 Role of FANCG in HRR and ICL repair

To further investigate the DNA repair pathway through which FANCG is thought to be involved, another assay termed homologous recombination repair (HRR) assay, 'HRR assay', which is a plasmid based reporter assay has been implemented to evaluate the ability of *FANCG* deficient cells to repair ICLs through the repair pathway HRR. The findings should point out the ability of the *FANCG* mutant cell lines in repairing ICLs through a specific repair pathway which is homologous recombination repair and hence the extent of involvement of FANCG protein in ICL repair through HRR. Details of the HRR assay are explained in the Methods (**Section 2.1.2.7** and **Fig. 2.1).**

3.2 Results

3.2.1 Validation and growth inhibition responses of cell lines used for metaphase analysis

3.2.1.1 Immunoblotting

Western blot analysis was performed to confirm the protein expression profile for FANCG in all cell lines prior to utilization in other experiments. **Figure 3.1** illustrates FANCG protein expression detected in cell lines AA8, NM3-gWT and NM3-TPR6 but not in NM3 the *FANCG* null cell line. The loading control β-actin **(Figure 3.1)** shows an equal amount of protein loaded for each cell line tested, thus validating the use of these cell lines in subsequent tests.

Figure 3.2 shows that in the SCneo transfected cell lines, FANCG is detected in NM3-gWT and NM3-S7A, NM3-S387A but not in NM3-VO, thus validating the use of these cell lines in subsequent tests.

Western blot of FANCG protein in NM3 cell lines

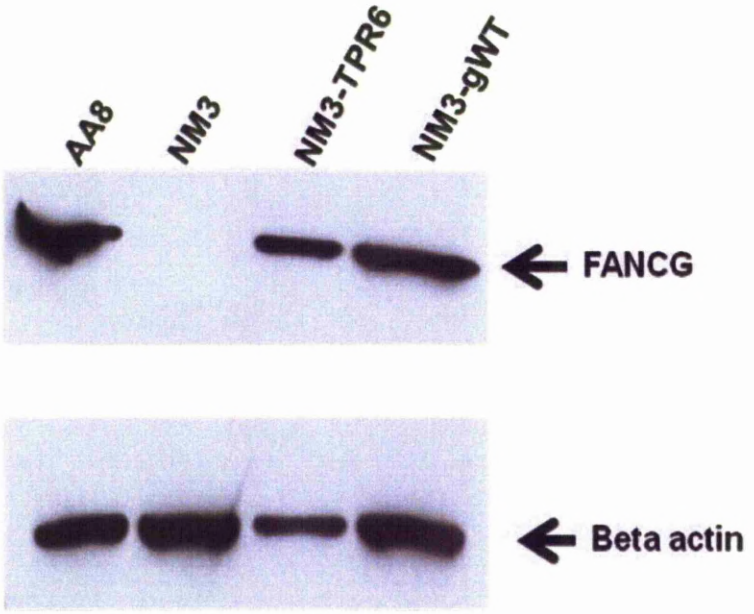

Figure (3.1): Western blot illustrating the absence of FANCG protein from the NM3 cell line and the presence of FANCG protein in cell lines AA8, NM3-TPR6 and FANCG-corrected cells NM3-gWT. – Beta actin antibody was used as loading control. NM3-TPR6 was obtained by transfecting NM3 with a human *fancg* cDNA mutated at a TPR motif (TPR6). NM3-TPR6 was not used in subsequent experiments.

Western blot of FANCG protein in NM3 cell lines

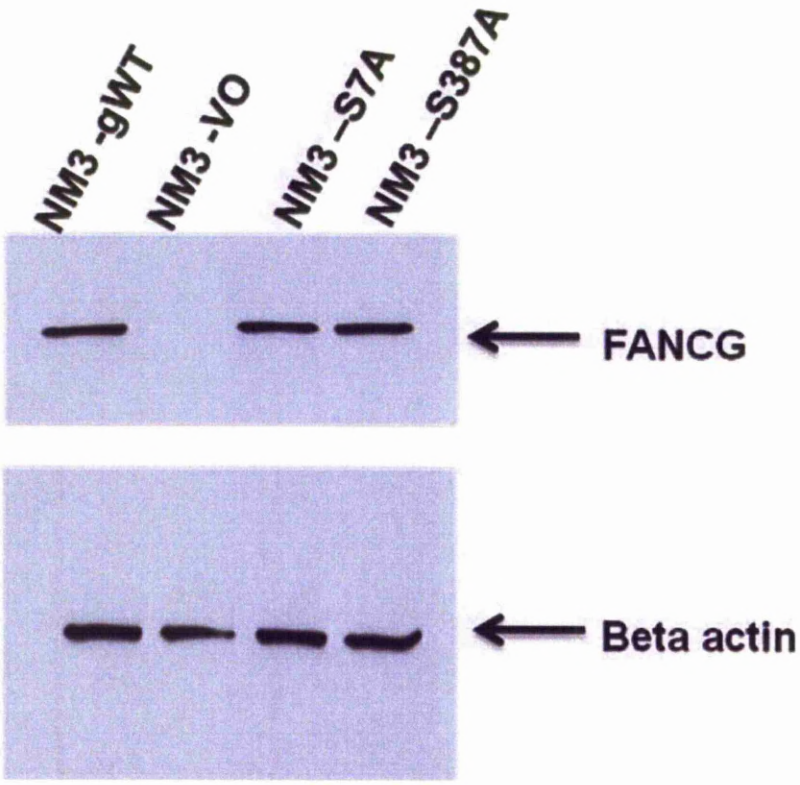

Figure (3.2): Western blot illustrating the absence of FANCG protein from the NM3-VO cell line and the presence of FANCG protein in cell lines NM3-S7A, NM3-S387A and FANCG-corrected cell line NM3-gWT. Beta actin antibody was used as loading control.

3.2.1.2 Growth inhibition assays results

To assess the degree of cellular hypersensitivity of these cell lines to the ICL inducing agent mitomycin C (MMC), growth inhibition assays were carried out as described in the Methods **(Section 2.1.2.5),** determining the GI-50, which is the dose of agent that allows 50% of the cells to grow was determined. From **Figure 3.3** it can be seen that NM3-VO was the most hypersensitive with a GI-50 value of 38 nM compared to 110 nM seen in NM3-gWT. NM3-VO is therefore 2.9-fold more hypersensitive to MMC than the corrected wild type NM3-gWT **(Fig. 3.3)**. These findings of NM3-VO hypersensitivity to MMC can be compared to the clonal survival experiments of **Wilson *et al*** in 2001 that showed about 4-fold hypersensitivity to MMC. From the graph it can be seen that NM3-S7A had a GI-50 value of 52.5 nM and is 2.1-fold hypersensitive to MMC and NM3-S387A has a GI-50 value of 57 nM and is 1.9-fold hypersensitive to MMC. These sensitivities observed here are comparable to the sensitivities reported by **Mi *et al.,*** in 2004 and by **Qiao *et al.,* (2004)** using a clonal survival assay. On the basis of the D37 values, which is the dose of agent that allows 37% of the cells to survive, NM3-VO is about 4.3 fold hypersensitive to MMC, NM3-S7A about 3 fold hypersensitive to MMC **(Qiao *et al.,* 2004)** and NM3-S387A about 2.6 fold hypersensitive to MMC **(Mi *et al.,* 2004).** This shows that mutating the phosphorylation sites with the FANCG protein leads to an increase in hypersensitivity, which reflects that phosphorylation of FANCG is required to get optimal levels of repair when exposed to DNA inter-strand linking agents. This highlights the importance of FANCG and its phospho-sites S7 and S387 in the ICL repair pathway.

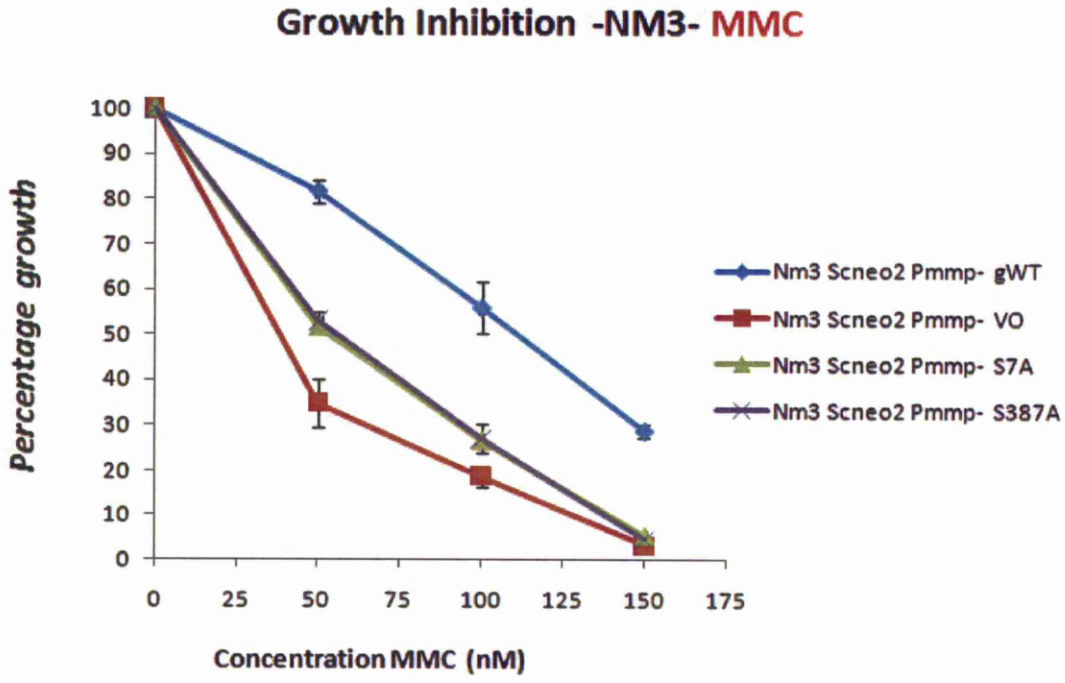

Figure (3.3): Illustrating MMC growth inhibition data using four cell lines: NM3-gWT, NM3-VO, NM3-S7A and NM3-S387A. Three experiments were performed. Error bars show the standard error of the mean.

3.2.2.1 Chromosome and chromatid aberration rates in control cell cultures

It can be noted that the number of aberrations per cell in untreated cell lines showed a spontaneous rate which did not exceed 0.12 aberration/cell as shown in **Tables; 3.1.A, 3.2.A, 3.3.A and Fig. 3.4.** Very few aberrations were recorded for untreated NM3–gWT, only one chromatid break as shown in **Table 3.3.A**. The highest number of aberrations for the untreated cells was that recorded for NM3–VO (0.12 aberration/cell) followed by NM3–S7A (0.1 aberration/cell) then NM3–S387A (0.08 aberration/cell). Also from the same **Tables 3.1.A, 3.2.A, 3.3.A and Fig. 3.5** it may be seen that the percentage of aberrant cells that have occurred spontaneously was lowest in NM3–gWT and highest in NM3–VO, whereas NM3–S7A and NM3–S387A presented similar numbers of aberrant cells spontaneously.

3.2.2.2 Chromosome and chromatid aberration rates in treated cell cultures

Table 3.1.A shows that using doses of 100 nM MMC resulted in NM3-VO, NM3-S7A, NM3-S387A producing higher rates of chromosomal aberrations per cell, 1.3, 0.84 and 0.74 aberration/cell respectively, compared to 0.44 aberration/cell found in NM3-gWT which represented about 3, 1.9 and 1.7 fold increases respectively. The same experimental conditions were obtained and despite slight variation, the readings of each experiment illustrated that the three mutant cell lines presented an increased number of CA compared to NM3-gWT. It is clear

that in mutant cell lines; NM3–VO, NM3–S7A, NM3–S387A and control cell line NM3–gWT that chromatid type aberrations predominate, involving both breaks and exchanges. To a lesser extent chromosome type aberrations such as dicentrics or rings have appeared as shown in **Tables 3.1.A, 3.2.A and 3.3.A.** These chromosome exchanges (dicentrics or rings) were not observed in the untreated cell lines cultures (controls), but were present, albeit rarely, in some of the NM3–VO and NM3–S7A MMC-treated cell line cultures. Based on their findings, **Sasaki and Tonomura, (1973)** made the assumption that these chromosome type aberrations may have been derivatives of some cells that have gone through at least a second cellular cycle of mitosis in culture. Although this may be possible, these structures may also be formed in some cells after the first mitotic division in culture. In the experiments described here, the time given for cellular division allowed one cycle of mitosis in culture, thus the aberrations recorded are most likely a reflection of the primary aberrations encountered post the first cellular division and not due to cells undergoing a second mitosis.

In the work described here, chromosome breaks were higher than chromosome exchanges in all cell lines. Chromosome breaks generally, were still considerably lower in numbers compared to chromatid breaks. This can especially be seen in treated mutant cell line cultures; NM3–VO, NM3–S7A and NM3–S387A in **Tables 3.1.A, 3.2.A and 3.3.A.**

Data-Table: Data summaries MMC treated cell lines and aberrations found in experiments

Table 3.1.A

Cell line	Treatment MMC nM	Total number of cells sampled	Chromatid based - aberrations		Chromosome based - aberrations		Gaps per cell	Total aberrations without Gaps	Aberrations Per cell	% Aberrant cells	*Total Chromatid Breaks - after aberration converting per cell*
			Ctid-break	Ctid-exch	Chro-break	Chro-exch					
NM3-gWT	0	50	0	0	0	0	0	0	0	0	0
NM3-gWT	100	50	9	11	2	0	0.12	22	0.44	34	0.96
NM3-VO	0	50	2	1	3	0	0.1	6	0.12	12	0.24
NM3-VO	100	50	23	38	4	0	0.24	65	1.3	60	2.92
NM3-S7A	0	50	0	0	1	0	0.1	1	0.02	2	0.04
NM3-S7A	100	50	15	15	12	0	0.48	42	0.84	50	1.58
NM3-S387A	0	50	0	0	1	0	0	1	0.02	2	0.04
NM3-S387A	100	50	20	9	8	0	0.26	37	0.74	38	1.3

Table abbreviations: Ctid-break: Chromatid break type aberration, Ctid-exch: Chromatid exchange type aberration, Ctid-exch: Chromatid exchange type aberration, Chro-break: Chromosome break type aberration, Chro-exch: Chromosome exchange type aberration.

Data-Table: Data summaries MMC treated cell lines and aberrations found in experiments

Table 3.2.A

Cell line	Treatment MMC nM	Total number of cells sampled	Chromatid based - aberrations		Chromosome based - aberrations		Gaps per cell	Total aberrations without Gaps	Aberrations Per cell	% Aberrant cells	*Total Chromatid Breaks - after aberration converting per cell*
			Ctid-break	Ctid-exch	Chro-break	Chro-exch					
NM3-gWT	0	50	0	0	0	0	0.04	0	0	0	0
NM3-gWT	50	50	2	1	0	0	0.14	3	0.06	6	0.08
NM3-gWT	100	50	6	12	0	0	0.06	18	0.36	22	0.92
NM3-VO	0	50	1	0	2	0	0.18	3	0.06	6	0.1
NM3-VO	50	50	8	5	6	0	0.2	19	0.38	24	0.68
NM3-VO	100	50	36	38	13	1	0.34	88	1.76	66	3.48
NM3-S7A	0	50	2	1	2	0	0.14	5	0.1	10	0.2
NM3-S7A	50	50	9	2	7	0	0.3	18	0.36	30	0.64
NM3-S7A	100	50	14	28	5	0	0.38	47	0.94	54	2.14
NM3-S387A	0	50	0	0	2	0	0.08	2	0.04	4	0.08
NM3-S387A	50	50	19	10	9	0	0.26	38	0.76	40	1.32
NM3-S387A	100	50	20	14	5	0	0.24	39	0.78	46	1.38

Table abbreviations: Ctid-break: Chromatid break type aberration, Ctid-exch: Chromatid exchange type aberration, Ctid-exch: Chromatid exchange type aberration, Chro-break: Chromosome break type aberration, Chro-exch: Chromosome exchange type aberration.

Data-Table: Data summaries MMC treated cell lines and aberrations found in experiments

Table 3.3.A

Cell line	Treatment MMC nM	Total number of cells sampled	Chromatid based - aberrations		Chromosome based - aberrations		Gaps per cell	Total aberrations without Gaps	Aberrations Per cell	% Aberrant cells	*Total Chromatid Breaks - after aberration converting per cell*
			Ctid-break	Ctid-exch	Chro-break	Chro-exch					
NM3-gWT	0	50	1	0	0	0	0.06	1	0.02	2	0.02
NM3-gWT	50	50	1	0	1	0	0.04	2	0.04	4	0.06
NM3-gWT	100	50	5	10	0	0	0.1	15	0.3	22	0.7
NM3-VO	0	50	2	0	2	0	0.1	4	0.08	8	0.12
NM3-VO	50	50	5	3	1	0	0.12	9	0.18	18	0.26
NM3-VO	100	50	7	17	6	1	0.26	31	0.62	38	1.54
NM3-S7A	0	50	0	0	1	0	0.14	1	0.02	2	0.04
NM3-S7A	50	50	7	4	1	2	0.12	14	0.28	24	0.52
NM3-S7A	100	50	18	26	3	1	0.1	48	0.96	52	1.96
NM3-S387A	0	50	2	0	2	0	0.02	4	0.08	8	0.12
NM3-S387A	50	50	26	14	10	0	0.24	50	1	52	1.62
NM3-S387A	100	50	44	24	14	0	0.26	82	1.64	70	2.96

Table abbreviations: Ctid-break: Chromatid break type aberration, Ctid-exch: Chromatid exchange type aberration, Ctid-exch: Chromatid exchange type aberration, Chro-break: Chromosome break type aberration, Chro-exch: Chromosome exchange type aberration.

From the **Pooled Table 3.4** it can be seen that when using the higher dose of 100 nM MMC the average aberrations per cell in the NM3–VO, NM3–S7A, NM3–S387A cell lines were 1.23, 0.91 and 1.05 respectively, which is 3.3 , 2.5 and 2.8 fold respectively higher than that of the corrected NM3–gWT cells. Also, using the higher dose of 100 nM MMC, the average percentage of aberrant cells in the NM3–VO, NM3–S7A, and NM3–S387A cell lines were about 54.6%, 52% and 51.3% aberrant cells respectively, which is 2.1, 2.5 and 2.8 fold respectively higher than that of the corrected wild type NM3–gWT cells. The average number of total chromatid breaks per cell (after converting all the exchanges into chromatid breaks as described in **Section 2.1.2.10.4, Table 2.1, Figs. 2.2, 2.3, 2.3 and 2.4** for the same higher dose of 100 nM MMC was in NM3–VO, NM3–S7A, NM3–S387A cell lines 2.65, 1.89 and 1.88 chromatid breaks/cell respectively, which is 3.1, 2.2 and 2.2 fold respectively higher than that of NM3–gWT cells.

This elevation in the level of structural aberrations in *FANCG* mutant cell lines can be clearly observed as average aberrations per cell **(Fig. 3.4),** average percentage aberrant cells **(Fig. 3.5),** or as average total chromatid breaks **(Fig. 3.6).** This indicates that the absence of FANCG or mutating its phospho-sites S7 or S387 will compromise the ICL repair pathway and this repair defect will be visualised as gross cytogenetic aberrations. As seen when using the higher dose of 100 nM MMC, most CAs are found in the complete absence of FANCG, then followed by high CAs rates in *FANCG* phospho-mutants S7 and S387, showing their importance in sustaining cellular resistance to inter-strand cross linking agent (MMC).

Table3.4: NM3- MMC – Average/ Standard error of the mean-(SE) - Table results for (Tables 3.1.A, 3.2.A and 3.3.A)

Table3.4

Cell line	Treatment MMC nM	Total number of cells sampled	Average Aberrations Per cell	SE of the mean of Aberrations per cell	Average % Aberrant cells	SE of the mean of % Aberrant cells	Average Total Chromatid Breaks (after converting exchanges) per cell	SE of the mean of Total Chromatid Breaks (after converting exchanges) per cell
NM3-gWT	0	150	0.01	0.01	0.67	0.67	0.01	0.01
NM3-gWT	50	100	0.05	0.01	5.00	1.00	0.07	0.01
NM3-gWT	100	150	0.37	0.04	26.00	4.00	0.86	0.08
NM3-VO	0	150	0.09	0.02	8.67	1.76	0.15	0.04
NM3-VO	50	100	0.28	0.10	21.00	3.00	0.47	0.21
NM3-VO	100	150	1.23	0.33	54.67	8.51	2.65	0.58
NM3-S7A	0	150	0.05	0.03	4.67	2.67	0.09	0.05
NM3-S7A	50	100	0.32	0.04	27.00	3.00	0.58	0.06
NM3-S7A	100	150	0.91	0.04	52.00	1.15	1.89	0.17
NM3-S387A	0	150	0.05	0.02	4.67	1.76	0.08	0.02
NM3-S387A	50	100	0.88	0.12	46.00	6.00	1.47	0.15
NM3-S387A	100	150	1.05	0.29	51.33	9.61	1.88	0.54

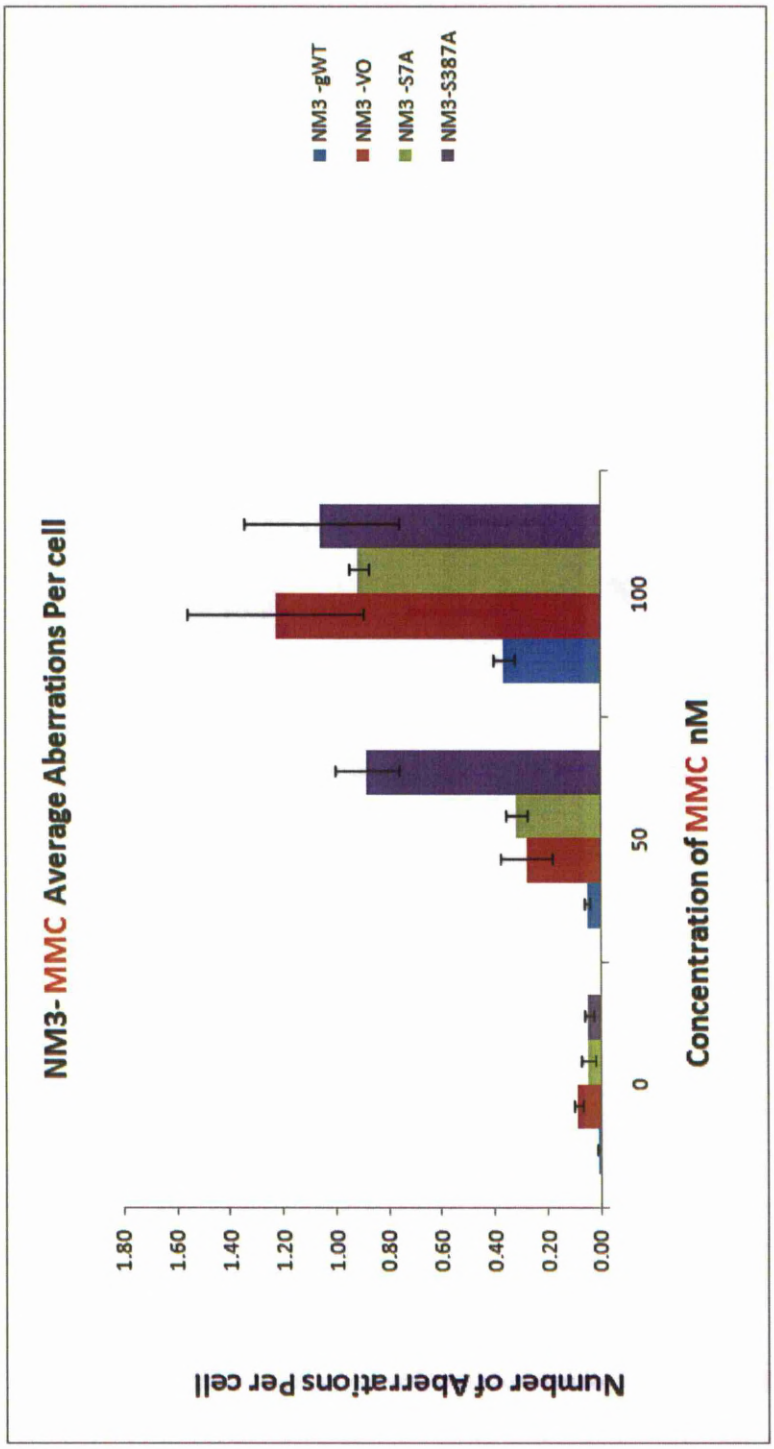

Figure (3.4): Illustrating MMC **Average Aberrations Per cell** data using four cell lines: NM3-gWT, NM3-VO, NM3-S7A and NM3-S387A. Three experiments were performed. Error bars show the standard error of the mean.

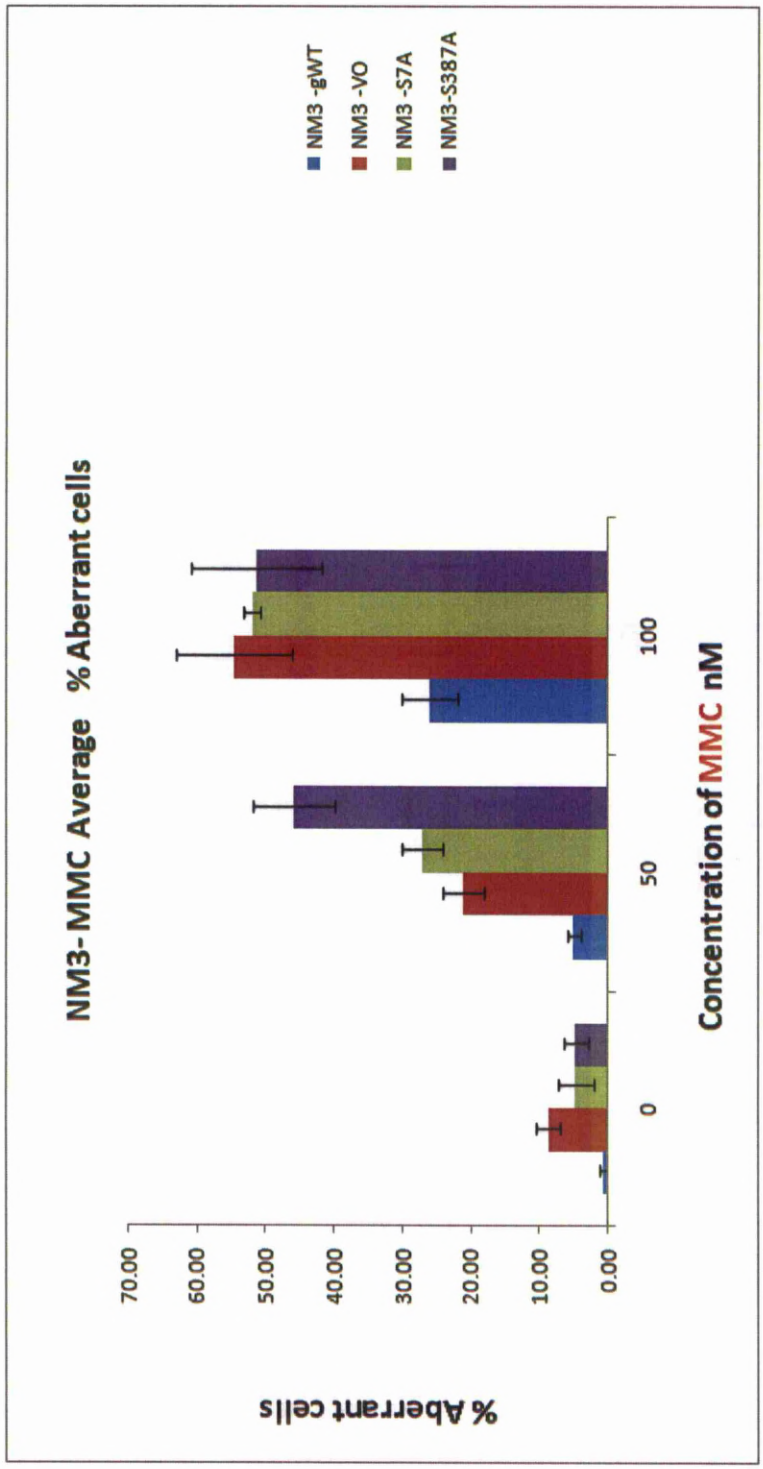

Figure (3.5): Illustrating MMC **Average percentage aberrant cells** data using four cell lines: NM3-gWT, NM3-VO, NM3-S7A and NM3-S387A. Three experiments were performed. Error bars show the standard error of the mean.

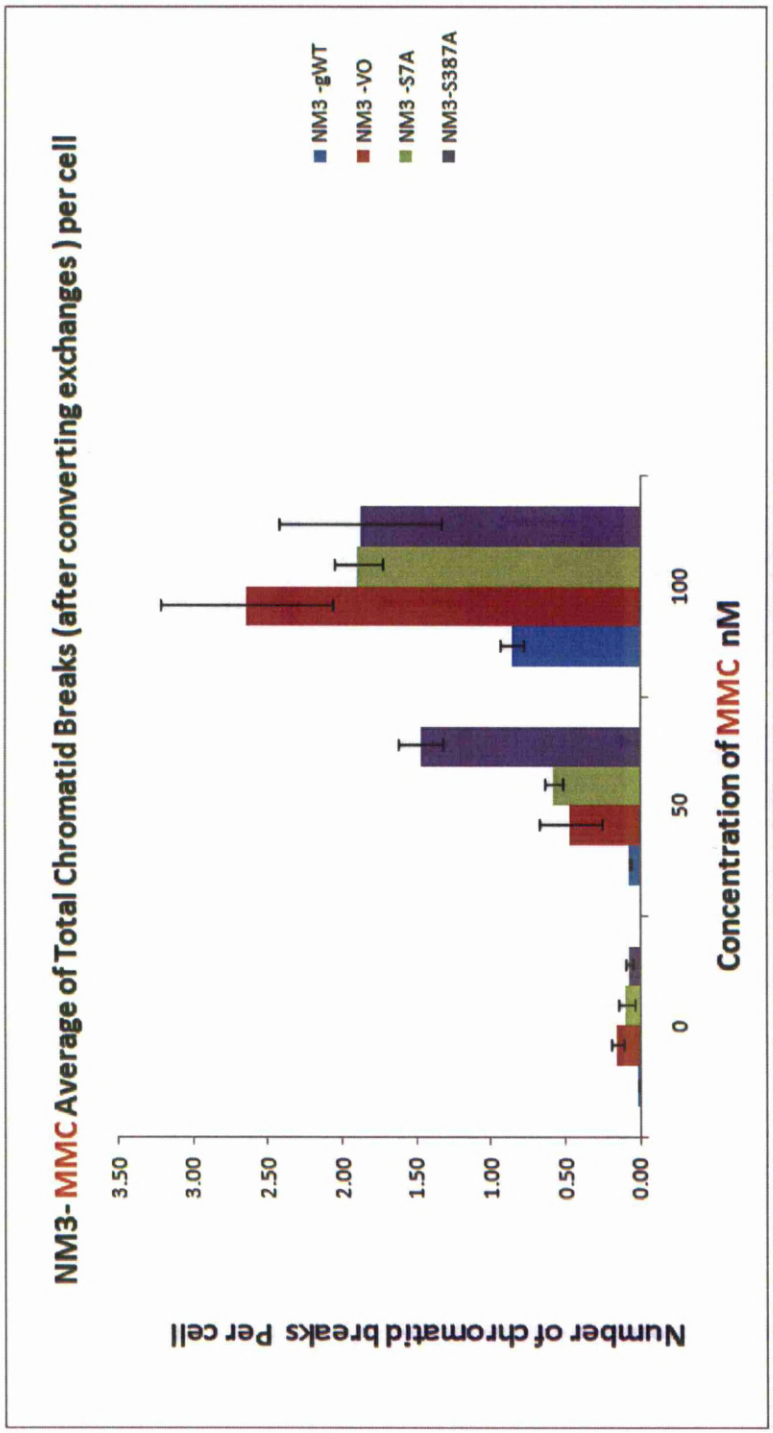

Figure (3.6): Illustrating MMC Average of Total Chromatid Breaks (after converting exchanges) per cell data using four cell lines: NM3-gWT, NM3-VO, NM3-S7A and NM3-S387A. Three experiments were performed. Error bars show the standard error of the mean.

3.2.2.3 Aberration types and predominance

Chromatid exchanges were either similar to or higher than chromatid breaks in NM3–gWT NM3–VO and NM3–S7A, particularly at the higher dose of 100 nM MMC. Whereas, in the NM3–S387A cell line it appears that chromatid breaks consistently exceeded chromatid exchanges, in both treated and untreated cellular cultures as seen in **Tables 3.1.A, 3.2.A and 3.3.A.** For example in **Table 3.1.A**, when treating NM3–S387A with a higher dose of 100 nM MMC, the number of chromatid breaks in fifty cells scored was 20 breaks compared to 9 chromatid exchanges, while NM3–S7A at the same MMC dose showed 15 chromatid breaks compared to 15 chromatid exchanges. Also, in **Tables 3.3.A**; at the higher dose of 100 nM MMC and fifty cells scored; NM3–S387A had 44 chromatid breaks compared to 24 chromatid exchanges, while NM3–S7A at the same MMC dose showed 18 chromatid breaks compared to 26 chromatid exchanges. This distinct difference in the types of chromatid aberrations suggests that phosphorylation of FANCG at serine-7 and serine-387 have distinct roles from one another in the repair of ICL.

For further analysis, the findings of the cytogenetic structural experiments presented in Tables tagged (A) were further extended in Tables tagged (B) where chromosome and chromatid exchanges were further subdivided into other more defined types such as dicentrics, rings, triradials, quadri-radials, taking into account the number of chromosomes and centromeres that are involved in complex exchanges. Also, in these tables the average number of total chromatid breaks per cell has been calculated after converting all the exchanges (chromosome and chromatid) into chromatid breaks as described in the Methods **(Section 2.1.2.10.4), Table 2.1, Figs. 2.2, 2.3, 2.3 and 2.4**.

From **Tables 3.1.B, 3.2.B and 3.3.B,** it can be seen that the predominant type of chromatid exchanges are those which involve two chromosomes (classified under complex arrangements). These chromatid exchanges involving two chromosomes are higher in occurrence than those involving three chromosomes. The involvement of more than three chromosomes in these complex arrangements does occur; however, it does so in a lesser extent, as illustrated in the same **Tables 3.1.B, 3.2.B and 3.3.B.** This can be seen in all cell lines especially in mutant cell lines, with the highest rate in *FANCG* null cell line NM3-VO.

3.2.2.4 Classification of cytogenetic aberrations

Both triradials and quadri-radials were noted separately despite the fact that they are classified together as chromatid exchanges. Monocentric, dicentric and tricentric triradials were noted. Also monocentric, dicentric, tricentric and quadri-centric quadri-radials were observed and recorded in **Tables 3.1.B, 3.2.B and 3.3.B.** The cytogenetic findings were recorded and classified in this way in order to account for the number of chromosomes involved in configuring any complex chromatid exchange-arrangement. This clear classification method allows the calculation of the minimal number of chromatid breaks required for the formation of any chromatid exchange by accounting for all the chromosomes that contribute to the formation of these complex chromatid exchange-arrangements.

EXPERIMENT – NM3- MMC

Table3.1.B

Cell line	Treatment MMC nM	No. Of cells scored	Triradials & no. Of centromeres			Quadri-radials & no. Of centromeres				Complex arrangements & no. Of chromosomes involved					No. Of Chromosome exchanges		No. Of Chromosome breaks	No. Of Chromatid breaks	No. Of TOTAL chromatid breaks [after converting all exchanges plus chromosome breaks]	Total Chromatid Breaks -after aberration converting per cell
			No. Of centromeres			No. Of centromeres				No. Of chromosomes					Type					
			1	2	3	1	2	3	4	2	3	4	5	Ring	Dicentric					
NM3-gWT	0	50	0	0	0	0	0	0	0	0	0	0	0	0	0		0	0	0	0
NM3-gWT	100	50	0	3	0	1	0	0	0	3	4	0	0	0	0		2	9	48	0.96
NM3-VO	0	50	0	0	0	1	0	0	0	0	0	0	0	0	0		3	2	12	0.24
NM3-VO	100	50	1	6	1	0	1	2	0	18	8	1	0	0	0		4	23	146	2.92
NM3-57A	0	50	0	0	0	0	0	0	0	0	0	0	0	0	0		1	0	2	0.04
NM3-57A	100	50	2	2	0	0	1	0	0	7	3	0	0	0	0		12	15	79	1.58
NM3-5387A	0	50	0	0	0	0	0	0	0	0	0	0	0	0	0		1	0	2	0.04
NM3-5387A	100	50	1	2	0	1	0	0	0	2	3	0	0	0	0		8	20	65	1.3

In order to calculate the total number of chromatid breaks, first chromosome breaks, chromosome exchanges and chromatid exchanges including triradials, quadri-radials and complex arrangements were converted to the minimal number of chromatid breaks required for the formation of each specific type of aberration. Then this minimal number of chromatid breaks required for the formation of those aberrations was added to the observed number of chromatid breaks. Then this total number of chromatid breaks has been presented as total chromatid breaks per cell.

EXPERIMENT – NM3-MMC

Table3.2.B

Cell line	Treatment MMC nM	No. Of cells scored	Triradials & no. Of centromeres			Quadri-radials & no. Of centromeres				Complex arrangements & no. Of chromosomes involved				No. Of Chromosome exchanges			No. Of Chromosome breaks	No. Of Chromatid breaks	No. Of TOTAL chromatid breaks [after converting all exchanges plus chromosome breaks]	Total Chromatid Breaks -after aberration converting per cell
			No. Of centromeres			No. Of centromeres				No. Of chromosomes				Type						
			1	2	3	1	2	3	4	2	3	4	5	Ring	Dicentric					
NM3-gWT	0	50	0	0	0	0	0	0	0	0	0	0	0	0	0		0	0	0	0
NM3-gWT	50	50	0	0	0	0	0	0	0	1	0	0	0	0	0		0	2	4	0.08
NM3-gWT	100	50	0	4	1	0	1	0	0	4	1	0	1	0	0		0	6	46	0.92
NM3-VO	0	50	0	0	0	0	0	0	0	0	0	0	0	0	0		2	1	5	0.1
NM3-VO	50	50	0	2	0	0	0	0	0	2	1	0	0	0	0		6	8	34	0.68
NM3-VO	100	50	6	2	0	2	3	0	1	18	5	1	0	0	1		13	36	174	3.48
NM3-S7A	0	50	0	0	0	0	0	0	0	0	1	0	0	0	0		2	2	10	0.2
NM3-S7A	50	50	0	1	0	0	0	1	0	0	0	0	0	0	0		7	9	32	0.64
NM3-S7A	100	50	3	6	0	0	3	0	0	10	3	3	0	0	0		5	14	107	2.14
NM3-S387A	0	50	0	0	0	0	0	0	0	0	0	0	0	0	0		2	0	4	0.08
NM3-S387A	50	50	2	1	0	0	1	0	0	4	1	1	0	0	0		9	19	66	1.32
NM3-S387A	100	50	6	1	0	1	2	0	0	3	1	0	0	0	0		5	20	69	1.38

In order to calculate the total number of chromatid breaks, first chromosome breaks, chromosome exchanges and chromatid exchanges including triradials, quadri-radials and complex arrangements were converted to the minimal number of chromatid breaks required for the formation of each specific type of aberration. Then this minimal number of chromatid breaks required for the formation of those aberrations was added to the observed number of chromatid breaks. Then this total number of chromatid breaks has been presented as total chromatid breaks per cell.

EXPERIMENT--NM3-MMC

Table3.3.B

Cell line	Treatment MMC nM	No. Of cells scored	Triradials & no. Of centromeres			Quadri-radials & no. Of centromeres				Complex arrangements & no. Of chromosomes involved				No. Of chromosomes				No. Of Chromosome exchanges		No. Of Chromosome breaks	No. Of Chromatid breaks	No. Of TOTAL chromatid breaks [after converting all exchanges plus chromosome breaks]	Total Chromatid Breaks -after aberration converting per cell
			No. Of centromeres			No. Of centromeres				No. Of chromosomes								Type					
			1	2	3	1	2	3	4	2	3	4	5	2	3	4	5	Ring	Dicentric				
NM3-gWT	0	50	0	0	0	0	0	0	0	0	0	0	0	0	0	0	0	0	0	0	1	1	0.02
NM3-gWT	50	50	0	0	0	0	0	0	0	0	0	0	0	0	0	0	0	0	0	1	1	3	0.06
NM3-gWT	100	50	1	1	1	0	1	0	0	4	2	0	0	0	0	0	0	0	0	0	5	35	0.7
NM3-VO	0	50	0	0	0	0	0	0	0	0	0	0	0	0	0	0	0	0	0	2	2	6	0.12
NM3-VO	50	50	0	0	0	0	2	0	0	1	0	0	0	0	0	0	0	0	0	1	5	13	0.26
NM3-VO	100	50	3	1	0	0	0	0	0	6	6	1	0	0	0	0	0	1	0	6	7	77	1.54
NM3-S7A	0	50	0	0	0	0	0	0	0	0	0	0	0	0	0	0	0	0	0	1	0	2	0.04
NM3-S7A	50	50	1	0	0	0	0	0	0	3	0	0	0	0	0	0	0	2	0	1	7	26	0.52
NM3-S7A	100	50	2	2	0	0	2	2	0	12	6	0	0	0	0	0	0	1	0	3	18	98	1.96
NM3-S387A	0	50	0	0	0	0	0	0	0	0	0	0	0	0	0	0	0	0	0	2	2	6	0.12
NM3-S387A	50	50	2	1	0	1	2	0	0	7	1	0	0	0	0	0	0	0	0	10	26	81	1.62
NM3-S387A	100	50	1	3	2	0	2	0	0	8	5	2	0	0	0	0	0	0	0	14	44	148	2.96

In order to calculate the total number of chromatid breaks, first chromosome breaks, chromosome exchanges and chromatid exchanges including triradials, quadri-radials and complex arrangements were converted to the minimal number of chromatid breaks required for the formation of each specific type of aberration. Then this minimal number of chromatid breaks required for the formation of those aberrations was added to the observed number of chromatid breaks. Then this total number of chromatid breaks has been presented as total chromatid breaks per cell.

3.2.3 Homologous recombination repair assay results

As can be seen from **Fig 3.7** the HRR-non-induced recombination frequencies of the selected cell lines are not very different from the spontaneous recombination frequency found in NM3-gWT, which was 1.4 X 10^{-6}. NM3-VO, NM3-S7A and NM3-S387A presented recombination frequencies of 1.2 X 10^{-6}, 2.2 X 10^{-6} and 1.7 X 10^{-6} respectively.

After exposure to100 nM MMC the induced level of recombination detected in the wild type cell line raised approximately 1000 fold compared to non-induced (from 1.4 x 10^{-6} to 10.3 x 10^{-4}). From **Fig 3.8,** NM3-VO, NM3-S7A and NM3-S387A exhibited reduced recombination frequencies of 1.8 X 10^{-4}, 3.4 X 10^{-4} and 4.9 X 10^{-4} respectively, which are equivalent to about 5.8, 3 and 2 fold reductions in HRR respectively compared to that of NM3-gWT 10.3 X 10^{-4}. The highest homologous recombination rate is seen in NM3-gWT and the lowest HRR rate is shown in NM3-VO, while an intermediate HRR rate is demonstrated by NM3-S7A and NM3-S387A cells. This indicates that homologous recombination is induced in all these cell lines post MMC treatment including the null cell line, indicating that some level of HRR takes place even in the absence of the FANCG protein. However, NM3-VO did exhibit the greatest reduction in HRR indicating the importance of FANCG in proficient HRR, while partial reduction in *FANCG* phospho-mutant NM3-S7A and NM3-S387A cell lines suggests the occurrence of partial or sub-optimal repair in these *FANCG* phospho-mutant cells. This is compared to the highest HR rate presented by NM3-gWT that suggests that for proficient HRR of ICL to occur, FANCG presence and its phosphorylation sites S7 and S387 are critical for ICL repair.

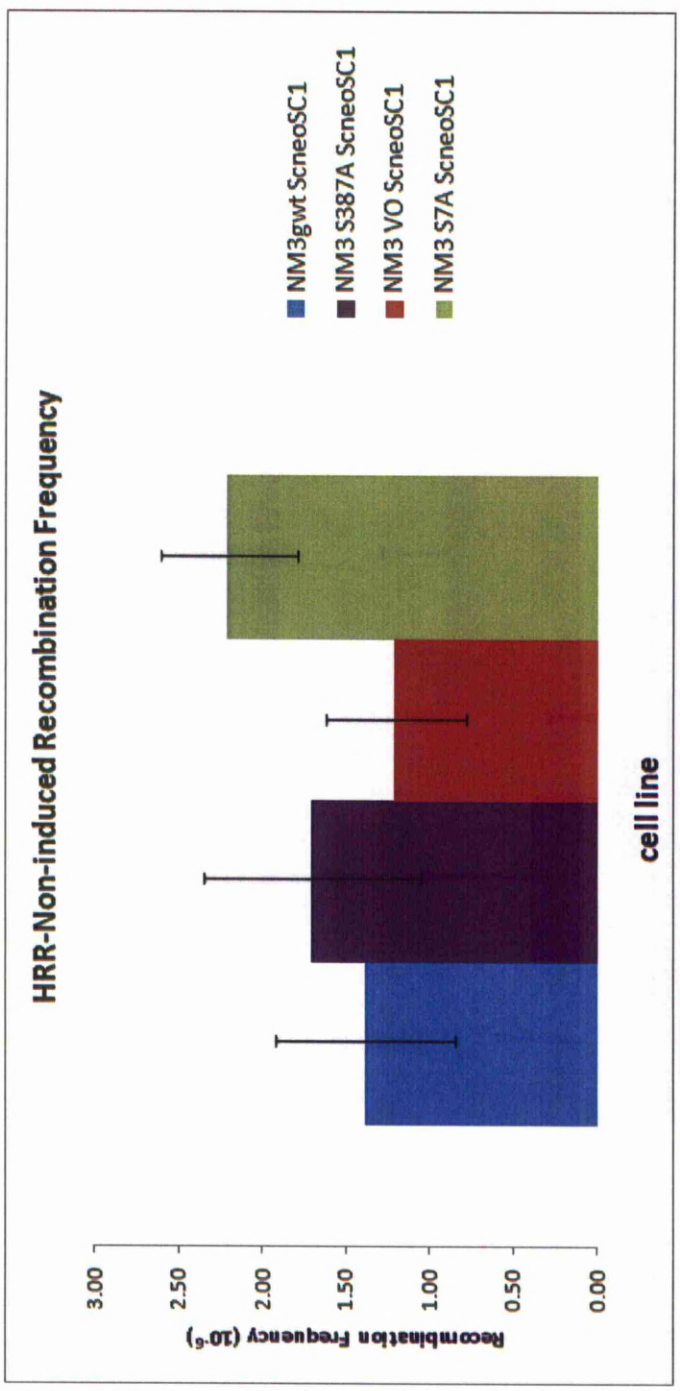

Figure (3.7): Illustrating **HRR-Non-induced recombination frequency** results. The data presented using four cell lines: NM3-gWT, NM3-VO, NM3-S7A and NM3-S387A. Three experiments were performed. Error bars show the standard error of the mean.

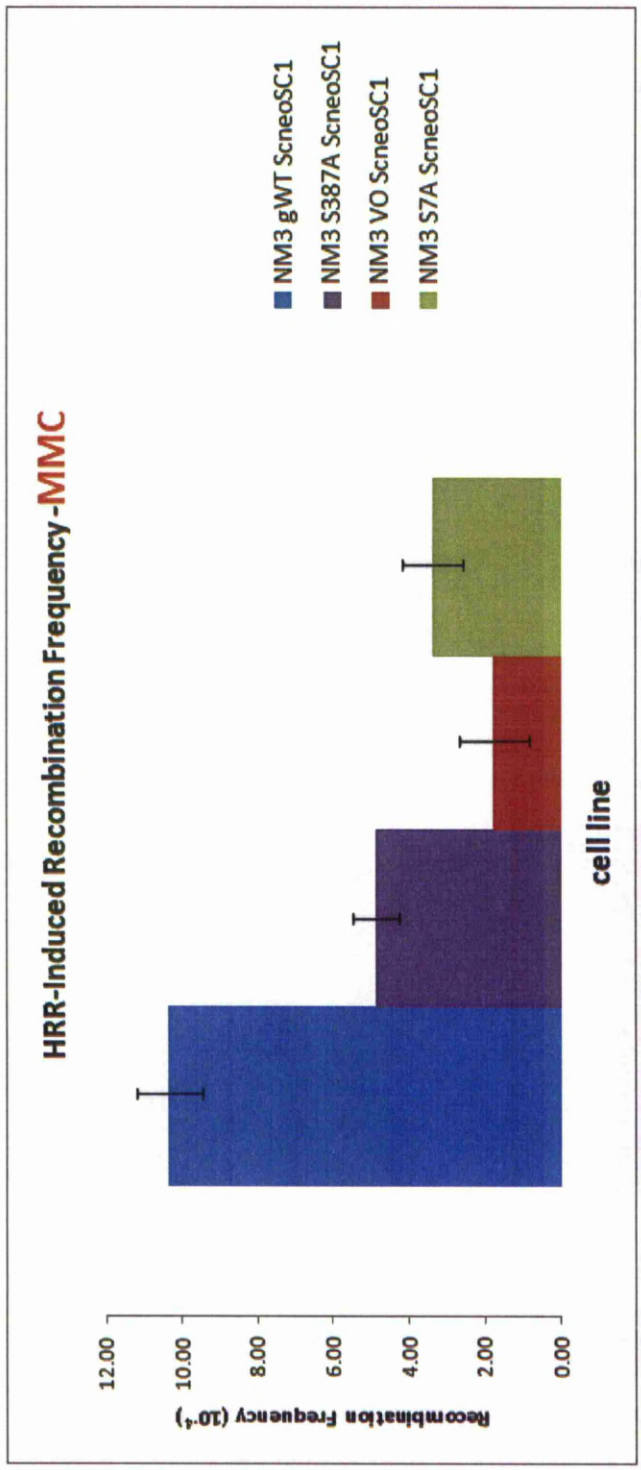

Figure (3.8): Illustrating **HRR-Induced recombination frequency** results after exposure to MMC. The data presented using four cell lines: NM3-gWT, NM3-VO, NM3-S7A and NM3-S387A. Three experiments were performed. Error bars show the standard error of the mean.

3.3 Discussion

The role of FANCG in ICL repair has been investigated in this chapter. Here, it has been shown that expression of FANCG is required for optimal repair of ICLs. This is based on the result that in the complete absence of FANCG, NM3-VO **(Fig. 3.1** and **Fig. 3.2)** cells are hypersensitive to the DNA inter-strand linking agent MMC. Furthermore, it has been shown that even if FANCG is being expressed, but carries specific mutations at known phosphorylation sites, then the function of FANCG is compromised as the cells are also hypersensitive to MMC. This indicates that FANCG must play a role in the repair processes to remove ICLs from the DNA and that post-translational modifications of FANCG are required for this.

It was also determined that NM3 *FANCG* null cells exhibit a severe reduction in homologous recombination repair in the vector-based assay. In addition, cells expressing the phosphorylation-site mutations S7A and S387A exhibit levels of HRR intermediate to that of the null and wild type cell lines. It is, however, important to remember that the HRR defects observed may not necessarily indicate a direct defect in homologous recombination. Failure to correctly process the ICLs induced by MMC (for example by ICL unhooking and subsequent steps may not generate substrates upon which homologous recombination can act. The reduction of HRR observed in NM3-VO, NM3-S7A or NM3-S387A may represent a defect or defects in the repair of ICLs that is upstream of HRR.

It is proposed that the first stage in ICLs repair is unhooking of the ICL (**Section 1.2.7.2** for details**).** It is known that the FA core complex is involved and promotes this process, but exactly how does this occur remains unclear **(Wang and Lambert, 2010)**. In addition, it is known that the FA core complex promotes translesion synthesis across the unhooked lesion **(Moldovan and**

D'Andrea, 2009; D'Andrea, 2010). FANCG is an integral part of the FA core complex and if not expressed this complex fails to form, so that unhooking and translesion synthesis will be compromised. In the cell lines carrying the specific phosphorylation mutations, the core complex does form and so that it might be assumed that the ICL unhooking and translesion synthesis is normal in these cell lines. This may explain why an intermediate cellular sensitivity is observed in these cell lines compared to the complete null, NM3-VO. However, it remains a possibility that the presence of a FANCG protein mutated at its phosphorylation sites in the core complex may result in sub-optimal activity of the complex even though FANCD2 mono-ubiquitination still occurs.

The accumulation of unrepaired ICLs is a serious cellular problem. ICLs lead to stalled replication forks that will require a combination of repair pathways to restart the replication process. The exact mechanism of mammalian ICLs repair is still not very clear **(Wang and Lambert, 2010)**. However, it is believed that removal of the unhooked ICLs may involve several repair pathways including NER and may involve several mismatch repair proteins including the MMR protein complexes MutSβ and MutLα **(Zhang *et al.*, 2007; Peng *et al.*, 2007).** In 2010, **Wang and Lambert** established through the use of yeast two hybrid analyses that FANCG interacts with ERCC1-XPF endonuclease which mediates the unhooking of ICLs **(Bhagwat *et al.*, 2009),** suggesting that FANCG is a key player in the ICL unhooking repair process, through functioning both in the FA core complex and in the ERCC1-XPF complex. It would be interesting to determine whether the XPF-ERCC1 complex forms in the phospho-specific mutated cell lines and whether the S7A and S387A proteins interact with XPF-ERCC1.

Once the ICLs are removed by a combination of unhooking and lesion removal then, the resulting double strand breaks have to be repaired by either HRR or NHEJ **(Sections 1.2.6.1** and

1.2.6.2 for details). Previous work in the Liverpool laboratory has shown that FANCG forms the G-BRCA2 complex **(Wilson *et al.*, 2008).** This complex, through its association with the HRR proteins BRCA2, and XRCC3, is postulated to be part of the HRR pathway. Here, further evidence is shown that this is the case as in the complete absence of FANCG (NM3-VO), HRR is severely compromised after exposure to MMC **(Fig 3.8).** Furthermore, if either S7 or S387 is mutated, the level of HRR detected is also reduced, but not to the extent seen in the null mutant. This supports the findings of **Wilson *et al.*, (2008),** who showed that phosphorylation of serine 7 is required for the G-BRCA2 complex to form. Therefore, if HRR is compromised then it is thought that NHEJ is the favoured pathway for double-strand breaks. This would mean if the error-prone NHEJ was taking place in the absence of error-free HRR, then this would be detectable as gross chromosome aberrations. It was also shown that NM3-S387A exhibited a reduction in HRR. It has been shown previously that the FANCG-S387A protein is able to form the G-BRCA2 complex **(Wilson *et al.*, 2008).** It may be that the NM3-S387A cells are proficient for homologous recombination *per se*, but are defective in processing ICLs upstream of homologous recombination.

From the results section it is clear that when FANCG is missing, a distinct abnormal cytogenetic profile is noted post MMC treatment. An elevated rate of chromosome aberrations, mainly of the chromatid type, was recorded in the *FANCG* mutant cells. This response of *FANCG* mutant cells to MMC is clearly seen in **Tables 3.1.A, 3.2.A and 3.3.A,** where the distribution profiles of chromatid aberrations is presented. *FANCG* mutant cell lines illustrated amplified cytotoxicity (elevated hypersensitivity) by the cross-linking agent MMC. Accumulation of chromosomal aberrations post exposure to MMC was observed. This suggests that the defective ICL repair

resulting from FANCG absence or mutating its phospho-sites S7 and S387 is visualised as gross cytogenetic aberrations.

The cytogenetic findings of predominance of chromatid type aberrations rather than chromosomal type aberrations post MMC treatment is in agreement with findings of **Godthelp *et al.*, (2006)** who reported predominance of MMC induced chromatid type aberrations (exchanges and breaks) utilizing FA human B lymphoblastoid cells. **Godthelp *et al.*, (2006)** reported predominance of chromatid breaks in HSC72 (FA-A) and HSC62 (FA-D1) cells, while EUFA423 (FA-D1) cells had predominance in chromatid exchanges.

The cytogenetic findings of predominance of chromatid exchanges is consistent with **Marx *et al.*, (1983)** who indicated the predominance of complex exchange configurations in diepoxybutane (DEB) - treated FA human lymphocytes. MMC induced chromatid exchanges have also been reported as the predominant aberration type in 1996 by **Busch *et al.*,** who used an MMC-sensitive rodent line, UV40 which is a *FANCG* mutant cell line mutated at exon 1 **(Lamerdin *et al.*, 2004).** These findings of predominance of chromatid exchanges are also consistent with **Wiegant *et al.*,** findings in 2006 who utilised V-C8 Chinese hamster mutant cell line defective in BRCA2 and have demonstrated higher levels of MMC induced CAs, particularly of the chromatid type compared to that of the wild-type cells. These findings of chromatid exchange aberrations predominance are consistent with our findings of chromatid exchange aberrations predominance in NM3-VO and NM3-S7A cells. This predominance of the chromatid exchange aberrations in NM3–VO and NM3–S7A cells suggest that NHEJ was the main available repair pathway in G-BRCA2 complex deficient NM3-VO and NM3-S7A cells to repair MMC induced DNA cross links, as exchanges reflect mis-repair by error prone-NHEJ.

Nevertheless, one paper by **Liu *et al.,*** in 1997 reported MMC-induced chromatid breaks to be predominant in UV40 (*FANCG* mutant).

On the other hand, the cytogenetic findings of predominance of the chromatid breaks in (NM3 - S387A) cells post MMC treatment is not an isolated finding, as others have also reported similar observations. Utilizing human dermal fibroblasts, **Latt *et al.,* (1975)** also reported increased MMC induced chromatid breaks. Prevalent MMC induced chromatid breaks with sporadic quadri-radials occurrence have been pointed out by **Duckworth-Rysiecki *et al.,* (1984)** using FA human lymphocytes post MMC or DEB treatment. Moreover, **Auerbach *et al.*, (1979)** had reported predominance of DEB induced chromatid breaks in FA human fetal cells. The predominance of DEB and MMC induced chromatid breaks have been also demonstrated by **Rosendorff and Bernstein, (1988)** using FA human lymphocytes and have been illustrated by **Tomkins *et al.*, (1998)** using a mouse cell line defective in FA (C) particularly post MMC exposure. These findings of chromatid breaks predominance are consistent with our findings chromatid breaks predominance in NM3 -S387A cells. This predominance of the chromatid breaks suggests that the NHEJ repair pathway in NM3 -S387A may have been less involved in the repair of (ICLs) and that HRR or other repair pathways may have been more available. In NM3 -S387A cells, the FANCG complexes are present (the FA-core and the G-BRCA2 complexes), nevertheless predominance of chromatid breaks is observed. It is not clear why chromatid breaks predominate in NM3 -S387A cells, however one can speculate that the occurrence of chromatid breaks rather than chromatid exchanges in NM3 -S387A could have resulted from partial FANCG activity that sustains its ability to suppress NHEJ. If so, this might explain the predominance of chromatid breaks in these cells, as intermediates of ICL repair in NM3-S387A would not be mis-repaired by NHEJ (that would lead to exchanges) but instead

would remain unrepaired, leading to the observed chromatid breaks. The sub-optimal FANCG activity in NM3 -S387A cells could have affected only processing double strand breaks down stream without affecting the unhooking step upstream. Alternatively, the formation of the G-ERCC1-XPF complex may be dependent on S387 phosphorylation reducing the unhooking of ICLs upstream which may have led to the prevalence of chromatid breaks.

Taken these findings together, these observations further support the view that the G-BRCA2 is very likely promotes proficient HRR to sustain genomic stability.

If HRR were compromised in the *FANCG* mutated cell lines then one would expect to observe an increase in the number of exchanges in these cell lines. From **Tables 3.1.A, 3.2.A and 3.3.A** it is clear that this is indeed the case, with NM3-VO and NM3-S7A having predominantly chromatid exchanges after MMC damage. This gives further evidence that in response to ICL damaging agents that action of FANCG is required through the three distinct complexes; FA core complex, G-ERCC1-XPF for unhooking and G-BRCA2 for HRR.

FANCG phospho-mutant cells S7A and S387A had intermediate levels of MMC hypersensitivity as shown by growth inhibition data **(Fig.3.3)**, intermediate levels of CA as shown by the average of total chromatid breaks per cell **(Fig.3.6)** at 100 nM MMC and illustrated intermediate levels of HRR as shown in **Fig.3.8.** This suggests the occurrence of partial repair in these phospho-mutant cells. The core complex which forms in NM3-S7A may contribute to this partial repair. In NM3-S387A, despite the fact that both the FA core and G-BRCA2 complexes are formed, the function of FANCG may have become sub-optimal due to the phospho-mutation at S387 site. Alternatively, phosphorylation of serine-387 may be required for the interaction of FANCG with the ERCC1-XPF endonuclease and reduced unhooking of ICLs might lead to the prevalence of

chromatid breaks in the NM3-S387A cell line. This possibility needs further investigation. The different predominating types of aberrations produced by NM3-S7A (chromatid exchanges) and NM3-S387A (chromatid breaks), indicate that NHEJ has been more active in NM3-S7A, probably due to the absence of G-BRCA2 complex resulting in more chromatid exchanges. Conversely, NHEJ has been less active in NM3-S387A, probably due to the presence of G-BRCA2 complex, and possibly also to continued suppression of NHEJ, even when *FANCG* is mutated at S387 resulting in the predominance of chromatid breaks. This signifies the importance of FANCG and its phosphorylation sites in determining the repair pathway in ICL repair.

It is worth mentioning that with the introduction of molecular cytogenetics, florescent in situ hybridization (F.I.S.H.) around the mid 90's, it revealed the more subtle chromosomal-exchanges that could not be detected through classical cytogenetics. Such chromosomal-exchanges would include small para-centric or peri-centric inversions, balanced or non-balanced translocations, micro-deletions, or amplifications. Florescent in situ hybridization implemented whole chromosome paints, whole arm chromosome paints, centromeric, telomeric and specific sequence probes in order to reveal a higher degree of chromosomal instability than previously reported **(Savage and Simpson, 1994; Savage, 2002; Obe *et al.*, 2002).** Had these methods been implemented in this project they would have possibly given a more in depth insight of the extent of instability encountered by FA cells and further explored the types of chromosome and chromatid aberrations produced by FA cells **(Van Limbergen, *et al.*, 2002; Sra *et al.*, 2005).**

As pointed earlier in this discussion the reduction in the HRR assay utilized may either reflect a direct defect in homologous recombination repair of the DSB generated during the course of ICL processing by the FA pathway, or alternatively, a defect in processing the ICL correctly to

generate a substrate upon which homologous recombination may act. In order to further elucidate the function of FANCG and the role of the phosphorylations in HRR and the FA pathway it was decided to carry out an investigation using an agent (phleomycin) that directly induces both single-strand and double-strand breaks in DNA. As these lesions may be acted upon by homologous recombination directly, without further processing (unlike ICLs), it should be possible to gain insight into whether FANCG and its phosphorylated isoforms function directly in homologous recombination. If, as suggested above, the G-BRCA2 complex has a direct role in homologous recombination repair, it would be anticipated that NM3-S7A and NM3-VO cells would be defective in the repair of the DNA strand-breaks induced by phleomycin. This hypothesis will be tested in the next chapter (Chapter-4).

3.4 Summary of the chapter

- It has been demonstrated that NM3 cell lines expressing FANCG proteins mutated at its serine 7 and serine 387 phosphorylation sites exhibit intermediate hypersensitivity to the inter-strand cross-linking agent MMC, indicating the importance of these post-translational modifications in ICL repair.
- Consistent with their cellular hypersensitivity to MMC, NM3-S7A and NM3-S387A cells exhibit reduced rates of MMC-induced homologous recombination repair in a plasmid-based reporter assay, at a level that is intermediate to that shown by the null mutant cell line (NM3-VO) and the wild type cell line (NM3-gWT).

- NM3-VO cells exhibit a large increase in MMC-induced chromosomal aberrations, these aberrations being predominantly chromatid aberrations, with chromatid exchanges being the most prevalent aberrations observed.
- Consistent with their intermediate cellular hypersensitivity to MMC, NM3-S7A and NM3-S387A cells exhibit increased levels of chromosomal aberrations in response to MMC, although these are at a lower level than those observed in NM3-VO.
- Despite showing similar overall increases in MMC-induced chromosomal aberrations, the predominant type of aberration differs in NM3-S7A and NM3-S387A. Chromatid exchanges are more common in NM3-S7A, while chromatid breaks are more common in NM3-S387A. This suggests different functions of FANCG are associated with these two phosphorylation sites of FANCG.
- As FANCG is known to participate in at least 3 different protein complexes in the FA pathway (FA core complex, G-BRCA2 complex and G-XPF-ERCC1 complex), it is possible that the differing functions of the phospho-Ser7-FANCG and phospho-Ser387-FANCG proteins are mediated through different protein complexes.
- As it is known that phosphorylation of FANCG at Ser7 is required for the formation of the G-BRCA2 complex (that contains two proteins, BRCA2 and XRCC3, known to participate in HRR), it seems likely that this complex is required for the repair, by HRR, of the double-strand breaks that arise indirectly from the processing of ICLs. This hypothesis will be tested in the next chapter using an agent (phleomycin) that induces direct DNA strand breaks.
- Given that mutation of S387A has no effect on the formation of the G-BRCA2 complex, it is proposed that this Ser387 phosphorylation is important "upstream" of HRR in the

repair of ICLs, possibly in unhooking or translesion synthesis stages. The observed reduction of HRR in NM3-S387A using the SCneo assay may result from the failure to process ICLs to a point where they are substrates for HRR. The presence of predominantly chromatid breaks in NM3-S387A also suggests that NHEJ is not significantly active in NM3-S387A (be it through the failure to generate double-strand breaks upon which NHEJ can act or continued suppression of NHEJ).

Chapter-4

Investigating the role of FANCG protein in the repair of induced DNA double strand breaks

4.1Introduction

4.1.1 DNA strand breaks

In chapter 3 it was shown that FANCG functions in the repair of ICL, most likely in upstream events that lead to the generation of a DNA double-strand break (DSB) and subsequently repair of that DSB by HRR. In this chapter, the focus is on the repair of another type of DNA damage, DNA strand breaks, and more specifically, directly-induced DNA double-strand breaks (DSBs). DSBs may be produced post exposure to exogenous elements such as chemical DNA-damaging agents, radiation or X-rays. DSBs may also appear at natural replication pause sites when DNA polymerases stall **(Rothstein *et al.*, 2000).**

4.1.2 NM3 cells hypersensitivity to radiomimetic agents

Evidence for FANCG being involved in other repair pathways other than the repair of ICL comes from work showing that the *FANCG* mutated cell line NM3, exhibited hypersensitivity not only to cross linking agents such as MMC, DEB and chlorambucil but also to radiomimetic agents bleomycin and streptonigrin and the monofunctional alkylating agent EMS. The

hypersensitivity of NM3 to bleomycin was 7.5 fold compared to 4.3 fold hypersensitivity to MMC (**Wilson *et al.*, 2001**). This hypersensitivity to bleomycin had also been reported in other *FANCG* mutant Chinese hamster ovary cell lines **(Busch *et al.*, 1996; Tebbs *et al.*, 2005).**

As previously mentioned the G-BRCA2 complex is composed of FANCD1/BRCA2-FANCD2-FANCG-XRCC3 (**Wilson *et al.*, 2008**) and research has shown that the CHO cell lines mutated for either *XRCC3* (irs1SF) or *BRCA2* (VC-8) are hypersensitive to radiomimetic agents **(Fuller and Painter, 1988; Overkamp *et al.*, 1993).** Given this information, further backed by research showing that both XRCC3 and BRCA2 interacted directly with FANCG **(Hussain *et al.*, 2003; Hussain *et al.*, 2004; Hussain *et al.*, 2006),** it was decided to investigate whether FANCG is involved in the repair of DSB induced by the radiomimetic agent, phleomycin. Furthermore, to investigate whether the post translational modifications of FANCG optimize this function, as they do for the repair of ICLs.

4.1.3 Cell lines used in this chapter

The cell lines used in this chapter are the same cell lines used in Chapter 3; NM3, NM3–VO, NM3–S7A, NM3–S387A and NM3–gWT.

4.2 Results

4.2.1 Survival assays results

To assess the degree of cellular hypersensitivity of these cell lines to phleomycin, initial survival experiments were carried out. From **Figure 4.1** it can be seen that NM3-VO is 4.6 fold hypersensitive to phleomycin compared to NM3-gWT in survival assays on the basis of D_{37} values (dose required to reduce survival to 37%). The NM3-S7A cell line was 3.6-fold hypersensitive to phleomycin, and is similar in response to NM3-VO **Fig. 4.1**. This shows that FANCG is involved in the repair of phleomycin-induced DNA damage and that phosphorylation of serine 7 is required for optimal repair of this damage. The D_{37} for NM3-S7A was 350 ng/ml and 270 ng/ml for NM3-VO, compared to a D_{37} of 1240 ng/ml for NM3-gWT cell line **(Fig. 4.1)**. NM3-S387A cell line survival data were very similar to NM3-gWT cell line **(Fig. 4.1)** suggesting that phosphorylation of serine 387 is not critical for the repair of phleomycin-induced DNA damage. Once established, the D_{37} value was the starting point for determining the doses required for the CA assay. The highest dose selected for testing reduced extensively the mitotic index (MI), but only to the extent where sufficient mitotic cells could still be found for chromosomal analysis. Triplicate cultures from each cell line for each dose were set allowing more cells to be scored and improving the assays' sensitivity.

4.2.2 Growth inhibition assays results

As phleomycin-hypersensitivity had not previously been shown in NM3 cells, growth inhibition assays were performed to confirm the survival assay results. NM3-VO has a GI-50 value of 265

ng/ml compared to 1030 ng/ml for NM3-gWT **(Fig. 4.2)**. This makes NM3-VO 3.9-fold hypersensitive to phleomycin compared to the corrected wild type NM3-gWT. NM3-S7A had a GI-50 value of 240 ng/ml and so is 4.3-fold hypersensitive to phleomycin. NM3-S387A had a GI-50 value of 690 ng/ml and so is only 1.5-fold more sensitive to phleomycin **(Fig. 4.2)**. Thus the results of the growth inhibition assays are consistent with findings of survival assays **Fig. 4.1**. This supports FANCG involvement in repairing DSBs and the importance of the phosphorylation of serine 7 in this repair.

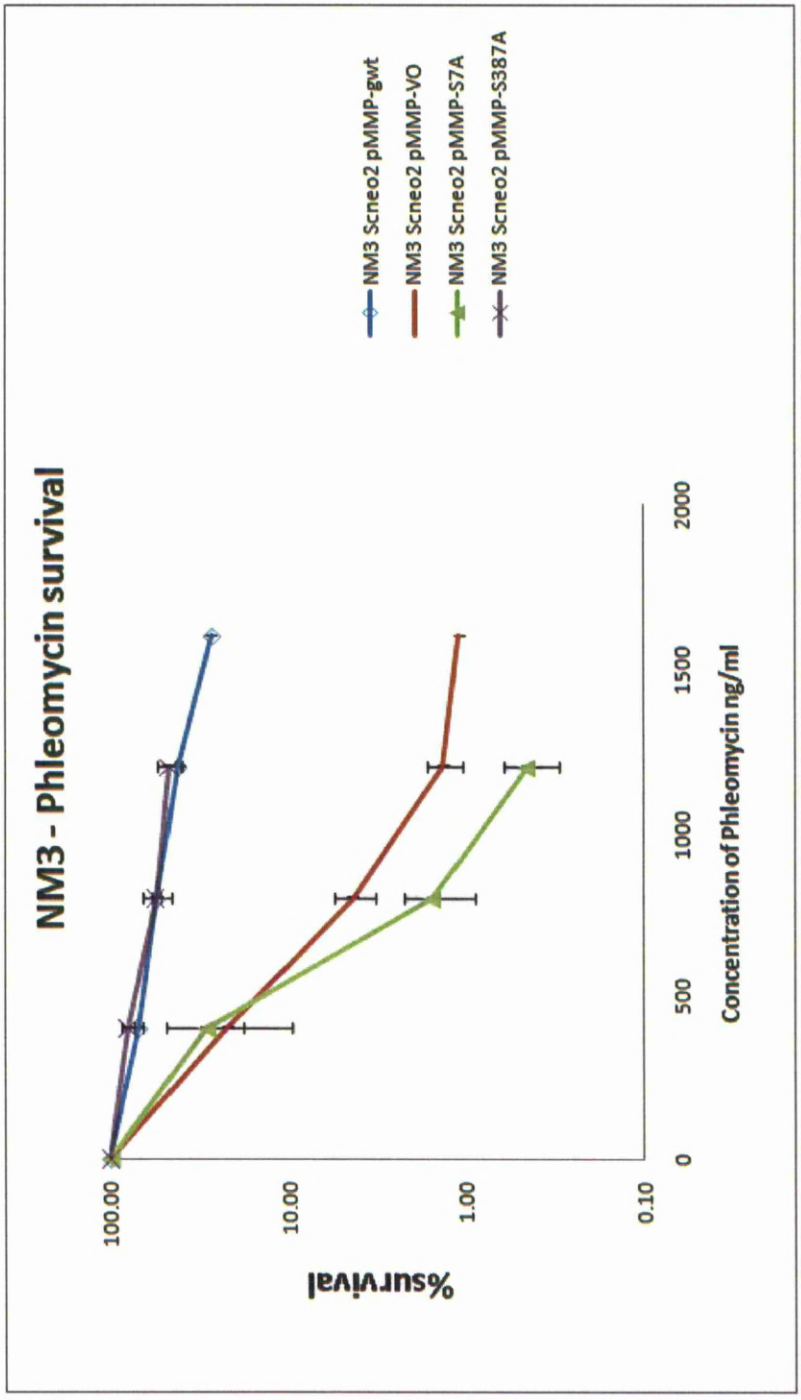

Figure (4.1): Illustrating Phleomycin survival data using four cell lines: NM3-VO, NM3-S7A, NM3-S387A and NM3-gWT. Cells were incubated for colony formation. As described previously cells plated in three 10-cm dishes at increasing numbers of cells per dish and were exposed continuously to the clastogen. After 10 days growth, colonies were fixed and stained with methylene blue for counting. Four experiments were performed for (NM3-VO and NM3-gWT) and two experiments for (NM3-S7A, NM3-S387A). Error bars show the standard error of the mean.

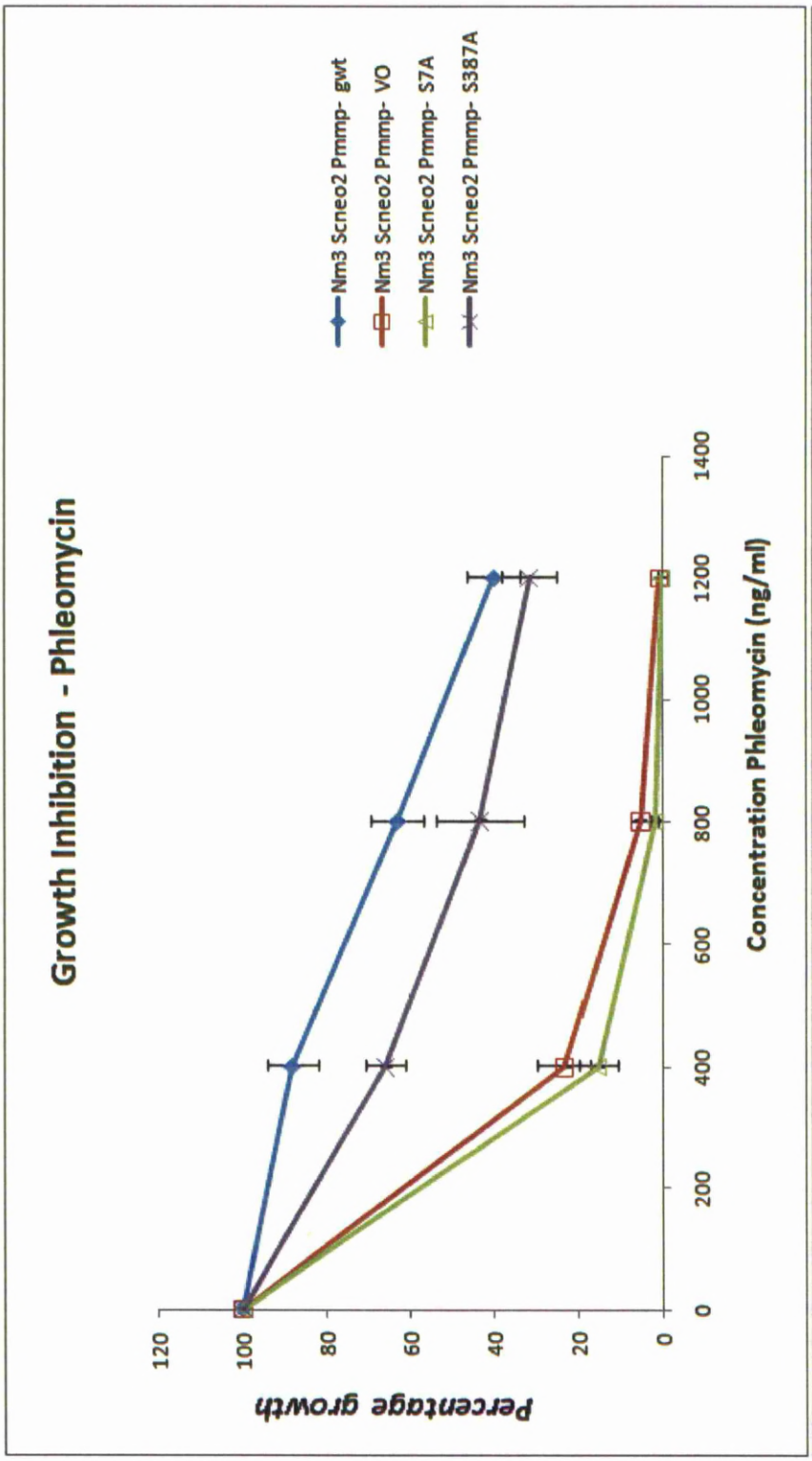

Figure (4.2): Illustrating phleomycin growth inhibition data using four cell lines: NM3-gWT, NM3-VO, NM3-S7A and NM3-S387A. Three experiments were performed. Error bars show standard error of the mean.

4.2.3 Chromosomal aberration analysis results

4.2.3.1 Preliminary metaphase analysis in NM3 and NM3-gWT post exposure to low doses of phleomycin

At this point it was decided to further investigate these findings at the chromosomal level through the exposure of NM3-VO and NM3-gWT to appropriate doses of phleomycin. In order to reach optimal experimental conditions, a reasonable growth index had to be obtained in metaphase spreads with minimal chromosomal overlapping **(Appendix-10)**. Initially, in the course of optimization, lower phleomycin doses were utilized and were gradually increased. **Tables 4.1 and 4.2** illustrate the type and number of chromosome aberrations presented when using these low doses of phleomycin. **Table 4.1** shows that using doses of 40 and 120 ng/ml phleomycin resulted in NM3 producing higher rates of chromosomal aberrations 0.16 and 0.23 aberration/cell respectively than that seen in NM3-gWT which are 0 and 0.01 aberration/cell respectively. The following experiment **(Table 4.2)** using doses of 80,120 and 160 ng/ml phleomycin resulted in CA rates in NM3 slightly higher that that shown by NM3-gWT **Table 4.1**. Also, when using the dose 120 ng/ml in both experiments **(Tables 4.1 and 4.2)** different numbers of CA per cell were obtained for NM3, 0.23 and 0.06 aberrations per cell respectively, despite using identical experimental conditions and this could not be explained. Although these readings illustrated that FANCG mutant cells presented an increased number of CA compared to NM3-gWT, it was decided to increase the phleomycin dose in an attempt to have a more distinct separation between the numbers of aberrations scored in the two cell lines and to avoid possible over lapping as a consequence of using low doses.

Table 4.3 demonstrates chromosome aberrations presented when using higher doses of phleomycin. Doses of 400, 600 and 800 ng/ml phleomycin resulted in NM3 producing chromosomal aberrations around 8-fold higher that NM3-gWT in response to the highest dose (800 ng/ml). There is a dose related increase in chromosomal aberrations in the NM3 cell line. However, NM3-gWT illustrated some resistance and presented fewer aberrations even at higher doses of phleomycin.

Table (4.1) Data summaries **phleomycin** treated cell lines and **structural** aberrations

Cell line	Treatment ng/ml	Total number of cells sampled	Chromatid based - aberrations		Chromosome based - aberrations		Gap per cell	Total aberrations without Gaps	Aberrations per cell
			Ctid-break	Ctid-exch	Chro-break	Chro-exch			
NM3-gWT	0	100	0	0	0	0	0.02	0	0
NM3-gWT	40	100	1	0	0	0	0	1	0.01
NM3-gWT	120	100	0	0	0	0	0.01	0	0
NM3-VO	0	100	1	6	0	0	0.05	7	0.07
NM3-VO	40	100	5	8	0	3	0.01	16	0.16
NM3-VO	120	100	11	8	0	4	0.07	23	0.23

Table abbreviations: Ctid-break: Chromatid break type aberration, Ctid**-exch:** Chromatid exchange type aberration, **Ctid-exch:** Chromatid exchange type aberration, **Chro-break:** Chromosome break type aberration, **Chro-exch:** Chromosome exchange type aberration.

Table (4.2) Data summaries **phleomycin** treated cell lines and **structural** aberrations.

Cell line	Treatment ng/ml	Total number of cells sampled	Chromatid based - aberrations		Chromosome based - aberrations		Gap per cell	Total aberrations without Gaps	Aberrations per cell
			Ctid-break	Ctid-exch	Chro-break	Chro-exch			
NM3-gWT	0	100	0	0	0	2	0.03	2	0.02
NM3-gWT	80	100	2	0	0	2	0.03	4	0.04
NM3-gWT	120	100	2	0	0	1	0.01	3	0.03
NM3-gWT	160	100	4	0	0	0	0.03	4	0.04
NM3-VO	0	100	1	1	0	0	0.03	2	0.02
NM3-VO	80	100	3	0	0	0	0.03	3	0.03
NM3-VO	120	100	4	1	0	1	0.01	6	0.06
NM3-VO	160	100	4	1	0	2	0.04	7	0.07

Table abbreviations: Ctid-break: Chromatid break type aberration, Ctid-**exch:** Chromatid exchange type aberration, **Ctid-exch:** Chromatid exchange type aberration, **Chro-break:** Chromosome break type aberration, **Chro-exch:** Chromosome exchange type aberration.

Table (4.3) Data summaries **phleomycin** treated cell lines and **structural** aberrations.

Cell line	Treatment ng/ml	Total number of cells sampled	Chromatid based - aberrations		Chromosome based - aberrations		Gap per cell	Total aberrations without Gaps	Aberrations per cell
			Ctid-break	Ctid-exch	Chro-break	Chro-exch			
NM3-gWT	0	100	2	0	0	0	0.01	2	0.02
NM3-gWT	400	100	3	0	0	1	0.04	4	0.04
NM3-gWT	600	100	4	0	0	0	0.03	4	0.04
NM3-gWT	800	100	3	0	0	0	0.01	3	0.03
NM3-VO	0	100	1	6	0	1	0.05	8	0.08
NM3-VO	400	100	8	2	1	2	0.04	13	0.13
NM3-VO	600	100	4	7	0	4	0.06	15	0.15
NM3-VO	800	100	8	13	0	3	0.14	24	0.24

Table abbreviations: Ctid-break: Chromatid break type aberration, Ctid**-exch:** Chromatid exchange type aberration, **Ctid-exch:** Chromatid exchange type aberration, **Chro-break:** Chromosome break type aberration, **Chro-exch:** Chromosome exchange type aberration.

4.2.3.2 The introduction of NM3-S7A cell line to phleomycin cytogenetic structural aberration assays using selected doses

After deciding the phleomycin doses to use in these cytogenetic experiments, a number of experiments were carried out using phleomycin doses of 1200 ng/ml and 1600 ng/ml on three cell lines; NM3-VO, NM3-S7A and NM3-gWT **Tables 4.4.A and 4.5.A**. However, the dose of 1600 ng/ml proved to be too high, resulting in excessive reduction of the mitotic index. Therefore, in the third experiment **Tables 4.6.A** the 1200 ng/ml dose was kept and a dose of 600 ng/ml used instead of 1600ng/ml. Another dose of 1000ng/ml phleomycin has been used in these experiments **(Table 4.7.A)**. The metaphase scores remained at 100 metaphases scored for the untreated negative controls, but was reduced to either 50 or 20 metaphases scored for the higher doses due to the prevalence of chromosomal aberrations. The percentage of aberrant cells was calculated and presented in **Tables 4.4.A, 4.5.A, 4.6.A and 4.7.A**.

4.2.3.3 The introduction of NM3-S387A cell line to phleomycin cytogenetic structural aberration assays using selected doses

Following the introduction of NM3-S7A cell line to the aberration assays, it was decided to include NM3-S387A cell line and use a phleomycin dose of 1000 ng/ml for these four cell lines; NM3-VO, NM3-S7A, NM3-S387A and NM3-gWT as shown in **Tables 4.7.A, 4.8.A, 4.9.A, 4.10.A and 4.11.A**.

4.2.3.4 Chromosome and chromatid aberration rates in control cell cultures

It can be noted that the number of aberrations per cell in untreated cell lines presented a spontaneous rate which did not exceed 0.16 aberration/cell as shown in **Tables 4.4.A, 4.5.A, 4.6.A, 4.7.A, 4.8.A, 4.9.A, 4.10.A and 4.11.A** and shown in **Figures 4.3, 4.4 and 4.5.** Virtually no aberrations were recorded for untreated NM3–gWT. The highest number of aberrations per cell for the untreated cells was that recorded for NM3– S7A 0.16 aberration/cell **(Table 4.9.A)** followed by NM3– VO 0.15 aberration/cell **(Table 4.4.A),** then NM3–VO 0.09 aberration/cell **(Table 4.8.A).** For NM3–S387A the highest number of aberrations per cell for the untreated cells was 0.06 aberrations per cell **(Table 4.9.A).** Also, from the same **Tables 4.4.A, 4.5.A, 4.6.A, 4.7.A, 4.8.A, 4.9.A, 4.10.A and 4.11.A and Figs. 4.3, 4.4 and 4.5** it can be seen that the percentage of aberrant cells that have occurred spontaneously was lowest in NM3–gWT and generally highest in both NM3–VO and NM3–S7A, followed by NM3–S387A.

4.2.3.5 Chromosome and chromatid aberration rates in treated cell cultures

Table 4.4.A shows that using doses of 1200 ng/ml phleomycin resulted in NM3-VO and NM3-S7A, producing higher rates of chromosomal aberrations per cell 1.72 and 2.61 aberrations per cell respectively compared to 0.1 aberration/cell found in NM3-gWT, which represents a 17.2- and 26.1-fold increase respectively. The same experimental conditions were used in **Table 4.5.A** and despite slight variation, the readings illustrated that *FANCG* mutant cell lines NM3-VO and NM3-S7A presented an increased number of CA compared to NM3-gWT. **Table 4.5.A** illustrates NM3-VO, NM3-S7A, producing higher rates of chromosomal aberrations per cell 1.6

and 3.25 aberration/cell respectively compared to 0.25 aberrations per cell found in NM3-gWT which represents about 6.4 and 13 fold increases respectively.

The same can be seen in **Table 4.7.A** when using doses of 1000 ng/ml phleomycin, where NM3-VO, NM3-S7A, produced higher rates of chromosomal aberrations per cell 1.18 and 1.5 aberration/cell respectively compared to 0.12 aberration/cell found in NM3-gWT, which represented 9.8 and 12.5 fold increase respectively. This suggests that in the absence of G-BRCA2 complex the phleomycin-induced damage repair pathway was defective, which led to increased levels of CAs in NM3-VO and NM3-S7A. On the other hand, NM3-S387A cells produced rates of chromosomal aberrations per cell similar to that of NM3-gWT cells as shown in **Tables 4.8.A, 4.9.A, 4.10.A, 4.11.A**. For example, in **Table 4.8.A** using a dose of 1000 ng/ml phleomycin, NM3-S387A cells produced 0.36 CA per cell compared to NM3-gWT with 0.32 CA per cell. This suggests that the mutation of the phosphorylation site FANCG-S387 did not affect the repair pathway for phleomycin-induced strand breaks and consequently that phosphorylation of FANCG at serine 387, unlike serine 7, is not required for efficient repair.

4.2.3.6 Average aberrations per cell, percentage aberrant cells and number of total chromatid breaks per cell

From the **Pooled Table 4.12** it can be seen that when using a dose of 1000 ng/ml phleomycin, the average aberrations per cell in the NM3–VO and NM3–S7A cell lines was 1.31 and 1.76 respectively, which is 5- and 6.8-fold respectively higher than that of the corrected wild type

NM3–gWT cells. NM3–S387A had 0.15 average aberrations per cell similar to the average for NM3–gWT (0.26 aberrations per cell).

In addition, for 1000 ng/ml phleomycin, the average percentage of aberrant cells in the NM3–VO and NM3–S7A was 56.8 and 67.2 % aberrant cells respectively, which is 3.1 and 3.7 fold higher than that of the corrected NM3–gWT cells. For NM3–S387A the average percentage of aberrant cells was 11.5% compared to an average of 18.2% for NM3–gWT **(Table 4.12).**

The average number of total chromatid breaks (after converting all the exchanges into chromatid breaks) per cell for 1000 ng/ml phleomycin was 3.25 and 4.12 chromatid breaks/cell in NM3–VO andNM3–S7A respectively, which is 7.2- and 9.2-fold higher than that of the corrected NM3–gWT cells. For NM3–S387A, the average number of total chromatid breaks was 0.27 chromatid breaks per cell compared to 0.45 chromatid breaks/cell for NM3–gWT **(Table 4.12).**

This elevation in structural aberrations in *FANCG* mutant cell lines NM3–VO and NM3–S7A can be clearly seen in graphs as average aberration per cell **(Fig. 4.3),** average percentage aberrant cells **(Fig. 4.4),** or as average total chromatid breaks per cell **(Fig. 4.5).** All of the NM3-phleomycin cytogenetic data shown in **Figs. 4.3, 4.4 and 4.5** supports one another and are consistent with the cellular survival and growth inhibition data. NM3–S387A and NM3–gWT cell lines exhibit proficient repair of phleomycin DNA induced damage and a reduced ability of NM3–VO and NM3–S7A cells to repair this phleomycin-induced DNA damage. This suggests that a mutation of the phosphorylation site FANCG-S387 did not affect the repair pathway for phleomycin induced DNA strand breaks, which is expected, as phosphorylation of this site is not required for the formation of the G-BRCA2 protein complex. It also suggests that in the absence of G-BRCA2 complex in NM3–VO and NM3–S7A cells, the repair pathway required to process phleomycin induced DNA damage in an error-free pathway, that does not result in chromosomal

aberrations was defective. It is likely that a more error-prone pathway, such as NHEJ, acted on these lesions instead.

Data-Table: Data summaries phleomycin treated cell lines and aberrations found in experiments

Table (4.4.A)

Cell line	Treatment Phleomycin ng/ml	Total number of cells sampled	Chromatid based - aberrations		Chromosome based - aberrations		Gaps per cell	Total aberrations without Gaps	Aberrations Per cell	% Aberrant cells	*Total Chromatid Breaks - after aberration converting per cell*
			Ctid-break	Ctid-exch	Chro-break	Chro-exch					
NM3-gWT	0	100	0	0	0	0	0.01	0	0	0	0
NM3-gWT	1200	100	2	5	1	2	0.06	10	0.1	6	0.36
NM3-gWT	1600	100	21	6	1	1	0.08	29	0.29	23	0.46
NM3-VO	0	100	5	0	8	2	0.18	15	0.15	14	0.29
NM3-VO	1200	100	66	89	7	9	0.26	172	1.72	60	4.17
NM3-VO	1600	100	91	141	9	9	0.23	250	2.5	78	5.93
NM3-S7A	0	100	2	0	1	0	0.09	3	0.03	3	0.04
NM3-S7A	1200	100	68	177	6	10	0.27	261	2.61	81	6.9
NM3-S7A	1600	100	90	118	7	13	0.3	228	2.28	80	5.9

Table abbreviations: Ctid-break: Chromatid break type aberration, Ctid-exch: Chromatid exchange type aberration, Chro-break: Chromosome break type aberration, Chro-exch: Chromosome exchange type aberration.

Data-Table: Data summaries **phleomycin** treated cell lines and aberrations found in experiments

Table (4.5.A)

Cell line	Treatment Phleomycin ng/ml	Total number of cells sampled	Chromatid based - aberrations		Chromosome based - aberrations		Gaps per cell	Total aberrations without Gaps	Aberrations Per cell	% Aberrant cells	*Total Chromatid Breaks - after aberration converting per cell*
			Ctid-break	Ctid-exch	Chro-break	Chro-exch					
NM3-gWT	0	100	0	0	0	0	0.01	0	0	0	0
NM3-gWT	1200	20	1	4	0	0	0.1	5	0.25	20	0.6
NM3-gWT	1600	20	3	5	0	0	0.1	8	0.4	30	0.8
NM3-VO	0	100	1	0	2	0	0.11	3	0.03	3	0.05
NM3-VO	1200	20	11	19	1	1	0.1	32	1.6	50	3.95
NM3-VO	1600	20	2	10	0	3	0.1	15	0.75	50	2.05
NM3-S7A	0	100	2	0	1	0	0.1	3	0.03	3	0.04
NM3-S7A	1200	20	18	42	2	3	0.3	65	3.25	75	7.3
NM3-S7A	1600	20	8	15	1	1	0.4	25	1.25	50	3

Table abbreviations: Ctid-break: Chromatid break type aberration, Ctid-exch: Chromatid exchange type aberration, Ctid-exch: Chromatid exchange type aberration, Chro-break: Chromosome break type aberration, Chro-exch: Chromosome exchange type aberration.

Data-Table: Data summaries **phleomycin** treated cell lines and aberrations found in experiments

Table (4.6.A)

Cell line	Treatment Phleomycin ng/ml	Total number of cells sampled	Chromatid based - aberrations		Chromosome based - aberrations		Gaps per cell	Total aberrations without Gaps	Aberrations Per cell	% Aberrant cells	*Total Chromatid Breaks - after aberration converting per cell*
			Ctid-break	Ctid-exch	Chro-break	Chro-exch					
NM3-gWT	0	100	1	0	1	0	0.03	2	0.02	2	0.03
NM3-gWT	600	50	5	2	0	0	0.08	7	0.14	10	0.2
NM3-gWT	1200	20	15	5	0	0	0.05	20	1	50	1.3
NM3-VO	0	100	1	0	4	3	0.02	8	0.08	7	0.21
NM3-VO	600	50	22	41	1	3	0.42	67	1.34	68	3.34
NM3-VO	1200	20	11	39	1	3	0.25	54	2.7	75	7.35
NM3-S7A	0	100	0	0	6	0	0.2	6	0.06	6	0.12
NM3-S7A	600	50	32	45	4	2	0.34	83	1.66	56	3.26
NM3-S7A	1200	20	6	34	0	0	0.1	40	2	75	4.6

Table abbreviations: Ctid-break: Chromatid break type aberration, Ctid-exch: Chromatid exchange type aberration, Ctid-exch: Chromatid exchange type aberration, Chro-break: Chromosome break type aberration, Chro-exch: Chromosome exchange type aberration.

Data-Table: Data summaries **phleomycin** treated cell lines and aberrations found in experiments

Table (4.7.A)

Cell line	Treatment Phleomycin ng/ml	Total number of cells sampled	Chromatid based - aberrations		Chromosome based - aberrations		Gaps per cell	Total aberrations without Gaps	Aberrations Per cell	% Aberrant cells	*Total Chromatid Breaks - after aberration converting per cell*
			Ctid-break	Ctid-exch	Chro-break	Chro-exch					
NM3-gWT	0	100	0	0	0	1	0	1	0.01	1	0.04
NM3-gWT	1000	100	5	7	0	0	0.02	12	0.12	7	0.19
NM3-VO	0	100	0	0	1	0	0.08	1	0.01	1	0.02
NM3-VO	1000	50	17	34	1	7	0.14	59	1.18	54	2.88
NM3-S7A	0	100	0	0	0	0	0.1	0	0	0	0
NM3-S7A	1000	50	14	50	5	6	0.3	75	1.5	72	4.1

Table abbreviations: Ctid-break: Chromatid break type aberration, Ctid-exch: Chromatid exchange type aberration, Ctid-exch: Chromatid exchange type aberration, Chro-break: Chromosome break type aberration, Chro-exch: Chromosome exchange type aberration.

Data-Table: Data summaries **phleomycin** treated cell lines and aberrations found in experiments

Table (4.8.A)

Cell line	Treatment Phleomycin ng/ml	Total number of cells sampled	Chromatid based - aberrations		Chromosome based - aberrations		Gaps per cell	Total aberrations without Gaps	Aberrations Per cell	% Aberrant cells	*Total Chromatid Breaks - after aberration converting per cell*
			Ctid-break	Ctid-exch	Chro-break	Chro-exch					
NM3-gWT	0	100	2	0	0	0	0.01	2	0.02	2	0.02
NM3-gWT	1000	50	5	7	1	3	0.06	16	0.32	30	0.74
NM3-VO	0	100	0	1	7	1	0.17	9	0.09	9	0.22
NM3-VO	1000	50	12	40	8	5	0.34	65	1.3	64	3.42
NM3-S7A	0	100	1	0	2	0	0.13	3	0.03	3	0.05
NM3-S7A	1000	50	33	52	8	11	0.3	104	2.08	72	5.26
NM3-S387A	0	100	4	0	2	0	0.13	6	0.06	6	0.08
NM3-S387A	1000	50	8	7	2	1	0.12	18	0.36	22	0.68

Table abbreviations: Ctid-break: Chromatid break type aberration, Ctid-exch: Chromatid exchange type aberration, Ctid-exch: Chromatid exchange type aberration, Chro-break: Chromosome break type aberration, Chro-exch: Chromosome exchange type aberration.

Data-Table: Data summaries **phleomycin** treated cell lines and aberrations found in experiments

Table (4.9.A)

Cell line	Treatment Phleomycin ng/ml	Total number of cells sampled	Chromatid based - aberrations		Chromosome based - aberrations		Gaps per cell	Total aberrations without Gaps	Aberrations Per cell	% Aberrant cells	*Total Chromatid Breaks - after aberration converting per cell*
			Ctid-break	Ctid-exch	Chro-break	Chro-exch					
NM3-gWT	0	100	1	0	0	0	0.06	1	0.01	1	0.01
NM3-gWT	1000	50	9	5	1	0	0.1	15	0.3	20	0.46
NM3-VO	0	100	3	0	7	0	0.18	10	0.1	9	0.17
NM3-VO	1000	50	23	42	6	10	0.26	81	1.62	66	4.06
NM3-S7A	0	100	6	0	10	0	0.33	16	0.16	16	0.26
NM3-S7A	1000	50	46	46	12	13	0.38	117	2.34	78	5.06
NM3-S387A	0	100	2	0	0	0	0.02	2	0.02	2	0.02
NM3-S387A	1000	50	3	0	0	0	0	3	0.06	6	0.06

Table abbreviations: Ctid-break: Chromatid break type aberration, Ctid-exch: Chromatid exchange type aberration, Ctid-exch: Chromatid exchange type aberration, Chro-break: Chromosome break type aberration, Chro-exch: Chromosome exchange type aberration.

Data-Table: Data summaries **phleomycin** treated cell lines and aberrations found in experiments

Table (4.10.A)

Cell line	Treatment Phleomycin ng/ml	Total number of cells sampled	Chromatid based - aberrations		Chromosome based - aberrations		Gaps per cell	Total aberrations without Gaps	Aberrations Per cell	% Aberrant cells	*Total Chromatid Breaks - after aberration converting per cell*
			Ctid-break	Ctid-exch	Chro-break	Chro-exch					
NM3-gWT	0	100	0	0	0	0	0.01	0	0	0	0
NM3-gWT	1000	50	15	8	0	0	0.14	23	0.46	28	0.76
NM3-VO	0	100	2	1	1	0	0.25	4	0.04	3	0.06
NM3-VO	1000	50	21	62	6	4	0.26	93	1.86	64	4.78
NM3-S7A	0	100	2	0	2	0	0.36	4	0.04	4	0.06
NM3-S7A	1000	50	50	62	2	2	0.48	116	2.32	74	5.16
NM3-S387A	0	100	1	0	0	1	0.02	2	0.02	2	0.05
NM3-S387A	1000	50	4	1	0	0	0.1	5	0.1	10	0.2

Table abbreviations: Ctid-break: Chromatid break type aberration, Ctid-exch: Chromatid exchange type aberration, Ctid-exch: Chromatid exchange type aberration, Chro-break: Chromosome break type aberration, Chro-exch: Chromosome exchange type aberration.

Data-Table: Data summaries **phleomycin** treated cell lines and aberrations found in experiments

Table (4.11.A)

Cell line	Treatment Phleomycin ng/ml	Total number of cells sampled	Chromatid based - aberrations		Chromosome based - aberrations		Gaps per cell	Total aberrations without Gaps	Aberrations Per cell	% Aberrant cells	*Total Chromatid Breaks - after aberration converting per cell*
			Ctid-break	Ctid-exch	Chro-break	Chro-exch					
NM3-gWT	0	50	0	0	0	0	0	0	0	0	0
NM3-gWT	600	50	0	0	0	0	0.02	0	0	0	0
NM3-gWT	1000	50	3	0	1	0	0.02	4	0.08	6	0.1
NM3-VO	0	50	0	0	0	0	0	0	0	0	0
NM3-VO	600	50	7	3	1	0	0.18	11	0.22	20	0.36
NM3-VO	1000	50	11	10	7	1	0.26	29	0.58	36	1.12
NM3-S7A	0	50	1	0	0	0	0.06	1	0.02	2	0.02
NM3-S7A	600	50	14	13	6	2	0.32	35	0.7	42	1.5
NM3-S7A	1000	50	18	7	1	2	0.26	28	0.56	40	1.02
NM3-S387A	0	50	1	0	0	0	0.02	1	0.02	2	0.02
NM3-S387A	600	50	1	0	3	0	0.04	4	0.08	6	0.14
NM3-S387A	1000	50	1	0	3	0	0.04	4	0.08	8	0.14

Table abbreviations: Ctid-break: Chromatid break type aberration, Ctid-exch: Chromatid exchange type aberration, Ctid-exch: Chromatid exchange type aberration, Chro-break: Chromosome break type aberration, Chro-exch: Chromosome exchange type aberration.

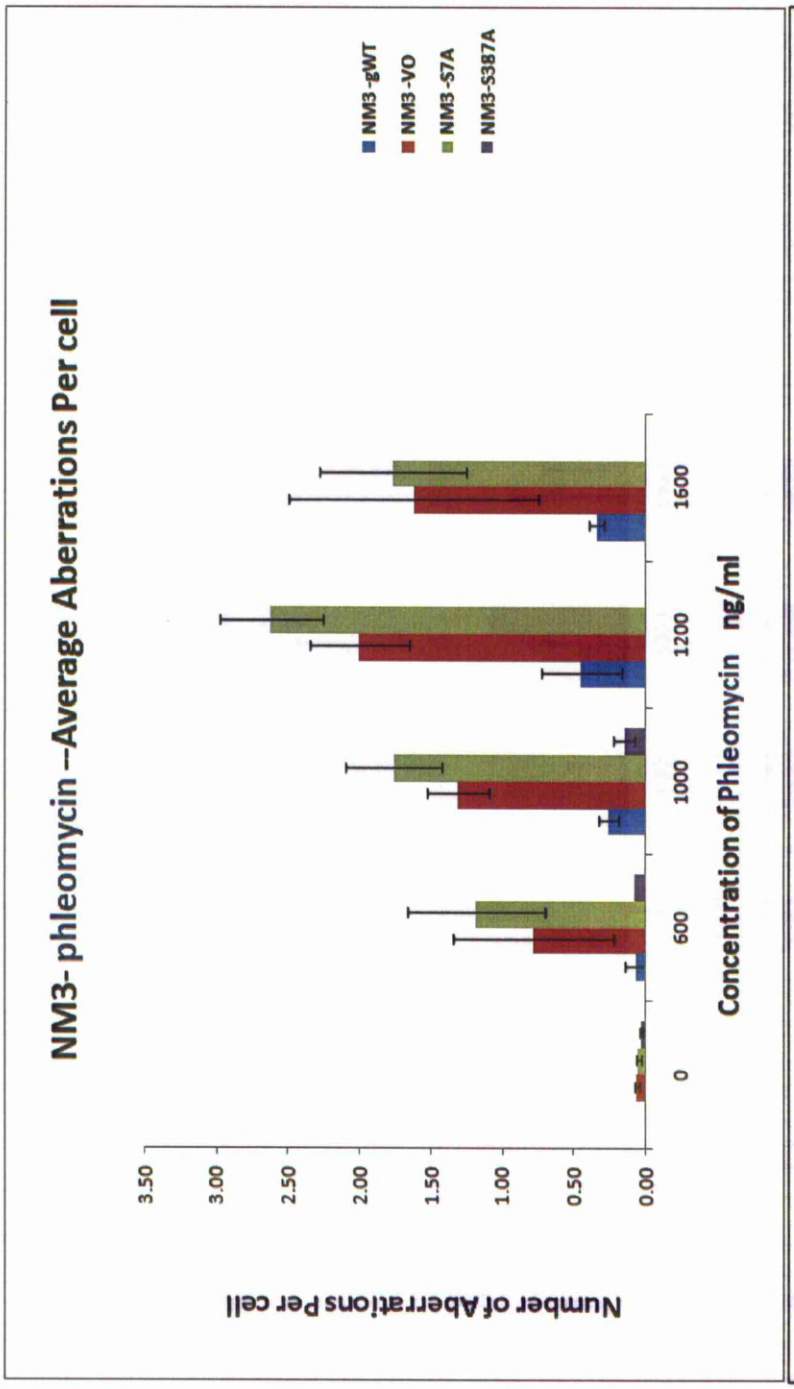

Figure (4.3): Illustrating phleomycin **Average Aberrations Per cell** data using four cell lines: NM3-gWT, NM3-VO, NM3-S7A and NM3-S387A. Eight experiments were performed as shown in **tables- (4.4.A, 4.5.A, 4.6.A, 4.7.A, 4.8.A, 4.9.A, 4.10.A and 4.11.A)**. NM3-S387A cell line was not used in doses (1200 ng/ml and 1600 ng/ml). Error bars show standard error of the mean.

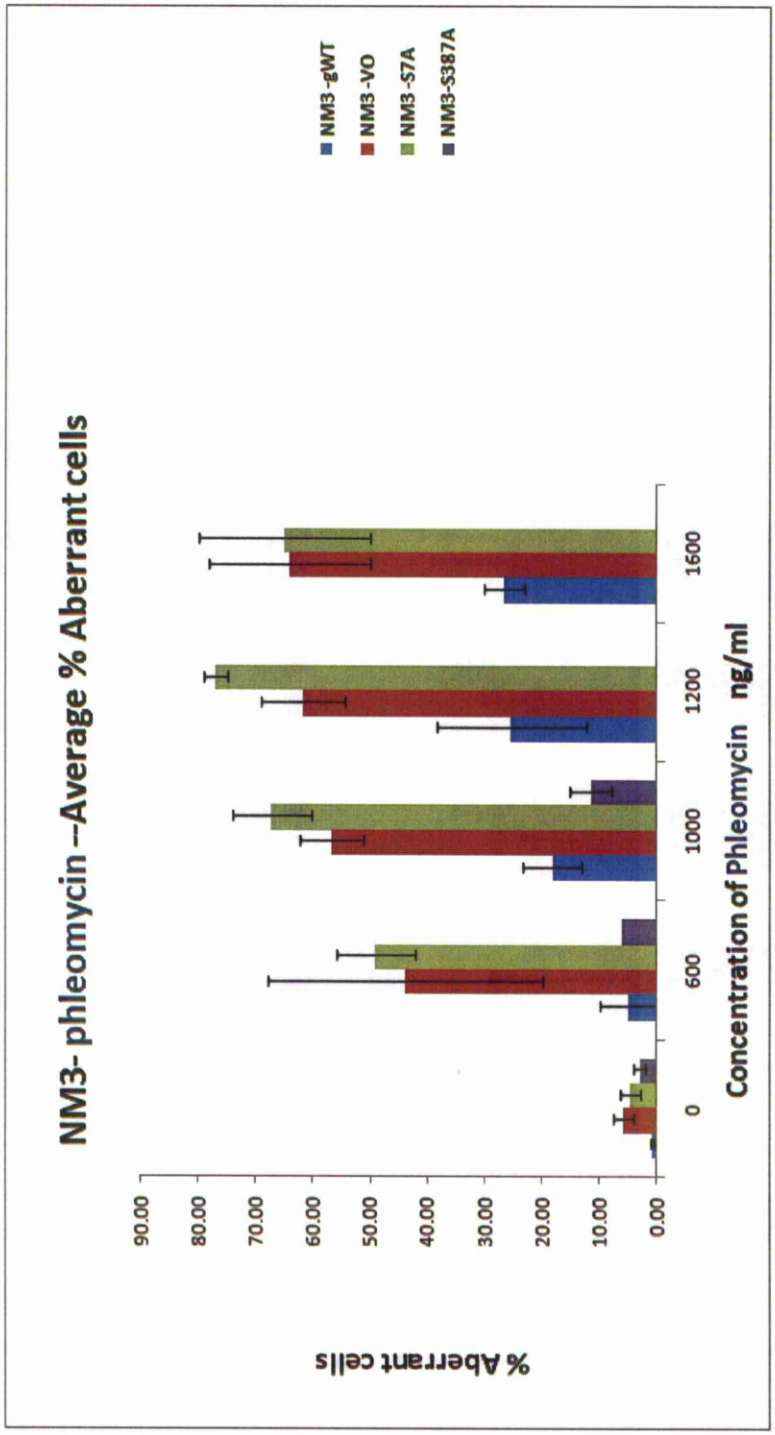

Figure (4.4): Illustrating phleomycin **Average Aberrations Per cell** data using four cell lines: NM3-gWT, NM3-VO, NM3-S7A and NM3-S387A. Eight experiments were performed as shown in **tables- (4.4.A, 4.5.A, 4.6.A, 4.7.A, 4.8.A, 4.9.A, 4.10.A and 4.11.A)**. NM3-S387A cell line was not used in doses (1200 ng/ml and 1600 ng/ml). Error bars show the standard error of the mean.

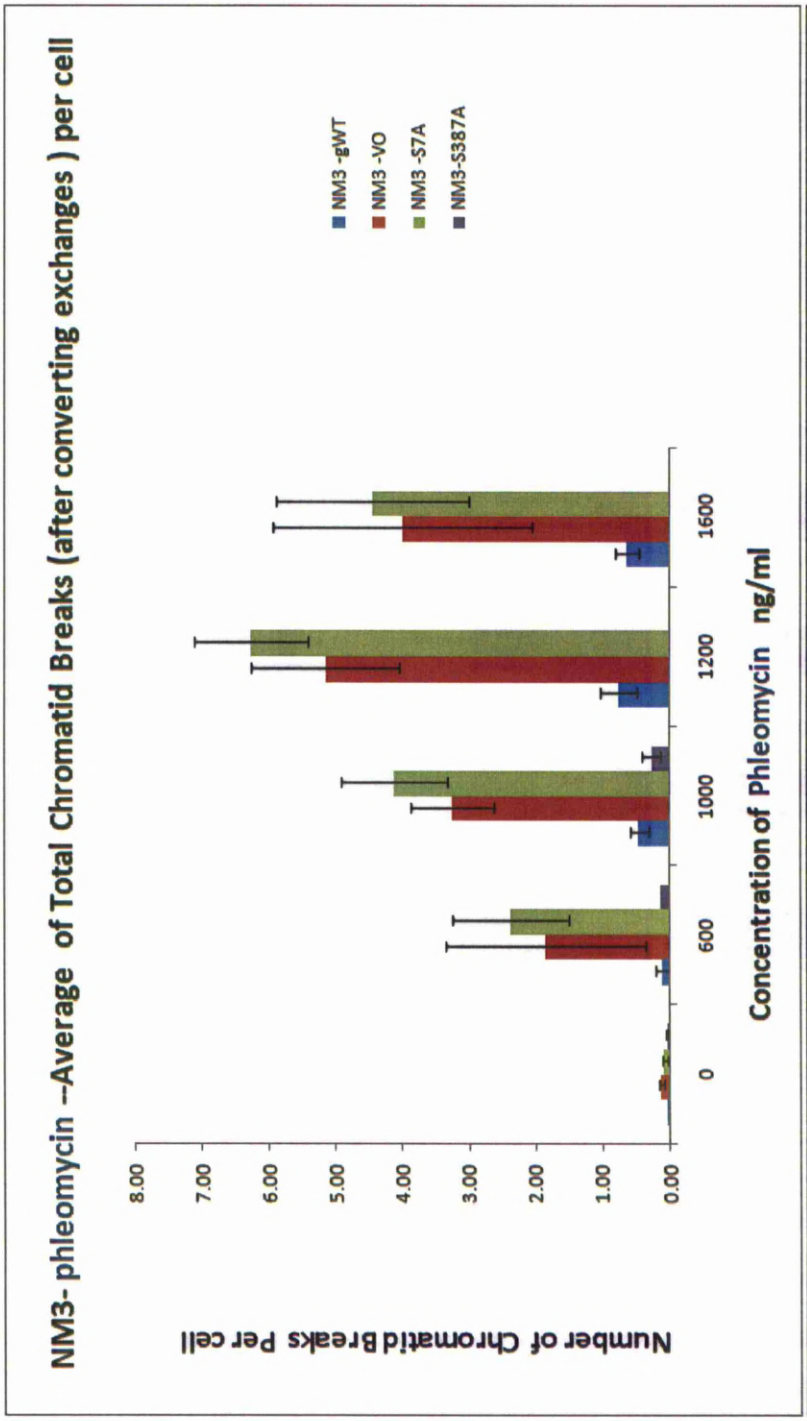

Figure (4.5): Illustrating phleomycin **Average Aberrations Per cell** data using four cell lines: NM3-gWT, NM3-VO, NM3-S7A and NM3-S387A. Eight experiments were performed as shown in **tables- (4.4.A, 4.5.A, 4.6.A, 4.7.A, 4.8.A, 4.9.A, 4.10.A and 4.11.A)**. NM3-S387A cell line was not used in doses (1200 ng/ml and 1600 ng/ml). Error bars show the standard error of the mean.

NM3-phleomycin - Average / Standard error of the mean-(SE) - Tables- results

Table (4.12) (Average and SE for tables- (4.4.A, 4.5.A, 4.6.A, 4.7.A, 4.8.A, 4.9.A, 4.10.A & 4.11.A)

Cell line	Treatment phleomycin ng/ml	Total number of cells sampled	Average Aberrations per cell	SE of the mean of Aberrations per cell	Average % Aberrant cells	SE of the mean of % Aberrant cells	Average Total Chromatid Breaks (after converting exchanges) per cell	SE of the mean of Total Chromatid Breaks (after converting exchanges) per cell
NM3-gWT	0	750	0.01	0.00	0.75	0.31	0.01	0.01
NM3-gWT	600	100	0.07	0.07	5.00	5.00	0.10	0.10
NM3-gWT	1000	300	0.26	0.07	18.20	5.06	0.45	0.14
NM3-gWT	1200	140	0.45	0.28	25.33	12.98	0.75	0.28
NM3-gWT	1600	120	0.35	0.06	26.50	3.50	0.63	0.17
NM3-VO	0	750	0.06	0.02	5.75	1.70	0.13	0.04
NM3-VO	600	100	0.78	0.56	44.00	24.00	1.85	1.49
NM3-VO	1000	250	1.31	0.22	56.80	5.61	3.25	0.62
NM3-VO	1200	140	2.01	0.35	61.67	7.26	5.16	1.10
NM3-VO	1600	120	1.63	0.87	64.00	14.00	3.99	1.94
NM3-S7A	0	750	0.05	0.02	4.63	1.73	0.07	0.03
NM3-S7A	600	100	1.18	0.48	49.00	7.00	2.38	0.88
NM3-S7A	1000	250	1.76	0.34	67.20	6.89	4.12	0.80
NM3-S7A	1200	140	2.62	0.36	77.00	2.00	6.27	0.84
NM3-S7A	1600	120	1.77	0.52	65.00	15.00	4.45	1.45
NM3-S387A	0	350	0.03	0.01	3.00	1.00	0.04	0.01
NM3-S387A	600	50	0.08		6.00		0.14	
NM3-S387A	1000	200	0.15	0.07	11.50	3.59	0.27	0.14

4.2.3.7 Aberration type and predominance

It is clear that in *FANCG* mutant cell lines; NM3–VO, NM3–S7A, NM3–S387A and in the control cell line NM3–gWT, that chromatid type aberrations predominate, involving breaks and exchanges as illustrated in **Tables 4.4.A, 4.5.A, 4.6.A, 4.7.A, 4.8.A, 4.9.A, 4.10.A and 4.11.A**. When comparing CA types in NM3–VO and NM3–S7A cells, it can also be seen that the occurrence of chromatid breaks in NM3–S7A cells is generally higher than that recorded in NM3–VO as seen in **Tables 4.4.A, 4.5.A, 4.6.A, 4.7.A, 4.8.A, 4.9.A, 4.10.A and 4.11.A**. From the same tables it can be noted that chromatid exchanges predominate in NM3–VO and NM3–S7A, while chromatid breaks predominate in NM3–gWT and NM3–S387A. From **Tables 4.4.B, 4.5.B, 4.6.B, 4.7.B, 4.8.B, 4.9.B, 4.10.B, and 4.11.B,** it can be seen that in NM3–VO and NM3–S7A, the predominant type of chromatid exchanges are exchanges that involve either two or three chromosomes (classified under complex arrangements). These chromatid exchanges involving two or three chromosomes seem to be higher in occurrence than those involving four chromosomes. The involvement of more than four chromosomes in these complex arrangements does occur; however, it does so in a lesser extent, as illustrated in the same **Tables 4.4.B, 4.5.B, 4.6.B, 4.7.B, 4.8.B, 4.9.B, 4.10.B, and 4.11.B.**

This variation in aberration type produced in these cell lines suggests the presence of different repair pathways used to process the phleomycin induced DNA damage. These findings suggest that NHEJ was the main available repair pathway in G-BRCA2 complex deficient NM3-VO and NM3-S7A cell lines to repair phleomycin induced DNA strand breaks, as exchanges reflect mis-repair by error prone-NHEJ. This data also suggests that HRR was the main available repair pathway in NM3-gWT and NM3-S387A cell lines in repairing phleomycin induced DNA

damage (DNA strand breaks), as fewer exchanges are observed in these two cell lines, that are both able to form the G-BRCA2 complex.

The presence of dicentrics or rings has been observed occasionally in untreated cultures (controls) and had been noted more often in treated cultures especially in NM3–VO and NM3–S7A cell lines as shown in **Tables 4.4.B, 4.5.B, 4.6.B, 4.7.B, 4.8.B, 4.9.B, 4.10.B and 4.11.B.** Generally, chromosome breaks were slightly higher than chromosome exchanges in all cell lines, especially NM3-gWT and NM3–S387A cell lines and were similar to the number of chromosome exchanges in NM3-VO and NM3–S7A. Chromosome breaks generally, were still considerably lower in numbers compared to chromatid breaks. This is particularly seen in treated *FANCG* mutant cell lines cultures NM3–VO and NM3–S7A as shown in **Tables 4.4.B, 4.5.B, 4.6.B, 4.7.B, 4.8.B, 4.9.B, 4.10.B and 4.11.B.** Whereas, NM3-gWT and NM3–S387A presented similarly low numbers of both chromosome breaks and chromatid breaks. Once again suggesting that HRR was the main available repair pathway in NM3-gWT and NM3 -S387A cell lines in repairing phleomycin induced DNA damage (DNA strand breaks).

EXPERIMENT – NM3- phleomycin

Table (4.4.B)

Cell line	Treatment ng/ml Phleomycin	No. Of cells scored	Triradials & no. Of centromeres			Quadri-radials & no. Of centromeres				Complex arrangements & no. Of chromosomes involved				Chromosome exchanges			No. Of Chromosome breaks	No. Of Chromatid breaks	No. Of TOTAL chromatid breaks [after converting all exchanges plus chromosome breaks]	Total Chromatid Breaks -after aberration converting per cell
			No. Of centromeres			No. Of centromeres				No. Of chromosomes				Type						
			1	2	3	1	2	3	4	2	3	4	5	Ring	Dicentric					
NM3-gWT	0	100	0	0	0	0	0	0	0	0	0	0	0	0	0		0	0	0	0
NM3-gWT	1200	100	2	0	0	0	0	0	0	0	1	1	1	0	2		1	2	36	0.36
NM3-gWT	1600	100	3	0	0	0	0	1	0	2	0	0	0	0	1		1	21	46	0.46
NM3-VO	0	100	0	0	0	0	0	0	0	0	0	0	0	0	2		8	5	29	0.29
NM3-VO	1200	100	12	13	1	1	3	1	2	29	19	5	3	5	4		7	66	417	4.17
NM3-VO	1600	100	13	9	3	3	5	1	1	6	30	11	2	8	1		9	91	593	5.93
NM3-S7A	0	100	0	0	0	0	0	0	0	0	0	0	0	0	0		1	2	4	0.04
NM3-S7A	1200	100	32	14	5	3	2	1	1	61	50	7	1	8	2		6	68	690	6.9
NM3-S7A	1600	100	10	8	1	1	0	1	0	56	23	8	14	4	9		7	90	590	5.9

In order to calculate the total number of chromatid breaks, first chromosome breaks, chromosome exchanges and chromatid exchanges including triradials, quadri-radials and complex arrangements were converted to the minimal number of chromatid breaks required for the formation of each specific type of aberration. Then this minimal number of chromatid breaks required for the formation of those aberrations was added to the observed number of chromatid breaks. Then this total number of chromatid breaks has been presented as total chromatid breaks per cell.

EXPERIMENT-- NM3- phleomycin

Table (4.5.B)

Cell line	Treatment ng/ml Phleomycin	No. Of cells scored	Triradials & no. Of centromeres			Quadri-radials & no. Of centromeres				Complex arrangements & no. Of chromosomes involved				No. Of Chromosome exchanges		No. Of Chromosome breaks	No. Of Chromatid breaks	No. Of TOTAL chromatid breaks [after converting all exchanges plus chromosome breaks]	Total Chromatid Breaks -after aberration converting per cell
			No. Of centromeres			No. Of centromeres				No. Of chromosomes				Type					
			1	2	3	1	2	3	4	2	3	4	5	Ring	Dicentric				
NM3-gWT	0	100	0	0	0	0	0	0	0	0	0	0	0	0	0	0	0	0	0
NM3-gWT	1200	20	1	0	0	0	0	0	0	2	1	0	0	0	0	0	1	12	0.6
NM3-gWT	1600	20	3	0	0	0	0	0	0	2	0	0	0	0	0	0	3	16	0.8
NM3-VO	0	100	0	0	0	0	0	0	0	0	0	0	0	0	0	2	1	5	0.05
NM3-VO	1200	20	4	4	0	0	0	0	0	4	6	1	0	1	0	1	11	79	3.95
NM3-VO	1600	20	0	1	1	0	0	0	0	7	1	0	0	1	2	0	2	41	2.05
NM3-S7A	0	100	0	0	0	0	0	0	0	0	0	0	0	0	0	1	2	4	0.04
NM3-S7A	1200	20	4	2	0	2	2	0	0	22	8	1	1	1	2	2	18	146	7.3
NM3-S7A	1600	20	0	2	0	0	1	1	0	7	3	1	0	1	0	1	8	60	3

In order to calculate the total number of chromatid breaks, first chromosome breaks, chromosome exchanges and chromatid exchanges including triradials, quadri-radials and complex arrangements were converted to the minimal number of chromatid breaks required for the formation of each specific type of aberration. Then this minimal number of chromatid breaks required for the formation of those aberrations was added to the observed number of chromatid breaks. Then this total number of chromatid breaks has been presented as total chromatid breaks per cell.

EXPERIMENT--NM3-phleomycin

Table (4.6.B)

Cell line	Treatment ng/ml Phleomycin	No. Of cells scored	Triradials & no. Of centromeres			Quadri-radials & no. Of centromeres				Complex arrangements & no. Of chromosomes involved				No. Of Chromosome exchanges		No. Of Chromosome breaks	No. Of Chromatid breaks	No. Of TOTAL chromatid breaks [after converting all exchanges plus chromosome breaks]	Total Chromatid Breaks -after aberration converting per cell
			No. Of centromeres			No. Of centromeres				No. Of chromosomes				Type					
			1	2	3	1	2	3	4	2	3	4	5	Ring	Dicentric				
NM3-gWT	100	0	0	0	0	0	0	0	0	0	0	0	0	0	0	1	1	3	0.03
NM3-gWT	50	600	0	1	0	0	0	0	0	1	0	0	0	0	0	0	5	10	0.2
NM3-gWT	20	1200	1	0	0	0	0	0	0	4	0	0	0	0	0	0	15	26	1.3
NM3-VO	100	0	0	0	0	0	0	0	0	0	0	0	0	0	3	4	1	21	0.21
NM3-VO	50	600	5	8	0	2	1	1	0	17	2	3	2	2	1	1	22	167	3.34
NM3-VO	20	1200	4	6	2	0	1	1	0	16	7	2	0	2	1	1	11	147	7.35
NM3-S7A	100	0	0	0	0	0	0	0	0	0	0	0	0	0	0	6	0	12	0.12
NM3-S7A	50	600	4	3	0	0	6	0	0	24	7	1	0	1	1	4	32	163	3.26
NM3-S7A	20	1200	3	3	0	0	2	0	0	21	4	1	0	0	0	0	6	92	4.6

In order to calculate the total number of chromatid breaks, first chromosome breaks, chromosome exchanges and chromatid exchanges including triradials, quadri-radials and complex arrangements were converted to the minimal number of chromatid breaks required for the formation of each specific type of aberration. Then this minimal number of chromatid breaks required for the formation of those aberrations was added to the observed number of chromatid breaks. Then this total number of chromatid breaks has been presented as total chromatid breaks per cell.

EXPERIMENT – NM3- phleomycin

Table (4.7.B)

Cell line	Treatment ng/ml Phleomycin	No. Of cells scored	Triradials & no. Of centromeres			Quadri-radials & no. Of centromeres				Complex arrangements & no. Of chromosomes involved					No. Of Chromosome exchanges			No. Of Chromosome breaks	No. Of Chromatid breaks	No. Of TOTAL chromatid breaks [after converting all exchanges plus chromosome breaks]	Total Chromatid Breaks -after aberration converting per cell
			No. Of centromeres			No. Of centromeres				No. Of chromosomes					Type						
			1	2	3	1	2	3	4	2	3	4	5		Ring	Dicentric					
NM3-gWT	0	100	0	0	0	0	0	0	0	0	0	0	0		1	0		0	0	4	0.04
NM3-gWT	1000	100	0	0	0	0	0	0	0	7	0	0	0		0	0		0	5	19	0.19
NM3-VO	0	100	0	0	0	0	0	0	0	0	0	0	0		0	0		1	0	2	0.02
NM3-VO	1000	50	4	9	1	1	1	0	0	13	5	0	0		5	2		1	17	144	2.88
NM3-S7A	0	100	0	0	0	0	0	0	0	0	0	0	0		0	0		0	0	0	0
NM3-S7A	1000	50	9	10	2	1	3	1	1	17	3	3	0		4	2		5	14	205	4.1

In order to calculate the total number of chromatid breaks, first chromosome breaks, chromosome exchanges and chromatid exchanges including triradials, quadri-radials and complex arrangements were converted to the minimal number of chromatid breaks required for the formation of each specific type of aberration. Then this minimal number of chromatid breaks required for the formation of those aberrations was added to the observed number of chromatid breaks. Then this total number of chromatid breaks has been presented as total chromatid breaks per cell.

EXPERIMENT--NM3- phleomycin

Table (4.8.B)

Cell line	Treatment ng/ml Phleomycin	No. Of cells scored	Triradials & no. Of centromeres			Quadri-radials & no. Of centromeres				Complex arrangements & no. Of chromosomes involved				No. Of Chromosome exchanges		No. Of Chromosome breaks	No. Of Chromatid breaks	No. Of TOTAL chromatid breaks [after converting all exchanges plus chromosome breaks]	Total Chromatid Breaks -after aberration converting per cell
			No. Of centromeres			No. Of centromeres				No. Of chromosomes				Type					
			1	2	3	1	2	3	4	2	3	4	5	Ring	Dicentric				
NM3-gWT	0	100	0	0	0	0	0	0	0	0	0	0	0	0	0	0	0	2	0.02
NM3-gWT	1000	50	2	0	0	0	0	0	0	4	1	0	0	0	3	1	5	37	0.74
NM3-VO	0	100	0	0	0	1	0	0	0	0	0	0	0	0	1	7	0	22	0.22
NM3-VO	1000	50	7	4	0	2	2	0	0	14	9	1	1	2	3	8	12	171	3.42
NM3-S7A	0	100	0	0	0	0	0	0	0	0	0	0	0	0	0	2	1	5	0.05
NM3-S7A	1000	50	9	9	1	0	2	0	0	11	14	2	2	7	4	8	33	263	5.26
NM3-S357A	0	100	0	0	0	0	0	0	0	0	0	0	0	0	0	2	4	8	0.08
NM3-S357A	1000	50	1	1	0	0	1	0	0	2	2	0	0	1	0	2	8	34	0.68

In order to calculate the total number of chromatid breaks, first chromosome breaks, chromosome exchanges and chromatid exchanges including triradials, quadri-radials and complex arrangements were converted to the minimal number of chromatid breaks required for the formation of each specific type of aberration. Then this minimal number of chromatid breaks required for the formation of those aberrations was added to the observed number of chromatid breaks. Then this total number of chromatid breaks has been presented as total chromatid breaks per cell.

EXPERIMENT– NM3- phleomycin

Table (4.9.B)

Cell line	Treatment ng/ml Phleomycin	No. Of cells scored	Triradials & no. Of centromeres			Quadri-radials & no. Of centromeres				Complex arrangements & no. Of chromosomes involved					No. Of Chromosome exchanges		No. Of Chromosome breaks	No. Of Chromatid breaks	No. Of TOTAL chromatid breaks [after converting all exchanges plus chromosome breaks]	Total Chromatid Breaks -after aberration converting per cell
			No. Of centromeres			No. Of centromeres				No. Of chromosomes					Type					
			1	2	3	1	2	3	4	2	3	4	5	Ring	Dicentric					
NM3-gWT	0	100	0	0	0	0	0	0	0	0	0	0	0	0	0		0	1	1	0.01
NM3-gWT	1000	50	0	0	0	1	1	0	0	3	0	0	0	0	0		1	9	23	0.46
NM3-VO	0	100	0	0	0	0	0	0	0	0	0	0	0	0	0		7	3	17	0.17
NM3-VO	1000	50	6	4	0	0	3	0	0	15	12	1	1	8	2		6	23	203	4.06
NM3-S7A	0	100	0	0	0	0	0	0	0	0	0	0	0	0	0		10	6	26	0.26
NM3-S7A	1000	50	8	5	1	1	1	0	0	21	8	1	0	5	8		12	46	253	5.06
NM3-S387A	0	100	0	0	0	0	0	0	0	0	0	0	0	0	0		0	2	2	0.02
NM3-S387A	1000	50	0	0	0	0	0	0	0	0	0	0	0	0	0		0	3	3	0.06

In order to calculate the total number of chromatid breaks, first chromosome breaks, chromosome exchanges and chromatid exchanges including triradials, quadri-radials and complex arrangements were converted to the minimal number of chromatid breaks required for the formation of each specific type of aberration. Then this minimal number of chromatid breaks required for the formation of those aberrations was added to the observed number of chromatid breaks. Then this total number of chromatid breaks has been presented as total chromatid breaks per cell.

EXPERIMENT – NM3- phleomycin

Table (4.10.B)

Cell line	Treatment ng/ml Phleomycin	No. Of cells scored	Triradials & no. Of centromeres			Quadri-radials & no. Of centromeres				Complex arrangements & no. Of chromosomes involved				No. Of Chromosome exchanges		No. Of Chromosome breaks	No. Of Chromatid breaks	No. Of TOTAL chromatid breaks [after converting all exchanges plus chromosome breaks]	Total Chromatid Breaks -after aberration converting per cell
			No. Of centromeres			No. Of centromeres				No. Of chromosomes				Type					
			1	2	3	1	2	3	4	2	3	4	5	Ring	Dicentric				
NM3-gWT	0	100	0	0	0	0	0	0	0	0	0	0	0	0	0	0	0	0	0
NM3-gWT	1000	50	2	1	0	0	0	1	0	4	0	0	0	0	0	0	15	38	0.76
NM3-VO	0	100	0	0	0	0	0	0	0	1	0	0	0	0	0	1	2	6	0.06
NM3-VO	1000	50	4	12	1	0	2	0	1	27	10	5	0	3	1	6	21	239	4.78
NM3-57A	0	100	0	0	0	0	0	0	0	0	0	0	0	0	0	2	2	6	0.06
NM3-57A	1000	50	7	7	0	2	2	0	0	22	17	5	0	2	0	2	50	258	5.16
NM3-5387A	0	100	0	0	0	0	0	0	0	0	0	0	0	0	1	0	1	5	0.05
NM3-5387A	1000	50	0	0	1	0	0	0	0	0	0	0	0	0	0	0	4	10	0.2

In order to calculate the total number of chromatid breaks, first chromosome breaks, chromosome exchanges and chromatid exchanges including triradials, quadri-radials and complex arrangements were converted to the minimal number of chromatid breaks required for the formation of each specific type of aberration. Then this minimal number of chromatid breaks required for the formation of those aberrations was added to the observed number of chromatid breaks. Then this total number of chromatid breaks has been presented as total chromatid breaks per cell.

EXPERIMENT-- NM3- phleomycin

Table (4.11.B)

Cell line	Treatment ng/ml Phleomycin	No. Of cells scored	Triradials & no. Of centromeres			Quadri-radials & no. Of centromeres				Complex arrangements & no. Of chromosomes involved					No. Of Chromosome exchanges		No. Of Chromosome breaks	No. Of Chromatid breaks	No. Of TOTAL chromatid breaks [after converting all exchanges plus chromosome breaks]	Total Chromatid Breaks -after aberration converting per cell
			No. Of centromeres			No. Of centromeres				No. Of chromosomes					Type					
			1	2	3	1	2	3	4	2	3	4	5	Ring	Dicentric					
NM3-gWT	0	50	0	0	0	0	0	0	0	0	0	0	0	0	0		0	0	0	0
NM3-gWT	600	50	0	0	0	0	0	0	0	0	0	0	0	0	0		0	0	0	0
NM3-gWT	1000	50	0	0	0	0	0	0	0	0	0	0	0	0	0		1	3	5	0.1
NM3-VO	0	50	0	0	0	0	0	0	0	0	0	0	0	0	0		0	0	0	0
NM3-VO	600	50	2	1	0	0	0	0	0	0	0	0	0	0	0		1	7	18	0.36
NM3-VO	1000	50	1	2	0	0	0	0	0	5	2	0	0	0	1		7	11	56	1.12
NM3-S7A	0	50	0	0	0	0	0	0	0	0	0	0	0	0	0		0	1	1	0.02
NM3-S7A	600	50	3	0	0	0	1	0	0	5	2	2	0	0	2		6	14	75	1.5
NM3-S7A	1000	50	2	1	0	0	0	0	1	3	0	0	0	1	1		1	18	51	1.02
NM3-S387A	0	50	0	0	0	0	0	0	0	0	0	0	0	0	0		0	1	1	0.02
NM3-S387A	600	50	0	0	0	0	0	0	0	0	0	0	0	0	0		3	1	7	0.14
NM3-S387A	1000	50	0	0	0	0	0	0	0	0	0	0	0	0	0		3	1	7	0.14

In order to calculate the total number of chromatid breaks, first chromosome breaks, chromosome exchanges and chromatid exchanges including triradials, quadri-radials and complex arrangements were converted to the minimal number of chromatid breaks required for the formation of each specific type of aberration. Then this minimal number of chromatid breaks required for the formation of those aberrations was added to the observed number of chromatid breaks. Then this total number of chromatid breaks has been presented as total chromatid breaks per cell.

4.2.3.8 Cytogenetic numerical aberration rates in control and treated cell cultures

CHO cell lines are immortalized cell lines with chromosomal counts ranging between 18-20 chromosomes per metaphase as observed in unstressed culture conditions. However, this numerical range increases when *FANCG* deficient CHO cell lines are exposed to phleomycin to reach 21 to 25+ chromosomes per metaphase as illustrated in **Tables 4.13, 4.14, 4.15, 4.16, and 4.17. Table 4.18** shows an average summary of **Tables 4.13, 4.14, 4.15, 4.16, and 4.17.** It can be noted, that while both NM3-VO and NM3-S7A exhibit an elevation of chromosome numbers when exposed to phleomycin doses of 1000 ng/ml, 1200 ng/ml and 1600 ng/ml, NM3-gWT demonstrates numerical stability spanning the usual range of 18-20 chromosomes when exposed to same doses of phleomycin.

Both NM3-VO and NM3-S7A exhibit elevated rates of chromosome numbers in **Tables 4.13, 4.14, 4.15, 4.16, and 4.17** compared to NM3-gWT. For example, in response to a dose of 1200 ng/ml, NM3-VO and NM3-S7A showed in **Table.4.13** an average chromosome number of 23.2 and 24.4 respectively, compared to an average of 19.52 chromosomes in NM3-gWT. Also in **Table.4.14,** in response to a dose of 1200 ng/ml, NM3-VO and NM3-S7A exhibit an average chromosome number of 23.5 and 24.5 respectively compared to an average of 17.85 chromosomes for NM3-gWT. This numerical elevation is also observable in **Table.4.16** in response to a dose of 1000 ng/ml, where NM3-VO and NM3-S7A showed an average chromosome number of 22.65 and 23.65 respectively compared to an average of 19.75 chromosomes presented in NM3-gWT. This data illustrates that NM3-S7A is exhibiting a degree

of chromosomal numerical instability similar to that of NM3-VO suggesting and supporting evidence indicating the importance of phosphorylation of FANCG-serine at position 7 in sustaining chromosomal integrity.

This chromosomal numerical elevation in FA-*FANCG* deficient cell lines NM3-VO and NM3-S7A was not observed in NM3-S387A cell line, which demonstrated wild type NM3-gWT chromosomal numerical levels spanning the usual range of 18-20 chromosomes when exposed to same doses of phleomycin, as shown in **Table 4.17.** These observations have been consistent and can be seen in **Fig. 4.6** and in **Table 4.18** that shows an average summary of **Tables 4.13, 4.14, 4.15, 4.16, and 4.17.**

Data- Table (4.13) -: Phleomycin treated NM3 cell lines - Average chromosome numbers count in experiment

Cell line	Treatment Phleomycin ng/ml	Total number of cells sampled	Average chromosome numbers count
NM3-gWT	0	100	19.14
NM3-gWT	1200	100	19.52
NM3-gWT	1600	100	19.48
NM3-VO	0	100	19.9
NM3-VO	1200	100	23.2
NM3-VO	1600	100	24.09
NM3-S7A	0	100	20.14
NM3-S7A	1200	100	24.4
NM3-S7A	1600	100	23.82

Data- Table (4.14) -: Phleomycin treated NM3 cell lines - Average chromosome numbers count in experiment

Cell line	Treatment Phleomycin ng/ml	Total number of cells sampled	Average chromosome numbers count
NM3-gWT	0	100	18.84
NM3-gWT	1200	20	17.85
NM3-gWT	1600	20	20.35
NM3-VO	0	100	19.97
NM3-VO	1200	20	23.5
NM3-VO	1600	20	21.8
NM3-S7A	0	100	19.82
NM3-S7A	1200	20	24.5
NM3-S7A	1600	20	23.65

Data- Table (4.15) -: Phleomycin treated NM3 cell lines - Average chromosome numbers count in experiment

Cell line	Treatment Phleomycin ng/ml	Total number of cells sampled	Average chromosome numbers count
NM3-gWT	0	100	19.06
NM3-gWT	600	20	19.3
NM3-gWT	1200	20	19.85
NM3-VO	0	100	19.53
NM3-VO	600	20	22.65
NM3-VO	1200	20	25.05
NM3-S7A	0	100	19.78
NM3-S7A	600	20	23.8
NM3-S7A	1200	20	22.25

Data- Table (4.16) -: Phleomycin treated NM3 cell lines - Average chromosome numbers count in experiment

Cell line	Treatment Phleomycin ng/ml	Total number of cells sampled	Average chromosome numbers count
NM3-gWT	0	50	19.02
NM3-gWT	1000	100	19.75
NM3-VO	0	100	19.73
NM3-VO	1000	20	22.65
NM3-S7A	0	100	19.8
NM3-S7A	1000	20	23.65

Data- Table (4.17) -: Phleomycin treated NM3 cell lines - Average chromosome numbers count in experiment

Cell line	Treatment Phleomycin ng/ml	Total number of cells sampled	Average chromosome numbers count
NM3-gWT	0	100	19.78
NM3-gWT	1000	20	21.35
NM3-VO	0	100	19.6
NM3-VO	1000	20	23
NM3-S7A	0	100	20.09
NM3-S7A	1000	20	23.5
NM3-S387A	0	100	19.97
NM3-S387A	1000	20	20.45

Data- Table (4.18) -: Phleomycin treated NM3 -Average Number of chromosome in five experiments as shown in tables (4.13, 4.14, 4.15, 4.16, and 4.17). STDEV: Standard deviation, SE: Standard error of the mean.

Cell line	Treatment phleomycin ng/ml	Total number of cells sampled	Average no. of chromosomes in All Experiments	STDEV of no. of chromosomes in All Experiments	SE of the mean of no. of chromosomes in All Experiments
NM3 -gWT	0	450	19.17	0.36	0.16
NM3 -gWT	600	20	19.30		
NM3 -gWT	1000	120	20.55	1.13	0.80
NM3 -gWT	1200	140	19.07	1.07	0.62
NM3 -gWT	1600	120	19.92	0.62	0.44
NM3 -VO	0	500	19.75	0.19	0.08
NM3 -VO	600	20	22.65		
NM3 -VO	1000	40	22.83	0.25	0.17
NM3 -VO	1200	140	23.92	0.99	0.57
NM3 -VO	1600	120	22.95	1.62	1.15
NM3 -S7A	0	500	19.93	0.17	0.08
NM3 -S7A	600	20	23.80		
NM3 -S7A	1000	40	23.58	0.11	0.06
NM3 -S7A	1200	140	23.72	1.27	0.73
NM3 -S7A	1600	120	23.74	0.12	0.09
NM3-S387A	0	100	19.97		
NM3-S387A	600				
NM3-S387A	1000	20	20.45		

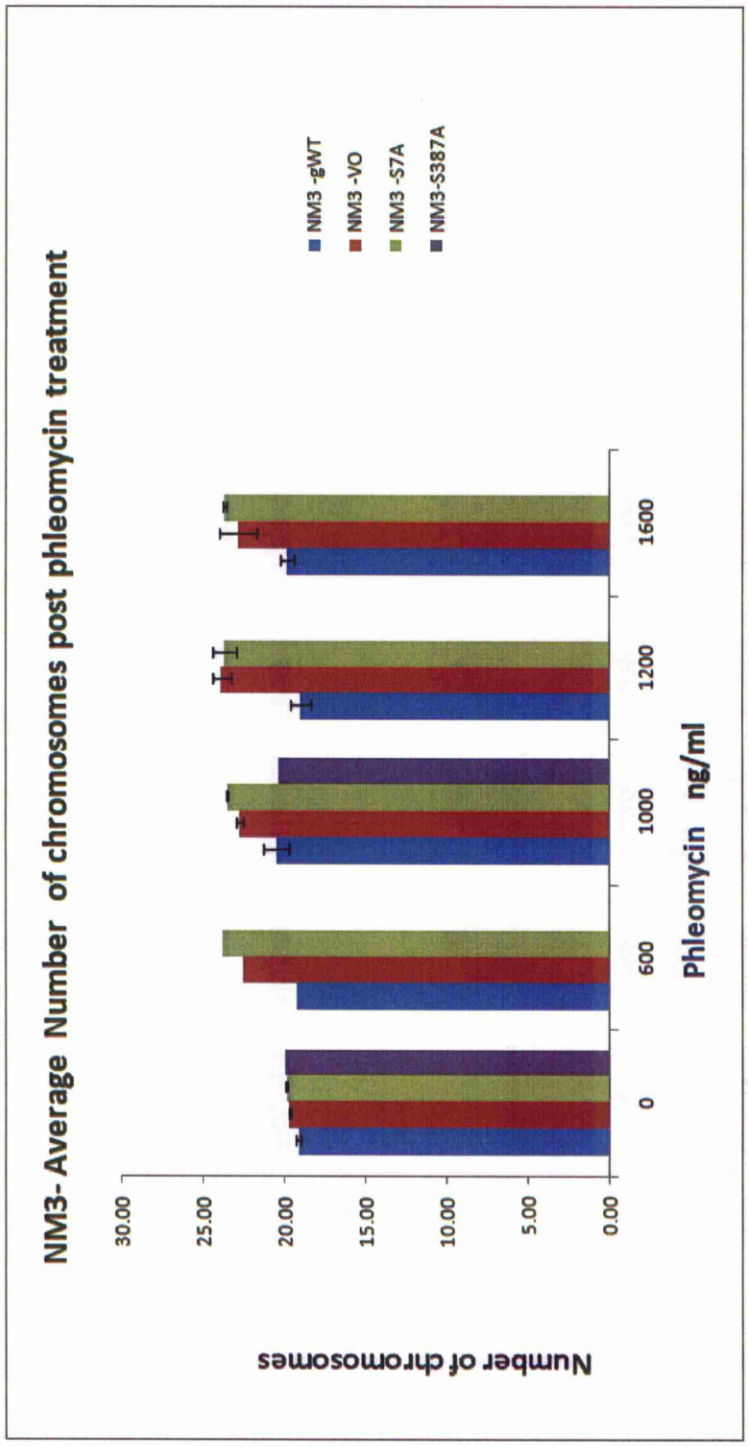

Figure (4.6): Illustrating phleomycin and **average chromosome numbers_data** using four cell lines: NM3-gWT, NM3-VO, NM3-S7A and NM3-S387A. Five experiments were performed as shown in **tables- (4.13, 4.14, 4.15, 4.16 and 4.17)**. NM3-S387A cell line was not used in doses (600 ng/ml, 1200 ng/ml and 1600 ng/ml) and was exposed once to (1000 ng/ml) as shown in **(Table 4.17)**. The dose 600 ng/ml was used once. Error bars show the standard error of the mean.

4.2.3.9 Chromatid Gaps in phleomycin-treated cell lines

Tables 4.4.A, 4.5.A, 4.6.A, 4.7.A, 4.8.A, 4.9.A, 4.10.A and 4.11.A illustrate the increase in the number of gaps scored in *FANCG* mutant cell lines NM3-VO and NM3-S7A particularly when using the higher doses of 1000 ng/ml, 1200 ng/ml and 1600 ng/ml of phleomycin. This elevation in scored gaps may indicate these gaps as actual breaks in response to clastogen treatment rather than staining variation. For example, NM3-VO and NM3-S7A exhibit gaps in **Table 4.4.A** at 4.3 and 4.5-fold higher than NM3-gWT at a phleomycin dose of 1200 ng/ml. NM3-VO and NM3-S7A cells also showed gaps **(Table 4.8.A)** at 5.7 and 5-fold higher rates than NM3-gWT at a phleomycin dose of 1000 ng/ml. Whereas, NM3-S387A exhibits a similar number of gaps to that observed in the wild type NM3-gWT for the same dose, as illustrated in **Tables 4.8.A, 4.9.A, 4.10.A and 4.11.A.** The numbers of gaps were small in comparison to the number of chromatid breaks induced. Therefore, even if they were considered as genuine clastogen-induced breaks, and included in the analyses described above, this would not alter the overall interpretation of the data.

4.2.4 Homologous recombination repair assay results

As can be seen from **Fig. 4.7**, the non-induced homologous recombination frequencies of the cell lines were very similar. The spontaneous recombination frequencies were 1.4 X 10^{-6} for NM3-gWT, 1.32 x 10^{6} for NM3-VO, 1.23 x 10^{6} for NM3-S7A and 1.53 x10^{6} for NM3-S387A.

This is compared to findings presented in **Fig. 4.8,** where the same cell lines were exposed to a dose of (800 ng/ml) phleomycin inducing DNA damage, and analyzed following a recovery

period allowing HRR to take place. As illustrated in **Fig. 4.8,** NM3-VO, NM3-S7A and NM3-S387A exhibited recombination frequencies of 3.23 X 10^{-4}, 0.5 X 10^{-4} and 5.6 X 10^{-4} respectively, which are equivalent to 2.8, 18 and 1.6 fold reduction in HRR respectively compared to that of NM3-gWT with a recombination frequency of 9 X 10^{-4}. The highest homologous recombination rate is observed in NM3-gWT and the lowest HRR rate is shown in NM3-S7A. It is interesting to note that NM3-S7A actually shows a much lower rate of HRR than the null mutant NM3-VO. The rate of HRR in NM3-S387A cells was only slightly reduced compared to wild type NM3-gWT cells. These findings are broadly consistent with survival, growth inhibition and cytogenetic data presented in this chapter.

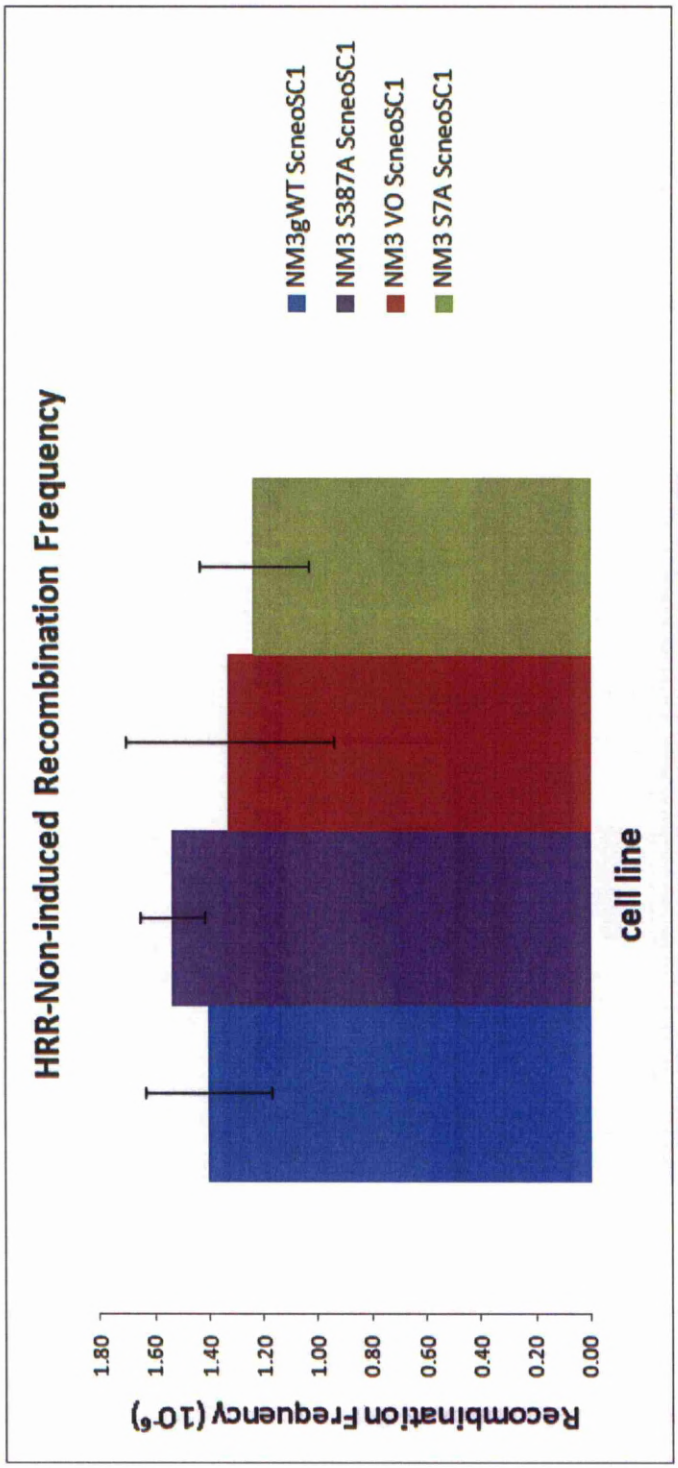

Figure (4.7): Illustrating **HRR-Non-induced recombination frequency** results. The data presented using four cell lines: NM3-gWT, NM3-VO, NM3-S7A and NM3-S387A. Three experiments were performed. Error bars show the standard error of the mean

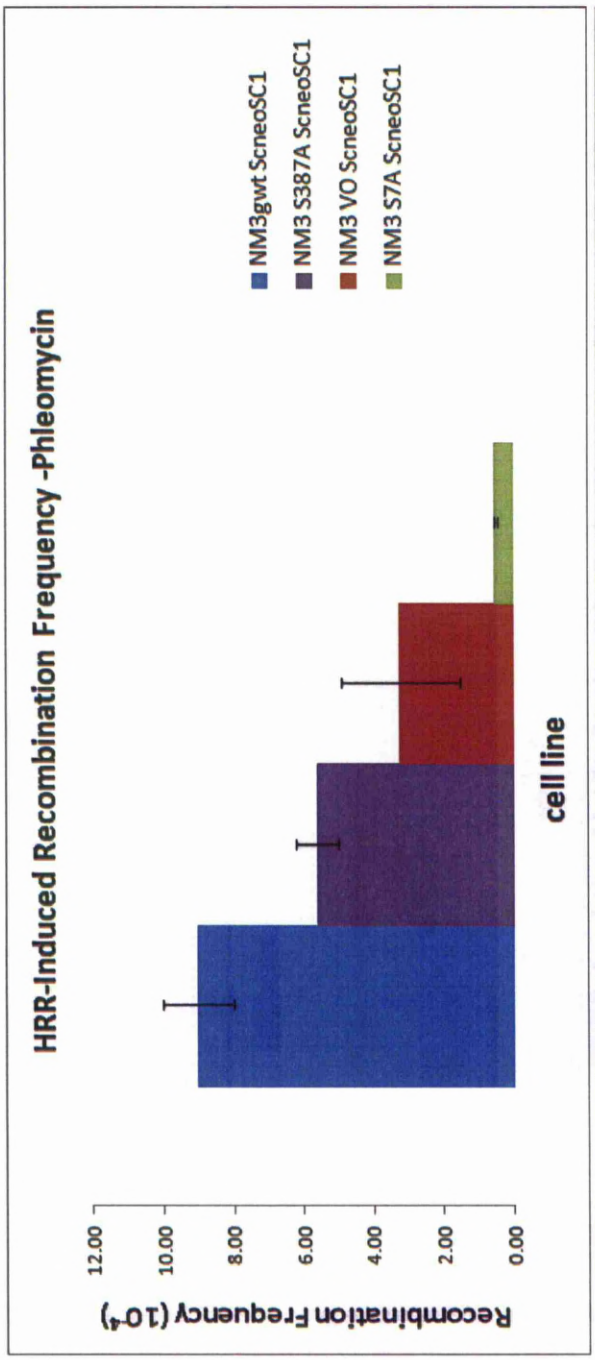

Figure (4.8): Illustrating **HRR Induced recombination frequency** results after exposure to phleomycin. The data presented using four cell lines: NM3-gWT, NM3-VO, NM3-S7A and NM3-S387A. Three experiments were performed. Error bars show the standard error of the mean.

4.2.5 MN assay

4.2.5.1 Optimizing the MN assay procedure

The micronucleus assay (**See section 2.1.2.10.2.1**) provides an alternate and more cost effective cytogenetic approach. The reason why the micronucleus assay has been chosen to be utilized is to have a better evaluation of the numerical instability seen in **Fig. 4.6**, **Tables: 4.13, 4.14, 4.15, 4.16, 4.17 and 4.18**. The increase in chromosome counts in both cell lines NM3-VO and NM3-S7A compared to NM3-gWT could be due to the presence of lagging chromosomes, centric, or acentric fragments with in a metaphase spread. The micronucleus assay is 'a cytokinesis-block method for the analysis of micronucli'. The technique is based on the use of cytochalasin B, an inhibitor of actin polymerisation, which blocks mitotic cytokinesis but not nuclear division in cultured cell lines. Micronuclei may contain either acentric chromosomal fragments, or lagged chromosomes that have failed to segregate into a daughter macronucleus during mitosis **(Hermine *et al.*, 1997).** Micronucleus testing could be carried out by utilizing immune-fluorescence labeling **(Lindh *et al.*, 2006).** Through the use of centromeric probes (or anti-kinetochore antibodies) chromosome breakage can be distinguished from chromosome loss. Chromosome migration impairment would result in increased frequency of micronuclei that enclose a single centromere while centrosome amplification would induce micronuclei with three or more centromeric signals. The use of micronucleus assay and crest staining allows an evaluation of spontaneous and drug induced numerical and structural instability.

For hamster cell lines a number of papers have implemented the MN assay **(Krishna *et al.*, 1989; Eastmond and Tucker 1989; Jones *et al.*, 1993; Lynch *et al.*, 1993; Gabriele *et al.*, 1995; Hermine *et al.*, 1997).** The literature regarding MN assay is considerably variant in the type of cell lines used, initial cellular densities, slide preparation, fixation, and staining methods. Most researchers have used or recommend the implementation of a cytocentrifuge to centrifuge cells directly onto slides to be scored for micronuclei **(Fenech and Morley, 1985; Fenech, 2000; Channarayappa *et al.*, 1990; Ellard *et al.*, 1991; Lynch *et al.*, 1993; Hermine *et al.*, 1997).** However, an alternative procedure for laboratories lacking a cytocentrifuge has been described in the literature **(Fenech, 2000)** and this was used in this study. The cellular density selected (5×10^5) ensured the presence of a dividing cellular population before and after adding both cytochalasian-B (Cyto-B) and MMC. This cellular density also ensured that the cellular confluence prior harvesting has been 60-70% and the dividing cells are allowed to accumulate in the bi-nucleated cellular state suitable for scoring. A free suspending router centrifuge has been used ensuring proficient collection of the pellet of cells prior fixation. The best fixation method without using a cytocentrifuge has been through the use of acetic acid and methanol fixation solution in 1:25 ratio respectively **(Fenech, 2000; Suzuki *et al.*, 2000).** Acetic acid-methanol fixation solution gave a better result compared to the methanol fixation method. Following fixation in culture tubes, the cells were dropped on horizontally held slides and allowed to dry for 10 minutes before staining. Staining has been conducted using either standard Giemsa stain (20% Giemsa solution) **(Ellard *et al.*, 1991; Jones *et al.*, 1993)**, or acridine orange fluorescent stain which is a more specific DNA dye **(Fenech, 2000; Suzuki *et al.*, 2000).** When using acridine orange the wet slides were immediately covered with cover glass slips prior to scoring. Both types of staining yield bi-nucleated cells that could be scored **(Fig. 4.9).**

4.2.5.2 Problems encountered in the MN procedure

Two problems hindered progress leading to the discontinuation of the optimization process for the MN assay and initiated consideration of other means to investigate numerical stability of FA cell lines. The main problem has been the low percentage of bi-nucleated cells produced from the pellet obtained. At best up to 30-35% of cells could be classified as viable cells wither they are mono-nucleated, bi-nucleated (**Fig. 4.9-A**), tri-nucleated or multinucleated. The other 60-65% of cells had an unclear-unspecific appearance **(Fig. 4.9-B)**. This percentage of bi-nucleated cells reduced when using MMC doses 300nM and 600nM. This problem has been persistent in control flasks despite altering cellular density, increasing Cyto-B incubation time up to 24 hours for CHO cells **(Gabriele *et al.*, 1995)** reducing Cyto-B final concentration or altering staining time

nor staining density or even briefly exposing cells to hypotonic treatment (0.075 M KCL) prior fixation **(Krishna *et al.*, 1989; Suzuki *et al.*, 2000).** It was concluded that the cells with an unclear appearance result as a consequence of the improper spreading of the bi-nucleated cells. This would be probably achieved proficiently through the use of a cytocentrifuge **(Channarayappa *et al.*, 1990),** ensuring proper cytoplasmic spreading to obtain proficient scoring.

The second problem, although minor, but worthy of reporting has been the appearance of the CHO bi-nucleated cells which fitted the scoring criteria however, at times the cytoplasmic boundary although encapsulates both nuclei and any micronuclei present but it didn't always

seem to be circular **(Fig. 4.9)** as seen in lymphocytes. Both of these problems seem to be resolved through the use of a cytocentrifuge.

Subsequent to the difficulties encountered in the micronucleus assay, the plan to investigate the numerical stability of FA cell lines, if time allowed, would have been through the implementation of fluorescent in situ hybridization (FISH) probes. Where the utilization of two selected centromeric probes for chromosomes number 2 **(Fatyol *et al.*, 1994)** and chromosome number 5 **(Faravelli *et al.*, 1998)** on metaphase spreads would reflect the loss or gain of these chromosomes (numerical instability) in FA cell lines spreads **(Griffin *et al.*, 2000)** which have been exposed to clastogens such as MMC or phleomycin. These two probes have been previously tested by other research groups for hamster chromosomes; they were therefore prefered as their use allows comparison to the previous studies. As it turned out, insufficient time resulted in discontinuing further research in this area. The expectation had these experiments been conducted successfully, would be to have observed aneuploidy and further chromosomal structural instability in mutant cell lines.

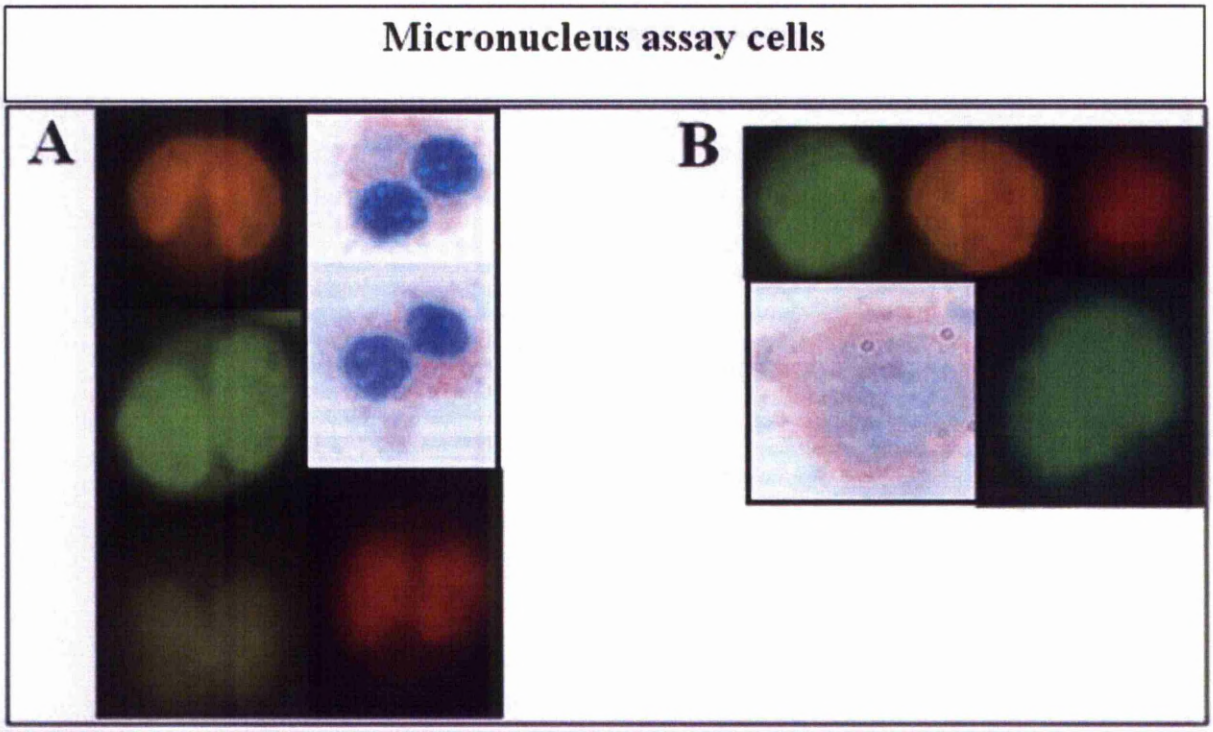

Figure (4.9): Illustrating two types of cells found in the micronucleus assay: (A): the formation of binucleated cells after induction with cytochalasian-B, shown using giemsa stain and acridine orange fluorescent stain. (B): non-dividing or badly spread cells.

4.3 Discussion

4.3.1 Discussion

The role of FANCG in DSBs repair has been investigated in this chapter. Here it has been shown that expression of FANCG is required for optimal repair of the DNA damage induced by phleomycin, an agent that induces a variety of DNA damage including DNA double-strand breaks. This is based on the result that in the complete absence of FANCG as in **NM3-VO (Figures 4.1 and 4.2),** the cells are hypersensitive to phleomycin. Furthermore, I also show that the phosphylation site at serine7 is important in this repair pathway but phosphorylation at serine 387 is much less important. This indicates that FANCG must play a role in the repair processes to repair phleomycin-induced DSBs and that post-translational modifications at FANCG serine 7 is also essential. The assays used to investigate FANCG role in HRR include: survival, growth inhibition assays, cytogenetic experiments (structurally and numerically analyzed) and HRR assays.

4.3.2 Survival and growth inhibition data

In this chapter, genetic evidence has been provided for a role of FANCG in HR as measured by different assays. Firstly, by survival assay and growth inhibition experiments, where it was shown that when exposed to phleomycin, hypersensitivity resulted in FANCG deficient cells. This observation gives support to the model presented in chapter 3, in that the G-BRCA2 complex is involved in HRR, probably in response to the presence of DSBs. This observation is

based on the results produced in the phospho-mutated cell line NM3-S7A. As previously stated, FANCG presence is required for the G-BRCA2 complex to form and is part of the core complex. In the serine 7 mutated cell line, the core complex still forms but the G-BRCA2 complex does not **(Wilson *et al.*, 2008).** This suggests that to repair the phleomycin induced DSBs, G-BRCA2 complex formation is required, as the level of hypersensitivity is similar to or greater than when the FANCG protein is totally absent. However, these results provide information about the post translational modifications of FANCG required to bring about repair of phleomycin induced damage, as when phosphorylation at serine 387 is prevented this leads to only a very slight hypersensitivity to phleomycin. This is in sharp contrast to the results described in chapter 3 where the level of sensitivity of the two phosphorylation site mutations resulted in similar MMC hypersensitivity.

4.3.3 Cytogenetic data

4.3.3.1 Chromosomal aberrations rate and type in FANCG cell lines

At the cytogenetic level, analyses of the rate of structural chromosomal aberrations, the type of observed chromosomal aberrations and chromosomal numerical aneuploidy all provide evidence, implicating FANCG in the process of HRR as discussed below.

G-BRCA2 deficient cells NM3-VO, NM3-S7A presented the highest CA rates in comparison with G-BRCA2 complex containing cells NM3-S387A and NM3-gWT, which presented the lower CAs rates, suggesting that the defective repair of phleomycin induced damage is resulting

from the absence of the G-BRCA2 complex. In comparing the types of aberrations presented when using phleomycin **(Tables 4.4.A, 4.5.A, 4.6.A, 4.7.A, 4.8.A, 4.9.A, 4.10.A and 4.11.A)** it can be clearly seen that chromatid-based aberrations (breaks and exchanges) were generally higher than chromosome-based aberrations in *FANCG* mutant cell lines. This is also true when using MMC (Chapter-3). One can assume that chromosome fragments may result from unrepaired DNA damage or the failure in chromosome exchange formation. The exchange type aberrations most likely result from mis-repaired DNA DSBs.

4.3.3.2 Chromatid lesions produced post treatment with DNA strand breakers

Tables 4.4.A, 4.5.A, 4.6.A, 4.7.A, 4.8.A, 4.9.A, 4.10.A and 4.11.A also indicate that chromosome exchanges and chromosome breaks particularly occurred in NM3–VO and NM3–S7A cells, however they were considerably lower in NM3–gWT and NM3–S387A cells. From the same tables, when comparing only NM3–VO and NM3–S7A cells, it can be seen that the occurrence of chromatid breaks in NM3–S7A cells is generally higher than that recorded in NM3–VO. However, chromatid exchanges predominate in NM3–VO and NM3–S7A cells, while chromatid breaks predominate in NM3–gWT and NM3–S387A cells in response to phleomycin treatment. **Tables 4.4.B, 4.5.B, 4.6.B, 4.7.B, 4.8.B, 4.9.B, 4.10.B, and 4.11.B,** illustrate that in NM3–VO and NM3–S7A cells the predominant type of chromatid exchanges are chromatid exchanges which involve either two or three chromosomes. This is consistent with data presented throughout the literature by various groups and is pointed out in following sections in this chapter **(Section 4.3.3.3).**

Although phleomycin induced DNA damage are likely to be double strand breaks, it is likely that the different NM3 cell lines process these DNA double strand breaks differently. This variation in aberration type produced in these cell lines suggests the presence of different repair pathways used to remove phleomycin induced damage. This predominance of the chromatid exchange aberrations in NM3–VO and NM3–S7A suggest that NHEJ was the main available pathway to process the phleomycin induced DNA damage due to the absence of the G-BRCA2 complex in these cells, as exchanges reflect mis-repair by error prone-NHEJ. This predominance of the chromatid breaks in NM3-gWT and NM3 -S387A cells suggests that NHEJ was not processing the phleomycin-induced damage, as HRR was functional due to the presence of the G-BRCA2 complex in these cells. Taken together, these observations support the hypothesis that the G-BRCA2 is very likely to play a role in promoting proficient HRR to maintain genomic integrity. HRR assays were conducted to further test this hypothesis **(Section 4.3.4).**

4.3.3.3 Cytogenetic data comparison to other repair deficient mutants

Consistent with the cytogenetic data showing high CA rates dominated by chromatid exchanges in G-BRCA2 complex deficient cells NM3–VO and NM3–S7A, chromatid exchanges were also documented by **Stackpole *et al.*, (2007)** in two Chinese hamster cell lines (irs3 and irs1SF) defective in the HRR genes *RAD51C* and *XRCC3* in response to particulate chromate Cr (VI), which is known to induce DNA double strand breaks **(Bryant *et al.*, 2006)**. **Mechilli *et al.*, (2008)** observed that after acetaldehyde treatment cell lines irs1SF and 51D1, deficient in HRR genes *XRCC3* and *RAD51D*, had higher chromatid breaks and exchanges in comparison to the

other cell lines including parental AA8, nucleotide excision repair deficient cell lines UV4, UV5 and UV61 or base excision repair deficient EM9 cell line. **Natarajan *et al.*, (2008)** on the other hand, have reported that HRR-deficient cell lines irs1SF/*XRCC3* and 51D1/*RAD51D* had higher X-ray induced chromatid exchanges, compared to parental AA8 cells. These data suggest that if HRR proteins are mutated or absent, then error-free HRR pathway is compromised, leaving the induced DNA double strand breaks to be repaired by error-prone NHEJ, which will cause genomic instability leading to the cytogenetically observed elevation in chromatid exchanges that cause cellular death.

These chromatid exchanges were also recorded (Chapter-3) in high rates in G-BRCA2 complex deficient cells NM3–VO and NM3–S7A post MMC exposure. This is consistent with findings presented throughout the literature by various groups using various FA cell lines treated with inter-strand cross-linking agents (**Marx *et al.*, 1983; Busch *et al.*, 1996; Lamerdin *et al.*, 2004; Wiegant *et al.*, 2006**) as detailed in Chapter-3 discussion. These data suggest that once the FA pathway is compromised, then NHEJ becomes the active DNA repair pathway producing these observed CA, which implies that the FA pathway may be important in suppressing NHEJ and promoting HRR to sustain genetic stability.

The cytogenetic data showing low wild type CA rates predominated by chromatid breaks in NM3–S387A, suggest that the G-BRCA2 complex is functional in this cell line and processed phleomycin induced DNA damage primarily through HRR. Thus phosphorylation of S387 did not severely affect the repair of directly induced DNA double strand breaks, in sharp contrast to the requirement of the site for proficient repair of MMC-induced ICLs. The reasons for these observations are not entirely clear, although it does seem that the phosphorylation of S387 is not required for proficient HRR. As discussed in the previous chapter, it may be that S387

phosphorylation is important in the events that convert an ICL into a double strand break that can then be repaired by HRR. Thus, it could be speculated that S387 phosphorylation is required for proficient processing of ICLs into double strand breaks or the suppression of NHEJ activity on ICL-repair intermediates, rather than the HRR of the indirectly produced double-strand breaks themselves.

4.3.3.4 Numerical instability in response to phleomycin applied to FA cell lines

The phleomycin hypersensitivity of NM3-VO and NM3-S7A is consistent, not only with elevated rates of chromosomal structural aberrations, but is also consistent with the numerical changes in these cells **(Fig. 4.6, Tables: 4.13, 4.14, 4.15, 4.16, 4.17 and 4.18)**. NM3-VO and NM3-S7A exhibited an increase of chromosomal number in response to phleomycin. This observed numerical increase in chromosomes is consistent with findings of **Ohshim, (2001)** of aneuploidy in nickel sulfate (NiSO4) induced V79 Chinese hamster cell line where the majority of the cells were hyperdiploid. The treated V79 cells had elevated rates of cells with both kinetochore-positive micronuclei and kinetochore-negative micronuclei.

NM3-gWT demonstrated chromosomal numerical stability spanning the usual range of 18-20 chromosomes when exposed to phleomycin. The increase in chromosomal number in NM3-VO and NM3-S7A may indicate either, an elevation in the rate of chromosomal miss-segregation, or a reflection of acentric chromosomal fragments resulting in a higher metaphase chromosomal count. This may suggest a possible effect of phleomycin on the spindle apparatus or on centrosomal stability which would give rise to abnormal chromosome segregation. This hypothesis could have been tested through an alternative approach. Two methods were available

to further investigate this observation. One method was the micronucleus assay **(Krishna *et al.*, 1989; Eastmond and Tucker 1989; Jones *et al.*, 1993; Lynch *et al.*, 1993; Gabriele *et al.*, 1995; Hermine *et al.*, 1997)** and the second method was through the use of fluorescent probes specific to hamster cell lines **(Griffin *et al.*, 2000)**. It was decided to attempt employing the micronucleus assay for that part of the project. However, problems were encountered with the assay and no useable data was generated (see results **Section 4.2.5.2).**

4.3.4 Homologous recombination repair assay data

To further confirm that FANCG is involved in the repair of DSBs through HRR the SCneo neomycin-resistance assay was employed. In response to phleomycin, there is a 1000-fold increase in the level of HRR detected in the wild type cells. This shows that HRR is taking place and the assay was working as expected. In the complete absence of FANCG the rate fell 2.8 fold showing conclusively that FANCG is involved in the repair of phleomycin induced DSBs. Interestingly, the most convincing support for the G-BRCA2 complex being involved comes from the phospho-mutant S7 cell line. The levels of HRR detected in this cell line are less than that detected in the cell line lacking FANCG expression. This is consistent with the results of the metaphase analysis, where in many experiments NM3-S7A exhibited higher levels of aberrations than NM3-VO. It is somewhat unexpected that the phosphorylation site mutant should exhibit a greater defect than the null mutant and the reasons for this are not known. This was not the case for mitomycin C, where the responses of NM3-S7A were intermediate between NM3-VO and NM3-gWT. As NM3-S7A does retain an intact FA core complex, this data provides evidence that the core complex is not required for the repair of phleomycin-induced DNA damage and that

the sensitivity of NM3-S7A is likely to be entirely attributable to its failure to form the G-BRCA2 complex. This hypothesis will be tested in the next chapter using a human *FANCA* deficient cell line, which lacks the FA core complex but retains an intact G-BRCA2 protein complex.

4.4 Summary of the chapter

- It has been demonstrated that the NM3-VO and NM3-S7A cell lines exhibit marked cellular hypersensitivity to phleomycin, an agent that induces DNA strand breaks (single and double strand breaks) and base damage. In contrast, the NM3-S387A cell line exhibits a response to phleomycin that is much more similar to wild type NM3-gWT cells.
- Consistent with this increased cellular hypersensitivity, NM3-VO and NM3-S7A cells exhibit elevated levels of induced structural chromosomal aberrations, with chromatid exchanges being the predominant type of aberration. In addition, both these cell lines also exhibit an increase in chromosome number in response to phleomycin. In contrast, NM3-S387A cells exhibit a response very similar to wild type for both these endpoints.
- Consistent with their cellular and chromosomal hypersensitivity, NM3-VO and NM3-S7A exhibit reduced rates of phleomycin-induced homologous recombination repair in a plasmid-based reporter assay. The HRR defect in NM3-S387A cells is much less severe than that observed for NM3-S7A.

- It is concluded that FANCG is required for cellular resistance to phleomycin and that in absence of the protein, homologous recombination repair fails to occur resulting in the observed chromosomal aberrations. Furthermore, phosphorylation of FANCG at Ser-7 is critical for the HRR of phleomycin-induced damage, as this post-translational modification of FANCG is required for the formation of the G-BRCA2 protein complex (containing BRCA2, FANCD2, FANCG and XRCC3).
- It is hypothesised that in the absence of the G-BRCA2 complex, as occurs in NM3-VO and NM3-S7A, HRR is compromised and phleomycin DNA damage is processed by NHEJ. Mis-repair by NHEJ leads to the observed elevation of chromosomal aberrations, particularly chromatid exchanges.
- Phosphorylation of FANCG at Ser-387 is not critical for the HRR of phleomycin-induced DNA damage, consistent with the observation that the G-BRCA2 complex forms normally in these cells.
- To test this hypothesis, the next chapter will examine the induction of chromosomal aberrations by phleomycin in a cell line that retains an intact G-BRCA2 complex, but lacks the FA core complex (a human *FANCA* mutant cell line).

Chapter-5

Investigating the role of FANCA protein in the repair of induced DNA double strand breaks and (ICLs)

5.1 Introduction

5.1.1 Cell lines used in this chapter

In this chapter focus has been made on the FANCA protein, which is known to be part of the FA core complex where it directly interacts with FANCG, but is not part of the FANCG-BRCA2 complex. The aim of this chapter is to examine the role of FANCA in response to the DNA damaging agents MMC and phleomycin and to determine whether any differences observed could be attributed to specific protein complexes. It has been previously reported that in the cells of patients carrying mutations in the *FANCA* gene are hypersensitive to MMC, but little is known about their sensitivity to x-rays. To determine the cellular sensitivities it was decided to use human *FANCA* mutated cell lines, corrected with the *FANCA* gene, exposing these cell lines to phleomycin and MMC.

The cell lines used in this chapter are human GM6914 fibroblast cells. The cell lines used are either wild type or corrected to wild type compared to *FANCA* defective cell lines.

Cell lines used include 6914-VO, 6914-S1449A and 6914-AWT. 6914-AWT is an immortalized FA-A human fibroblast cell line transduced with full length human *FANCA* cDNA tagged with Flag in the pMMP vector. 6914-VO is a *FANCA* mutant immortalized human fibroblast cell line transduced with empty pMMP vector. 6914-VO cell line does not express FANCA protein (*FANCA*-null cells). 6914-S1449A is a *FANCA* mutant immortalized human fibroblast cell line transduced with human *FANCA* cDNA that has been mutated via site-directed mutagenesis in *FANCA* at serine 1449 to alanine (S1449A).

5.1.2 Investigation of the induction of chromosome aberrations in GM6914 fibroblasts

Similar to Chapter- three and four, classical cytogenetic analysis has been implemented in this chapter (Chapter-5) investigating and determining (using plain Giemsa stain) structural chromosomal aberrations, classifying and analyzing metaphase spreads. The selected cell lines were cultured in the presence and absence of a radiomimetic agent (phleomycin) and a cross-linking agent (MMC). Metaphase spreads were scored and analyzed for chromosomal breakage as well as the formation of radials. Findings of *FANCA* mutant cell lines were compared with findings from corrected control cells. Cellular cultures without the DNA clastogenic agent were used to measure the spontaneous breakage rate. Results were reported as the number of aberrations per cell, the percentage of aberrant cells and the total number of chromatid breaks per cell.

5.2 Results

5.2.1 GM6914 fibroblasts to phleomycin growth inhibition results

From **Figure 5.1** it can be seen that the *FANCA* deficient cell line, 6914-AVO, showed a GI-50 value of 925 ng/ml compared to a value of 1200 ng/ml for the corrected 6914-AWT cell line. This meant that 6914-VO is around 1.3-fold hypersensitive to phleomycin compared to the corrected wild type 6914-AWT **(Fig.5.1)**. These findings show that 6914–VO is only very slightly hypersensitive to phleomycin, indicating that in these cells, which lack *FANCA*, the machinery to repair the phleomycin induced damage is present and functioning almost as well as in the corrected cells. Certainly these *FANCA* deficient cells do not exhibit the levels of phleomycin hypersensitivity observed in *FANCG* deficient cells (Chapter 4). This suggests that the FA core complex does not play an important role in the repair of phleomycin-induced damage and implies that the unaffected G-BRCA2 complex functions independently of FANCA.

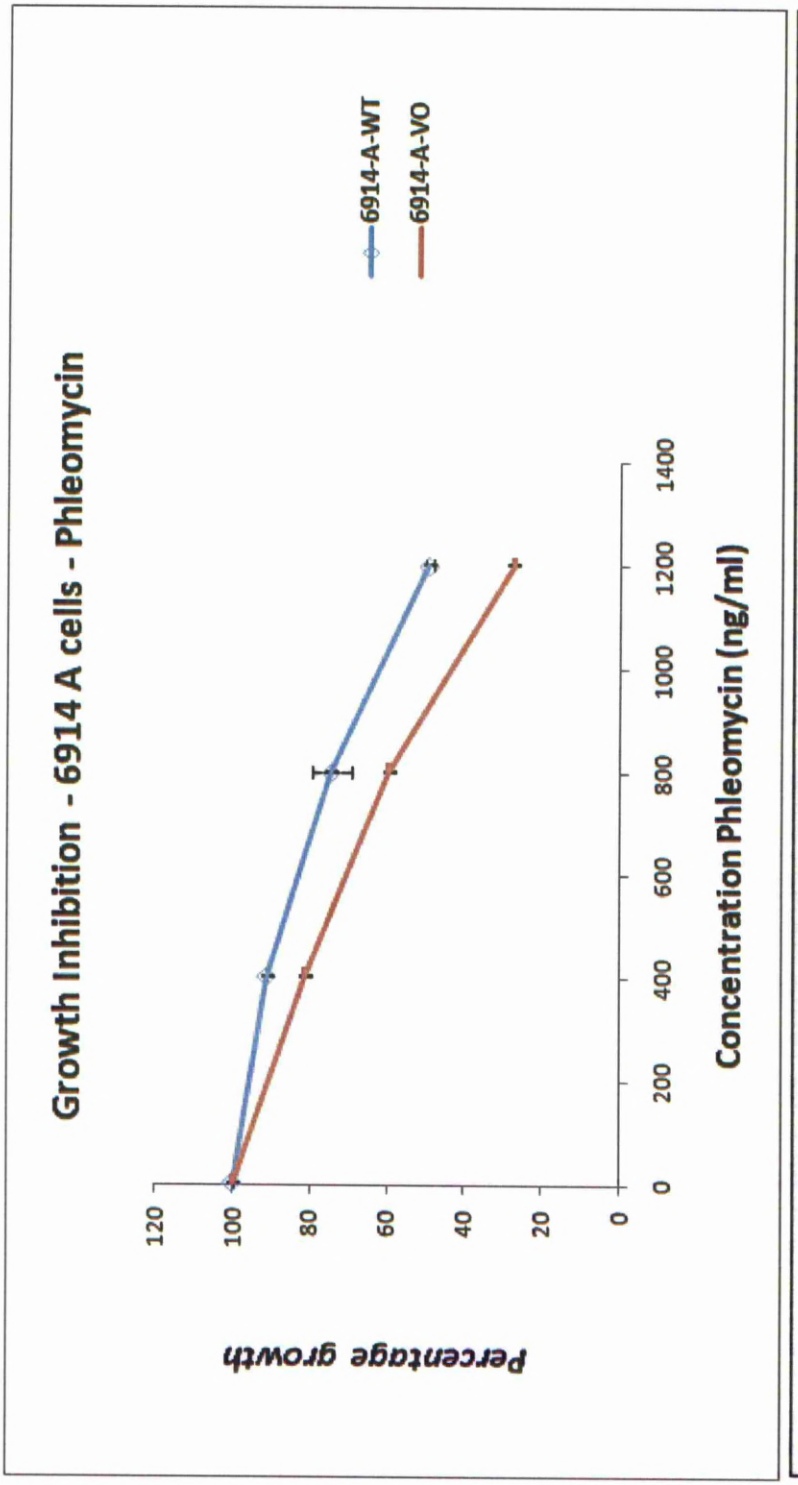

Figure (5.1): Illustrating phleomycin growth inhibition data using two cell lines: 6914-A-WT and 6914-A-VO. Two experiments were performed. Error bars show the standard error of the mean.

5.2.2 GM6914 fibroblasts cytogenetic findings

5.2.2.1 GM6914 fibroblasts chromosomal aberration analysis results to phleomycin

This finding that FANCA was not hypersensitive to DNA damage induced by phleomycin was, further investigated at the chromosomal level. Phleomycin at a dose of 1000 ng/ml was used and produced the cytogenetic profile for *FANCA* deficient cells in response to phleomycin exposure as illustrated by **Tables 5.1-A, 5.2-A and 5.3-A**. Frequencies of both induced and spontaneous chromosome and chromatid aberrations in treated and untreated cell lines cultures 6914-VO, 6914-S1449A and 6914-AWT are presented in **Tables 5.1-A, 5.2-A and 5.3-A**.

5.2.2.1.1 GM6914 fibroblasts chromosome and chromatid aberration rates in control cell cultures

It can be noted that the number of aberrations per cell in untreated cell lines presented a spontaneous rate which did not exceed 0.04 as shown in **Tables 5.1-A, 5.2-A and 5.3-A** and **Fig. 5.2.** Hardly any aberrations were recorded for all untreated 6914-VO, 6914-S1449A and 6914-AWT fibroblasts. The highest number of aberrations per cell for the untreated cells was that recorded for both, 6914-VO and 6914-S1449A as 0.04 aberration/cell followed by 6914-VO, 6914-S1449A and 6914-AWT as 0.02 aberration/cell as shown in **Tables 5.1-A, 5.2-A and 5.3-**

A. Also, from the same **Tables 5.1-A, 5.2-A, 5.3-A and Fig. 5.3** it can be seen that the percentage of aberrant cells that have occurred spontaneously was not very different amongst the various *FANCA* fibroblasts; 6914-VO, 6914-S1449A and 6914-AWT. This ranged from 0% to 4% aberrant cells, which is the number of aberrant cells occurring spontaneously as seen in three independent experiments (replicates) presented in **Tables 5.1-A, 5.2-A and 5.3-A.**

5.2.2.1.2 GM6914 fibroblasts chromosome and chromatid aberration rates in treated cell cultures to phleomycin

Table 5.1-A shows that using doses of 1000 ng/ml phleomycin resulted in 6914-VO and 6914-S1449A fibroblasts producing rates of chromosomal aberrations per cell of 0.16 and 0.2 aberration/cell respectively compared to 0.0 aberration/cell found in 6914-AWT indicating that *FANCA* mutant cell lines 6914-VO and 6914-S1449A are insensitive to phleomycin. Keeping the same experimental conditions and despite slight variation, the readings of each experiment illustrated that *FANCA* mutant fibroblasts presented similar numbers of CA compared to 6914-AWT as shown in **Tables 5.2-A and 5.3-A** confirming and supporting growth inhibition findings of *FANCA* deficient cells 6914-VO insensitivity to phleomycin. This also indicates that phleomycin-induced damage (DNA strand breaks) is being repaired without the presence of the FANCA protein or its phosphorylation at serine 1449. This suggests the presence of a repair pathway that processes DNA strand breaks independently of both FANCA protein and the action of the FA-core complex.

Data-Table: summaries phleomycin treated 6914 cell lines and aberrations found in experiment

Table (5.1-A)

Cell line	Treatment phleomycin ng/ml	Total number of cells sampled	Chromatid based - aberrant cells		Chromosome - aberrant cells		Gaps per cell	Total aberrations without Gaps	Aberrations Per cell	% Aberrant cells	*Total Chromatid Breaks - after aberration converting per cell*
			Ctid-break	Ctid-exch	Chro-break	Chro-exch					
6914 AWT	0	50	0	0	0	0	0.02	0	0	0	0
6914 AWT	1000	50	4	0	0	0	0	4	0.08	8	0.08
6914 AVO	0	50	1	0	0	1	0	2	0.04	4	0.1
6914 AVO	1000	50	7	1	1	0	0.16	9	0.18	14	0.22
6914 S1449A	0	50	1	0	0	0	0.04	1	0.02	2	0.02
6914 S1449A	1000	50	15	2	1	1	0.2	19	0.38	30	0.52

Table abbreviations: Ctid-break: Chromatid break type aberration, Ctid-exch: Chromatid exchange type aberration, Chro-break: Chromosome break type aberration, Chro-exch: Chromosome exchange type aberration.

Data-Table: summaries phleomycin treated 6914 cell lines and aberrations found in experiment

Table (5.2-A)

Cell line	Treatment phleomydin ng/ml	Total number of cells sampled	Chromatid based - aberrant cells		Chromosome - aberrant cells		Gaps per cell	Total aberrations without Gaps	Aberrations Per cell	% Aberrant cells	*Total Chromatid Breaks - after aberration converting per cell*
			Ctid-break	Ctid-exch	Chro-break	Chro-exch					
6914 AWT	0	50	0	0	0	0	0	0	0	0	0
6914 AWT	1000	50	6	1	0	0	0.08	7	0.14	10	0.18
6914 AVO	0	50	1	0	0	0	0.02	1	0.02	2	0.02
6914 AVO	1000	50	8	0	1	0	0.18	9	0.18	14	0.2
6914 S1449A	0	50	1	0	0	0	0.06	1	0.02	2	0.02
6914 S1449A	1000	50	14	0	2	0	0.16	16	0.32	24	0.36

Table abbreviations: Ctid-break: Chromatid break type aberration, Ctid-exch: Chromatid exchange type aberration, Ctid-exch: Chromatid exchange type aberration, Chro-break: Chromosome break type aberration, Chro-exch: Chromosome exchange type aberration.

Data-Table: summaries phleomycin treated 6914 cell lines and aberrations found in experiment

Table (5.3-A)

Cell line	Treatment phleomycin ng/ml	Total number of cells sampled	Chromatid based - aberrant cells		Chromosome - aberrant cells		Gaps per cell	Total aberrations without Gaps	Aberrations Per cell	% Aberrant cells	*Total Chromatid Breaks - after aberration converting per cell*
			Ctid-break	Ctid-exch	Chro-break	Chro-exch					
6914 AWT	0	50	1	0	0	0	0.04	1	0.02	2	0.02
6914 AWT	1000	50	35	3	3	0	0.2	41	0.82	52	1.04
6914 AVO	0	50	0	0	0	0	0.06	0	0	0	0
6914 AVO	1000	50	23	0	0	0	0.12	23	0.46	30	0.46
6914 S1449A	0	50	2	0	0	0	0.08	2	0.04	4	0.04
6914 S1449A	1000	50	23	0	0	0	0.28	23	0.46	34	0.46

Table abbreviations: Ctid-break: Chromatid break type aberration, Ctid-exch: Chromatid exchange type aberration, Chro-break: Chromosome break type aberration, Chro-exch: Chromosome exchange type aberration.

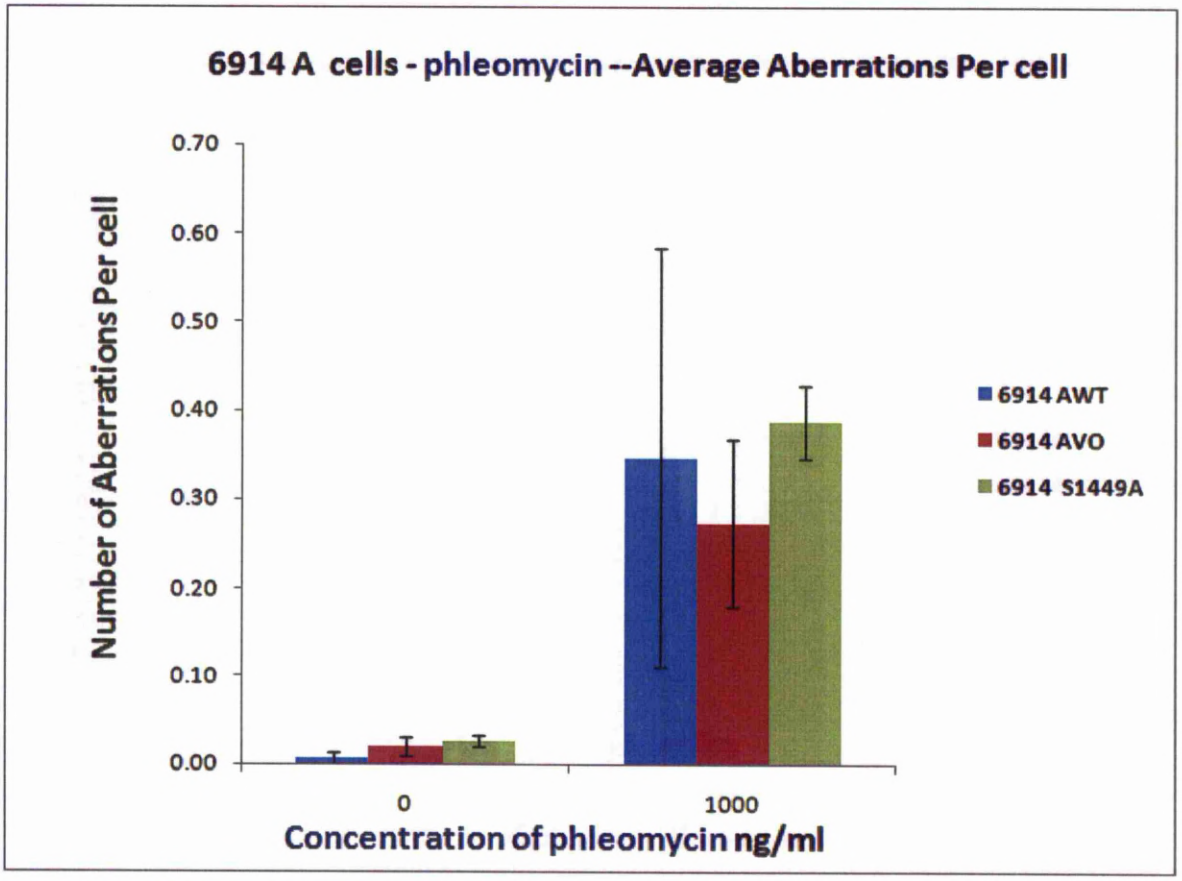

Figure (5.2): Illustrating phleomycin **Average Aberrations Per cell** data using three cell lines: 6914A-WT, 6914A-VO, 6914- S1449A. Three experiments were performed. Error bars show the standard error of the mean.

From the **Pooled Table 5.4,** it can be seen for1000 ng/ml phleomycin, the average aberrations per cell in the 6914-AWT, 6914-VO and 6914-S1449A cell lines were 0.35, 0.27 and 0.39 aberration/cell respectively. Using the same 1000 ng/ml phleomycin dose it can be seen that the average percentage of aberrant cells in the 6914-AWT, 6914-VO and 6914-S1449A cell lines was about 23.3%, 19.3% and 29.3% aberrant cells respectively. Finding of the average number of total chromatid breaks (after converting all the exchanges into chromatid breaks) per cell for the same 1000 ng/ml phleomycin dose was in 6914-AWT, 6914-VO and 6914-S1449A cell lines 0.43, 0.29 and 0.45 chromatid breaks/cell respectively. All of these cytogenetic findings clearly illustrate that *FANCA* mutant cell lines 6914-VO and 6914-S1449A produce chromosome aberrations rates similar to that of the corrected wild type when exposed to phleomycin.

This resemblance in cytogenetic profile in *FANCA* mutant and wild type cell lines to phleomycin is illustrated in graphs as average aberration per cell **(Fig. 5.2),** average percentage aberrant cells **(Fig. 5.3),** or as average total chromatid breaks **(Fig. 5.4).** This is consistent with growth inhibition findings, supporting the suggestion that the machinery to repair double strand breaks is active in *FANCA* mutant cell lines as in the corrected wild type cells, indicating the role of the G-BRCA2 complex in the repair of phleomycin induced damage independently of FANCA and the FA core complex.

Average/Standard error of the mean (SE) - Tables-Results for Human cells 6914 cells phleomycin

Table (5.4)

Cell line	Treatment phleomycin ng/ml	Total number of cells sampled	Average Aberrations Per cell	SE of the mean of Aberrations per cell	Average % Aberrant cells	SE of the mean of % Aberrant cells	Average Total Chromatid Breaks (after converting exchanges) per cell	SE of the mean of Total Chromatid Breaks (after converting exchanges) per cell
6914 AWT	0	150	0.01	0.01	0.67	0.67	0.01	0.01
6914 AWT	1000	150	0.35	0.24	23.33	14.34	0.43	0.30
6914 AVO	0	150	0.02	0.01	2.00	1.15	0.04	0.03
6914 AVO	1000	150	0.27	0.09	19.33	5.33	0.29	0.08
6914 *S1449A*	0	150	0.03	0.01	2.67	0.67	0.03	0.01
6914 *S1449A*	1000	150	0.39	0.04	29.33	2.91	0.45	0.05

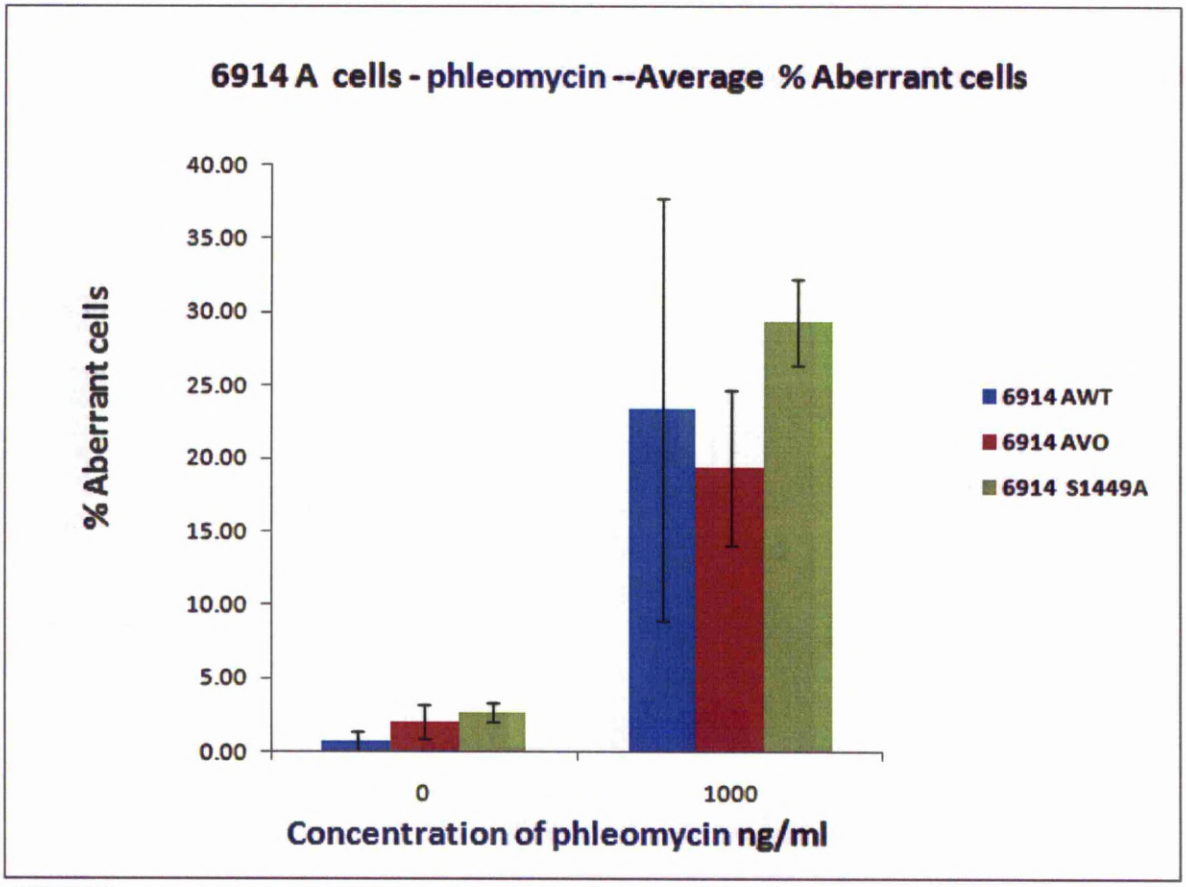

Figure (5.3): Illustrating phleomycin **Average percentage aberrant cells** data using three cell lines: 6914A-WT, 6914A-VO, 6914- S1449A. Three experiments were performed. Error bars show the standard error of the mean.

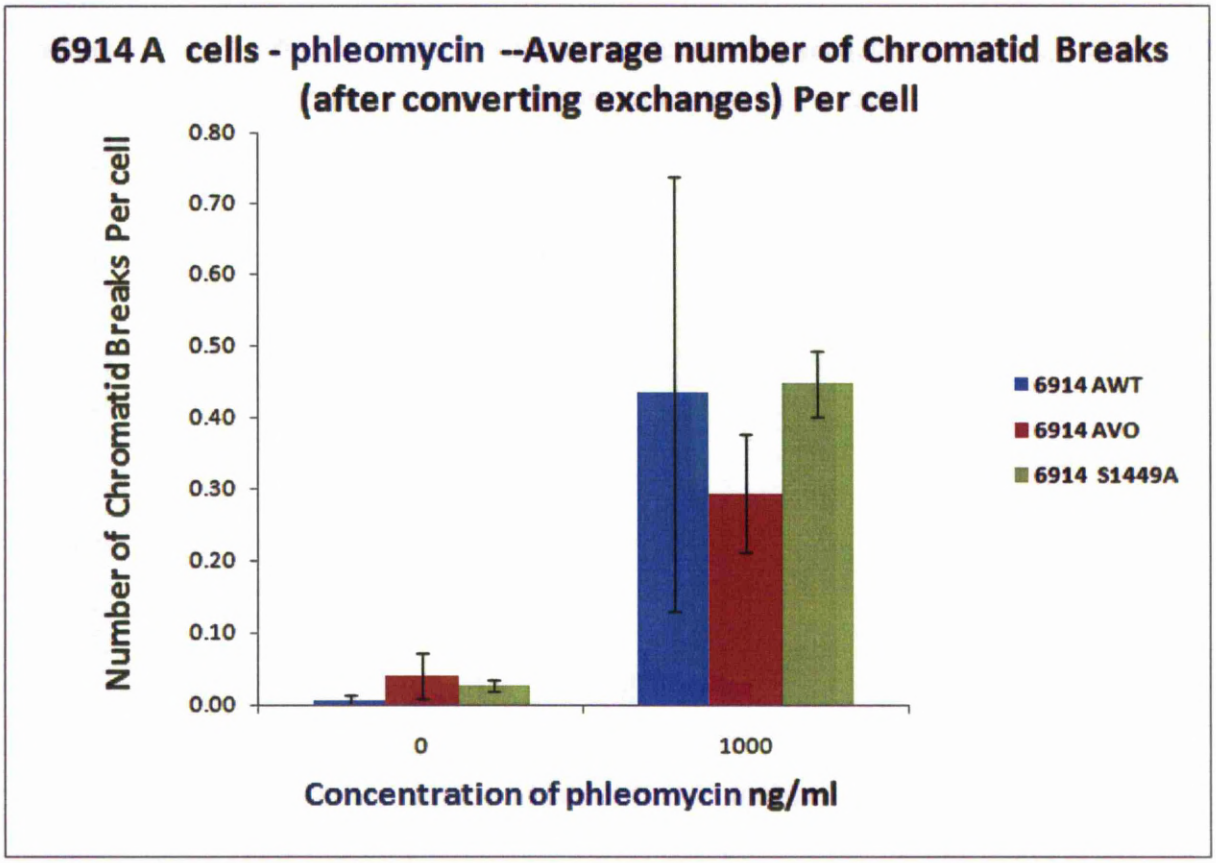

Figure (5.4): Illustrating phleomycin **Average of Total Chromatid Breaks (after converting exchanges) per cell** data using three cell lines: 6914A-WT, 6914A-VO, 6914-S1449A. Three experiments were performed. Error bars show the standard error of the mean.

5.2.2.1.3 The cytogenetic aberration types and predominance in GM6914 fibroblasts to phleomycin

It is clear that in *FANCA* mutant cell lines 6914-VO, 6914-S1449A and 6914-AWT, the chromatid type aberrations predominate, involving specifically breaks but not exchanges at the chromatid level. Occasionally, chromosome type aberrations (such as dicentrics or rings) have been observed in treated cultures as shown in **Tables 5.1-A, 5.2-A and 5.3-A.** These chromosome exchanges (dicentrics or rings) were rarely observed in the untreated cell lines cultures (controls), but were present once as a dicentric recorded in 6914-VO untreated cell lines culture **(Tables 5.1-A and 5.1-B)**. Chromosome breaks and chromosome exchanges in all cell lines were similarly low, with no distinct elevation in any of type of CA as illustrated in **Tables 5.1-A, 5.2-A, 5.3-A, 5.1-B, 5.2-B and 5.3-B.** The occurrence of chromatid breaks and the absence of chromatid exchanges tend to suggest that the G-BRCA2 complex is modulating proficient HRR and that NHEJ is not actively involved in the repair of phleomycin induced damage in these cells.

EXPERIMENT—6914A- phleomycin

Table (5.1-B)

Cell line	Treatment ng/ml Phleomycin	No. Of cells scored	Triradials & no. Of centromeres			Quadri-radials & no. Of centromeres				Complex arrangements & no. Of chromosomes involved				No. Of Chromosome exchanges		No. Of Chromosome breaks	No. Of Chromatid breaks	No. Of TOTAL chromatid breaks [after converting all exchanges plus chromosome breaks]	Total Chromatid Breaks -after aberration converting per cell
			No. Of centromeres			No. Of centromeres				No. Of chromosomes				Type					
			1	2	3	1	2	3	4	2	3	4	5	Ring	Dicentric				
6914-AWT	0	50	0	0	0	0	0	0	0	0	0	0	0	0	0	0	0	0	0
6914-AWT	1000	50	0	0	0	0	0	0	0	0	0	0	0	0	0	0	4	4	0.08
6914-AVO	0	50	0	0	0	0	0	0	0	0	0	0	0	0	1	0	1	5	0.1
6914-AVO	1000	50	0	0	0	0	0	0	0	1	0	0	0	0	0	1	7	11	0.22
6914-S1449A	0	50	0	0	0	0	0	0	0	0	0	0	0	0	0	0	1	1	0.02
6914-S1449A	1000	50	0	1	0	0	0	0	0	1	0	0	0	0	1	1	15	26	0.52

In order to calculate the total number of chromatid breaks, first chromosome breaks, chromosome exchanges and chromatid exchanges including triradials, quadri-radials and complex arrangements were converted to the minimal number of chromatid breaks required for the formation of each specific type of aberration. Then this minimal number of chromatid breaks required for the formation of those aberrations was added to the observed number of chromatid breaks. Then this total number of chromatid breaks has been presented as total chromatid breaks per cell.

EXPERIMENT—6914A- phleomycin

Table (5.2-B)

Cell line	Treatment ng/ml Phleomycin	No. Of cells scored	Triradials & no. Of centromeres			Quadri-radials & no. Of centromeres				Complex arrangements & no. Of chromosomes involved				No. Of Chromosome exchanges		No. Of Chromosome breaks	No. Of Chromatid breaks	No. Of TOTAL chromatid breaks [after converting all exchanges plus chromosome breaks]	Total Chromatid Breaks -after aberration converting per cell
			No. Of centromeres			No. Of centromeres				No. Of chromosomes				Type					
			1	2	3	1	2	3	4	2	3	4	5	Ring	Dicentric				
6914-AWT	0	50	0	0	0	0	0	0	0	0	0	0	0	0	0	0	0	0	0
6914-AWT	1000	50	0	1	0	0	0	0	0	0	0	0	0	0	0	0	6	9	0.18
6914-AVO	0	50	0	0	0	0	0	0	0	0	0	0	0	0	0	0	1	1	0.02
6914-AVO	1000	50	0	0	0	0	0	0	0	0	0	0	0	0	0	1	8	10	0.2
6914-S1449A	0	50	0	0	0	0	0	0	0	0	0	0	0	0	0	0	1	1	0.02
6914-S1449A	1000	50	0	0	0	0	0	0	0	0	0	0	0	0	0	2	14	18	0.36

In order to calculate the total number of chromatid breaks, first chromosome breaks, chromosome exchanges and chromatid exchanges including triradials, quadri-radials and complex arrangements were converted to the minimal number of chromatid breaks required for the formation of each specific type of aberration. Then this minimal number of chromatid breaks required for the formation of those aberrations was added to the observed number of chromatid breaks. Then this total number of chromatid breaks has been presented as total chromatid breaks per cell.

EXPERIMENT—6914A- phleomycin

Table (5.3-B)

Cell line	Treatment ng/ml Phleomycin	No. Of cells scored	Triradials & no. Of centromeres			Quadri-radials & no. Of centromeres				Complex arrangements & no. Of chromosomes involved					No. Of Chromosome exchanges		No. Of Chromosome breaks	No. Of Chromatid breaks	No. Of TOTAL chromatid breaks [after converting all exchanges plus chromosome breaks]	Total Chromatid Breaks -after aberration converting per cell
			No. Of centromeres			No. Of centromeres				No. Of chromosomes					Type					
			1	2	3	1	2	3	4	2	3	4	5	Ring	Dicentric					
6914-AWT	0	50	0	0	0	0	0	0	0	0	0	0	0	0	0		0	1	1	0.02
6914-AWT	1000	50	0	1	0	0	0	1	0	1	0	0	0	0	0		0	35	52	1.04
6914-AVO	0	50	0	0	0	0	0	0	0	0	0	0	0	0	0		0	0	0	0
6914-AVO	1000	50	0	0	0	0	0	0	0	0	0	0	0	0	0		0	23	23	0.46
6914-S1449A	0	50	0	0	0	0	0	0	0	0	0	0	0	0	0		0	2	2	0.04
6914-S1449A	1000	50	0	0	0	0	0	0	0	0	0	0	0	0	0		0	23	23	0.46

In order to calculate the total number of chromatid breaks, first chromosome breaks, chromosome exchanges and chromatid exchanges including triradials, quadri-radials and complex arrangements were converted to the minimal number of chromatid breaks required for the formation of each specific type of aberration. Then this minimal number of chromatid breaks required for the formation of those aberrations was added to the observed number of chromatid breaks. Then this total number of chromatid breaks has been presented as total chromatid breaks per cell.

5.2.2.2 GM6914 fibroblasts chromosomal aberration analysis results to MMC

In order to validate the phleomycin results, and confirm the FA phenotype of the 6914-VO cells, it was decided to perform MMC experiments at the chromosome level. It was previously shown that *FANCA* mutated cell lines used in this study are hypersensitive to MMC **(Collins *et al.*, 2009)** and so aberrations should be detected at the chromosome level. The first experiments were to find the appropriate doses of MMC to be used. Initially, in the course of procedure optimization different MMC doses were utilized. Three doses were used eventually a lower dose of 30 nM, a middle dose of 50 nM and a higher dose of 100 nM MMC. **Tables 5.5.A, 5.6.A, 5.7.A and 5.8.A** illustrate the type and number of chromosome aberrations presented when exposed to MMC. Frequencies of both induced and spontaneous chromosome and chromatid aberrations in treated and untreated cell lines cultures 6914-AWT, 6914-VO and 6914-S1449A are presented in **Tables 5.5.A, 5.6.A, 5.7.A and 5.8.A.**

5.2.2.2.1 GM6914 fibroblasts chromosome and chromatid aberration rates in control cell cultures to MMC

It can be noted that the number of aberrations per cell in untreated cell lines presented a spontaneous rate which did not exceed 0.1 as shown in **Tables 5.5.A, 5.6.A, 5.7.A, 5.8.A** and **Fig. 5.5**. The highest number of aberrations per cell for the untreated cells was that recorded for 6914-S1449A as 0.1 aberration/cell followed by 6914-AWT as 0.06 aberration/cell then 6914-

VO and 6914-S1449A presenting a value of 0.04 aberration/cell. Also from the **Pooled Table 5.9 and Fig. 5.6** it can be illustrated that the average percentage of aberrant cells that have occurred spontaneously was generally lowest in 6914-VO 1.5% aberrant cells and highest in 6914-S1449A 4.5% aberrant cells, where as 6914-AWT presented close numbers of aberrant cells 2% aberrant cells to both *FANCA* mutant cell lines reflecting a similar spontaneous rate in all cell lines.

5.2.2.2.2 GM6914 fibroblasts chromosome and chromatid aberration rates in treated cell cultures to MMC

Table 5.5-A shows that using doses of 100 nM MMC resulted in 6914-VO and 6914-S1449A producing higher rates of chromosomal aberrations per cell 1.58 and 2 aberration/cell respectively compared to 0.44 aberration/cell found in 6914-AWT which represented about 3.6 and 4.5 fold increase respectively. However, this dose considerably reduced metaphase spreads in 6914-S1449A fibroblasts and a lower dose of 30 nM MMC was used in the following experiment. **Table 5.6-A** shows that using doses of 30 nM MMC resulted in 6914-VO and 6914-S1449A producing slightly higher rates of chromosomal aberrations per cell 0.58 and 0.94 aberration/cell respectively compared to 0.48 aberration/cell found in 6914-AWT which represented about 1.2 and 2 fold increase respectively. Nevertheless, in following experiments this elevation of CA became more evident as seen in **Tables 5.7-A and 5.8-A.** For example, **Table 5.7-A** shows that using doses of 30 nM MMC resulted in 6914-VO and 6914-S1449A producing higher rates of chromosomal aberrations per cell 1.86 and 0.94 aberration/cell

respectively compared to 0.16 aberration/cell found in 6914-AWT which represented about 11.6 and 5.9 fold increase respectively. Similarly, **Table 5.8-A** shows that using doses of 30 nM MMC resulted in 6914-VO and 6914-S1449A producing higher rates of chromosomal aberrations per cell 2.86 and 1.68 aberration/cell respectively compared to 0.4 aberration/cell found in 6914-AWT which represented about 7.2 and 4.2 fold increase respectively.

A third MMC dose of 50 nM MMC was adopted in later experiments keeping the previous 30 and 100 nM MMC doses in order to cover the dose range that would produce enough metaphase spreads to be scored with a readable and reliable cytogenetic profile. The same experimental conditions were obtained and despite slight variation, the readings of each experiment illustrated that *FANCA* mutant cells presented an increased number of CA compared to 6914-AWT. **Table 5.8-A** shows that using doses of 50 nM MMC resulted in 6914-VO and 6914-S1449A producing higher rates of chromosomal aberrations per cell 2.8, and 1.86 aberration/cell respectively compared to 0.64 aberration/cell found in 6914-AWT which represented about 4.3 and 2.9 fold increase respectively. **Table 5.7-A** shows that using doses of 50 nM MMC resulted in 6914-VO and 6914-S1449A producing higher rates of chromosomal aberrations per cell 1.58, and 1.84 aberration/cell respectively compared to 0.2 aberration/cell found in 6914-AWT which represented about 7.9 and 9.2 fold increase respectively. This elevation in CA is evident in the three doses used 30, 50 and 100 nM MMC, however occasionally the higher dose reduced the number of metaphase spreads in 6914-VO and 6914-S1449A. Doses of 30 and 100 nM MMC were used in three experiments while the intermediate dose of 50 nM MMC was used in two experiments.

It is clear that in *FANCA* mutant cell lines 6914-VO, 6914-S1449A and control cell line 6914-AWT chromatid type aberrations predominate, involving breaks and exchanges at the chromatid

level. Chromosome type aberrations such as dicentrics or rings occasionally appeared as shown in **Tables 5.5.A, 5.6.A, 5.7.A and 5.8.A.** These dicentrics or rings were almost completely absent in all the untreated cell lines cultures (controls) but were occasionally present in some of *FANCA* mutant 6914-VO, 6914-S1449A treated cell lines cultures.

On the other hand, chromosome breaks were higher than chromosome exchanges in all cell lines. Chromosome breaks generally, were still considerably lower in numbers compared to chromatid breaks. This can be especially seen in treated *FANCA* mutant cell lines cultures 6914-VO, 6914-S1449A in **Tables 5.5.A, 5.6.A, 5.7.A and 5.8.A.**

Data-Table: summaries MMC treated 6914 cell lines and aberrations found in experiment

Table (5.5-A)

Cell line	Treatment MMC nM	Total number of cells sampled	Chromatid based - aberrant cells		Chromosome - aberrant cells		Gaps per cell	Total aberrations without Gaps	Aberrations Per cell	% Aberrant cells	*Total Chromatid Breaks - after aberration converting per cell*
			Ctid-break	Ctid-exch	Chro-break	Chro-exch					
6914 AWT	0	50	0	0	0	0	0.02	0	0	0	0
6914 AWT	100	50	12	7	2	1	0.16	22	0.44	40	0.76
6914 AVO	0	50	1	0	0	1	0	2	0.04	4	0.1
6914 AVO	100	50	31	47	1	0	0.24	79	1.58	54	4.28
6914 S1449A	0	50	1	0	0	0	0.04	1	0.02	2	0.02
6914 S1449A	100	9	9	6	2	1	0.56	18	2	88.9	0.62

Table abbreviations: Ctid-break: Chromatid break type aberration, Ctid-exch: Chromatid exchange type aberration, Ctid-exch: Chromatid exchange type aberration, Chro-break: Chromosome break type aberration, Chro-exch: Chromosome exchange type aberration.

Data-Table: summaries MMC treated 6914 cell lines and aberrations found in experiment

Table (5.6-A)

Cell line	Treatment MMC nM	Total number of cells sampled	Chromatid based - aberrant cells		Chromosome - aberrant cells		Gaps per cell	Total aberrations without Gaps	Aberrations Per cell	% Aberrant cells	*Total Chromatid Breaks - after aberration converting per cell*
			Ctid-break	Ctid-exch	Chro-break	Chro-exch					
6914 AWT	0	50	0	0	0	0	0	0	0	0	0
6914 AWT	30	50	16	4	4	0	0.16	24	0.48	24	0.76
6914 AWT	100	50	3	3	0	0	0.12	6	0.12	12	0.26
6914 AVO	0	50	1	0	0	0	0.02	1	0.02	2	0.02
6914 AVO	30	50	9	17	3	0	0.2	29	0.58	48	1.38
6914 AVO	100	50	33	56	2	1	0.34	92	1.84	68	4.6
6914 S1449A	0	50	1	0	0	0	0.06	1	0.02	2	0.02
6914 S1449A	30	50	15	31	1	0	0.24	47	0.94	38	2.4
6914 S1449A	100	5	11	14	0	0	0	25	5	80	18

Table abbreviations: Ctid-break: Chromatid break type aberration, Ctid-exch: Chromatid exchange type aberration, Ctid-exch: Chromatid exchange type aberration, Chro-break: Chromosome break type aberration, Chro-exch: Chromosome exchange type aberration.

Data-Table: summaries MMC treated 6914 cell lines and aberrations found in experiment

Table (5.7-A)

Cell line	Treatment MMC nM	Total number of cells sampled	Chromatid based - aberrant cells		Chromosome - aberrant cells		Gaps per cell	Total aberrations without Gaps	Aberrations Per cell	% Aberrant cells	*Total Chromatid Breaks - after aberration converting per cell*
			Ctid-break	Ctid-exch	Chro-break	Chro-exch					
6914 AWT	0	50	2	1	0	0	0	3	0.06	6	0.14
6914 AWT	30	50	3	5	0	0	0.04	8	0.16	14	0.44
6914 AWT	50	50	1	9	0	0	0.14	10	0.2	12	0.48
6914 AWT	100	50	17	31	1	0	0.24	42	0.84	50	2.62
6914 AVO	0	50	0	0	0	0	0.16	0	0	0	0
6914 AVO	30	50	37	52	4	0	0.48	93	1.86	76	4.62
6914 AVO	50	50	32	46	1	0	0.24	79	1.58	62	3.82
6914 AVO	100	20	19	43	1	0	0.15	63	3.15	90	9.2
6914 S1449A	0	50	5	0	0	0	0.06	5	0.1	10	0.1
6914 S1449A	30	50	27	18	2	0	0.16	47	0.94	50	1.62
6914 S1449A	50	50	38	49	5	0	0.34	92	1.84	68	4.24
6914 S1449A	100	50	41	46	2	0	0.22	89	1.78	72	4.18

Table abbreviations: Ctid-break: Chromatid break type aberration, Ctid-exch: Chromatid exchange type aberration, Ctid-exch: Chromatid exchange type aberration, Chro-break: Chromosome break type aberration, Chro-exch: Chromosome exchange type aberration.

Data-Table: summaries **MMC treated** 6914 cell lines and aberrations found in experiment

Table (5.8-A)

Cell line	Treatment MMC nM	Total number of cells sampled	Chromatid based - aberrant cells		Chromosome - aberrant cells		Gaps per cell	Total aberrations without Gaps	Aberrations Per cell	% Aberrant cells	*Total Chromatid Breaks - after aberration converting per cell*
			Ctid-break	Ctid-exch	Chro-break	Chro-exch					
6914 AWT	0	50	1	0	0	0	0.04	1	0.02	2	0.02
6914 AWT	30	50	14	4	2	0	0.36	20	0.4	30	0.64
6914 AWT	50	50	15	15	2	0	0.22	32	0.64	32	1.32
6914 AVO	0	50	0	0	0	0	0.06	0	0	0	0
6914 AVO	30	50	49	93	1	0	0.16	143	2.86	82	7.58
6914 AVO	50	50	46	91	3	0	0.3	140	2.8	88	8.02
6914 S1449A	0	50	2	0	0	0	0.08	2	0.04	4	0.04
6914 S1449A	30	50	32	44	8	0	0.34	84	1.68	60	4.06
6914 S1449A	50	50	45	48	0	0	0.34	93	1.86	64	4.22

Table abbreviations: Ctid-break: Chromatid break type aberration, Ctid-exch: Chromatid exchange type aberration, Ctid-exch: Chromatid exchange type aberration, Chro-break: Chromosome break type aberration, Chro-exch: Chromosome exchange type aberration.

Average/Standard error of the mean (SE) – Table - results for Human cells 6914 MMC

Table (5.9)

Cell line	Treatment MMC nM	Total number of cells sampled	Average Aberrations Per cell	SE of the mean of Aberrations per cell	Average % Aberrant cells	SE of the mean of % Aberrant cells	Average Total Chromatid Breaks (after converting exchanges) per cell	SE of the mean of Total Chromatid Breaks (after converting exchanges) per cell
6914 AWT	**0**	**200**	**0.02**	**0.01**	**2.00**	**1.41**	**0.04**	**0.03**
6914 AWT	**30**	**150**	**0.35**	**0.10**	**22.67**	**4.67**	**0.61**	**0.09**
6914 AWT	**50**	**100**	**0.42**	**0.22**	**22.00**	**10.00**	**0.90**	**0.42**
6914 AWT	**100**	**200**	**0.47**	**0.21**	**34.00**	**11.37**	**1.21**	**0.72**
6914 AVO	**0**	**200**	**0.02**	**0.01**	**1.50**	**0.96**	**0.03**	**0.02**
6914 AVO	**30**	**150**	**1.77**	**0.66**	**68.67**	**10.48**	**4.53**	**1.79**
6914 AVO	**50**	**100**	**2.19**	**0.61**	**75.00**	**13.00**	**5.92**	**2.10**
6914 AVO	**100**	**170**	**2.19**	**0.49**	**70.67**	**10.48**	**6.03**	**1.59**
6914 *S1449A*	**0**	**200**	**0.05**	**0.02**	**4.50**	**1.89**	**0.05**	**0.02**
6914 *S1449A*	**30**	**150**	**1.19**	**0.25**	**49.33**	**6.36**	**2.69**	**0.72**
6914 *S1449A*	**50**	**100**	**1.85**	**0.01**	**66.00**	**2.00**	**4.23**	**0.01**
6914 *S1449A*	**100**	**114**	**2.93**	**1.04**	**80.30**	**4.88**	**7.60**	**5.30**

From the **Pooled Table 5.9** it can be seen that when using the higher dose of 100 nM MMC the average aberrations per cell in the 6914-VO and 6914-S1449A cell lines was about 2.19 and 2.93 aberration/cell respectively which was about 4.7 and 6.2 fold respectively higher than that of the corrected wild type 6914-AWT cells which is 0.47 aberrations per cell. Also using the higher dose of 100 nM MMC the average percentage of aberrant cells in the 6914-VO and 6914-S1449A cell lines was about 70.6% and 80.3% aberrant cells respectively which was about 2.1 and 2.4 fold respectively higher than that of the corrected wild type 6914-AWT cells which is 34% aberrant cells. The findings of the average number of total chromatid breaks (after converting all the exchanges into chromatid breaks) per cell for the same higher dose of 100 nM MMC was in 6914-VO and 6914-S1449A cell lines 6.03 and 7.6 chromatid breaks/cell respectively which was about 5 and 6.3 fold respectively higher than that of the corrected wild type 6914-AWT which is about 1.21 chromatid breaks/cell. This *FANCA* mutant cell line cytogenetic profile indicates very clearly and supports the hypersensitivity of *FANCA* mutant cell lines to MMC as observed throughout the literature and pointed out in the discussion. This *FANCA* mutant cellular hypersensitivity to MMC indicate that MMC induced damage (DNA ICLs) are being left unrepaired in the absence of FANCA protein or when its phosphorylation at serine 1449 is mutated to alanine. This suggests that the repair pathway required in processing ICLs has been compromised by the absence of both FANCA protein and the FA-core complex action.

This elevation in cytogenetic structural aberration level in *FANCA* mutant cell lines is shown in graphs as average aberration per cell **(Fig. 5.5),** average percentage aberrant cells **(Fig. 5.6),** or as average total chromatid breaks as shown in **Fig. 5.7.**

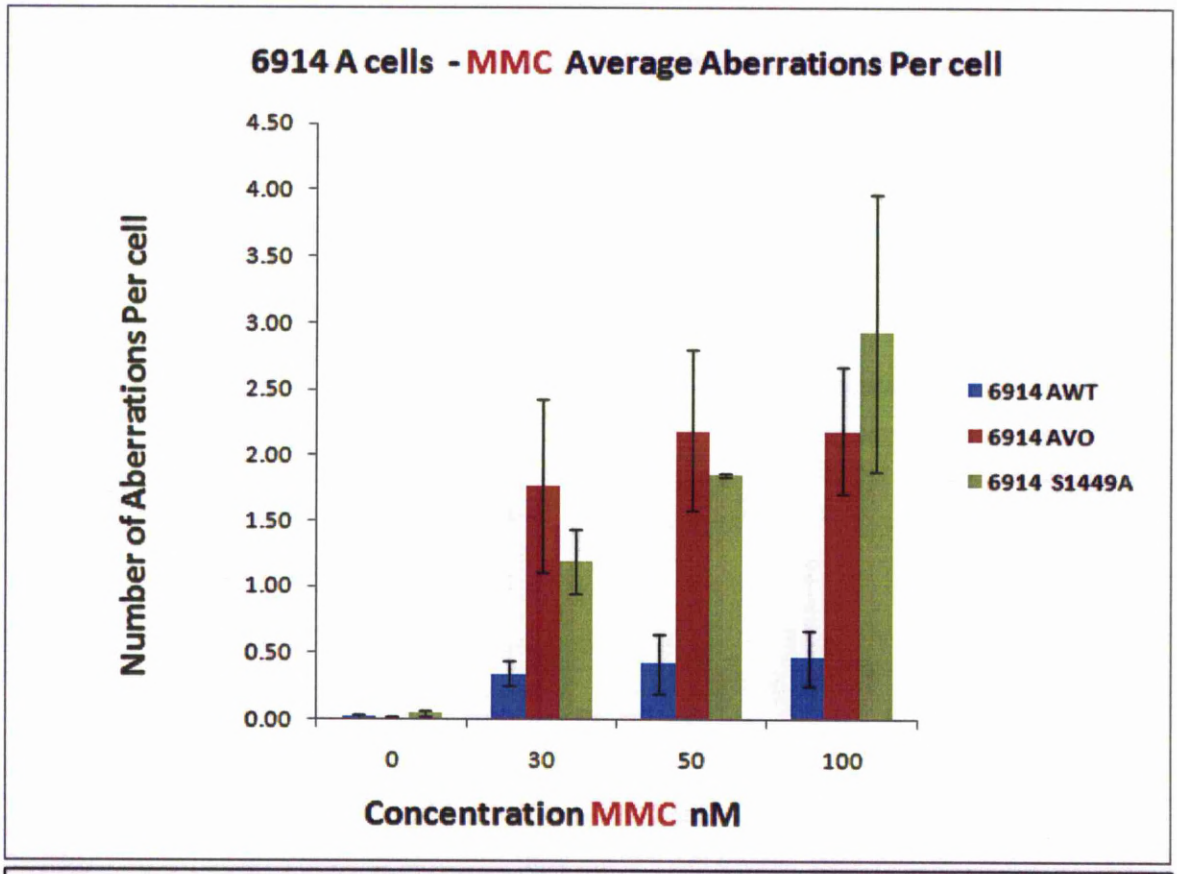

Figure (5.5): Illustrating MMC **Average Aberrations Per cell** data using three cell lines: 6914A-WT, 6914A-VO, 6914- S1449A. Four experiments were performed as shown in Tables 5.5-A, 5.6-A, 5.7-A and 5.8-A. Error bars show the standard error of the mean.

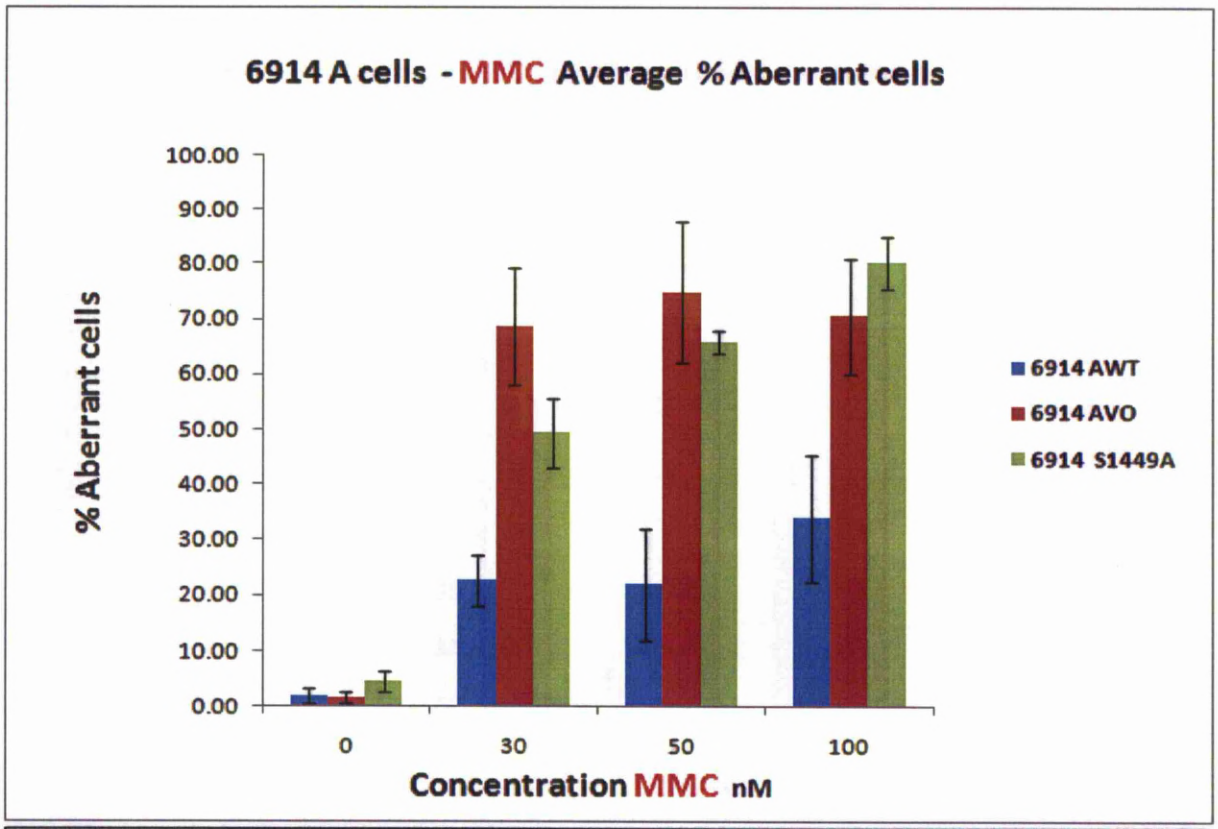

Figure (5.6): Illustrating MMC **Average percentage aberrant cells** data using three cell lines: 6914A-WT, 6914A-VO, 6914- S1449A. Four experiments were performed as shown in Tables 5.5-A, 5.6-A, 5.7-A and 5.8-A. Error bars show the standard error of the mean.

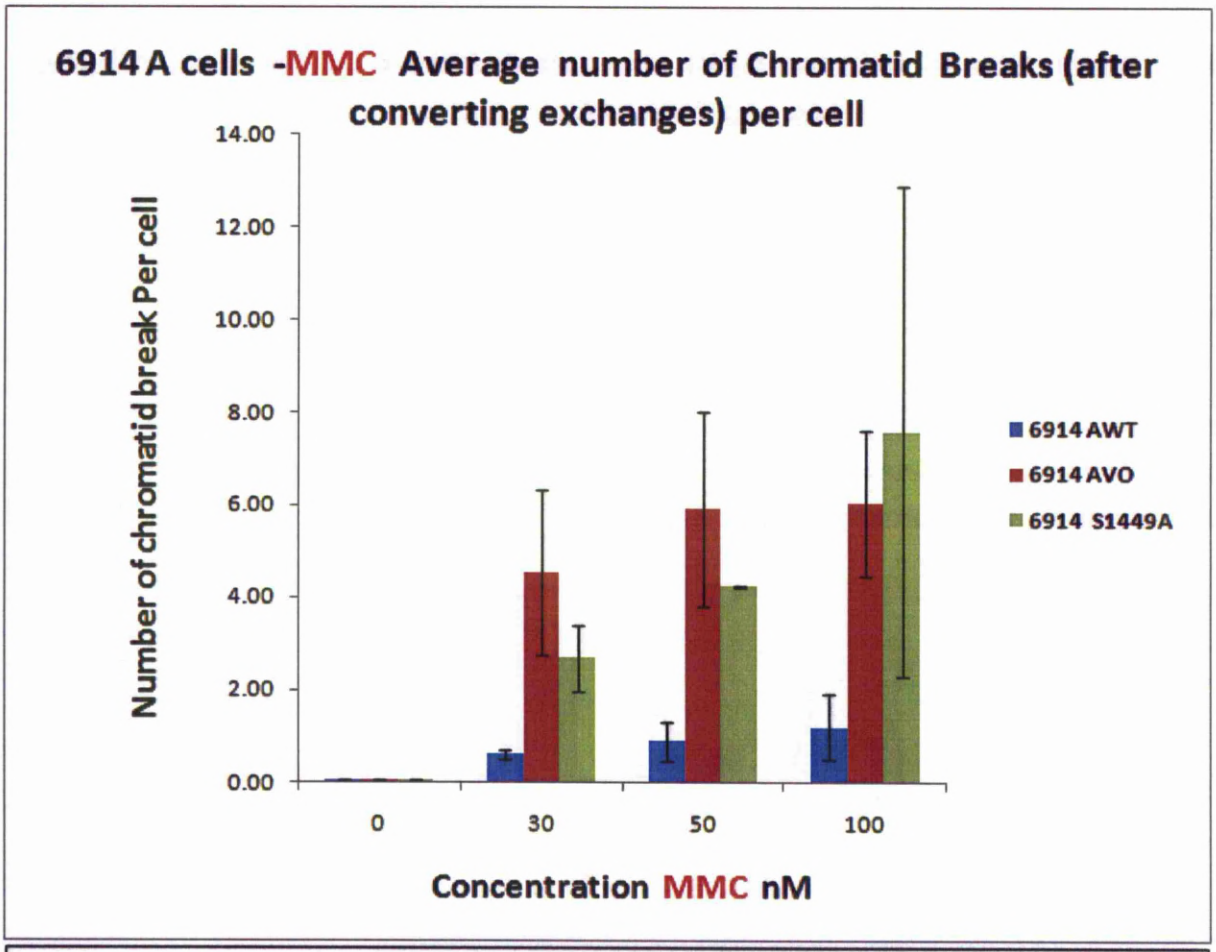

Figure (5.7): Illustrating MMC **Average of Total Chromatid Breaks (after converting exchanges) per cell** data using three cell lines: 6914A-WT, 6914A-VO, 6914- S1449A. Four experiments were performed as shown in Tables 5.5-A, 5.6-A, 5.7-A and 5.8-A. Error bars show the standard error of the mean.

5.2.2.2.3 The cytogenetic aberration types and predominance in GM6914 fibroblasts to MMC

Chromatid exchanges were higher than chromatid breaks, making chromatid exchanges the predominant chromosomal lesion observed in *FANCA* mutant 6914-VO and 6914-S1449A cell line cultures especially in 6914-VO as seen in **Tables 5.5.A, 5.6.A, 5.7.A and 5.8.A.**

From **Tables 5.5.B, 5.6.B, 5.7.B and 5.8.B**, it can be seen that the predominant type of chromatid exchanges are chromatid exchanges which involve two and three chromosomes (classified under complex arrangements). These chromatid exchanges involving two or three chromosomes seem to be higher in occurrence than those involving four or five chromosomes. The involvement of more than three chromosomes in these complex arrangements does occur; however it does so to a lesser extent as illustrated in the same **Tables 5.5.B, 5.6.B, 5.7.B and 5.8.B**. The same tables demonstrate that triradials and quadri-radials appear highest in treated 6914-VO followed by 6914-S1449A compared to the corrected wild type, which is typical of and consistent with FA cells cytogenetic profile. These findings tend to suggest that NHEJ was the main available repair pathway in 6914-VO and 6914-S1449A cell lines to repair ICLs.

EXPERIMENT—6914A-MMC

Table (5.5-B)

Cell line	Treatment nM MMC	No. Of cells scored	Triradials & no. Of centromeres			Quadri-radials & no. Of centromeres				Complex arrangements & no. Of chromosomes involved				No. Of Chromosome exchanges		No. Of Chromosome breaks	No. Of Chromatid breaks	No. Of TOTAL chromatid breaks [after converting all exchanges plus chromosome breaks]	Total Chromatid Breaks -after aberration converting per cell
			No. Of centromeres			No. Of centromeres				No. Of chromosomes				Type					
			1	2	3	1	2	3	4	2	3	4	5	Ring	Dicentric				
6914-AWT	0	50	0	0	0	0	0	0	0	0	0	0	0	0	0	0	0	0	0
6914-AWT	100	50	0	2	0	0	0	0	0	4	1	0	0	1	0	2	12	38	0.76
6914-AVO	0	50	0	0	0	0	0	0	0	0	0	0	0	0	1	0	1	5	0.1
6914-AVO	100	50	3	4	0	4	5	0	0	10	11	5	5	0	0	1	31	214	4.28
6914-S1449A	0	50	0	0	0	0	0	0	0	0	0	0	0	0	0	0	1	1	0.02
6914-S1449A	100	9	0	0	0	0	0	0	0	5	1	0	0	1	0	2	9	31	0.62

In order to calculate the total number of chromatid breaks, first chromosome breaks, chromosome exchanges and chromatid exchanges including triradials, quadri-radials and complex arrangements were converted to the minimal number of chromatid breaks required for the formation of each specific type of aberration. Then this minimal number of chromatid breaks required for the formation of those aberrations was added to the observed number of chromatid breaks. Then this total number of chromatid breaks has been presented as total chromatid breaks per cell.

EXPERIMENT—6914A-MMC

Table (5.6-B)

Cell line	Treatment nM MMC	No. Of cells scored	Triradials & no. Of centromeres			Quadri-radials & no. Of centromeres				Complex arrangements & no. Of chromosomes involved				No. Of Chromosome exchanges		No. Of Chromosome breaks	No. Of Chromatid breaks	No. Of TOTAL chromatid breaks [after converting all exchanges plus chromosome breaks]	Total Chromatid Breaks -after aberration converting per cell
			No. Of centromeres			No. Of centromeres				No. Of chromosomes				Type					
			1	2	3	1	2	3	4	2	3	4	5	Ring	Dicentric				
6914-AWT	0	50	0	0	0	0	0	0	0	0	0	0	0	0	0	0	0	0	0
6914-AWT	30	50	0	0	1	0	0	0	0	2	1	0	0	0	0	4	16	38	0.76
6914-AWT	100	50	0	0	0	0	0	0	0	1	2	0	0	0	0	0	3	13	0.26
6914-AVO	0	50	0	0	0	0	0	0	0	0	0	0	0	0	0	0	1	1	0.02
6914-AVO	30	50	1	5	0	1	1	1	0	5	2	1	0	0	0	3	9	69	1.38
6914-AVO	100	50	2	7	1	0	4	1	0	17	18	3	3	1	0	2	33	230	4.6
6914-S1449A	0	50	0	0	0	0	0	0	0	0	0	0	0	0	0	0	1	1	0.02
6914-S1449A	30	50	0	7	1	2	1	0	0	9	9	2	0	0	0	1	15	120	2.4
6914-S1449A	100	5	1	0	0	0	0	0	0	2	3	2	6	0	0	0	11	90	18

In order to calculate the total number of chromatid breaks, first chromosome breaks, chromosome exchanges and chromatid exchanges including triradials, quadri-radials and complex arrangements were converted to the minimal number of chromatid breaks required for the formation of each specific type of aberration. Then this minimal number of chromatid breaks required for the formation of those aberrations was added to the observed number of chromatid breaks. Then this total number of chromatid breaks has been presented as total chromatid breaks per cell.

EXPERIMENT—6914A-MMC

Table (5.7-B)

Cell line	Treatment nM MMC	No. Of cells scored	Triradials & no. Of centromeres			Quadri-radials & no. Of centromeres				Complex arrangements & no. Of chromosomes involved				No. Of Chromosome exchanges		No. Of Chromosome breaks	No. Of Chromatid breaks	No. Of TOTAL chromatid breaks [after converting all exchanges plus chromosome breaks]	Total Chromatid Breaks -after aberration converting per cell
			No. Of centromeres			No. Of centromeres				No. Of chromosomes				Type					
			1	2	3	1	2	3	4	2	3	4	5	Ring	Dicentric				
6914-AWT	0	50	0	0	0	0	0	0	0	0	1	0	0	0	0	0	3	7	0.14
6914-AWT	30	50	0	1	0	1	0	0	0	1	1	1	0	0	0	0	3	22	0.44
6914-AWT	50	50	0	3	0	0	1	0	0	4	1	0	0	0	0	0	1	24	0.48
6914-AWT	100	50	5	3	2	4	0	0	0	4	10	3	0	0	0	1	17	131	2.62
6914-AVO	0	50	0	0	0	0	0	0	0	0	0	0	0	0	0	0	0	0	0
6914-AVO	30	50	9	3	0	3	1	0	1	15	13	5	2	0	0	4	37	231	4.62
6914-AVO	50	50	2	7	1	1	6	0	0	14	7	6	2	0	0	1	32	191	3.82
6914-AVO	100	20	0	9	0	2	3	0	0	10	11	3	5	0	0	1	19	184	9.2
6914-S1449A	0	50	0	0	0	0	0	0	0	0	0	0	0	0	0	0	5	5	0.1
6914-S1449A	30	50	2	6	0	0	1	0	0	7	1	1	0	0	0	2	27	81	1.62
6914-S1449A	50	50	9	9	0	1	2	0	0	9	16	2	1	0	0	5	38	212	4.24
6914-S1449A	100	50	7	3	0	2	1	0	0	13	13	5	2	0	0	2	41	209	4.18

In order to calculate the total number of chromatid breaks, first chromosome breaks, chromosome exchanges and chromatid exchanges including triradials, quadri-radials and complex arrangements were converted to the minimal number of chromatid breaks required for the formation of each specific type of aberration. Then this minimal number of chromatid breaks required for the formation of those aberrations was added to the observed number of chromatid breaks. Then this total number of chromatid breaks has been presented as total chromatid breaks per cell.

EXPERIMENT—6914A-MMC

Table (5.8-B)

Cell line	Treatment nM MMC	No. Of cells scored	Triradials & no. Of centromeres			Quadri-radials & no. Of centromeres				Complex arrangements & no. Of chromosomes involved				No. Of Chromosome exchanges			No. Of Chromosome breaks	No. Of Chromatid breaks	No. Of TOTAL chromatid breaks [after converting all exchanges plus chromosome breaks]	Total Chromatid Breaks -after aberration converting per cell
			No. Of centromeres			No. Of centromeres				No. Of chromosomes				Type						
			1	2	3	1	2	3	4	2	3	4	5	Ring	Dicentric					
6914-AWT	0	50	0	0	0	0	0	0	0	0	0	0	0	0	0		0	1	1	0.02
6914-AWT	30	50	2	0	0	0	0	0	0	1	0	1	0	0	0		2	14	32	0.64
6914-AWT	50	50	1	4	0	1	0	0	0	5	3	1	0	0	0		2	15	66	1.32
6914-AVO	0	50	0	0	0	0	0	0	0	0	0	0	0	0	0		0	0	0	0
6914-AVO	30	50	3	11	1	6	3	0	0	26	33	7	3	0	0		1	49	379	7.58
6914-AVO	50	50	5	16	0	3	3	1	0	24	21	7	11	0	0		3	46	401	8.02
6914-S1449A	0	50	0	0	0	0	0	0	0	0	0	0	0	0	0		0	0	2	0.04
6914-S1449A	30	50	4	11	1	5	3	2	0	7	8	2	1	0	0		8	32	203	4.06
6914-S1449A	50	50	3	5	1	1	2	1	0	15	14	6	0	0	0		0	45	211	4.22

In order to calculate the total number of chromatid breaks, first chromosome breaks, chromosome exchanges and chromatid exchanges including triradials, quadri-radials and complex arrangements were converted to the minimal number of chromatid breaks required for the formation of each specific type of aberration. Then this minimal number of chromatid breaks required for the formation of those aberrations was added to the observed number of chromatid breaks. Then this total number of chromatid breaks has been presented as total chromatid breaks per cell.

5.3 Discussion

DNA-damaging agents such as radiomimetic agents or cross-linking agents activate FANCD2 mono-ubiquitination, leading to its targeting to nuclear foci that also contain HRR proteins BRCA1 and FANCD1/BRCA2. The question addressed in this chapter is whether or not FANCA protein is involved in modulating proficient HRR as found for FANCG (as discussed in chapter four). To investigate this, *FANCA* mutant cell lines 6914-VO and 6914-S1449A were employed and tested for hypersensitivity to both a DNA strand break inducer (phleomycin) and an inter-strand crosslink inducer (MMC). The cytogenetic profile for the selected cell lines 6914-AWT, 6914-VO and 6914-S1449A was also analyzed. The obtained data were compared to data presented in the literature when available.

Growth inhibition experiments **(Fig. 5.1)** show low hypersensitivity of *FANCA* deficient cell line 6914-VO to phleomycin suggesting that the FANCA protein is not essential to process DNA strand breaks induced by phleomycin. This phleomycin insensitivity is illustrated through growth inhibition assays is backed up by the lack of phleomycin induced chromosomal aberrations in the cytogenetic profile for mutant cell lines 6914-VO and 6914-S1449 which also suggests that the phosphorylation activity at S1449 is not critical in processing DNA strand breaks. Despite this lack of hypersensitivity in response to phleomycin, the expected hypersensitivities and cytogenetic profiles were observed after MMC induced damage. FANCA and its phosphorylation at S1449 seem critical in processing ICLs induced by MMC.

This may go some way in explaining the lack of published work in the literature concerning FANCA hypersensitivity to radiomimetic agents (phleomycin). Whereas there is a lot published about FANCA hypersensitivity to cross-linking agents (MMC). Over the years data has emerged

that allowed further characterization of the FANC proteins and the roles they may play in different repair pathways. For example, in 2005, **Nakanishi *et al.,*** tested whether cells from FA patients (groups A, G, and D2) and mouse *FANCA*$^{-/-}$ cells with a targeted mutation are impaired for this HR repair pathway. **Nakanishi *et al.,* (2005)** utilized a number of *FANC* deficient cells including EUFA326 FA-G and GM6914 FA-A cells to test for their involvement in HRR and single-strand annealing (SSA) repair pathways and concluded that FANCG and FANCA promote HRR of chromosomal double-strand breaks (DSBs). This is in agreement with my findings in chapter four which support the involvement of FANCG in HRR; however the data that I have generated in chapter five tend to suggest that FANCA protein is less involved in HRR in response to phleomycin damage but is still involved in HRR pathway involved in repairing ICLs induced damage.

Also in support of my findings that FANCA is less involved in DNA strand breaks repair through HRR comes from preliminary HRR assays data produced by (Vijayashree Mysore at the Jones laboratory) to *FANCA* human cell lines exposed to phleomycin (unpublished data). The data illustrate similar levels of HRR produced by *FANCA* mutant cell lines 6914-VO, 6914-S1449A and the corrected wild type cell line 6914-AWT following phleomycin treatment indicating their insensitivity to phleomycin which is consistent with both my growth inhibition and cytogenetic findings for *FANCA* human cell lines 6914-VO, 6914-S1449A and 6914-AWT to phleomycin in chapter five. Also consistent with my findings that *FANCA* mutant cell lines 6914-VO and 6914-S1449A are hypersensitive to MMC treatment are HRR assays produced independently by (Vijayashree Mysore at the Jones laboratory) illustrating reduced levels of HRR produced by *FANCA* mutant cell lines 6914-VO and 6914-S1449A post MMC treatment

which had 3.2 and 2.7 fold respectively reduced recombination frequency compared to that of the corrected wild type 6914-AWT.

Also consistent with my growth inhibition and cytogenetic findings are growth inhibition data produced independently by (Vijayashree Mysore at the Jones laboratory) to *FANCA* human cell lines exposed to phleomycin and MMC (not published). The data indicate *FANCA* mutant cell lines 6914-VO and 6914-S1449A insensitivity to phleomycin and illustrates increased hypersensitivity by *FANCA* mutant cell lines 6914-VO and 6914-S1449A following MMC treatment which were 3.7 and 3.4 fold respectively hypersensitive compared to the corrected wild type 6914-AWT.

The observed hypersensitivity recorded in cytogenetic experiments as elevation in CA as illustrated in **Pooled Table 5.9** can be compared to previous findings made by **Duckworth-Rysiecki *et al.,*** in 1986 where GM6914 cells expressed cellular hypersensitivity to MMC and elevated chromosomal instability. **Table 5.9** illustrates that when using the higher dose of 100 nM MMC the average aberrations per cell in the 6914-VO and 6914-S1449A cell lines was about 2.19 and aberration/cell respectively which was about 4.7 and 6.2 fold respectively higher than that of the corrected wild type 6914-AWT cells which is 0.47 aberration/cell. Also finding of the average number of total chromatid breaks (after converting all the exchanges into chromatid breaks) per cell for the same higher dose of 100 nM MMC was in 6914-VO and 6914-S1449A cell lines about 6.03 and 7.6 chromatid breaks/cell respectively which is about 5 and 6.3 fold respectively higher than that of the corrected wild type 6914-AWT which is about 1.21 chromatid breaks/cell. Consistent with these findings, **Duckworth-Rysiecki *et al.,* (1986)** using cytogenetic analysis reported that GM6914 cells also had an elevated chromosome aberrations

rate of about 4-fold when exposed to MMC 0.1 μg/ml MMC for 30 minutes compared to their equivalent controls. In support of these findings, **Duckworth-Rysiecki *et al.*** also reported using survival assays in 1986 that GM6914 cells were 8 fold hypersensitive to MMC compared to their equivalent controls. **Duckworth-Rysiecki *et al.*** also pointed out their observation of about 3-fold hypersensitivity of GM6914 cells to another DNA-cross-linking clastogen (nitrogen mustard) compared to their equivalent control (GM637) cells. However, in contrast to my cytogenetic findings of chromatid exchanges being predominant in *FANCA* mutant fibroblasts 6914-VO and 6914-S1449A, **Duckworth-Rysiecki *et al.*, (1986)** reports the predominance of chromatid breaks and chromatid gaps post MMC treatment.

From growth inhibition graphs produced by **Collins *et al.*, (2009)** for 6914-VO and 6914-S1449A cells were estimated to be about 5, 2.3 fold higher respectively in sensitivity to MMC treatment compared to corrected wild type 6914-AWT. Also from graphs produced by **Collins *et al.*, (2009)** presenting cytogenetic data, the average number of aberrations per metaphase cell for 6914-VO and 6914-S1449A was calculated to be 6.8, 3.6 aberration/metaphase respectively which is about 3, 1.6 fold higher respectively in response to MMC treatment compared to that produced by the corrected wild type 6914-AWT which is 2.3 aberration/metaphase. **Collins *et al.*, (2009)** suggested that this intermediate cellular hypersensitivity that they had observed in 6914-S1449A cells may indicate partial repair of the DNA damage induced by MMC.

This cellular hypersensitivity to MMC observed by **Collins *et al.*, (2009)** is generally consistent with the cytogenetic findings for *FANCA* mutant cell lines 6914-VO and 6914-S1449A presented in **Tables 5.5.A, 5.6.A, 5.7.A, 5.8.A and 5.9** that show increased MMC-induced chromosomal aberrations. However, whilst **Collins *et al.*, (2009)** found the phenotype of 6914-S1449A to be

intermediate that of 6914-VO and 6914-AWT, I found very similar levels of chromosomal aberrations were induced in the phosphorylation and null mutants.

5.4 Summary of the chapter

- It has been demonstrated that GM6914-VO and GM6914-S1449A cells exhibit little or no increased sensitivity to phleomycin in a growth inhibition assay.
- Consistent with the lack of cellular hypersensitivity, GM6914-VO and GM6914-S1449A cells exhibit a similar level of induced chromosomal aberrations to the wild type cell line GM6914-AWT in response to phleomycin.
- In contrast, both GM6914-VO and GM6914-S1449A cells exhibit increased levels of chromosomal aberrations in response to MMC. This is consistent with the cellular hypersensitivity to MMC previously reported for these cell lines **(Collins *et al.*, 2009)**.
- Unpublished data from the Jones laboratory indicates that while GM6914-VO and GM6914-S1449A cells exhibit reduced HRR in response to MMC, there is little or no defect in HRR following phleomycin treatment.
- It is concluded that while FANCA is required for cellular resistance to inter-strand cross-linking agents and the proficient repair of ICL, it is not required for the repair of phleomycin-induced DNA strand breaks.
- Given that the G-BRCA2 complex is formed in cells deficient for FANCA (such as GM6914-VO), the data in this chapter provide further evidence that this complex is

specifically required for the homologous recombination repair of DNA strand breaks, such as those induced by phleomycin.

- To further support the model that G-BRCA2 complex modulates proficient HRR of phleomycin-induced DNA strand breaks and not the nuclear FA-core complex, Chapter-6 will focus on processing DNA lesions (DNA strand breaks and ICLs) in the absence of the G-BRCA2 complex but in the presence the FA core complex. This will involve utilization of *FANCD2* deficient human cell lines. Cells that are deficient for *FANCD2* form a functional FA core complex but will lack the G-BRCA2 complex. In addition, cells expressing a FANCD2 protein mutated at a phosphorylation site required for the interaction of FANCD2 with BRCA2 will be investigated **(Zhi *et al.*, 2009)**.

Chapter-6

Investigating the role of the FANCD2 protein in the repair of DNA double strand breaks and inter-strand cross-links

6.1 Introduction

6.1.1 Introduction

In this chapter the role of FANCD2 in response to DNA double strand break and inter strand cross link damage has been investigated. It has been shown that FANCD2 is a member of the G-BRCA2 complex but is not part of the FA core complex, although it is mono-ubiquitinated by this complex in response to DNA damage **(Sections 1.4.9.3** and **1.4.9.4).** By studying the role of FANCD2 in response to DNA strand breaking or inter-strand cross-linking agents, it is hoped that the results would provide further insight into the role of the G-BRCA2 complex in HRR induced by phleomycin damage. To do this the human *FANCD2* deficient cell line PD20 will be exposed to phleomycin and MMC, growth inhibition assays and chromosomal analysis will be conducted as previously described, **(Methods Sections 2.1.2.5, 2.1.2.10.2.2 and 2.1.2.10.3).** In doing so, the types of chromosomal aberrations induced may give some insight into the role of the FANCD2 in the G-BRCA2 complex.

6.1.2 Cell lines utilized in this chapter

The *FANCD2* deficient cell line used in these studies was PD20, a human patient derived fibroblast cell line. PD20 was transduced with either an empty pMMP vector or with pMMP containing full-length *FANCD2* cDNA (referred to as PD20-D2WT), the *FANCD2* (K561R) mono-ubiquitination mutant (referred to as PD20-K561R), *FANCD2* (S331A) phospho-mutant (referred to as PD20-S331A) or *FANCD2* (S331D) phospho-mutant (referred to as PD20-S331D). PD20-3-15 was chromosomally corrected with human chromosome 3p. All described in detail in the methods section and in (**Garcia-Higuera *et al.*, 2001; Zhi *et al.*, 2009**).

6.2 Results

6.2.1 Growth inhibition assays results of PD20 cells to phleomycin

The role of FANCD2 in response to phleomycin is shown in **Figure 6.1**. From the graph it can be seen that the *FANCD2* deficient cell line, PD20, has a GI-50 value of 295 ng/ml compared to a value of 985 ng/ml for PD20-D2WT making PD20 3.3-fold hypersensitive to phleomycin. PD20-S331A had a GI-50 value of 520 ng/ml (1.9-fold hypersensitive), PD20-S331D had a GI-50 value of 840 ng/ml (1.2-fold), PD20-K561R had a GI-50 value of 490 ng/ml (2-fold hypersensitive). PD20-315 had a GI-50 value of 1005 ng/ml compared to 985 ng/ml for PD20 D2WT, confirming a wild type phenotype for both cell lines **(Fig. 6.1)**. Thus, PD20 cells were the most hypersensitive to phleomycin, PD20-S331A and PD20-K561R exhibited intermediate

sensitivity, while the phospho-mimetic cell line PD20-S331D, was only slightly sensitive to phleomycin compared to the two wild type cell lines.

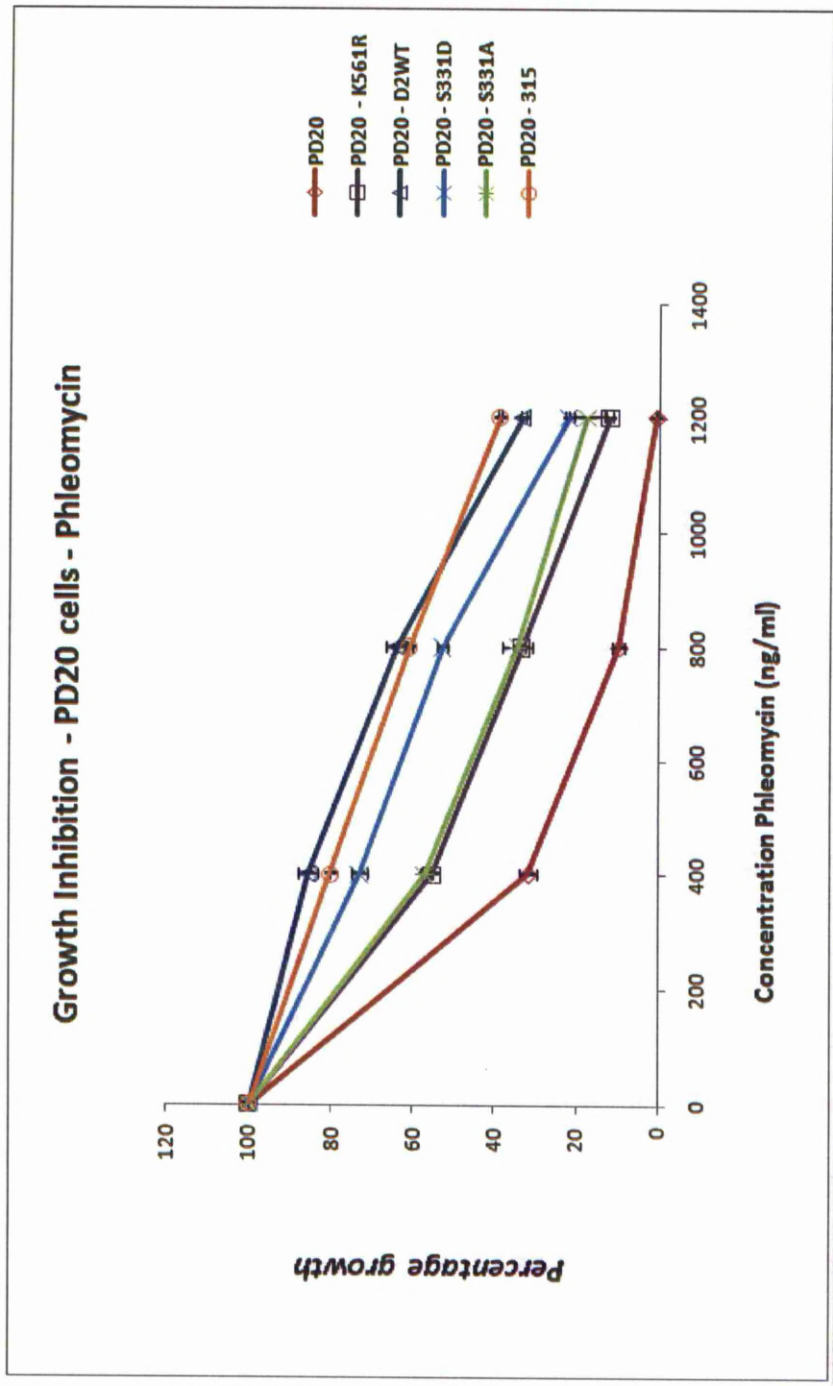

Figure (6.1): Illustrating phleomycin growth inhibition data using six cell lines: PD20, PD20-S331A, PD20-S331D, PD20-K561R, PD20-315 and PD20-D2WT. Three experiments were performed. Error bars show the standard error of the mean.

6.2.2 Metaphase analysis in PD20 cells

6.2.2.1 Phleomycin-induced chromosomal aberration in PD20 cell lines

After the growth inhibition results showed that FANCD2 played a role in the repair of phleomycin induced damage it was decided to further investigate these results to observe what was happening at the chromosomal level. This was carried out by exposing these cell lines to 500 and 1000 ng/ml of phleomycin to produce the cytogenetic profile for *FANCD2* mutant and wild type corrected cells as illustrated in **Tables 6.1-A, 6.2-A and 6.3-A**. Frequencies of chromosome and chromatid aberrations in treated and untreated cell lines cultures PD20, PD20-S331A, PD20-S331D, PD20-K561R, PD20-315 and PD20-D2WT are presented in **Tables 6.1-A, 6.2-A and 6.3-A**.

6.2.2.1.1 Spontaneous chromosome and chromatid aberrations

It can be noted that the number of aberrations per cell in untreated cell lines presented a spontaneous rate which did not exceed 0.04 as shown in **Tables 6.1-A, 6.2-A and 6.3-A** and **Fig. 6.2.** Very few aberrations were recorded for all untreated PD20, PD20-S331A, PD20-S331D, PD20-K561R, PD20-315 and PD20-D2WT fibroblasts. The highest number of aberrations per cell for the untreated cells was that recorded for PD20-K561R as 0.04, followed by PD20-D2WT as 0.02 **(Tables 6.1-A, 6.2-A, 6.3-A) and (Fig. 6.3).** In addition, from the same Tables it can be

seen that the percentage of aberrant cells that have occurred spontaneously were similar for all cell lines, ranging from 0% to 4%.

6.2.2.1.2 Phleomycin-induced chromosome and chromatid aberrations

Table 6.1-A shows that using a dose of 1000 ng/ml phleomycin resulted in 1 and 0.32 chromosomal aberrations per cell in PD20 and PD20-D2WT respectively, making PD20 3.1-fold hypersensitive to the induction of chromosomal aberrations. This indicates that *FANCD2* deficient cell line PD20 is hypersensitive to phleomycin and is unable to correctly repair or process phleomycin induced damage (DNA strand breaks), which then lead to the observed chromosomal aberrations.

The same experimental conditions were used in **Table 6.2-A** and two more cell lines were added to the cytogenetic assay to test a total of four cell lines; PD20, PD20-S331A, PD20-K561R and PD20-D2WT. The number of chromosomal aberrations per cell was 0.56 for PD20, 0.52 for PD20-S331A, 0.24 for PD20-K561R and 0.2 for PD20-D2WT. Thus PD20 and PD20-S331A showed a similar increase in aberrations, 2.8-fold and 2.6-fold respectively compared to PD20-D2WT; whereas, the response of PD20-K561R was much more similar to that observed for PD20-D2WT.

In a third experiment **(Table 6.3-A)** a dose of 1000 ng/ml phleomycin produced higher chromosomal aberrations per cell in PD20, 0.48 compared to 0.26 found in PD20-D2WT representing a 1.9 fold increase. On the other hand, PD20-S331A and PD20-K561R cells produced rates of chromosomal aberrations per cell similar to that of PD20-D2WT cells as

shown in **Table 6.3-A.** It is noted that the result for PD20-S331A **(Table 6.2-A)** is at variance to that reported in **Table 6.3-A**, where the response was much more similar to that of PD20 cells.

So far, **Tables 6.1-A, 6.2-A and 6.3-A** indicate the hypersensitivity of G-BRCA2 complex deficient cell line PD20 to phleomycin, suggesting its inability to correctly process phleomycin induced damage (DNA strand breaks). This observation has been consistent in these three experiments. Also, PD20-K561R cells have been consistent in showing CA rates similar or close to that shown by the corrected wild type **(Tables 6.2-A and 6.3-A)**. While for PD20-S331A cells the results illustrated an initial elevation in CAs, but this elevation reduced in the following experiment as shown in **Tables 6.2-A and 6.3-A.** In order to test for consistency more experiments were performed employing these *FANCD2* cell lines PD20, PD20-S331A, PD20-K561R and PD20-D2WT. Unfortunately, these further experiments suffered an unidentified technical problem and due to time limitations these experiments could not be repeated as explained in the discussion section. The numbers of chromosomal aberrations recorded in each of the cell lines in these experiments proved to be highly variable and have been disregarded. Experiments which seem to have encountered this unknown problem are presented in an appendix at the end of this chapter.

Data-Table: summaries phleomycin treated PD20 cell lines and aberrations found in experiment

Table (6.1-A)

Cell line	Treatment phleomycin ng/ml	Total number of cells sampled	Chromatid based - aberrant cells		Chromosome - aberrant cells		Gaps per cell	Total aberrations without Gaps	Aberrations Per cell	% Aberrant cells	*Total Chromatid Breaks - after aberration converting per cell*
			Ctid-break	Ctid-exch	Chro-break	Chro-exch					
PD20 –D2WT	0	50	1	0	0	0	0	1	0.02	2	0.02
PD20 –D2WT	500	50	5	0	0	0	0	5	0.1	8	0.1
PD20 –D2WT	1000	50	15	1	0	0	0.12	16	0.32	24	0.36
PD20	0	50	0	0	0	0	0.08	0	0	0	0
PD20	500	50	17	2	3	1	0.3	23	0.46	30	0.7
PD20	1000	50	47	3	0	0	0.36	50	1	50	1.1

Table abbreviations: Ctid-break: Chromatid break type aberration, Ctid-exch: Chromatid exchange type aberration, Chro-break: Chromosome break type aberration, Chro-exch: Chromosome exchange type aberration.

Data-Table: summaries phleomycin treated PD20 cell lines and aberrations found in experiment

Table (6.2-A)

Cell line	Treatment phleomycin ng/ml	Total number of cells sampled	Chromatid based - aberrant cells		Chromosome - aberrant cells		Gaps per cell	Total aberrations without Gaps	Aberrations Per cell	% Aberrant cells	*Total Chromatid Breaks - after aberration converting per cell*
			Ctid-break	Ctid-exch	Chro-break	Chro-exch					
PD20 –D2WT	0	50	0	0	0	0	0.02	0	0	0	0
PD20 –D2WT	500	50	8	0	0	0	0	8	0.16	14	0.16
PD20 –D2WT	1000	50	10	0	0	0	0.12	10	0.2	16	0.2
PD20	0	50	0	0	0	0	0.08	0	0	0	0
PD20	500	50	5	1	0	0	0.08	6	0.12	8	0.14
PD20	1000	50	26	1	1	0	0.12	28	0.56	38	0.6
PD20 –S331A	0	50	0	0	0	0	0	0	0	0	0
PD20 –S331A	500	50	0	0	0	0	0	0	0	0	0
PD20 –S331A	1000	50	26	0	0	0	0.2	26	0.52	36	0.52
PD20 –K561R	0	50	0	0	0	0	0.06	0	0	0	0
PD20 –K561R	500	50	4	1	0	0	0.04	5	0.1	6	0.12
PD20 –K561R	1000	50	10	2	0	0	0.16	12	0.24	16	0.32

Table abbreviations: Ctid-break: Chromatid break type aberration, Ctid-exch: Chromatid exchange type aberration, Chro-break: Chromosome break type aberration, Chro-exch: Chromosome exchange type aberration.

Data-Table: summaries phleomycin treated PD20 cell lines and aberrations found in experiment

Table (6.3-A)

Cell line	Treatment phleomycin ng/ml	Total number of cells sampled	Chromatid based - aberrant cells		Chromosome - aberrant cells		Gaps per cell	Total aberrations without Gaps	Aberrations Per cell	% Aberrant cells	*Total Chromatid Breaks - after aberration converting per cell*
			Ctid-break	Ctid-exch	Chro-break	Chro-exch					
PD20 –D2WT	0	50	0	0	0	0	0.02	0	0	0	0
PD20 –D2WT	500	50	1	1	2	0	0	4	0.08	8	0.14
PD20 –D2WT	1000	50	10	2	0	1	0.04	13	0.26	18	0.38
PD20	0	50	0	0	0	0	0.02	0	0	0	0
PD20	500	50	5	1	0	0	0.1	6	0.12	10	0.14
PD20	1000	50	21	0	1	2	0.16	24	0.48	34	0.62
PD20 –S331A	0	50	0	0	0	0	0.04	0	0	0	0
PD20 –S331A	500	50	7	0	0	0	0.06	7	0.14	14	0.14
PD20 –S331A	1000	50	14	1	0	0	0.1	15	0.3	22	0.32
PD20 –K561R	0	50	2	0	0	0	0.04	2	0.04	4	0.04
PD20 –K561R	500	50	0	0	0	0	0.02	0	0	0	0
PD20 –K561R	1000	50	6	2	0	0	0.06	8	0.16	12	0.24

Table abbreviations: Ctid-break: Chromatid break type aberration, Ctid-exch: Chromatid exchange type aberration, Ctid-exch: Chromatid exchange type aberration, Chro-break: Chromosome break type aberration, Chro-exch: Chromosome exchange type aberration.

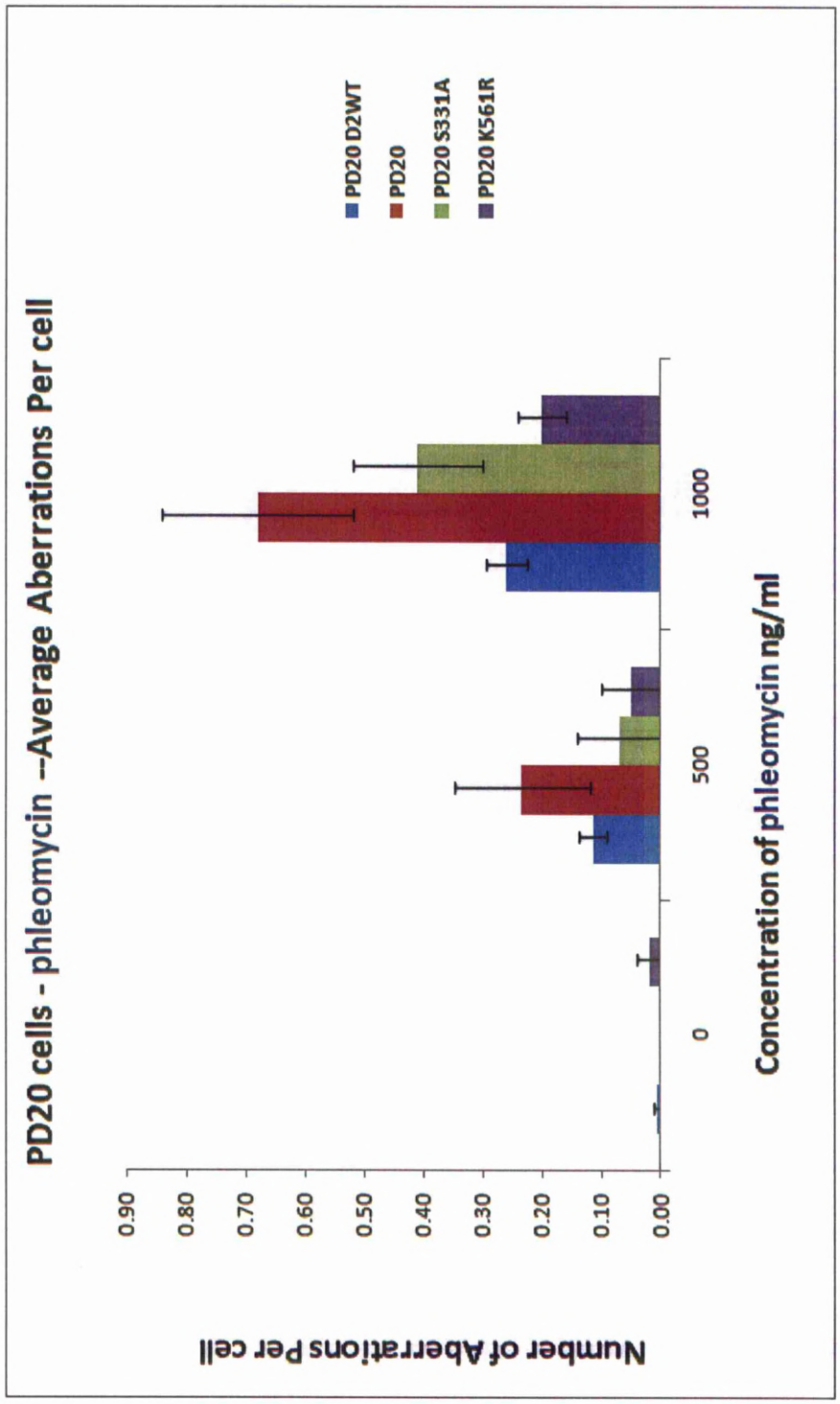

Figure (6.2): Illustrating phleomycin **Average Aberrations Per cell** data using four cell lines: (PD20, PD20-S331A, PD20-K561R and PD20-D2WT). Three experiments were performed. Error bars show the standard error of the mean.

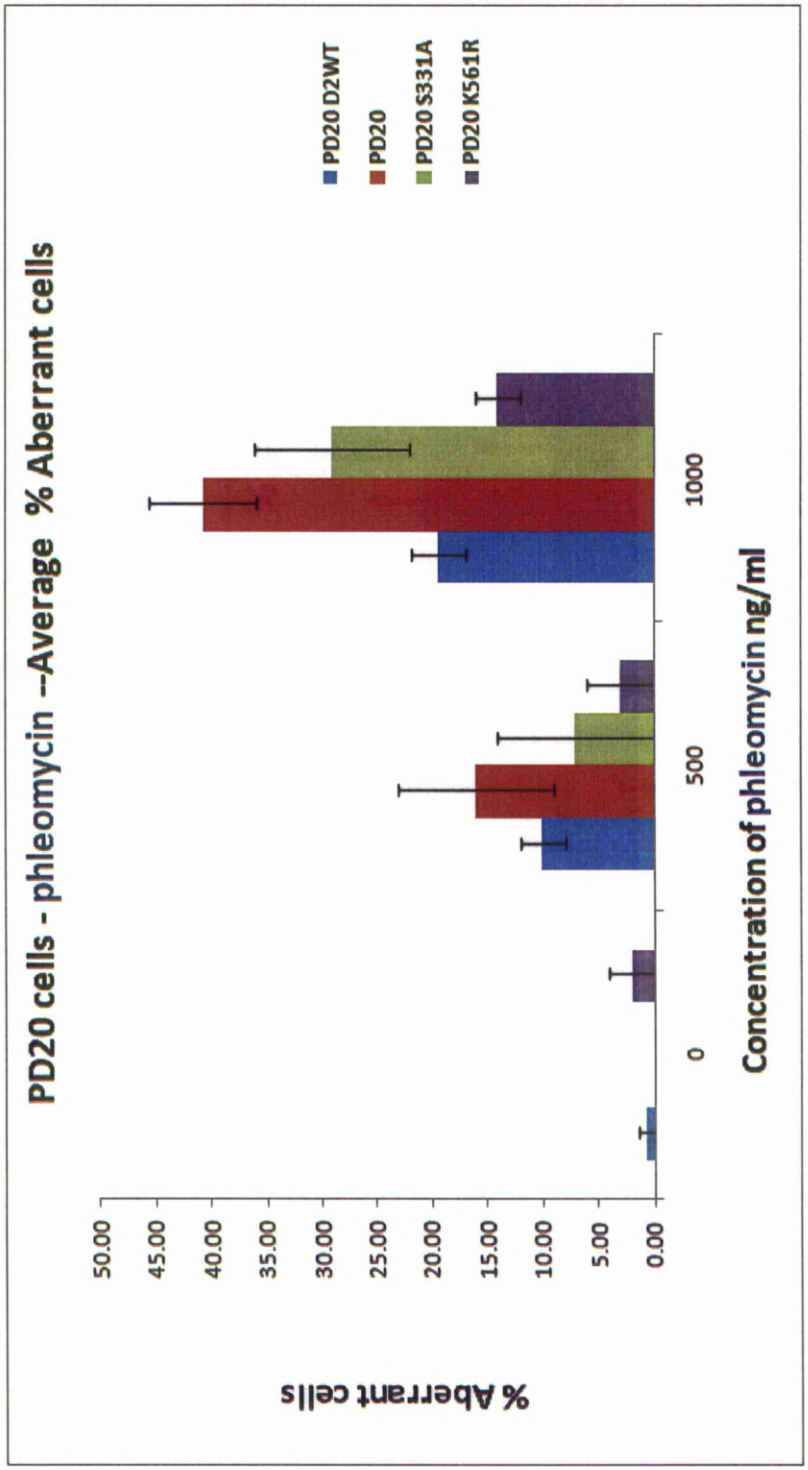

Figure (6.3): Illustrating phleomycin **Average percentage aberrant cells** data using four cell lines: (PD20, PD20-S331A, PD20-K561R and PD20-D2WT). Three experiments were performed. Error bars show the standard error of the mean.

6.2.2.1.3 Aberrations per cell, percentage aberrant cells and total chromatid breaks per cell

From the **Pooled Table 6.4** it can be seen that when using a dose of 1000 ng/ml phleomycin, the average aberrations per cell were 0.68 for PD20, 0.41 for PD20-S331A, 0.20 for PD20-K561R and 0.26 for PD20-D2WT. Thus, PD20 and PD20-S331A showed an increase in aberrations, 2.6-fold and 1.6-fold respectively compared to PD20-D2WT; whereas, the response of PD20-K561R was much more similar to that observed for PD20-D2WT.

Also using the dose of 1000 ng/ml phleomycin the average percentage of aberrant cells were 40.7% for PD20, 29% for PD20-S331A, 14% for PD20-K561R and 19.3% aberrant cells for PD20-D2WT. Thus, PD20 and PD20-S331A showed an increase in aberrations, 2.1-fold and 1.5-fold respectively compared to PD20-D2WT; whereas, the response of PD20-K561R was much more similar to that observed for PD20-D2WT, as shown in **Table 6.4.** The average number of total chromatid breaks (after converting all the exchanges into chromatid breaks) per cell for the same dose of 1000 ng/ml phleomycin was 0.77 for PD20, 0.42 for PD20-S331A, 0.28 for PD20-K561R and 0.31 chromatid breaks/cell for PD20-D2WT. Thus PD20 and PD20-S331A showed an increase in aberrations, 2.5-fold and 1.4-fold respectively compared to PD20-D2WT; whereas, the response of PD20-K561R was much more similar to that observed for PD20-D2WT, as shown in **Table 6.4.**

This elevation in cytogenetic structural aberrations in *FANCD2* mutant cell lines PD20 and PD20-S331A is presented in graphs as average aberration per cell **(Fig. 6.2),** average percentage aberrant cells **(Fig.6.3),** or as average total chromatid breaks per cell **(Fig. 6.4).**

Phleomycin cytogenetic findings presented in **Tables 6.1-A, 6.2-A and 6.3-A** and illustrated in **Figs. 6.1, 6.2 and 6.3** support the growth inhibition data in pointing out the ability of PD20-D2WT cell line to repair phleomycin DNA induced damage and the reduced ability of PD20 and PD20-S331A cells in repairing phleomycin DNA induced damage. This suggests that a mutation of the phosphorylation site FANCD2-S331 did affect the repair pathway for phleomycin induced DNA strand breaks. The *in vivo* interaction of FANCD2 with BRCA2 requires S331 phosphoryaltion **(Zhi *et al.*, 2009),** so mutating it would compromise this interaction and the formation of the G-BRCA2 complex. Phleomycin cytogenetic findings also suggest that in the absence of G-BRCA2 complex in PD20 cells, the repair pathway usually employed to handle phleomycin induced DNA damage was defective. On the other hand, while growth inhibition data point out PD20-K561R hypersensitivity to phleomycin, cytogenetic data show CAs rates of PD20-K561R, similar to that presented by PD20-D2WT.

While unrepaired phleomycin induced damage is cytogenetically detected in non-phosphorylated S331 FANCD2 **(Tables 6.2-A),** presumably due to a compromised G-BRCA2 complex, FANCD2-K561R cells exhibited a cytogenetic response after phleomycin treatment that was very similar to wild type cells **(Tables 6.2-A and 6.3-A).** It should be remembered that mono-ubiquitination is not required for the formation of the G-BRCA2 protein complex and differs from PD20-S331A cells in this respect. PD20 cells, that fail to express FANCD2 (and therefore also lack the G-BRCA2 complex) illustrated the highest CA numbers, particularly at the highest dose of phleomycin **(Tables 6.1-A, 6.2-A and 6.3-A).** Further validation for these findings is required, as they are based on a limited number of experiments. Unfortunately attempts to do this were hampered by inconsistencies in subsequent experiments.

Average /Standard error of the mean (SE) - Table-Results for Human PD20 cells - phleomycin

Table (6.4)

Cell line	Treatment phleomycin ng/ml	Total number of cells sampled	Average Aberrations Per cell	SE of the mean of Aberrations per cell	Average % Aberrant cells	SE of the mean of % Aberrant cells	Average Total Chromatid Breaks (after converting exchanges) per cell	SE of the mean of Total Chromatid Breaks (after converting exchanges) per cell
PD20 D2WT	0	150	0.01	0.01	0.67	0.67	0.01	0.01
PD20 D2WT	500	150	0.11	0.02	10.00	2.00	0.13	0.02
PD20 D2WT	1000	150	0.26	0.03	19.33	2.40	0.31	0.06
PD20	0	150	0.00	0.00	0.00	0.00	0.00	0.00
PD20	500	150	0.23	0.11	16.00	7.02	0.33	0.19
PD20	1000	150	0.68	0.16	40.67	4.81	0.77	0.16
PD20 *S331A*	0	100	0.00	0.00	0.00	0.00	0.00	0.00
PD20 *S331A*	500	100	0.07	0.07	7.00	7.00	0.07	0.07
PD20 *S331A*	1000	100	0.41	0.11	29.00	7.00	0.42	0.10
PD20 *K561R*	0	100	0.02	0.02	2.00	2.00	0.02	0.02
PD20 *K561R*	500	100	0.05	0.05	3.00	3.00	0.06	0.06
PD20 *K561R*	1000	100	0.20	0.04	14.00	2.00	0.28	0.04

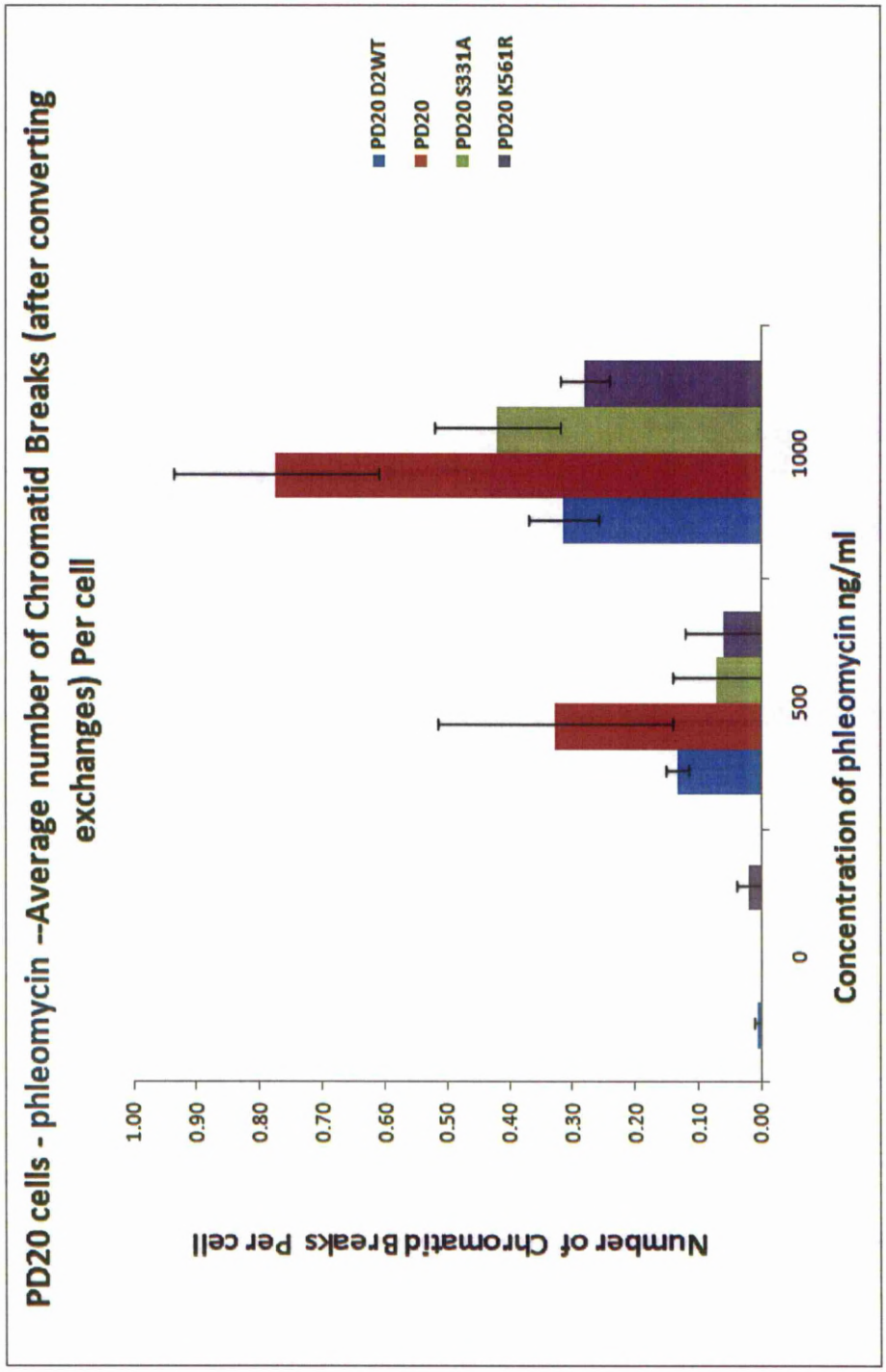

Figure (6.4): Illustrating phleomycin Average of Total Chromatid Breaks (after converting exchanges) per cell data using four cell lines: (PD20, PD20-S331A, PD20-K561R and PD20-D2WT). Three experiments were performed. Error bars show the standard error of the mean.

6.2.2.1.4 Types of cytogenetic aberrations induced by phleomycin

Generally, chromatid type aberrations predominated, involving mostly chromatid breaks and to a lesser extent, chromatid exchanges, in *FANCD2* cell lines PD20, PD20-S331A, PD20-K561R and PD20-D2WT **(Tables 6.1-A, 6.2-A and 6.3-A).** When comparing CA types in PD20, PD20-S331A, PD20-K561R and PD20-D2WT cells, it can also be seen that the occurrence of chromatid breaks in PD20 cells is generally higher than that recorded in PD20-S331A and PD20-K561R mutant cell lines. It can be seen that chromatid breaks predominate in all cell lines used. From **(Tables 6.1-B, 6.2-B and 6.3-B),** it can be seen that chromatid exchanges only emerge occasionally in the form of triradials, quadri-radials or complex arrangements which involve either two or three chromosomes.

This aberration type (chromatid breaks) predominance in these cell lines suggests an absence of repair pathways, such as HRR, used to repair phleomycin induced damage. In addition, these findings also suggest that NHEJ may have been less involved as an alternative repair pathway to HRR in cell lines deficient in the G-BRCA2 complex (PD20 and PD20-S331A), as mis-repair by error-prone NHEJ is likely to have led to exchange-type aberrations.

Dicentrics or rings were not observed in untreated *FANCD2* cultures (controls) and were rarely observed in treated cultures **(Tables 6.1-B, 6.2-B and 6.3-B).** Generally, chromosome breaks were slightly higher than chromosome exchanges in the PD20 cell line and were absent in PD20-S331A and PD20-K561R. PD20-D2WT presented as shown in **Tables 6.3-A and 6.3-B,** a couple of chromosome breaks and a dicentric which is low as explained earlier. Chromosome breaks, were still considerably lower in numbers compared to chromatid breaks. This can be seen in treated *FANCD2* mutant cell lines cultures PD20, PD20-S331A, PD20-K561R **(Tables 6.1-A,**

6.2-A and 6.3-A). Whereas, the corrected wild type PD20-D2WT and PD20-K561R presented the lowest numbers of chromatid breaks.

PD20-D2WT growth inhibition data showing wild type levels of hypersensitivity to phleomycin is consistent with the cytogenetic data presented in **Tables 6.1-A, 6.2-A, 6.3-A, 6.1-B, 6.2-B and 6.3-B.** However, PD20-K561R growth inhibition data showing an intermediate level of hypersensitivity to phleomycin is not consistent with the cytogenetic data presented in **Tables 6.1-A, 6.2-A, 6.3-A, 6.1-B, 6.2-B and 6.3-B** as PD20-K561R showed levels of CAs that were similar to PD20 D2WT.

EXPERIMENT—PD20- phleomycin

Table (6.1-B)

Cell line	Treatment ng/ml Phleomycin	No. Of cells scored	Triradials & no. Of centromeres			Quadri-radials & no. Of centromeres				Complex arrangements & no. Of chromosomes involved				No. Of Chromosome exchanges		No. Of Chromosome breaks	No. Of Chromatid breaks	No. Of TOTAL chromatid breaks [after converting all exchanges plus chromosome breaks]	Total Chromatid Breaks -after aberration converting per cell
			No. Of centromeres			No. Of centromeres				No. Of chromosomes				Type					
			1	2	3	1	2	3	4	2	3	4	5	Ring	Dicentric				
PD20 D2WT	0	50	0	0	0	0	0	0	0	0	0	0	0	0	0	0	1	1	0.02
PD20 D2WT	500	50	0	0	0	0	0	0	0	0	0	0	0	0	0	0	5	5	0.1
PD20 D2WT	1000	50	0	1	0	0	0	0	0	0	0	0	0	0	0	0	15	18	0.36
PD20	0	50	0	0	0	0	0	0	0	0	0	0	0	0	0	0	0	0	0
PD20	500	50	0	0	1	0	0	0	0	1	0	0	0	1	0	3	17	35	0.7
PD20	1000	50	0	0	0	0	0	0	0	2	1	0	0	0	0	0	47	55	1.1

In order to calculate the total number of chromatid breaks, first chromosome breaks, chromosome exchanges and chromatid exchanges including triradials, quadri-radials and complex arrangements were converted to the minimal number of chromatid breaks required for the formation of each specific type of aberration. Then this minimal number of chromatid breaks required for the formation of those aberrations was added to the observed number of chromatid breaks. Then this total number of chromatid breaks has been presented as total chromatid breaks per cell.

EXPERIMENT—PD20- phleomycin

Table (6.2-B)

Cell line	Treatment ng/ml Phleomycin	No. Of cells scored	Triradials & no. Of centromeres			Quadri-radials & no. Of centromeres				Complex arrangements & no. Of chromosomes involved				No. Of Chromosome exchanges		No. Of Chromosome breaks	No. Of Chromatid breaks	No. Of TOTAL chromatid breaks [after converting all exchanges plus chromosome breaks]	Total Chromatid Breaks -after aberration converting per cell
			No. Of centromeres			No. Of centromeres				No. Of chromosomes				Type					
			1	2	3	1	2	3	4	2	3	4	5	Ring	Dicentric				
PD20 D2WT	0	50	0	0	0	0	0	0	0	0	0	0	0	0	0	0	0	0	0
PD20 D2WT	500	50	0	0	0	0	0	0	0	0	0	0	0	0	0	0	8	8	0.16
PD20 D2WT	1000	50	0	0	0	0	0	0	0	0	0	0	0	0	0	0	10	10	0.2
PD20	0	50	0	0	0	0	0	0	0	0	0	0	0	0	0	0	0	0	0
PD20	500	50	0	0	0	0	0	0	0	1	0	0	0	0	0	0	5	7	0.14
PD20	1000	50	0	0	0	0	0	0	0	1	0	0	0	0	0	1	26	30	0.6
PD20 S331A	0	50	0	0	0	0	0	0	0	0	0	0	0	0	0	0	0	0	0
PD20 S331A	500	50	0	0	0	0	0	0	0	0	0	0	0	0	0	0	0	0	0
PD20 S331A	1000	50	0	0	0	0	0	0	0	0	0	0	0	0	0	0	26	26	0.52
PD20 K561R	0	50	0	0	0	0	0	0	0	0	0	0	0	0	0	0	0	0	0
PD20 K561R	500	50	0	0	0	0	1	0	0	0	0	0	0	0	0	0	4	6	0.12
PD20 K561R	1000	50	0	2	0	0	0	0	0	0	0	0	0	0	0	0	10	16	0.32

In order to calculate the total number of chromatid breaks, first chromosome breaks, chromosome exchanges and chromatid exchanges including triradials, quadri-radials and complex arrangements were converted to the minimal number of chromatid breaks required for the formation of each specific type of aberration. Then this minimal number of chromatid breaks required for the formation of those aberrations was added to the observed number of chromatid breaks. Then this total number of chromatid breaks has been presented as total chromatid breaks per cell.

EXPERIMENT—PD20- phleomycin

Table (6.3-B)

Cell line	Treatment ng/ml Phleomycin	No. Of cells scored	Triradials & no. Of centromeres			Quadri-radials & no. Of centromeres				Complex arrangements & no. Of chromosomes involved				No. Of Chromosome exchanges		No. Of Chromosome breaks	No. Of Chromatid breaks	No. Of TOTAL chromatid breaks [after converting all exchanges plus chromosome breaks]	Total Chromatid Breaks -after aberration converting per cell
			No. Of centromeres			No. Of centromeres				No. Of chromosomes				Type					
			1	2	3	1	2	3	4	2	3	4	5	Ring	Dicentric				
PD20 D2WT	0	50	0	0	0	0	0	0	0	0	0	0	0	0	0	0	0	0	0
PD20 D2WT	500	50	0	0	0	0	0	0	0	1	0	0	0	0	0	2	1	7	0.14
PD20 D2WT	1000	50	0	1	0	0	0	0	0	1	0	0	0	0	1	0	10	19	0.38
PD20	0	50	0	0	0	0	0	0	0	0	0	0	0	0	0	0	0	0	0
PD20	500	50	0	0	0	0	0	0	0	1	0	0	0	0	0	0	5	7	0.14
PD20	1000	50	0	0	0	0	0	0	0	0	0	0	0	1	1	1	21	31	0.62
PD20 S331A	0	50	0	0	0	0	0	0	0	0	0	0	0	0	0	0	0	0	0
PD20 S331A	500	50	0	0	0	0	0	0	0	0	0	0	0	0	0	0	7	7	0.14
PD20 S331A	1000	50	0	0	0	0	0	0	0	1	0	0	0	0	0	0	14	16	0.32
PD20 K561R	0	50	0	0	0	0	0	0	0	0	0	0	0	0	0	0	2	2	0.04
PD20 K561R	500	50	0	0	0	0	0	0	0	0	0	0	0	0	0	0	0	0	0
PD20 K561R	1000	50	0	2	0	0	0	0	0	0	0	0	0	0	0	0	6	12	0.24

In order to calculate the total number of chromatid breaks, first chromosome breaks, chromosome exchanges and chromatid exchanges including triradials, quadri-radials and complex arrangements were converted to the minimal number of chromatid breaks required for the formation of each specific type of aberration. Then this minimal number of chromatid breaks required for the formation of those aberrations was added to the observed number of chromatid breaks. Then this total number of chromatid breaks has been presented as total chromatid breaks per cell.

6.2.2.1.5 Phleomycin-PD20 cytogenetic experiments with high variability due to an unidentified technical problem

These include five experiments reported in **Tables 6.5-A, 6.6-A, 6.7-A, 6.8-A, 6.9-A, 6.5-B, 6.6-B, 6.7-B, 6.8-B and 6.9-B** and shown in an appendix to this chapter. Here, the observed cytogenetic structural aberration levels in *FANCD2* cell lines PD20-D2WT, PD20, PD20-S331A and PD20-K561R show inconsistency for all endpoints recorded including average aberrations per cell, average percentage aberrant cells and average total chromatid breaks per cell. This suggests the occurrence of a problem which could be connected to the cells utilized. For example, using a dose of 1000 ng/ml phleomycin resulted in PD20-D2WT fibroblasts rates of chromosomal aberrations per cell that did not exceed 0.32 aberration/cell in initial experiments **(Tables 6.1-A, 6.2-A and 6.3-A).** However, in the subsequent experiments this value increased up to 0.64 aberration/cell in **Table 6.7-A,** and up to 1.4 aberration/cell in **Table 6.9-A.** This could indicate a number of possibilities that will be explored in the discussion section. Another example confirming a problem is when PD20 shows at a dose of 1000 ng/ml phleomycin average chromosomal aberrations per cell rates of 0.34, 0.3, 0.72, 0.82 and 1.2 aberrations per cell. However, PD20-D2WT at the same dose shows average chromosomal aberrations per cell rates of 0.4, 0.25, 0.64, 0.5 and 1.4 **(Tables 6.5-A, 6.6-A, 6.7-A, 6.8-A and 6.9-A).** Thus, similar CA rates obtained for both PD20 and PD20-D2WT.

The second dose of 1500 ng/ml phleomycin was employed to rule out the possibility that the observed inconsistency problem may be related to drug batch potency, but this was clearly not the problem as this higher dose of 1500 ng/ml phleomycin significantly reduced the mitotic index.

6.2.3 Growth inhibition assays results of PD20 cells to MMC

As anticipated, the *FANCD2* mutated cell lines all showed hypersensitivity to MMC, with the PD20 cell line having a GI-50 value of 29 nM compared to a value of 107 nM for PD20-D2WT **(Fig. 6.5)**. This means PD20 cell line is 3.7-fold hypersensitive to MMC. PD20-S331A had a GI-50 value of 37 nM and so is 2.9-fold hypersensitive to MMC. PD20-K561R had a GI-50 value of 42 nM and so is 2.6-fold more hypersensitive to MMC. PD20-315 and PD20-S331D had GI-50 values of 102 and 103 nM respectively, similar to the GI-50 value of that of PD20-D2WT, illustrating wild type behavior for these cell lines **(Fig. 6.5)**.

6.2.4 MMC- PD20 cytogenetic experiments that have suffered an unidentified technical problem

As for the later phleomycin experiments these MMC-experiments (three independent experiments) shown in **Tables 6.10-A, 6.11-A, 6.12-A, 6.10-B, 6.11-B and 6.12-B** (in the appendix of this chapter) exhibited an unacceptable level of variability and were inconsistent with the growth inhibition data. The observed level of cytogenetic structural aberrations in *FANCD2* cell lines PD20-D2WT, PD20, PD20-S331A and PD20-K561R do not correlate with growth inhibition findings. The cytogenetic data indicates there may be a problem with the corrected wild type cell line which expressed the highest rates of chromosomal aberrations in average aberration per cell, in average percentage aberrant cells, and in average total chromatid breaks per cell. For example, using a dose of 100 nM MMC for PD20-D2WT resulted in rates of chromosomal aberrations per cell of 0.38, 0.8 and 0.45 which were similar to, or exceeded those,

of the PD20 *FANCD2* deficient cell line with rates of 0.24, 0.35 and 0.3 aberration/cell **(Tables 6.10-A, 6.11-A and 6.12-A).**

Another dose of 300 nM MMC was employed to rule out the possibility that the observed inconsistency problem may be related to drug batch potency, but this was clearly not the problem as this higher dose of MMC significantly reduced the mitotic index.

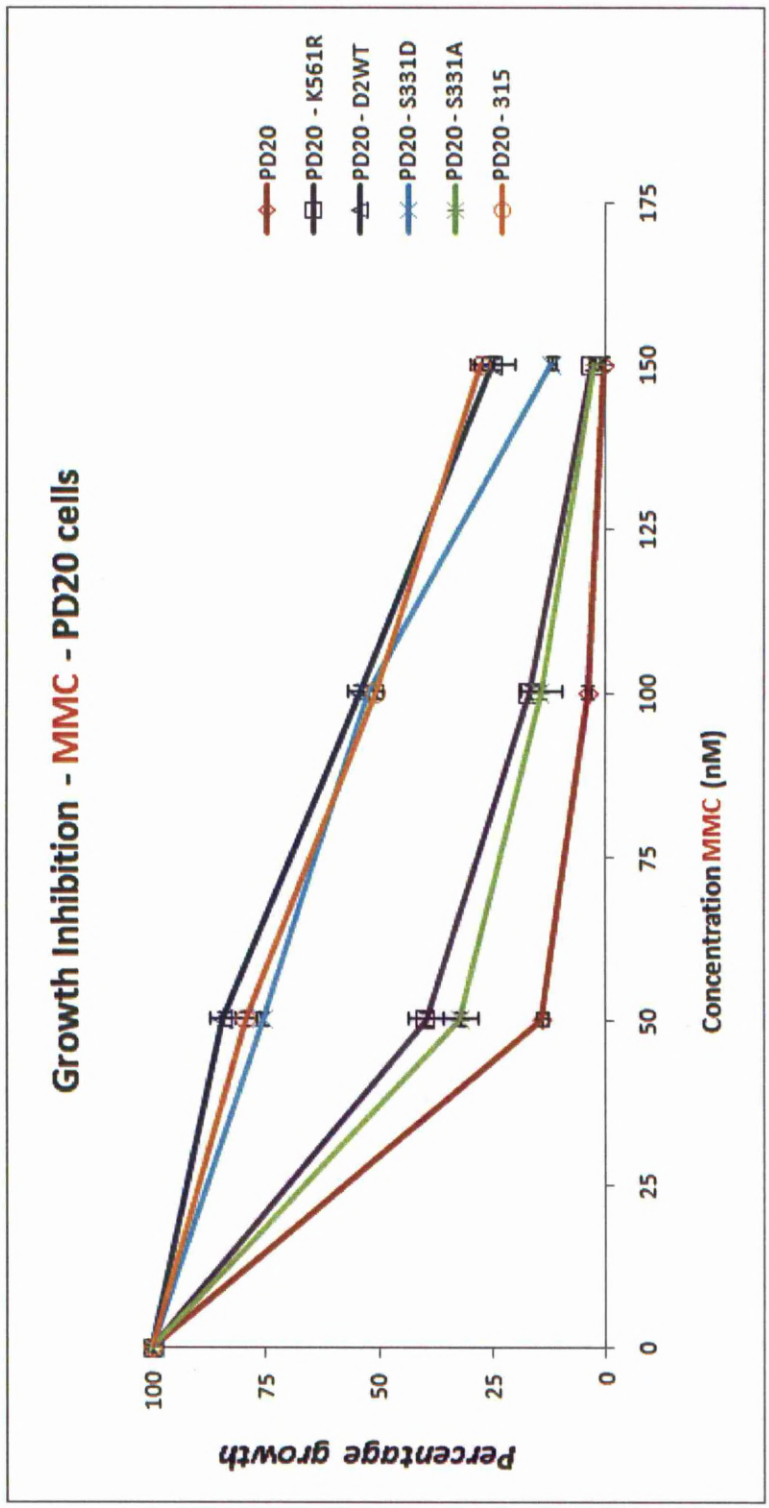

Figure (6.5): Illustrating MMC growth inhibition data using six cell lines: PD20, PD20-S331A, PD20-S331D, PD20-K561R, PD20-315 and PD20-D2WT. Four experiments were performed. Error bars show the standard error of the mean.

6.3 Discussion

6.3.1 Requirement of post-translational modifications of FANCD2 for efficient DNA repair

The results presented here show that in response to the DNA damaging agents phleomycin and MMC, it is necessary to have an intact FANCD2 protein that has the ability to be mono-ubiquitinated at lysine 561 and phosphorylated at serine 331. PD20 cells, that lack FANCD2, are 3.7 fold hypersensitive to MMC and 3.3 fold hypersensitive to phleomycin. The importance of post-translation modifications is also evident, as in the cell line PD20-K561R, where mono-ubiquitination is abolished, hypersensitivity to both MMC and phleomycin is observed, although the response of this cell line is intermediate between PD20 and PD20 D2WT. This intermediate sensitivity would appear to indicate that both isoforms of FANCD2 are required for optimal repair. This demonstration that the short isoform of FANCD2 is likely to have an active role is a novel finding that has not been reported previously. Similarly, phosphorylation of S331 is required to achieve optimal repair for both DNA damaging agents with the PD20-S331A cell line exhibiting intermediate sensitivity to both MMC and phleomycin. This phosphorylation site lies within the binding region of FANCD2 and BRCA2 **(Hussain *et al.*, 2006)** and phosphorylation of S331 has been shown to be required for the *in vivo* interaction of FANCD2 with BRCA2 **(Zhi *et al.*, 2009).** Growth inhibition experiments were performed first, early in the course of this investigation, using FANCD2 cell lines PD20-D2WT, PD20, PD20-S331A and PD20-K561R and prior to the latter cytogenetic experiments in which excessive variability was encountered.

These findings so far suggest that an intact mono-ubiquitinated and phosphorylated FANCD2 is required for optimal processing of DNA lesions (double strand breaks and ICLs) via the G-BRCA2 and the FA-ID complexes. In addition, the intermediate sensitivity observed in both PD20-K561R and PD20-S331A also suggest functionally active roles for both FANCD2-S and the non-S331 phosphorylated FANCD2 in the repair of both MMC-induced and phleomycin-induced DNA damage. As yet, the roles of these unmodified proteins have to be identified.

6.3.2 Functions of S331-phosphorylated FANCD2 and non-ubiquitinated FANCD2

The phosphorylation of FANCD2 at S331 is required for its interaction with BRCA2, thus a mutation at *FANCD2*-S331 will prevent this interaction thereby compromising the formation of the G-BRCA2 complex. It can therefore be hypothesized that the intermediate hypersensitivity to clastogens observed in PD20-S331A is a result of the absence of the G-BRCA2 complex and compromised HRR of DNA double strand breaks, regardless of whether they are directly induced or arise from the processing of inter-strand cross-links. In the two usable experiments with phleomycin **(Tables 6.2-A and 6.3-A)** the level of phleomycin-induced chromosomal aberrations were similar to the null mutant PD20 or intermediate between PD20 and PD20 D2WT, consistent with the hypothesis that absence of the G-BRCA2 complex results in these aberrations. It should be noted, that while the S331A mutation has been reported to slightly reduce FANCD2 mono-ubiquitination, mono-ubiquitinated FANCD2is still expressed at quite high levels in PD20-S331A cells **(Zhi *et al.*, 2009).**

Conversely, a mutation at the *FANCD2* mono-ubiquitination site K561 sustains the interaction between FANCD2 and BRCA2, the G-BRCA2 complex is formed and modulates proficient repair of phleomycin damage via HRR. This may explain the wild type cytogenetic profile observed for PD20-K561R after phleomycin treatment **(Tables 6.2-A and 6.3-A)**. The intermediate hypersensitivity illustrated by PD20-K561R to both phleomycin and MMC suggests the occurrence of partial DNA lesion repair, most likely through the action of the non-monoubiquitinated FANCD2-S expressed in PD20-K561R. This indicates that FANCD2-S may have an independent active role in mechanisms involved in DNA repair post phleomycin and MMC exposure. This is also supported by findings of **Oestergaard *et al.*, (2007)** indicating the requirements of Ubiquitin specific protease 1 (USP1) mediated FANCD2 deubiquitination for DNA cross link repair. **Oestergaard *et al.*, (2007)** and **Kim *et al.*, (2009)** illustrated that USP1 deficient cells exhibited about 2-fold hypersensitivity to MMC, thus supporting a role that FANCD2-S may play in DNA cross link repair.

It might be further speculated that mono-ubiquitination of FANCD2 is not required for proficient HRR, but other steps in the repair process, such as inhibition or suppression of NHEJ in inter-strand cross-link repair **(Pace *et al.*, 2010; Adamo *et al.*, 2010)**, stabilization of stalled or broken replication forks **(Thompson *et al.*, 2005; Thompson and Hinz, 2009)** for phleomycin-induced damage or localization of FANCD2 to chromatin.

To summarize, the intermediate sensitivity of PD20-S331A and PD20-K561R to DNA damaging agents may be due to different reasons and differing roles of the FANCD2 protein. These roles might include a direct involvement in HRR of some DNA damages (requiring phosphorylation of S331) or independently, and upstream or in parallel, of HRR (requiring mono-ubiquitination of K561R). It would be interesting to create a PD20 cell line that expressed a *FANCD2* cDNA

with both S331A and K561R mutations, as it might be predicted that this cell line would exhibit a response similar to PD20 null cells. Nevertheless, as these findings and speculations are based on a limited number of experiments as shown in **Tables 6.1-A, 6.2-A and 6.3-A,** they need further validation by performing further experiments. Unfortunately (see below), it was not possible to generate further data as part of this study.

6.3.3 Problems encountered with metaphase analysis of PD20 cell lines

Experiments to examine the chromosomal aberrations induced in the PD20 cell lines by MMC were conducted in parallel with the problematic phleomycin experiments shown in **Tables 6.5-A, 6.6-A, 6.7-A, 6.8-A and 6.9-A, 6.5-B, 6.6-B, 6.7-B, 6.8-B and 6.9-B.** Thus, the same cell lines that gave rise to the inconsistent phleomycin experiments were used in parallel experiments with MMC. These MMC-experiments are shown in **Tables 6.10-A, 6.11-A, 6.12-A, 6.10-B, 6.11-B and 6.12-B** in the appendix to this chapter. The observed cytogenetic structural aberration levels in *FANCD2* cell lines PD20-D2WT, PD20, PD20-S331A and PD20-K561R were inconsistent with growth inhibition findings and were not analyzed further.

Several possibilities may explain what might have caused the variability in these experiments. A first possibility would be that the cells used may have somehow lost the inserted cDNA construct or that construct had in some way become inactivated, thereby reverting the cells to their original uncorrected PD20 phenotype. A second possibility would be that a cross contamination of cell lines may have occurred between the various PD20 cell lines. A third possibility is that cell lines may have acquired resistance to the clastogens through genetic changes acquired during

continued culture. Such changes might include changes in the metabolism of the clastogens or transport of the clastogen into the cell.

The practical way to confirm the findings of this chapter and continue to develop our understanding of the aims of this section would be to use *FANCD2* cell lines PD20-D2WT, PD20, PD20-S331A and PD20-K561R after re-confirming their protein profile expression through Western blots and checking their clastogen sensitivity via growth inhibition or survival assays before using them into cytogenetic assays. PD20-K561R are expected to express the non-mono-ubiquitinated FANCD2-S, whereas FANCD2 expression would be completely absent in PD20 cells compared to the corrected wild type PD20-D2WT and PD20-S331A, where both FANCD2 forms are expressed illustrated as two bands in Western blots. Use of a phospho-antibody could be performed to confirm the validity of PD20-S331A cells. The cytogenetic profile in response to phleomycin or MMC treatment may resemble or compare to the hypersensitivity profile recorded in this chapter using growth inhibition curves as shown in **Figures 6.1 and 6.5.**

6.4 Summary of the chapter

- It has been demonstrated that *FANCD2*-deficient PD20 cells exhibit increased hypersensitivity to the radiomimetic compound phleomycin, in addition to their previously reported hypersensitivity to the inter-strand cross-linking agent MMC **(Whitney *et al.*, 1995; Jakobs *et al.*, 1996)**.
- PD20 cells expressing FANCD2 proteins that cannot be mono-ubiquitinated at K561 or phosphorylated at S331, exhibit intermediate sensitivity to both MMC and phleomycin.

- Consistent with their cellular hypersensitivity to phleomycin, PD20 cells exhibit increased levels of induced chromosomal aberrations, with chromatid breaks being the predominant type of aberration **(Tables 6.1-A, 6.2-A and 6.3-A)**.
- PD20-S331A cells, that are unable to form the G-BRCA2 protein complex, also exhibit an increase in phleomycin-induced chromosomal aberrations that were similar in number and type to those seen in PD20 cells **(Tables 6.2-A and 6.3-A)**.
- In contrast, PD20-K561R cells, that are able to form the G-BRCA2 complex, do not exhibit an increase in phleomycin-induced chromosomal aberrations **(Tables 6.2-A and 6.3-A)**.
- It is therefore proposed that the observed increase in chromosomal aberrations is due to the absence of the G-BRCA2 protein complex and that this complex is particularly important for the repair of phleomycin-induced DNA damage.
- The intermediate phleomycin (and MMC) hypersensitivity observed in PD20-S331A and PD20-K561R is a consequence of FANCD2 having multiple roles in DNA repair. In addition, the data clearly indicate that non mono-ubiquitinated FANCD2 has a functional role in the cellular resistance to clastogens.
- The predominance of chromatid breaks in phleomycin treated PD20 and PD20-S331A cells suggests that unrepaired DNA breaks resulting from defective HRR are not processed by NHEJ (that would likely result in chromatid exchanges), but rather these remain unrepaired leading to the observed chromatid breaks.

6.5 Appendix of chapter-6

Data-Table: summaries phleomycin treated PD20 cell lines and aberrations found in experiment

Table (6.5-A)

Cell line	Treatment phleomycin ng/ml	Total number of cells sampled	Chromatid based - aberrant cells		Chromosome - aberrant cells		Gaps per cell	Total aberrations without Gaps	Aberrations Per cell	% Aberrant cells	*Total Chromatid Breaks -after aberration converting per cell*
			Ctid-break	Ctid-exch	Chro-break	Chro-exch					
PD20 –D2WT	0	50	0	0	0	0	0.04	0	0	0	0
PD20 –D2WT	500	50	8	0	1	0	0.1	9	0.18	14	0.2
PD20 –D2WT	1000	50	19	0	1	0	0.24	20	0.4	26	0.42
PD20	0	50	1	0	0	0	0.04	1	0.02	2	0.02
PD20	500	50	19	0	1	0	0.06	20	0.4	28	0.42
PD20	1000	50	16	0	1	0	0.14	17	0.34	24	0.36
PD20 –S331A	0	50	1	0	0	0	0.06	1	0.02	2	0.02
PD20 –S331A	500	50	0	0	0	0	0.14	0	0	0	0
PD20 –S331A	1000	50	8	0	1	0	0.06	9	0.18	14	0.2
PD20 –K561R	0	50	1	0	0	0	0.02	1	0.02	2	0.02
PD20 –K561R	500	50	5	0	0	0	0.06	5	0.1	10	0.1
PD20 –K561R	1000	50	16	1	4	0	0.22	21	0.42	22	0.56

Table abbreviations: Ctid-break: Chromatid break type aberration, Ctid-exch: Chromatid exchange type aberration, Ctid-exch: Chromatid exchange type aberration, Chro-break: Chromosome break type aberration, Chro-exch: Chromosome exchange type aberration.

Data-Table: summaries phleomycin treated PD20 cell lines and aberrations found in experiment

Table (6.6-A)

Cell line	Treatment phleomycin ng/ml	Total number of cells sampled	Chromatid based - aberrant cells		Chromosome - aberrant cells		Gaps per cell	Total aberrations without Gaps	Aberrations Per cell	% Aberrant cells	*Total Chromatid Breaks -after aberration converting per cell*
			Ctid-break	Ctid-exch	Chro-break	Chro-exch					
PD20 –D2WT	0	20	1	0	0	0	0	1	0.05	5	0.05
PD20 –D2WT	500	20	4	0	1	0	0.1	5	0.25	20	0.3
PD20 –D2WT	1000	20	5	0	0	0	0.05	5	0.25	20	0.25
PD20	0	20	1	0	0	0	0.05	1	0.05	5	0.05
PD20	500	20	3	0	1	0	0.1	4	0.2	15	0.25
PD20	1000	20	5	0	0	1	0.15	6	0.3	25	0.45
PD20 –S331A	0	20	0	0	0	0	0	0	0	0	0
PD20 –S331A	500	20	2	3	0	0	0.05	5	0.25	25	0.55
PD20 –S331A	1000	20	6	1	0	0	0.1	7	0.35	35	0.45
PD20 –K561R	0	20	0	0	0	0	0	0	0	0	0
PD20 –K561R	500	20	0	1	0	0	0.2	1	0.05	5	0.3
PD20 –K561R	1000	20	1	0	0	0	0	1	0.05	5	0.05

Table abbreviations: Ctid-break: Chromatid break type aberration, Ctid-exch: Chromatid exchange type aberration, Ctid-exch: Chromatid exchange type aberration, Chro-break: Chromosome break type aberration, Chro-exch: Chromosome exchange type aberration.

Data-Table: summaries phleomycin treated PD20 cell lines and aberrations found in experiment

Table (6.7-A)

Cell line	Treatment phleomycin ng/ml	Total number of cells sampled	Chromatid based - aberrant cells		Chromosome - aberrant cells		Gaps per cell	Total aberrations without Gaps	Aberrations Per cell	% Aberrant cells	*Total Chromatid Breaks -after aberration converting per cell*
			Ctid-break	Ctid-exch	Chro-break	Chro-exch					
PD20 –D2WT	0	50	2	0	0	0	0.08	2	0.04	4	0.04
PD20 –D2WT	1000	50	27	2	2	1	0.28	32	0.64	32	0.78
PD20 –D2WT	1500	50	46	7	9	2	0.22	64	1.28	64	1.92
PD20	0	50	0	0	0	0	0.02	0	0	0	0
PD20	1000	50	25	6	4	1	0.12	36	0.72	34	1
PD20	1500	50	25	2	1	0	0.16	28	0.56	34	0.64
PD20 –S331A	0	50	0	0	0	0	0.06	0	0	0	0
PD20 –S331A	1000	50	13	0	0	1	0.02	14	0.28	22	0.34
PD20 –S331A	1500	50	30	1	3	1	0.26	35	0.7	38	0.84
PD20 –K561R	0	50	1	0	0	0	0.04	1	0.02	2	0.02
PD20 –K561R	1000	50	14	0	0	0	0.02	14	0.28	22	0.28
PD20 –K561R	1500	50	28	1	1	0	0.14	30	0.6	42	0.64

Table abbreviations: Ctid-break: Chromatid break type aberration, Ctid-exch: Chromatid exchange type aberration, Ctid-exch: Chromatid exchange type aberration, Chro-break: Chromosome break type aberration, Chro-exch: Chromosome exchange type aberration.

Data-Table: summaries **phleomycin** treated PD20 cell lines and aberrations found in experiment

Table (6.8-A)

Cell line	Treatment phleomycin ng/ml	Total number of cells sampled	Chromatid based - aberrant cells		Chromosome - aberrant cells		Gaps per cell	Total aberrations without Gaps	Aberrations Per cell	% Aberrant cells	*Total Chromatid Breaks -after aberration converting per cell*
			Ctid-break	Ctid-exch	Chro-break	Chro-exch					
PD20 –D2WT	0	50	0	0	0	0	0.04	0	0	0	0
PD20 –D2WT	1000	50	24	0	0	1	0.2	25	0.5	42	0.56
PD20 –D2WT	1500	50	38	4	2	3	0.34	47	0.94	40	1.36
PD20	0	50	1	0	0	0	0	1	0.02	2	0.02
PD20	1000	50	40	1	0	0	0.24	41	0.82	54	0.84
PD20	1500	50	79	1	5	3	0.36	88	1.76	68	2.06
PD20 –S331A	0	50	0	0	0	0	0	0	0	0	0
PD20 –S331A	1000	50	30	0	0	0	0.22	30	0.6	38	0.6
PD20 –S331A	1500	50	23	4	1	1	0.32	29	0.58	34	0.74
PD20 –K561R	0	50	2	0	1	0	0.1	3	0.06	6	0.08
PD20 –K561R	1000	50	13	1	1	2	0.02	17	0.34	26	0.5
PD20 –K561R	1500	50	77	6	0	0	0.44	83	1.66	62	1.84

Table abbreviations: Ctid-break: Chromatid break type aberration, Ctid-exch: Chromatid exchange type aberration, Ctid-exch: Chromatid exchange type aberration, Chro-break: Chromosome break type aberration, Chro-exch: Chromosome exchange type aberration.

Data-Table: summaries phleomycin treated PD20 cell lines and aberrations found in experiment

Table (6.9-A)

Cell line	Treatment phleomycin ng/ml	Total number of cells sampled	Chromatid based - aberrant cells		Chromosome - aberrant cells		Gaps per cell	Total aberrations without Gaps	Aberrations Per cell	% Aberrant cells	*Total Chromatid Breaks -after aberration converting per cell*
			Ctid-break	Ctid-exch	Chro-break	Chro-exch					
PD20 –D2WT	0	20	0	0	0	0	0	0	0	0	0
PD20 –D2WT	1000	20	25	0	2	1	0.45	28	1.4	65	1.65
PD20 –D2WT	1500	20	49	2	1	1	0.25	53	2.65	95	3.15
PD20	0	20	0	0	0	0	0	0	0	0	0
PD20	1000	20	23	1	0	0	0.15	24	1.2	55	1.3
PD20	1500	20	58	0	2	0	0.45	60	3	90	3.1
PD20 –S331A	0	20	1	0	0	0	0.05	1	0.05	5	0.05
PD20 –S331A	1000	20	29	1	2	0	0.15	32	1.6	60	1.75
PD20 –S331A	1500	20	17	0	0	0	0.55	17	0.85	50	0.85
PD20 –K561R	0	20	3	1	0	0	0	4	0.2	10	0.25
PD20 –K561R	1000	20	15	1	1	1	0.1	18	0.9	35	1.15
PD20 –K561R	1500	20	38	2	1	0	0.4	41	2.05	80	2.35

Table abbreviations: Ctid-break: Chromatid break type aberration, Ctid-exch: Chromatid exchange type aberration, Ctid-exch: Chromatid exchange type aberration, Chro-break: Chromosome break type aberration, Chro-exch: Chromosome exchange type aberration.

EXPERIMENT—PD20- phleomycin

Table (6.5-B)

Cell line	Treatment ng/ml Phleomycin	No. Of cells scored	Triradials & no. Of centromeres			Quadri-radials & no. Of centromeres				Complex arrangements & no. Of chromosomes involved				No. Of Chromosome exchanges		No. Of Chromosome breaks	No. Of Chromatid breaks	No. Of TOTAL chromatid breaks [after converting all exchanges plus chromosome breaks]	Total Chromatid Breaks -after aberration converting per cell
			No. Of centromeres			No. Of centromeres				No. Of chromosomes				Type					
			1	2	3	1	2	3	4	2	3	4	5	Ring	Dicentric				
PD20 D2WT	0	50	0	0	0	0	0	0	0	0	0	0	0	0	0	0	0	0	0
PD20 D2WT	500	50	0	0	0	0	0	0	0	0	0	0	0	0	0	1	8	10	0.2
PD20 D2WT	1000	50	0	0	0	0	0	0	0	0	0	0	0	0	0	1	19	21	0.42
PD20	0	50	0	0	0	0	0	0	0	0	0	0	0	0	0	0	1	1	0.02
PD20	500	50	0	0	0	0	0	0	0	0	0	0	0	0	0	1	19	21	0.42
PD20	1000	50	0	0	0	0	0	0	0	0	0	0	0	0	0	1	16	18	0.36
PD20 S331A	0	50	0	0	0	0	0	0	0	0	0	0	0	0	0	0	1	1	0.02
PD20 S331A	500	50	0	0	0	0	0	0	0	0	0	0	0	0	0	0	0	0	0
PD20 S331A	1000	50	0	0	0	0	0	0	0	0	0	0	0	0	0	1	8	10	0.2
PD20 K561R	0	50	0	0	0	0	0	0	0	0	0	0	0	0	0	0	1	1	0.02
PD20 K561R	500	50	0	0	0	0	0	0	0	0	0	0	0	0	0	0	5	5	0.1
PD20 K561R	1000	50	0	0	0	0	0	0	0	0	1	0	0	0	0	4	16	28	0.56

In order to calculate the total number of chromatid breaks, first chromosome breaks, chromosome exchanges and chromatid exchanges including triradials, quadri-radials and complex arrangements were converted to the minimal number of chromatid breaks required for the formation of each specific type of aberration. Then this minimal number of chromatid breaks required for the formation of those aberrations was added to the observed number of chromatid breaks. Then this total number of chromatid breaks has been presented as total chromatid breaks per cell.

EXPERIMENT—PD20- phleomycin

Table (6.6-B)

Cell line	Treatment ng/ml Phleomycin	No. Of cells scored	Triradials & no. Of centromeres			Quadri-radials & no. Of centromeres				Complex arrangements & no. Of chromosomes involved				No. Of Chromosome exchanges		No. Of Chromosome breaks	No. Of Chromatid breaks	No. Of TOTAL chromatid breaks [after converting all exchanges plus chromosome breaks]	Total Chromatid Breaks -after aberration converting per cell
			No. Of centromeres			No. Of centromeres				No. Of chromosomes				Type					
			1	2	3	1	2	3	4	2	3	4	5	Ring	Dicentric				
PD20 D2WT	0	20	0	0	0	0	0	0	0	0	0	0	0	0	0	0	1	1	0.05
PD20 D2WT	500	20	0	0	0	0	0	0	0	0	0	0	0	0	0	1	4	6	0.3
PD20 D2WT	1000	20	0	0	0	0	0	0	0	0	0	0	0	0	0	0	5	5	0.25
PD20	0	20	0	0	0	0	0	0	0	0	0	0	0	0	0	0	1	1	0.05
PD20	500	20	0	0	0	0	0	0	0	0	0	0	0	0	0	1	3	5	0.25
PD20	1000	20	0	0	0	0	0	0	0	0	0	0	0	1	0	0	5	9	0.45
PD20 S331A	0	20	0	0	0	0	0	0	0	0	0	0	0	0	0	0	0	0	0
PD20 S331A	500	20	1	0	0	0	1	0	0	0	1	0	0	0	0	0	2	11	0.55
PD20 S331A	1000	20	0	1	0	0	0	0	0	0	0	0	0	0	0	0	6	9	0.45
PD20 K561R	0	20	0	0	0	0	0	0	0	0	0	0	0	0	0	0	0	0	0
PD20 K561R	500	20	0	0	1	0	0	0	0	0	0	0	0	0	0	0	0	6	0.3
PD20 K561R	1000	20	0	0	0	0	0	0	0	0	0	0	0	0	0	0	1	1	0.05

In order to calculate the total number of chromatid breaks, first chromosome breaks, chromosome exchanges and chromatid exchanges including triradials, quadri-radials and complex arrangements were converted to the minimal number of chromatid breaks required for the formation of each specific type of aberration. Then this minimal number of chromatid breaks required for the formation of those aberrations was added to the observed number of chromatid breaks. Then this total number of chromatid breaks has been presented as total chromatid breaks per cell.

EXPERIMENT—PD20- phleomycin

Table (6.7-B)

Cell line	Treatment ng/ml Phleomycin	No. Of cells scored	Triradials & no. Of centromeres			Quadri-radials & no. Of centromeres				Complex arrangements & no. Of chromosomes involved				No. Of Chromosome exchanges		No. Of Chromosome breaks	No. Of Chromatid breaks	No. Of TOTAL chromatid breaks [after converting all exchanges plus chromosome breaks]	Total Chromatid Breaks -after aberration converting per cell
			No. Of centromeres			No. Of centromeres				No. Of chromosomes				Type					
			1	2	3	1	2	3	4	2	3	4	5	Ring	Dicentric				
PD20 D2WT	0	50	0	0	0	0	0	0	0	0	0	0	0	0	0	0	2	2	0.04
PD20 D2WT	1000	50	0	0	0	0	0	0	0	2	0	0	0	0	1	2	27	39	0.78
PD20 D2WT	1500	50	0	2	1	0	0	1	0	3	0	0	0	0	2	9	46	96	1.92
PD20	0	50	0	0	0	0	0	0	0	0	0	0	0	0	0	0	0	0	0
PD20	1000	50	0	1	0	0	0	0	0	5	0	0	0	0	1	4	25	50	1
PD20	1500	50	0	1	0	0	0	0	0	1	0	0	0	0	0	1	25	32	0.64
PD20 S331A	0	50	0	0	0	0	0	0	0	0	0	0	0	0	0	0	0	0	0
PD20 S331A	1000	50	0	0	0	0	0	0	0	0	0	0	0	0	1	0	13	17	0.34
PD20 S331A	1500	50	0	0	0	0	0	0	0	1	0	0	0	0	1	3	30	42	0.84
PD20 K561R	0	50	0	0	0	0	0	0	0	0	0	0	0	0	0	0	1	1	0.02
PD20 K561R	1000	50	0	0	0	0	0	0	0	0	0	0	0	0	0	0	14	14	0.28
PD20 K561R	1500	50	0	0	0	0	0	0	0	1	0	0	0	0	0	1	28	32	0.64

In order to calculate the total number of chromatid breaks, first chromosome breaks, chromosome exchanges and chromatid exchanges including triradials, quadri-radials and complex arrangements were converted to the minimal number of chromatid breaks required for the formation of each specific type of aberration. Then this minimal number of chromatid breaks required for the formation of those aberrations was added to the observed number of chromatid breaks. Then this total number of chromatid breaks has been presented as total chromatid breaks per cell.

EXPERIMENT—PD20- phleomycin

Table (6.8-B)

Cell line	Treatment g/ml Phleomycin	No. Of cells scored	Triradials & no. Of centromeres			Quadri-radials & no. Of centromeres				Complex arrangements & no. Of chromosomes involved					No. Of chromosome exchanges		No. Of Chromosome breaks	No. Of Chromatid breaks	No. Of TOTAL chromatid breaks [after converting all exchanges plus chromosome breaks]	Total Chromatid Breaks -after aberration converting per cell
			No. Of centromeres			No. Of centromeres				No. Of chromosomes					Type					
			1	2	3	1	2	3	4	2	3	4	5		Ring	Dicentric				
PD20 D2WT	0	50	0	0	0	0	0	0	0	0	0	0	0		0	0	0	0	0	0
PD20 D2WT	1000	50	0	0	0	0	0	0	0	0	0	0	0		0	1	0	24	28	0.56
PD20 D2WT	1500	50	0	0	0	0	0	0	0	2	1	1	0		0	3	2	38	68	1.36
PD20	0	50	0	0	0	0	0	0	0	0	0	0	0		0	0	0	1	1	0.02
PD20	1000	50	0	0	0	0	0	0	0	1	0	0	0		0	0	0	40	42	0.84
PD20	1500	50	0	0	0	0	0	0	0	1	0	0	0		0	3	5	79	103	2.06
PD20 S331A	0	50	0	0	0	0	0	0	0	0	0	0	0		0	0	0	0	0	0
PD20 S331A	1000	50	0	0	0	0	0	0	0	0	0	0	0		0	0	0	30	30	0.6
PD20 S331A	1500	50	0	0	0	0	0	0	0	4	0	0	0		0	1	1	23	37	0.74
PD20 K561R	0	50	0	0	0	0	0	0	0	0	0	0	0		0	0	1	2	4	0.08
PD20 K561R	1000	50	0	0	0	0	0	0	0	1	0	0	0		0	2	1	13	25	0.5
PD20 K561R	1500	50	0	1	0	0	0	0	0	4	1	0	0		0	0	0	77	92	1.84

In order to calculate the total number of chromatid breaks, first chromosome breaks, chromosome exchanges and chromatid exchanges including triradials, quadri-radials and complex arrangements were converted to the minimal number of chromatid breaks required for the formation of each specific type of aberration. Then this minimal number of chromatid breaks required for the formation of those aberrations was added to the observed number of chromatid breaks. Then this total number of chromatid breaks has been presented as total chromatid breaks per cell.

EXPERIMENT—PD20- phleomycin

Table (6.9-B)

Cell line	Treatment ng/ml Phleomycin	No. Of cells scored	Triradials & no. Of centromeres			Quadri-radials & no. Of centromeres				Complex arrangements & no. Of chromosomes involved				No. Of Chromosome exchanges		No. Of Chromosome breaks	No. Of Chromatid breaks	No. Of TOTAL chromatid breaks [after converting all exchanges plus chromosome breaks]	Total Chromatid Breaks -after aberration converting per cell
			No. Of centromeres			No. Of centromeres				No. Of chromosomes				Type					
			1	2	3	1	2	3	4	2	3	4	5	Ring	Dicentric				
PD20 D2WT	0	20	0	0	0	0	0	0	0	0	0	0	0	0	0	0	0	0	0
PD20 D2WT	1000	20	0	0	0	0	0	0	0	0	0	0	0	1	0	2	25	33	1.65
PD20 D2WT	1500	20	0	0	0	0	0	0	0	0	2	0	0	1	0	1	49	63	3.15
PD20	0	20	0	0	0	0	0	0	0	0	0	0	0	0	0	0	0	0	0
PD20	1000	20	1	0	0	0	0	0	0	0	0	0	0	0	0	0	23	26	1.3
PD20	1500	20	0	0	0	0	0	0	0	0	0	0	0	0	0	2	58	62	3.1
PD20 S331A	0	20	0	0	0	0	0	0	0	0	0	0	0	0	0	0	1	1	0.05
PD20 S331A	1000	20	0	0	0	0	0	0	0	1	0	0	0	0	0	2	29	35	1.75
PD20 S331A	1500	20	0	0	0	0	0	0	0	0	0	0	0	0	0	0	17	17	0.85
PD20 K561R	0	20	0	0	0	0	0	0	0	1	0	0	0	0	0	0	3	5	0.25
PD20 K561R	1000	20	0	0	0	0	0	0	0	1	0	0	0	1	0	1	15	23	1.15
PD20 K561R	1500	20	1	0	0	0	0	0	0	0	1	0	0	0	0	1	38	47	2.35

In order to calculate the total number of chromatid breaks, first chromosome breaks, chromosome exchanges and chromatid exchanges including triradials, quadri-radials and complex arrangements were converted to the minimal number of chromatid breaks required for the formation of each specific type of aberration. Then this minimal number of chromatid breaks required for the formation of those aberrations was added to the observed number of chromatid breaks. Then this total number of chromatid breaks has been presented as total chromatid breaks per cell.

Data-Table: summaries MMC treated PD20 cell lines and aberrations found in experiment

Table (6.10-A)

Cell line	Treatment MMC nM	Total number of cells sampled	Chromatid based - aberrant cells		Chromosome - aberrant cells		Gaps per cell	Total aberrations without Gaps	Aberrations Per cell	% Aberrant cells	*Total Chromatid Breaks -after aberration converting per cell*
			Ctid-break	Ctid-exch	Chro-break	Chro-exch					
PD20 –D2WT	0	50	0	0	0	0	0	0	0	0	0
PD20 –D2WT	30	50	3	3	0	0	0	6	0.12	10	0.2
PD20 –D2WT	50	50	8	5	0	0	0.06	13	0.26	18	0.48
PD20 –D2WT	100	50	6	13	0	0	0.08	19	0.38	28	0.92
PD20	0	50	0	0	0	0	0	0	0	0	0
PD20	30	50	3	5	0	0	0.12	8	0.16	12	0.42
PD20	50	50	5	4	0	0	0.02	9	0.18	14	0.4
PD20	100	50	8	3	1	0	0.06	12	0.24	18	0.38
PD20 –S331A	0	50	0	0	0	0	0	0	0	0	0
PD20 –S331A	30	50	2	8	0	0	0.08	10	0.2	14	0.5
PD20 –S331A	50	50	5	7	0	0	0.06	12	0.24	18	0.44
PD20 –S331A	100	50	7	12	0	0	0.06	19	0.38	22	0.82
PD20 –K561R	0	50	0	0	0	0	0	0	0	0	0
PD20 –K561R	30	50	2	5	1	0	0.08	8	0.16	12	0.3
PD20 –K561R	50	50	13	9	2	0	0.26	24	0.48	38	0.78
PD20 –K561R	100	50	6	7	0	1	0.12	14	0.28	20	0.54

Table abbreviations: Ctid-break: Chromatid break type aberration, Ctid-exch: Chromatid exchange type aberration, Ctid-exch: Chromatid exchange type aberration, Chro-break: Chromosome break type aberration, Chro-exch: Chromosome exchange type aberration.

Data-Table: summaries MMC treated PD20 cell lines and aberrations found in experiment

Table (6.11-A)

Cell line	Treatment MMC nM	Total number of cells sampled	Chromatid based - aberrant cells		Chromosome - aberrant cells		Gaps per cell	Total aberrations without Gaps	Aberrations Per cell	% Aberrant cells	*Total Chromatid Breaks -after aberration converting per cell*
			Ctid-break	Ctid-exch	Chro-break	Chro-exch					
PD20 –D2WT	0	20	1	0	0	0	0	1	0.05	5	0.05
PD20 –D2WT	30	20	3	1	0	0	0.15	4	0.2	20	0.25
PD20 –D2WT	50	20	5	8	0	0	0.15	13	0.65	40	1.35
PD20 –D2WT	100	20	6	7	3	0	0.3	16	0.8	55	1.9
PD20	0	20	0	0	0	0	0	0	0	0	0
PD20	30	20	5	3	0	0	0.1	8	0.4	4	0.65
PD20	50	20	4	4	1	0	0.05	9	0.45	30	0.95
PD20	100	20	4	3	0	0	0.15	7	0.35	35	0.6
PD20 –S331A	0	20	0	0	0	0	0	0	0	0	0
PD20 –S331A	30	20	4	6	0	0	0.05	10	0.5	35	1.1
PD20 –S331A	50	20	4	1	0	1	0.2	6	0.3	30	0.4
PD20 –S331A	100	20	8	17	1	0	0.1	26	1.3	70	2.5
PD20 –K561R	0	20	0	0	0	0	0.05	0	0	0	0
PD20 –K561R	30	20	3	6	3	0	0	12	0.6	35	1.25
PD20 –K561R	50	20	1	6	0	0	0	7	0.35	25	1.05
PD20 –K561R	100	20	3	5	0	0	0.25	8	0.4	30	1

Table abbreviations: Ctid-break: Chromatid break type aberration, Ctid-exch: Chromatid exchange type aberration, Ctid-exch: Chromatid exchange type aberration, Chro-break: Chromosome break type aberration, Chro-exch: Chromosome exchange type aberration.

Data-Table: summaries MMC treated PD20 cell lines and aberrations found in experiment

Table (6.12-A)

Cell line	Treatment MMC nM	Total number of cells sampled	Chromatid based - aberrant cells		Chromosome - aberrant cells		Gaps per cell	Total aberrations without Gaps	Aberrations Per cell	% Aberrant cells	*Total Chromatid Breaks -after aberration converting per cell*
			Ctid-break	Ctid-exch	Chro-break	Chro-exch					
PD20 –D2WT	0	20	0	0	0	0	0	0	0	0	0
PD20 –D2WT	30	20	8	8	0	0	0.15	16	0.8	45	1.4
PD20 –D2WT	100	20	5	4	0	0	0.1	9	0.45	40	0.85
PD20 –D2WT	300	20	32	26	1	1	0.2	60	3	80	6.44
PD20	0	20	1	0	0	0	0.05	1	0.05	5	0.05
PD20	30	20	1	0	0	0	0.05	1	0.05	5	0.05
PD20	100	20	3	12	0	0	0.1	15	0.3	50	2.05
PD20	300	12	11	6	2	0	0.25	19	1.58	75	2.75
PD20 –S331A	0	20	0	0	0	0	0.1	0	0	0	0
PD20 –S331A	30	20	5	6	0	0	0.15	11	0.55	25	1.4
PD20 –S331A	100	20	5	19	3	0	0.4	27	1.35	65	3.45
PD20 –S331A	300	20	19	29	1	0	0.1	49	2.45	75	5.7
PD20 –K561R	0	20	1	0	0	1	0.05	2	0.1	10	0.25
PD20 –K561R	30	20	23	8	4	0	0.25	35	1.75	65	2.75
PD20 –K561R	100	20	23	14	1	0	0.3	38	1.9	80	3.5
PD20 –K561R	300	3	2	2	1	0	0.67	5	1.67	100	3

Table abbreviations: Ctid-break: Chromatid break type aberration, Ctid-exch: Chromatid exchange type aberration, Ctid-exch: Chromatid exchange type aberration, Chro-break: Chromosome break type aberration, Chro-exch: Chromosome exchange type aberration.

EXPERIMENT—PD20- MMC

Table (6.10-B)

Cell line	Treatment MMC nM	No. Of cells scored	Triradials & no. Of centromeres			Quadri-radials & no. Of centromeres				Complex arrangements & no. Of chromosomes involved					No. Of Chromosome exchanges			No. Of Chromosome breaks	No. Of Chromatid breaks	No. Of TOTAL chromatid breaks [after converting all exchanges plus chromosome breaks]	Total Chromatid Breaks -after aberration converting per cell
			No. Of centromeres			No. Of centromeres				No. Of chromosomes					Type						
			1	2	3	1	2	3	4	2	3	4	5		Ring	Dicentric					
PD20 D2WT	0	50	0	0	0	0	0	0	0	0	0	0	0		0	0		0	0	0	0
PD20 D2WT	30	50	0	1	0	0	2	0	0	0	0	0	0		0	0		0	3	10	0.2
PD20 D2WT	50	50	0	2	0	0	0	0	0	1	2	0	0		0	0		0	8	24	0.48
PD20 D2WT	100	50	2	2	0	0	1	0	0	3	5	0	0		0	0		0	6	46	0.92
PD20	0	50	0	0	0	0	0	0	0	0	0	0	0		0	0		0	0	0	0
PD20	30	50	0	2	1	0	0	0	0	1	1	0	0		0	0		0	3	21	0.42
PD20	50	50	1	0	0	0	0	0	0	1	1	1	0		0	0		0	5	20	0.4
PD20	100	50	1	0	0	0	0	0	0	1	1	0	0		0	0		1	8	19	0.38
PD20 S331A	0	50	0	0	0	0	0	0	0	0	0	0	0		0	0		0	0	0	0
PD20 S331A	30	50	1	2	0	0	0	0	0	3	2	0	0		0	0		0	2	25	0.5
PD20 S331A	50	50	0	1	0	0	2	0	0	3	1	0	0		0	0		0	5	22	0.44
PD20 S331A	100	50	1	3	0	0	0	0	0	5	3	0	0		0	0		0	7	41	0.82
PD20 K561R	0	50	0	0	0	0	0	0	0	0	0	0	0		0	0		0	0	0	0
PD20 K561R	30	50	0	1	0	0	0	0	0	4	0	0	0		0	0		1	2	15	0.3
PD20 K561R	50	50	0	0	0	0	1	0	0	6	2	0	0		0	0		2	13	39	0.78
PD20 K561R	100	50	0	3	0	0	2	0	0	2	0	0	0		1	0		0	6	27	0.54

In order to calculate the total number of chromatid breaks, first chromosome breaks, chromosome exchanges and chromatid exchanges including triradials, quadri-radials and complex arrangements were converted to the minimal number of chromatid breaks required for the formation of each specific type of aberration. Then this minimal number of chromatid breaks required for the formation of those aberrations was added to the observed number of chromatid breaks. Then this total number of chromatid breaks has been presented as total chromatid breaks per cell.

EXPERIMENT—PD20- MMC

Table (6.11-B)

Cell line	Treatment MMC nM	No. Of cells scored	Triradials & no. Of centromeres			Quadri-radials & no. Of centromeres				Complex arrangements & no. Of chromosomes involved				No. Of Chromosome exchanges		No. Of Chromosome breaks	No. Of Chromatid breaks	No. Of TOTAL chromatid breaks [after converting all exchanges plus chromosome breaks]	Total Chromatid Breaks -after aberration converting per cell
			No. Of centromeres			No. Of centromeres				No. Of chromosomes				Type					
			1	2	3	1	2	3	4	2	3	4	5	Ring	Dicentric				
PD20 D2WT	0	20	0	0	0	0	0	0	0	0	0	0	0	0	0	0	1	1	0.05
PD20 D2WT	30	20	0	0	0	0	1	0	0	0	0	0	0	0	0	0	3	5	0.25
PD20 D2WT	50	20	0	0	0	0	0	0	0	5	3	0	0	0	0	0	5	27	1.35
PD20 D2WT	100	20	0	0	0	0	0	0	0	1	6	0	0	0	0	3	6	38	1.9
PD20	0	20	0	0	0	0	0	0	0	0	0	0	0	0	0	0	0	0	0
PD20	30	20	0	0	0	0	0	0	0	2	1	0	0	0	0	0	5	13	0.65
PD20	50	20	0	1	0	0	0	0	0	1	2	0	0	0	0	1	4	19	0.95
PD20	100	20	0	0	0	0	0	0	0	2	1	0	0	0	0	0	4	12	0.6
PD20 S331A	0	20	0	0	0	0	0	0	0	0	0	0	0	0	0	0	0	0	0
PD20 S331A	30	20	1	1	0	0	0	0	0	3	0	1	0	0	0	0	4	22	1.1
PD20 S331A	50	20	0	0	0	0	0	0	0	1	0	0	0	1	0	0	4	8	0.4
PD20 S331A	100	20	1	3	0	0	2	0	0	10	1	0	0	0	0	1	8	50	2.5
PD20 K561R	0	20	0	0	0	0	0	0	0	0	0	0	0	0	0	0	0	0	0
PD20 K561R	30	20	0	2	0	0	0	0	0	3	1	0	0	0	0	3	3	25	1.25
PD20 K561R	50	20	0	0	0	0	0	0	0	2	3	1	0	0	0	0	1	21	1.05
PD20 K561R	100	20	0	1	0	0	0	1	0	2	1	0	0	0	0	0	3	20	1

In order to calculate the total number of chromatid breaks, first chromosome breaks, chromosome exchanges and chromatid exchanges including triradials, quadri-radials and complex arrangements were converted to the minimal number of chromatid breaks required for the formation of each specific type of aberration. Then this minimal number of chromatid breaks required for the formation of those aberrations was added to the observed number of chromatid breaks. Then this total number of chromatid breaks has been presented as total chromatid breaks per cell.

EXPERIMENT—PD20- MMC

Table (6.12-B)

Cell line	Treatment MMC nM	No. Of cells scored	Triradials & no. Of centromeres			Quadri-radials & no. Of centromeres				Complex arrangements & no. Of chromosomes involved				No. Of Chromosome exchanges		No. Of Chromosome breaks	No. Of Chromatid breaks	No. Of TOTAL chromatid breaks [after converting all exchanges plus chromosome breaks]	Total Chromatid Breaks -after aberration converting per cell
			No. Of centromeres			No. Of centromeres				No. Of chromosomes				Type					
			1	2	3	1	2	3	4	2	3	4	5	Ring	Dicentric				
PD20 D2WT	0	20	0	0	0	0	0	0	0	0	0	0	0	0	0	0	0	0	0
PD20 D2WT	30	20	0	2	0	0	0	0	0	5	1	0	0	0	0	0	8	28	1.4
PD20 D2WT	100	20	0	0	0	0	0	0	0	2	2	0	0	0	0	0	5	17	0.85
PD20 D2WT	300	20	3	3	2	1	0	0	0	9	4	4	0	0	1	1	32	130	6.44
PD20	0	20	0	0	0	0	0	0	0	0	0	0	0	0	0	0	1	1	0.05
PD20	30	20	0	0	0	0	0	0	0	0	0	0	0	0	0	0	1	1	0.05
PD20	100	20	0	2	0	0	2	1	0	3	4	0	0	0	0	0	3	41	2.05
PD20	300	12	0	2	1	0	1	0	0	2	0	0	0	0	0	2	11	31	2.75
PD20 S331A	0	20	0	0	0	0	0	0	0	0	0	0	0	0	0	0	0	0	0
PD20 S331A	30	20	0	1	1	0	0	0	0	1	3	0	0	0	0	0	5	28	1.4
PD20 S331A	100	20	1	1	2	0	1	0	0	9	5	0	0	0	0	3	5	69	3.45
PD20 S331A	300	20	1	4	1	0	1	0	0	14	5	1	2	0	0	1	19	114	5.7
PD20 K561R	0	20	0	0	0	0	0	0	0	0	0	0	0	1	0	0	1	5	0.25
PD20 K561R	30	20	0	0	0	0	0	0	0	4	4	0	0	0	0	4	23	55	2.75
PD20 K561R	100	20	2	1	0	0	0	0	0	5	5	1	0	0	0	1	23	70	3.5
PD20 K561R	300	3	0	1	0	0	0	0	0	1	0	0	0	0	0	1	2	9	3

In order to calculate the total number of chromatid breaks, first chromosome breaks, chromosome exchanges and chromatid exchanges including triradials, quadri-radials and complex arrangements were converted to the minimal number of chromatid breaks required for the formation of each specific type of aberration. Then this minimal number of chromatid breaks required for the formation of those aberrations was added to the observed number of chromatid breaks. Then this total number of chromatid breaks has been presented as total chromatid breaks per cell.

Chapter-7

General discussion

7.1 Discussion

7.1.1 Introduction

Fanconi anaemia is a human disorder characterized by cancer susceptibility and cellular sensitivity to DNA cross links and other replication fork stalling agents. Cells derived from FA patients have been shown to undergo premature senescence, spontaneously accrue chromosome aberrations and accumulate in G2 phase of the cell cycle **(Thompson and Hinz, 2009).** When exposed to ICL agents, like MMC, a covalent bond results in opposite strands of DNA becoming linked or cross-linked. The chemistry of guanine disposes itself to react with these cross linking agents and the majority of ICLs occur between guanines. These lesions are extremely toxic and block both transcription and DNA replication. The failure of a cell to repair such lesions leads to chromosome breaks and complex radial structure formation. The aim of this project was to further investigate the links between FA proteins and HRR, thereby strengthening the emerging data that the FA pathway is not linear, but is composed of multifunctional proteins that form different sub-complexes with specific functions. Here, the role that FANCG, FANCA and FANCD2 play promoting cell survival in response to two chemical DNA damaging agents MMC (ICL) and phleomycin (DSB) has been investigated. The loss of function of these proteins when exposed to MMC, leads to increased radial formations and chromosomal breaks. In the case of

phleomycin, it appears that only the loss of FANCG and FANCD2 functions affects cell survival and consequent chromosome aberrations. Furthermore, it has also been shown that the loss of specific phosphorylation sites in FANCG and FANCD2 affects cellular survival and the amount of chromosomal damage detected.

7.1.2 DNA inter-strand cross-link repair

7.1.2.1 Unhooking

The repair of ICLs is coupled to DNA replication. Regardless of which stage of the cell cycle cells are treated with MMC, they will accumulate a 4N complement of DNA **(Akkari *et al.*, 2001).** Additionally, chromosomal damage and DSBs formation only occur following transit through S-phase of the cell cycle **(Akkari *et al.*, 2001).** Recent work has shown the importance of mono-ubiquitinated FANCD2 in ICL repair. Mono-ubiquitinated FANCD2 is required for incisions at the site of the cross-link, in the TLS step and HRR **(Long *et al.*, 2011).** This biochemical and genetic information place the FA, TLS and HRR machinery in a common pathway for ICLs repair. This is shown in the proposed model illustrated in **Fig.7.1.**

The FA-core complex mediated mono-ubiquitination of FANCD2 acts upstream of both TLS and HRR **(Niedzwiedz *et al.*, 2004; Hirano *et al.*, 2005; Wilson *et al.*, 2008; Long *et al.*, 2011).** FAN1 exhibits a 5' flap endonuclease activity with an associated 5'to 3'exonuclease activity **(Kratz *et al.*, 2010; MacKay *et al.*, 2010; Crossan and Patel, 2011).** This FAN1 activity could be connected to crosslink repair **(Raschle *et al.*, 2008).** Thus, FANCD2 recruitment of FAN1 to

the site of DNA cross-links may be one mechanism by which one nuclease is recruited. On the other hand, *FAN1* depletion is associated with normal kinetics of γ-H2AX foci formation, which is a marker of DNA double strand breaks **(Crossan and Patel, 2011),** suggesting that FAN1 is not essential for generating DSBs or HRR.

The biochemical endonuclease activity of XPF-ERCC1 results in strand incision when ICLs are encountered **(Sijbers *et al.*, 1996; Raschle *et al.*, 2008).** It has been shown that the biochemical activity of XPF-ERCC1 can be altered in a way nicking dsDNA 4 nucleotides before ICLs **(Fischer *et al.*, 2008; Crossan and Patel, 2011),** suggesting that XPF-ERCC1 alone is adequate to execute both incisions at the site of an ICL.

Discovery of the *SLX4* gene may reveal another part of DNA cross-link repair process **(Fekairi *et al.*, 2009, Svendesen *et al.*, 2009, Munoz *et al.*, 2009).** Human SLX4 interacts with the SLX1, which is a structure specific endonuclease. The SLX4-SLX1 complex is involved in *in vitro* resolution of Holliday junctions. Both cross-link repair nucleases XPF-ERCC1 and MUS81-EME1 interact with SLX4, which also enhances their biochemical action *in vitro* **(Fekairi *et al.*, 2009, Svendesen *et al.*, 2009, Munoz *et al.*, 2009).** DNA cross-linking agent hypersensitivity has been found in *Drosophila, C. elegans,* mouse, yeast and human cells depleted of SLX4 **(Liao *et al.*, 2007; Crossan and Patel, 2011).** Thus, it would be reasonable to propose a model in which SLX4 has an analogous role in XPF-ERCC1 recruitment to inter-strand cross-links sites to that of XPA in nucleotide excision repair (NER). XPA recruits ERCC1 to UV damaged DNA sites in NER **(Volker *et al.*, 2001).** XPA deficient cells are hypersensitive to UV but not to DNA cross-linking agents. On the other hand, SLX4 depletion does not bring about cellular hypersensitivity to UV irradiation but leads to hypersensitivity to DNA inter-strand cross-linking agents. Thus, it is possible that SLX4 segregates XPF-ERCC1 activity into ICL repair from its

function in repairing UV induced DNA damage. The mechanics of Fanconi anaemia pathway dependent incisions at the site of ICLs remain unclear to this date.

Figure (7.1): The proposed model to repair ICLs and double strand DNA breaks via FANCG complexes

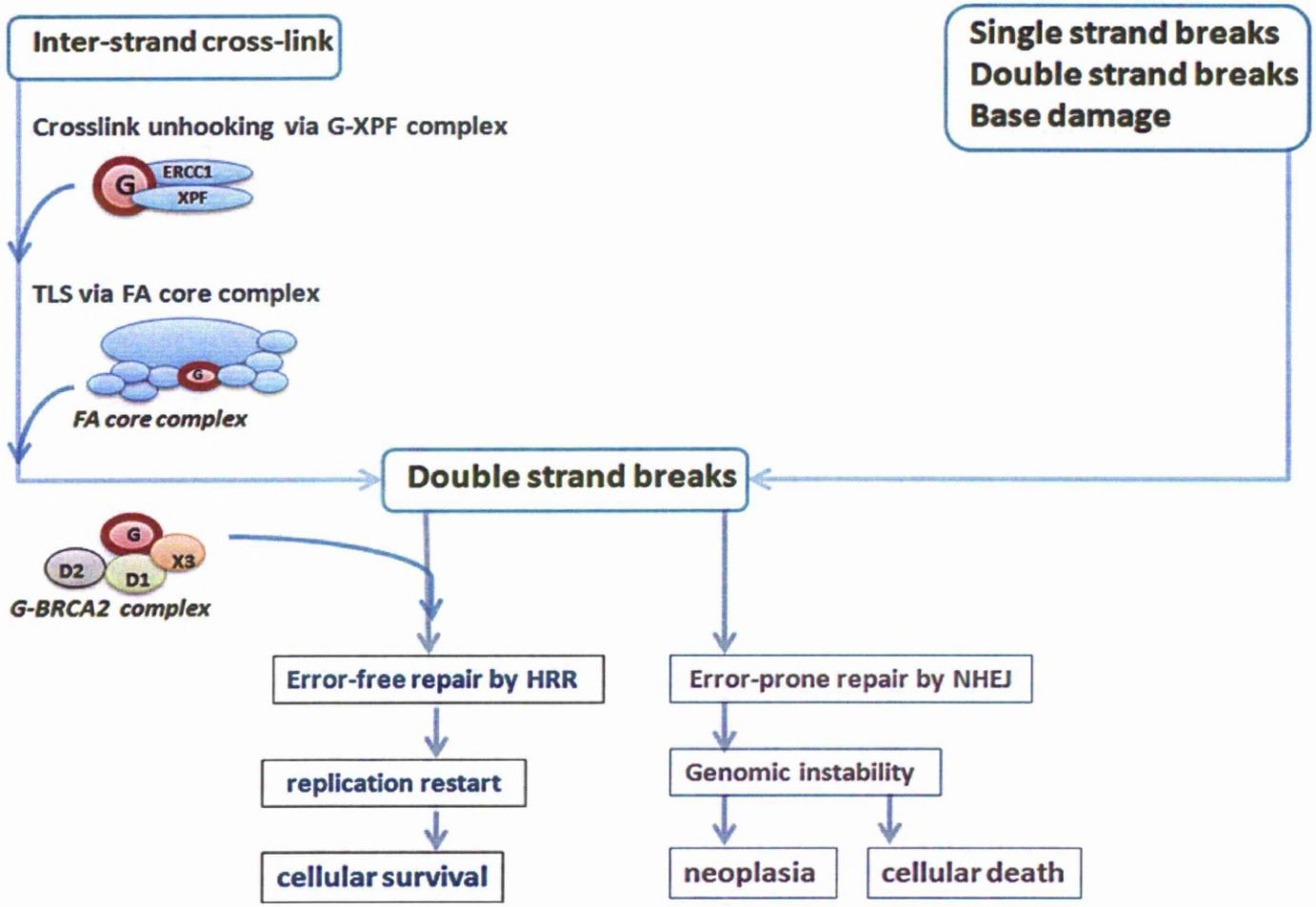

Figure (7.1): summarizing the model to repair ICLs and double strand DNA breaks via FANCG complexes in the presence or absence of the FA pathway. Abbreviations G; FANCG, D2;FANCD2, D1; FANCD1, X3; XRCC3, XPF; xeroderma pigmentosum group F, ERCC1; excision repair protein, TLS; translesion synthesis, FA: Fanconi anaemia, HRR; homologous recombination repair, NHEJ; non-homologous end joining.

7.1.2.2 Processing of Double Strand Breaks in ICL Repair

As previously stated, DSB repair occurs through either HRR or NHEJ. ICL repair, from the results presented here, seems to require the core complex to suppress the NHEJ pathway. In the cell lines where the core complex does not form, due to absence of either FANCG (NM3) or FANCA (GM9614), the number of exchanges at the chromosome level increases in response to MMC. This suggests that NHEJ acts upon the DSB that arise from ICL cross-links that are not processed by the FA pathway. NHEJ appears to be suppressed in cell lines that have a functional core complex. It has yet to be determined whether this is due to a direct inhibition of NHEJ or the FA pathway processing ICLs in a way that does not create substrates for NHEJ or protects ICL repair intermediates from NHEJ binding proteins. The G-BRCA2 complex seems to play a role in ICL repair as in the serine 7 mutated cell line (NM3-S7A), the core complex forms and the number of exchanges detected in response to MMC increase, although the highest CA level detected has been recorded in the complete absence of FANCG. It seems most likely that in the absence of the G-BRCA2 complex, the DSBs produced from the FA pathway acting upon a cross-link, become available for processing by NHEJ due to the absence of HRR, and these DSBs then result in increased numbers of chromatid exchanges. An alternative explanation, that seems more unlikely, is that the S7A-FANCG mutated protein has sub-optimal activity in the FA core complex, even though the core complex forms in NM3-S7A cells and FANCD2 is mono-ubiquitinated.

To summarize the sequence, it appears that after cross-link unhooking, the resultant DSB is repaired by HRR, with the FA core complex and FANCD2 mono-ubiquitination somehow playing a role in suppressing NHEJ. Recent data **(Adamo *et al.*, 2010)** suggest that FA pathway

proteins are likely to direct DNA cross-links into accurate HRR, rather than error-prone NHEJ, nevertheless the exact mechanism is still undetermined. **Adamo *et al.*, (2010)** showed that FANCD2 is critical in avoiding NHEJ repair of meiotic DSBs. In eukaryotes, the repair of DSBs repair can either be through error-prone repair pathway NHEJ or error-free repair pathway HRR. Rigorous regulation of DNA repair pathways is required to avoid inaccurate end-joining which could lead to harmful or lethal cellular effects such as genomic instability, chromosomal radial formation or apoptosis **(Kitao and Takata, 2010). Bunting *et al.*, (2010)** and **Bouwman *et al.*, (2010)** demonstrated NHEJ and HRR *in vivo* competition. **Bouwman *et al.*, (2010)** illustrated using *BRCA1* mutant cells, that repair through HRR pathway is restored by deleting the NHEJ factor 53BP1 thereby preventing radial chromosome arrangements and tumor formation. This suggests that the characteristic acquired FA cellular phenotype post exposure to inter-strand cross-linking agents, is most likely a result of inaccurate end-joining of non-homologous chromosomes **(Bunting and Nussenzweig, 2010).**

Experimental evidence supported a role of FA proteins in promoting DNA repair via HRR through NHEJ suppression **(Pace *et al.*, 2010; Adamo *et al.*, 2010).** **Adamo *et al.*, (2010)** showed that treatment of human wild type MO59K cells with FANCD2 siRNAs resulted in sensitivity to mitomycin C (MMC). However, when FANCD2 was depleted in DNA-PKcs-deficient MO59J cells, no increase in MMC-sensitivity was observed. Furthermore, chemical inhibition of NHEJ with the DNA-PKcs-specific inhibitor NU7026 in FA-deficient cells substantially corrects the characteristic FA phenotype of inter-strand cross-linking agent hypersensitivity and chromosomal instability **(Adamo *et al.*, 2010)**. In NHEJ, the DNA-PKcs enzyme is recruited to DNA breaks and is activated by the KU70/KU80 heterodimer. Two studies in 2010 show that disruption of Ku70, Ku80 or DNA-PKcs in *FANCD2*-deficient human

cells reverses cellular hypersensitivity to cross-linking agents, reduces chromosome instability, and promotes HRR **(Pace *et al.*, 2010; Adamo *et al.*, 2010).**

7.1.2.3 Determining the role of the G-BRCA2 complex (comprising BRCA2-FANCD2-FANCG-XRCC3) in ICL and DSB repair

In Chapter 3, the involvement of FANCG and the G-BRCA2 complex in the error free HRR pathway of DNA inter-strand cross links was investigated using the CHO NM3 cell lines. Growth inhibition assays demonstrated that FANCG and its two phosphorylation sites at Serine 7 and Serine 387 are important in sustaining resistance to the cross linking agent MMC. The MMC-hypersensitivity presented by the *FANCG* mutant cell lines is supported by cytogenetic analysis. Rates of chromosomal aberrations were elevated in the *FANCG* mutant cell lines, especially in the complete absence of FANCG protein (NM3-VO), as shown in the summary **Table 7.1.** In *FANCG* deficient cells, NM3-VO, all known protein complexes containing FANCG protein will be absent; the FA nuclear core complex, the G-BRCA2 complex and the G-ERCC1-XPF complex. In contrast, cell lines NM3-S7A and NM3-S387A, known to form one or more of these three complexes exhibit intermediate MMC-sensitivity and induction of chromosomal aberrations. NM3-S7A cells contain a fully assembled and presumably active FA-core complex, but are deprived of the G-BRCA2 complex **(Wilson *et al.*, 2008)**. The status of the G-ERCC1-XPF complex is unknown in NM3-S7A and the other phospho-mutant cell line NM3-S387A. Given that NM3-S7A cells show compromised ICL repair ability, as evidenced by their hypersensitivity to MMC and elevated chromosomal aberrations, this most likely indicates the

requirement of the G-BRCA2 complex for successful and complete ICL repair and restoration of DNA replication. It is proposed that NM3-S7A cells were able to process ICLs through the action of the G-ERCC1-XPF complex and the FA-core complex by unhooking ICLs and performing TLS, but the resulting DSBs could not be repaired by HRR, due to the absence of the G-BRCA2 complex. This is consistent with the reduction of HRR in MMC-treated NM3-S7A cells as measured using the SCneo recombination assay. In the absence of the G-BRCA2 complex and HRR, it is likely that the DSBs arising from the upstream processing of ICL in NM3-S7A are available as substrates for error-prone mis-repair by NHEJ. This is consistent with the increased levels and predominance of chromatid exchanges in MMC-treated NM3-S7A cells. In contrast, NM3-S387A cells that have an intact G-BRCA2 complex did not show chromatid exchanges as the predominant MMC-induced aberration.

To further investigate the role of S7-FANCG phosphorylation and the G-BRCA2 complex in the repair of DSBs by HRR, the radio-mimetic agent phleomycin was used **(Sleigh, 1976; Povirk *et al.*, 1981).** Phleomycin induces direct double-strand breaks (DSB) into DNA. It also induces single-strand breaks and base damage and if these remain unrepaired prior to DNA replication, it is likely they will result in broken replication forks and replication fork-associated DSBs. However, phleomycin is not known to induce ICL.

Consistent with the hypothesis that the G-BRCA2 complex is required for the repair of DSBs, NM3-S7A and NM3-VO cells that lack this protein complex, exhibit significant hypersensitivity to phleomycin. This suggests that the G-BRCA2 complex is involved in homologous recombinational repair of DSBs, whatever their origin, be it direct induction of DSBs by phleomycin or indirectly arising DSBs from the partial repair of ICLs. In contrast, NM3-S387A that retains an intact G-BRCA2 complex shows minimal hypersensitivity to phleomycin.

Consistent with NHEJ processing the unrepaired phleomycin-induced DSBs, both NM3-VO and NM3-S7A exhibit large increases in chromosomal aberrations with chromatid exchanges being the predominant type of aberration. The absence of the G-BRCA2 complex in NM3-S7A (and NM3-VO) cells prevented DNA double strand processing in an error-free manner through HRR, resulting the observed hypersensitivity and elevation in CA rate as illustrated in summary **Table 7.1.** For MMC, NM3-S7A displayed an intermediate response, while for phleomycin, it's cellular and chromosomal hypersensitivity were as severe as (if not more severe) than that observed for the null mutant. In NM3-VO, all FANCG-containing protein complexes will be absent, yet this cell line has a response to phleomycin similar to NM3-S7A. This strongly suggests that repair of phleomycin-induced DNA damage does not require either the FA core or the G-ERCC1-XPF protein complexes.

Consistent with the idea that the repair of phleomycin-induced DNA damage requires the G-BRCA2 complex, but not the FA core complex or G-ERCC1-XPF complexes, levels of HRR in NM3-VO and NM3-S7A were reduced compared to wild type NM3-gWT cells. In fact, it appeared that HRR was more severely compromised in NM3-S7A than it was in NM3-VO. The reasons for this are presently unclear, but one possibility may be that the presence of the FA core complex and G-ERCC1-XPF (containing the mutated FANCG-S7A protein) might somehow interfere with the processing, or hinder the repair, of phleomycin-induced DNA damage.

Further evidence for the involvement of the G-BRCA2 complex in the homologous recombination repair of phleomycin-induced DSBs comes from the analysis of NM3-S387A and human *FANCA* mutant cell line GM6914. It is known that the G-BRCA2 complex forms in both these cell lines **(Wilson *et al.*, 2008; Wilson *et al.*, 2010)**. NM3-S387A cells do not exhibit significant cellular hypersensitivity to phleomycin compared with wild type NM3-gWT control

cells. In addition, the levels of phleomycin induced chromosomal aberrations and the types of aberrations induced (predominantly chromatid breaks) are similar to NM3-gWT. While HRR levels after phleomycin are somewhat reduced in NM3-S387A cells, the defect is much less severe than that observed for NM3-S7A (Chapter 4). Thus, whatever the defect is in NM3-S387A cells that results in MMC-hypersensitivity, it is clear that this defect has little effect on the repair of phleomycin-induced DNA damage.

GM6914 cells, like NM3-S387A cells, presumably have a functional G-BRCA2 complex, as it is known that the formation of this complex is independent of the FANCA protein, the FA core complex and FANCD2 mono-ubiquitination **(Wilson *et al.*, 2008; Wilson *et al.*, 2010)**. For phleomycin, GM6914 (GM6914-VO) cells showed a response that was very similar its wild type cDNA corrected counterpart (GM6914-AWT). Cellular sensitivity and the induction of chromosomal aberrations were similar in GM6914-VO and GM6914-AWT cells (Chapter 5) **(Table 7.2)** and similar levels of HRR have been observed in these two cell lines (Mysore, Wilson and Jones unpublished). These data, therefore provide further evidence that the G-BRCA2 complex is important for HRR of phleomycin-induced DSB. Furthermore, they also indicate that the repair of this damage does not require the formation of the FA core complex or FANCD2 mono-ubiquitination, as neither of these things occur in GM6914 *FANCA* mutant cells.

Table (7.1): FANCG cell lines findings to MMC and phleomycin

		FANCG COMPLEXES			Hypersensitivity		HRR RF		CA Rate		Most abundant CA Types		Predominant CA	
		FA-Core Complex	G-BRCA2 Complex	G-XPF-ERCC1 Complex	MMC	Phleomycin	MMC	Phleomycin	MMC	Phleomycin	MMC	Phleomycin	MMC	Phleomycin
FANCG cell lines	NM3-gWT	yes	yes	yes	Low	Low	High	High	Low	Low	Chromatid breaks & exchanges	Chromatid breaks & exchanges	Chromatid exchanges	Chromatid breaks
	NM3-VO	NO	yes	NO	Highest	High	Low	Low	Highest	High	Chromatid breaks & exchanges	Chromatid breaks & exchanges	Chromatid exchanges	Chromatid exchanges
	NM3-S7A	yes	NO	?	Intermediate	High	Low	Low	High	Highest	Chromatid breaks & exchanges	Chromatid breaks & exchanges	Chromatid exchanges	Chromatid exchanges
	NM3-S387A	yes	yes	?	Intermediate	Low	Intermediate	Intermediate	High	Low	Chromatid breaks & exchanges	Chromatid breaks & exchanges	Chromatid breaks	Chromatid breaks

Table (7.1): Summarizing FANCG cell lines growth inhibition, homologous recombination repair and cytogenetic analysis findings to MMC and phleomycin (Chapter-3 and Chapter-4). Table abbreviations: HRR; homologous recombination repair, RF; recombination frequency, CA chromosomal aberration.

Table (7.2): FANCA cell lines findings to MMC and phleomycin

FANCA cell lines	FANCG COMPLEXES			Hypersensitivity		HRR RF		CA Rate		Most abundant CA Types		Predominant CA	
	FA-Core Complex	G-BRCA2 Complex	G-XPF-ERCC1 Complex	MMC	Phleomycin	MMC	Phleomycin	MMC	Phleomycin	MMC	Phleomycin	MMC	Phleomycin
FANCA-WT	yes	yes	yes	Low	Low	High	High	Low	Low	Chromatid breaks & exchanges	Chromatid breaks	Chromatid exchanges	Chromatid breaks
FANCA-VO	NO	yes	yes	Highest	Low	Low	High	High	Low	Chromatid breaks & exchanges	Chromatid breaks	Chromatid exchanges	Chromatid breaks
FANCA-S1449A	yes	yes	yes	Intermediate	Low	Low	High	High	Low	Chromatid breaks & exchanges	Chromatid breaks	Chromatid exchanges	Chromatid breaks
FANCA-S1449D	yes	yes	yes	Intermediate	Low	Intermediate	High						

Table (7.2): Summarizing FANCA cell lines growth inhibition, homologous recombination repair and cytogenetic analysis findings to MMC and phleomycin (Chapter-5). Table abbreviations: HRR; homologous recombination repair, RF; recombination frequency, CA chromosomal aberration.

Further support for the G-BRCA2 complex modulating proficient HRR in processing DNA strand breaks, and not the nuclear FA-core complex is presented in Chapter 6. The *FANCD2* deficient cell line PD20 exhibited hypersensitivity to phleomycin while the phospho-mutant cell line PD20-S331A and mono-ubiquitination mutant cell line PD20-K561R showed an intermediate level of hypersensitivity, while the phospho-mimetic PD20 S331D showed wild type behavior **(Table 7.3)**. This intermediate hypersensitivity observed in *FANCD2* phospho-mutant PD20-S331A and mono-ubiquitination mutant PD20-K561R to phleomycin, suggest a role for both FANCD2-S and non-phosphorylated FANCD2 S331 in partial repair of DNA double strand breaks. The wild type behavior in PD20 S331D is predicted as the mutation in PD20 S331D did not affect FANCD2 mono-ubiquitination, nor did it affect the interaction between FANCD2 with BRCA2 to form the G-BRCA2 complex, thus sustaining both phleomycin and MMC cellular resistance.

Despite showing similar cellular hypersensitivity to phleomycin, the induction of chromosomal aberrations in PD20-S331A and PD20-K561R was distinct. In the limited number of experiments performed with these cell lines, it appeared that the response of PD20-K561R was more similar to that of the wild type PD20-D2WT, while the response of PD20-S331A was closer to that of the null mutant PD20-VO. This difference in result may possibly be explained with respect to the formation of the G-BRCA2 complex in these cells. Phosphorylation of Serine 331 has been shown to be required for its interaction with BRCA2 and therefore formation of the complete G-BRCA2 complex **(Zhi *et al.*, 2009)**. The lack of the G-BRCA2 complex, and an inability to process phleomycin-induced DSBs by HRR, most likely explains the induction of chromosomal aberrations in PD20-S331A cells. On the other hand, mono-ubiquitination of FANCD2 is not required for formation of the G-BRCA2, thus the presence of the complex in PD20-K561R cells

is consistent with the lack of increased chromosomal aberrations compared to PD20-D2WT cells and a normal ability to perform HRR. Certainly, recent unpublished data (Wilson and Jones, personal communication) shows that while both PD20-K561R and PD20-S331A cells show reduced HRR in the SCneo recombination assay, the defect is much more severe in PD20-S331A cells. HRR is less than 2-fold reduced in PD20-K561R compared to PD20-D2WT. However, while the levels of HRR observed in these two cell lines are broadly consistent with the induction of chromosomal aberrations, it is not consistent with their intermediate and similar cellular sensitivities to phleomycin. One possibility is that the mono-ubiquitination is important for a function of FANCD2, other than that in the G-BRCA2 protein complex.

Thus the intermediate hypersensitivity observed in PD20-K561R cells might possibly be explained by the failure to mono-ubiquitinate FANCD2-S to FANCD2-L. This in turn leads to failure of FANCD2 to bind chromatin and the failure of FANCD2 to form nuclear foci. Thus, while the G-BRCA2 complex can form in PD20-K561R cells, HRR may operate at reduced efficiency. Alternatively, mono-ubiquitinated FANCD2 has been implicated in a DNA damage cell cycle checkpoint response **(Taniguchi *et al.*, 2002b; Andreassen *et al.*, 2004)** and this may also go some way in explaining the intermediate response to phleomycin in K561R cells. A role for mono-ubiquitinated FANCD2 in the repair of DNA damage or cellular responses, such as cell cycle control to DNA damage, upon phleomycin exposure is consistent with the intermediate response of PD20-S331A cells. While the G-BRCA2 complex does not form in these cells, they still express mono-ubiquitinated FANCD2. It is clear that further experimentation is required to fully determine the role(s) of FANCD2, unfortunately attempts to repeat the initial experiments with PD20 cells were hindered due to unexplained variability.

It is interesting to note that the predominant chromosomal aberrations induced by phleomycin in *FANCG*-deficient cells (NM3) and *FANCD2*-deficient cells (PD20) were different. Chromatid exchanges were prevalent in NM3, while chromatid breaks were prevalent in PD20. Neither cell line is able to form the G-BRCA2 complex, but the reason for the difference in aberration type is unknown. It might possibly relate to functions of FANCG and FANCD2 outside of the G-BRCA2 complex. FANCG is a component of the FA core complex and G-ERCC1-XPF complexes and mono-ubiquitinated FANCD2 has other functions as just discussed. However, the prevalence of exchanges in the *FANCG*-deficient cells does suggest illegitimate-processing of breaks by NHEJ, while the prevalence of breaks in *FANCD2*-deficent cells suggests a lack of repair by either HRR or NHEJ. Alternatively, the difference might simply be due to a species-specific difference between hamster (NM3) and human (PD20) cells.

Support that G-BRCA2 complex may modulate proficient HRR also comes from XRCC3 and BRCA2 data in the literature. Employing CHO cell line mutants of *XRCC3* (irs1SF), **Fuller and Painter, (1988)** illustrated their cellular hypersensitivity to ionizing radiation (DNA strand breaking agent). **Fuller and Painter, (1988)** also reported elevated numbers of chromatid exchanges in irslSF cells post cellular exposure to irradiation. These findings are in agreement with phleomycin growth inhibition and cytogenetic findings of *FANCG* deficient cells which have shown phleomycin hypersensitivity and chromatid exchange type aberration predominance. This agreement supports the model which explains hypersensitivity to DNA strand breaking agents and the predominance of chromatid exchanges in G-BRCA2 deficient cell lines at least in CHO cells. The use of different model systems could be the reason why chromatid exchanges were observed in CHO cells NM3-VO and NM3-S7A, while chromatid breaks were observed in human PD20 cells.

BRCA2 cell mutants exhibit hypersensitivity to several DNA damaging agents including cross-linking, mono-functional alkylating agents **(Overkamp *et al.*, 1993). Rahden-Staron *et al.*, (2003)** showed that BRCA2 defective CHO V-C8 cells were hypersensitive, to topoisomerase I inhibition by camptothecin. Topoisomerases intracellular level is vital in ionizing radiation and oxidative damage repair **(Davies *et al.*, 1988; 1990). Pommier *et al.*, (1994)** has suggested that radiation and inhibitory drug induced DSBs may be repaired through a common pathway.

These two homologous recombination repair proteins XRCC3 and BRCA2 interact directly with FANCG **(Hussain *et al.*, 2003; Hussain *et al.*, 2004; Hussain *et al.*, 2006).** These observations further support the model that proposes the G-BRCA2 complex containing FANCG, BRCA2, FANCD2 and XRCC3 to modulate proficient HRR in DNA lesion repair.

Table (7.3): FANCD2 cell lines findings to MMC and phleomycin

		FANCG COMPLEXES			Hypersensitivity		CA Rate		Most abundant CA		Predominant CA Type	
		FA-Core Complex	G-BRCA2 Complex	G-XPF-ERCC1 Complex	MMC	Phleomycin	MMC	Phleomycin	MMC	Phleomycin	MMC	Phleomycin
FANCD2 cell lines	PD20-D2WT	yes	yes	yes	Low	Low		Low		Chromatid breaks		Chromatid breaks
	PD20	yes	NO	yes	Highest	Highest		Highest		Chromatid breaks		Chromatid breaks
	PD20-S331A	yes	NO	yes	Intermediate	Intermediate		High		Chromatid breaks		Chromatid breaks
	PD20-K561R	yes	yes	yes	Intermediate	Intermediate		Low		Chromatid breaks		Chromatid breaks
	PD20S331D	yes	yes	yes	Low	Low						
	PD20-315	yes	yes	yes	Low	Low						

Table (7.3): Summarizing FANCD2 cell lines growth inhibition findings to MMC and phleomycin and cytogenetic analysis findings for phleomycin experiments in **Tables 6.1-A, 6.2-A and 6.3-A** (Chapter- 6)

7.1.3 Conclusions

Inter-strand cross-link repair requires multiple repair processes regulated through phosphorylation of FANC proteins which may assist in determining the sequential order of these processes. Phosphorylation of FANCG at serine-7 has a distinct function independent of the FA-core complex and arbitrates the formation of the G-BRCA2 complex. The G-BRCA2 complex forms separately from the FA-core complex and modulates error-free HRR proficiency. The G-BRCA2 complex operates either downstream (as in ICL repair) or independently of the FA core complex (as in DSB repair), dependent on the type of DNA lesion encountered.

The G-BRCA2 complex promotes error free HRR. In the absence of the G-BRCA2 complex, directly induced DSBs (phleomycin) or DSBs arising from incomplete or partial repair of ICLs (MMC) are processed through error-prone NHEJ, resulting in the induction of chromosomal aberrations and genomic instability. FANCG, its phospho-site S7 and the G-BRCA2 complex are essential in restoring wild type ability to repair DNA strand breaks through proficient HRR, which is also part of proficient ICL repair.

The FANCG phospho-site S387 is required for proficient ICL repair, but is not essential for the repair of DNA double strand breaks. The role of S387-phosphorylation in ICL repair is unknown. FA core complex formation and FANCD2 mono-ubiquitination appear to be independent of this phosphorylation event, although it is possible that the failure to phosphorylate S387 will lead to sub-optimal processing of ICL prior to the HRR step. Another possibility might be that phosphorylation of S387 is required for formation of the G-ERCC1-XPF complex, responsible for unhooking of ICL. A final possibility, given that the phosphorylation occurs in mitosis, it may be the case that phosphorylation of S387 is required to

"switch off" suppression of NHEJ by the FA core complex. It could be speculated that NHEJ is required to repair remaining ICL-associated DSBs that have evaded repair by HRR during S-phase. This explanation would at least be consistent with the additional chromatid breaks observed in NM3-S387A cells after MMC.

FANCD2, its phospho-site S331 and its mono-ubiquitination site K561 are important in restoring wild type ability to repair DNA strand breaks through proficient HRR. Both FANCD2-S and non-phosphorylated FANCD2 S331 seem to have a function or an active role in DNA double strand break and ICL repair.

FANCA and the FA-core complex are not critically required for the repair of DNA strand breaks that are induced directly (as for phleomycin) However, FANCA and the FA core complex are required for the processing of ICL upstream of HRR (ICL unhooking and lesion bypass) and in the suppression of NHEJ by the FA pathway.

References

Adachi, D., Oda, T., Yagasaki, H., Nakasato, K., Taniguchi, T., D'Andrea, A. D., Asano, S. and Yamashita, T. (2002). Heterogeneous activation of the Fanconi anaemia pathway by patient-derived FANCA mutants. *Human Molecular Genetics* **11**, 3125-3134.

Adamo, A., Collis, S. J., Adelman, C. A., Silva, N., Horejsi, Z., Ward, J. D., Martinez-Perez, E., Boulton, S. J. and La Volpe, A. (2010). Preventing Nonhomologous End Joining Suppresses DNA Repair Defects of Fanconi Anaemia. *Molecular Cell* **39**, 25-35.

Akkari, Y. M. N., Bateman, R. L., Reifsteck, C. A., D'Andrea, A. D., Olson, S. B. and Grompe, M. (2001). The 4N cell cycle delay in Fanconi anaemia reflects growth arrest in late S phase. *Molecular Genetics and Metabolism* **74**, 403-412.

Alter, B. P. (2003). Cancer in Fanconi anaemia, 1927-2001. *Cancer* **97**, 425-440.

Ameziane, N., Errami, A., Leveille, F., Fontaine, C., de Vries, Y., van Spaendonk, R. M. L., de Winter, J. R., Pals, G. and Joenje, H. (2008). Genetic subtyping of Fanconi anaemia by comprehensive mutation screening. *Human Mutation* **29**, 159-166.

Andreassen, P. R., D'Andrea, A. D. and Taniguchi, T. (2004). ATR couples FANCD2 monoubiquitination to the DNA-damage response. *Genes and Development* **18**, 1958-1963.

Apostolou, S., Whitmore, S. A., Crawford, J. and other authors (1996). Positional cloning of the Fanconi anaemia group A gene. *Nature Genetics* **14**, 324-328.

Auerbach, A. D. and Wolman, S. R. (1976). Susceptibility of Fanconi's anaemia fibroblasts to chromosome damage by carcinogens. *Nature* **261**, 494-496.

Auerbach, A. D., Warburton, D., Bloom, A. D. and Chaganti, R. S. K. (1979). Prenatal detection of the Fanconi anaemia gene by cytogenetic methods. *American Journal of Human Genetics* **31**, 77-81.

Auerbach, A. D., Rogatko, A. and Schroederkurth, T. M. (1989). International Fanconi Anaemia Registry: relation of clinical symptoms to diepoxybutane sensitivity. *Blood* **73**, 391-396.

Auerbach, A. D. (1993). Fanconi anaemia diagnosis and the diepoxybutane (DEB) test. *Experimental Hematology* **21**, 731-733.

Balcome, S., Park, S., Dorr, D. R. Q., Hafner, L., Phillips, L. and Tretyakova, N. (2004). Adenine-containing DNA-DNA cross-links of antitumor nitrogen mustards. *Chemical Research in Toxicology* **17**, 950-962.

Barlow, J. H., Lisby, M. and Rothstein, R. (2008). Differential regulation of the cellular response to DNA double-strand breaks in G1. *Molecular Cell* **30**, 73-85.

Barnes, D. E. and Lindahl, T. (2004). Repair and genetic consequences of endogenous DNA base damage in mammalian cells. *Annual Review of Genetics* **38**, 445-476.

Barre, F. X., Soballe, B., Michel, B., Aroyo, M., Robertson, M. and Sherratt, D. (2001). Circles: The replication-recombination-chromosome segregation connection. *Proceedings of the National Academy of Sciences of the United States of America* **98**, 8189-8195.

Baynton, K., Bresson-Roy, A. and Fuchs, R. P. P. (1999). Distinct roles for Rev1p and Rev7p during translesion synthesis in Saccharomyces cerevisiae. *Molecular Microbiology* **34**, 124-133.

Bhagwat, N., Olsen, A. L., Wang, A. T., Hanada, K., Stuckert, P., Kanaar, R., D'Andrea, A., Niedernhofer, L. J. and McHugh, P. J. (2009). XPF-ERCC1 Participates in the Fanconi Anaemia Pathway of Cross-Link Repair. *Molecular and Cellular Biology* **29**, 6427-6437.

Bio-world http://www.bio-world.com/productinfo/4_847_60_444/1087/Phleomycin.html.

Bizanek, R., Chowdary, D., Arai, H., Kasai, M., Hughes, C. S., Sartorelli, A. C., Rockwell, S. and Tomasz, M. (1993). Adducts of mitomycin C and DNA in EMT6 mouse mammary tumor cells: effects of hypoxia and dicumarol on adduct patterns. *Cancer Research* **53**, 5127-5134.

Blom, E., van de Vrugt, H. J., de Vries, Y., de Winter, J. P., Arwert, F. and Joenje, H. (2004). Multiple TPR motifs characterize the Fanconi anaemia FANCG protein. *DNA Repair* **3**, 77-84.

Blommaert, F. A., Vandijkknijnenburg, H. C. M., Dijt, F. J., Denengelse, L., Baan, R. A., Berends, F. and Fichtingerschepman, A. M. J. (1995). Formation of DNA Adducts by the Anticancer Drug Carboplatin: Different. Nucleotide Sequence Preferences in Vitro and in Cells. *Biochemistry* **34**, 8474-8480.

Bodell, W. J., Aida, T., Berger, M. S. and Rosenblum, M. L. (1985). Repair of O6-(2-chloroethyl)guanine mediates the biological effects of chloroethylnitrosoureas. *Environmental Health Perspectives* **62**, 119-126.

Bodell, W. J., Tokuda, K. and Ludlum, D. B. (1988). Differences in DNA Alkylation Products Formed in Sensitive and Resistant Human Glioma Cells Treated with N-(2-Chloroethyl)-N-nitrosourea. *Cancer Research* **48**, 4489-4492.

Bodell, W. J. (1990). Molecular dosimetry for sister-chromatid exchange induction and cytotoxicity by monofunctional and bifunctional alkylating agents. *Mutation Research* **233**, 203-210.

Brabec, V. and Leng, M. (1993). DNA interstrand cross-links of trans-diamminedichloroplatinum(II) are preferentially formed between guanine and complementary cytosine residues. *Proceedings of the National Academy of Sciences of the United States of America* **90**, 5345-5349.

Brash, D. E., Rudolph, J. A., Simon, J. A., Lin, A., McKenna, G. J., Baden, H. P., Halperin, A. J. and Ponten, J. (1991). A role for sunlight in skin cancer: UV-induced p53 mutations in squamous cell carcinoma. *Proceedings of the National Academy of Sciences of the United States of America* **88**, 10124-10128.

Brendel, M. and Ruhland, A. (1984). Relationships between functionality and genetic toxicology of selected DNA-damaging agents. *Mutation Research* **133**, 51-85.

Bryant, H. E., Ying, S. M. and Helleday, T. (2006). Homologous recombination is involved in repair of chromium-induced DNA damage in mammalian cells. *Mutation Research-Fundamental and Molecular Mechanisms of Mutagenesis* **599**, 116-123.

Buchwald, M. (1995). Complementation groups: one or more per gene. *Nature Genetics* **11**, 228-230.

Bunting, S. F., Callen, E., Wong, N. and other authors (2010). 53BP1 Inhibits Homologous Recombination in Brca1-Deficient Cells by Blocking Resection of DNA Breaks. *Cell* **141**, 243-254.

Bunting, S. F. and Nussenzweig, A. (2010). Dangerous Liaisons: Fanconi Anaemia and Toxic Nonhomologous End Joining in DNA Crosslink Repair. *Molecular Cell* **39**, 164-166.

Busch, D. B., Zdzienicka, M. Z., Natarajan, A. T. and other authors (1996). A CHO mutant, UV40, that is sensitive to diverse mutagens and represents a new complementation group of mitomycin C sensitivity. *Mutation Research-DNA Repair* **363**, 209-221.

Callen, E., Samper, E., Ramirez, M. J. and other authors (2002). Breaks at telomeres and TRF2-independent end fusions in Fanconi anaemia. *Human Molecular Genetics* **11**, 439-444.

Callen, E., Casado, J. A., Tischkowitz, M. D. and other authors (2005). A common founder mutation in FANCA underlies the world's highest prevalence of Fanconi anaemia in Gypsy families from Spain. *Blood* **105**, 1946-1949.

Cantor, S. B., Bell, D. W., Ganesan, S. and other authors (2001). BACH1, a novel helicase-like protein, interacts directly with BRCA1 and contributes to its DNA repair function. *Cell* **105**, 149-160.

Castella, M., Pujol, R., Callen, E. and other authors (2011). Origin, functional role, and clinical impact of Fanconi anaemia FANCA mutations. *Blood* **117**, 3759-3769.

Cervenka, J., Arthur, D. and Yasis, C. (1981). Mitomycin-C test for diagnostic differentiation of idiopathic aplastic aneamia and Fanconi aneamia. *Pediatrics* **67**, 119-127.

Champeil, E. and Tomasz, M. (2006). Novel synthesis of DNA-mitomycin C adducts formed at N2 of guanine. *Abstracts of Papers of the American Chemical Society* **232**, 22-22.

Champeil, E., Bargonetti, J. and Tomasz, M. (2010). Differential toxicity of DNA adducts of mitomycin C. *Journal of nucleic acids* **2010**.

Chan, K. L., Palmai-Pallag, T., Ying, S. and Hickson, I. D. (2009). Replication stress induces sister-chromatid bridging at fragile site loci in mitosis. *Nature Cell Biology* **11**, 753-U120.

Chandra, S., Levran, O., Jurickova, I. and other authors (2005). A rapid method for retrovirus-mediated identification of complementation groups in Fanconi anaemia patients. *Molecular Therapy* **12**, 976-984.

Channarayappa, Nath, J. and Ong, T. (1990). Micronuclei assay in cytokinesis-blocked binucleated and conventional mononucleated methods in human peripheral lymphocytes. *Teratogenesis Carcinogenesis and Mutagenesis* **10**, 273-279.

Chen, J., Ghorai, M. K., Kenney, G. and Stubbe, J. (2008). Mechanistic studies on bleomycin-mediated DNA damage: multiple binding modes can result in double-stranded DNA cleavage. *Nucleic Acids Research* **36**, 3781-3790.

Ciccia, A., Ling, C., Coulthard, R. and other authors (2007). Identification of FAAP24, a Fanconi anaemia core complex protein that interacts with FANCM. *Molecular Cell* **25**, 331-343.

Ciccia, A., McDonald, N. and West, S. C. (2008). Structural and functional relationships of the XPF/MUS81 family of proteins. In *Annual Review of Biochemistry*, pp. 259-287.

Cochrane, J. E. and Skopek, T. R. (1994). Mutagenicity of butadiene and its epoxide metabolites: II. Mutational spectra of butadiene, 1,2-epoxybutene and diepoxybutane at the hprt locus in splenic T cells from exposed B6C3F1 mice. *Carcinogenesis* **15**, 719-723.

Collins, N. B., Wilson, J. B., Bush, T., Thomashevski, A., Roberts, K. J., Jones, N. J. and Kupfer, G. M. (2009). ATR-dependent phosphorylation of FANCA on serine 1449 after DNA damage is important for FA pathway function. *Blood* **113**, 2181-2190.

Collis, S. J., Barber, L. J., Ward, J. D., Martin, J. S. and Boulton, S. J. (2006). C-elegans FANCD2 responds to replication stress and functions in interstrand cross-link repair. *DNA Repair* **5**, 1398-1406.

Crossan, G. P. & Patel, K. J. (2011). The Fanconi anaemia pathway orchestrates incisions at sites of crosslinked DNA. *J Pathol*, Published online 25 October 2011 in Wiley Online Library. *J Pathol* 2012 Jan;2226(2012):2326-2037. doi: 2010.1002/path.3002. Epub 2011 Oct 2025

D'Andrea, A. D. (2010). Mechanisms of disease Susceptibility Pathways in Fanconi's Anaemia and Breast Cancer. *New England Journal of Medicine* **362**, 1909-1919.

Daniels, M. J., Wang, Y. M., Lee, M. Y. and Venkitaraman, A. R. (2004). Abnormal cytokinesis in cells deficient in the breast cancer susceptibility protein BRCA2. *Science* **306**, 876-879.

Davies, S. M., Robson, C. N., Davies, S. L. and Hickson, I. D. (1988). Nuclear topoisomerase II levels correlate with the sensitivity of mammalian cells to intercalating agents and epipodophyllotoxins. *Journal of Biological Chemistry* **263**, 17724-17729.

Davies, S. M., Davies, S. L., Hall, A. G. and Hickson, I. D. (1990). Isolation and partial characterisation of a mammalian cell mutant hypersensitive to topoisomerase II inhibitors and X-rays. *Mutation Research* **235**, 111-118.

Davies, A. A., Masson, J. Y., McLlwraith, M. J., Stasiak, A. Z., Stasiak, A., Venkitaraman, A. R. and West, S. C. (2001). Role of BRCA2 in control of the RAD51 recombination and DNA repair protein. *Molecular Cell* 7, 273-282.

Davies, O. R. and Pellegrini, L. (2007). Interaction with the BRCA2 C terminus protects RAD51-DNA filaments from disassembly by BRC repeats. *Nature Structural and Molecular Biology* **14**, 475-483.

de Oca, R. M., Andreassen, P. R., Margossian, S. P., Gregory, R. C., Taniguchi, T., Wang, X. Z., Houghtaling, S., Grompe, M. and D'Andrea, A. D. (2005). Regulated interaction of the Fanconi anaemia protein, FANCD2, with chromatin. *Blood* **105**, 1003-1009.

de Winter, J. P., Waisfisz, Q., Rooimans, M. A. and other authors (1998). The Fanconi anaemia group G gene FANCG is identical with XRCC9. *Nature Genetics* **20**, 281-283.

de Winter, J. P., van der Weel, L., de Groot, J. and other authors (2000a). The Fanconi anaemia protein FANCF forms a nuclear complex with FANCA, FANCC and FANCG. *Human Molecular Genetics* **9**, 2665-2674.

de Winter, J. P., Rooimans, M. A., van der Weel, L. and other authors (2000b). The Fanconi anaemia gene FANCF encodes a novel protein with homology to ROM. *Nature Genetics* **24**, 15-16.

Deakyne, J. S. and Mazin, A. V. (2011). Fanconi anaemia: at the Crossroads of DNA repair. *Biochemistry-Moscow* **76**, 36-48.

Deans, A. J. and West, S. C. (2011). DNA interstrand crosslink repair and cancer. *Nature Reviews Cancer* **11**, 467-480.

Demuth, I., Wlodarski, M., Tipping, A. J. and other authors (2000). Spectrum of mutations in the Fanconi anaemia group G gene, FANCG/XRCC9. *European Journal of Human Genetics* **8**, 861-868.

DePinho, R. A. (2000). The age of cancer. *Nature* **408**, 248-254.

Dorsman, J. C., Levitus, M., Rockx, D. and other authors (2007). Identification of the Fanconi anaemia complementation group I gene, FANCI. *Cellular Oncology* **29**, 211-218.

Dronkert, M. L. G. and Kanaar, R. (2001). Repair of DNA interstrand cross-links. *Mutation Research-DNA Repair* **486**, 217-247.

Duckworthrysiecki, G., Hulten, M., Mann, J. and Taylor, A. M. R. (1984). Clinical and cytogenetic diversity in Fanconis anaemia. *Journal of Medical Genetics* **21**, 197-203.

Duckworthrysiecki, G., Toji, L., Ng, J., Clarke, C. and Buchwald, M. (1986). Characterization of a simian virus 40-transformed Fanconi anaemia fibroblast cell line. *Mutation Research* **166**, 207-214.

Duncan, B. K. and Miller, J. H. (1980). Mutagenic deamination of cytosine residues in DNA. *Nature* **287**, 560-561.

Eastmond, D. A. and Tucker, J. D. (1989). Kinetochore localization in micronucleated cytokinesis-blocked Chinese-Hamster Ovary cells - A new and rapid assay for identifying aneuploidy-inducing agents. *Mutation Research* **224**, 517-525.

Ellard, S., Mohammed, Y., Dogra, S., Wolfel, C., Doehmer, J. and Parry, J. M. (1991). The use of genetically engineered V79 Chinese hamster cultures expressing rat liver CYP1A1, 1A2 and 2B1 cDNAs in micronucleus assays. *Mutagenesis* **6**, 461-470.

Esashi, F., Galkin, V. E., Yu, X., Egelman, E. H. and West, S. C. (2007). Stabilization of RAD51 nucleoprotein filaments by the C-terminal region of BRCA2. *Nature Structural and Molecular Biology* **14**, 468-474.

Esmer, C., Sanchez, S., Ramos, S., Molina, B., Frias, S. and Carnevale, A. (2004). DEB test for Fanconi anaemia detection in patients with atypical phenotypes. *American Journal of Medical Genetics Part A* **124A**, 35-39.

Ewig, R. A. G. and Kohn, K. W. (1977). DNA Damage and Repair in Mouse Leukemia L1210 Cells Treated with Nitrogen Mustard, 1,3-Bis(2-chloroethyl)-1-nitrosourea, and Other Nitrosoureas. *Cancer Research* **37**, 2114-2122.

Ewig, R. A. G. and Kohn, K. W. (1978). DNA-protein cross-linking and DNA interstrand cross-linking by haloethylnitrosoureas in L1210 cells. *Cancer Research* **38**, 3197-3203.

Eyfjord, J. E. and Bodvarsdottir, S. K. (2005). Genomic instability and cancer: Networks involved in response to DNA damage. *Mutation Research-Fundamental and Molecular Mechanisms of Mutagenesis* **592**, 18-28.

Faivre, L., Guardiola, P., Lewis, C. and other authors (2000). Association of complementation group and mutation type with clinical outcome in Fanconi anaemia. *Blood* **96**, 4064-4070.

Faravelli, M., Moralli, D., Bertoni, L., Attolini, C., Chernova, O., Raimondi, E. and Giulotto, E. (1998). Two extended arrays of a satellite DNA sequence at the centromere and at the short-arm telomere of Chinese hamster chromosome 5. *Cytogenetics and Cell Genetics* **83**, 281-286.

Fatyol, K., Cserpan, I., Praznovszky, T., Kereso, J. and Hadlaczky, G. (1994). Cloning and molecular characterization of a novel chromosome specific centromere sequence of Chinese hamster. *Nucleic Acids Research* **22**, 3728-3736.

Featherstone, C. and Jackson, S. P. (1999). Ku, a DNA repair protein with multiple cellular functions? *Mutation Research-DNA Repair* **434**, 3-15.

Fekairi, S., Scaglione, S., Chahwan, C. and other authors (2009). Human SLX4 Is a Holliday Junction Resolvase Subunit that Binds Multiple DNA Repair/Recombination Endonucleases. *Cell* **138**, 78-89.

Feldser, D. M., Hackett, J. A. and Greider, C. W. (2003). Opinion - Telomere dysfunction and the initiation of genome instability. *Nature Reviews Cancer* **3**, 623-627.

Fenech, M. and Morley, A. A. (1985). Measurement of micronuclei in lymphocytes. *Mutation Research* **147**, 29-36.

Fenech, M. (2000). The in vitro micronucleus technique. *Mutation Research-Fundamental and Molecular Mechanisms of Mutagenesis* **455**, 81-95.

Fisher, L. A., Bessho, M. and Bessho, T. (2008). Processing of a psoralen DNA interstrand cross-link by XPF-ERCC1 complex in vitro. *Journal of Biological Chemistry* **283**, 1275-1281.

Folias, A., Matkovic, M., Bruun, D., Reid, S., Hejna, J., Grompe, M., D'Andrea, A. and Moses, R. (2002). BRCA1 interacts directly with the Fanconi anaemia protein FANCA. *Human Molecular Genetics* **11**, 2591-2597.

Fracasso, P. M. and Sartorelli, A. C. (1986). Cytotoxicity and DNA lesions produced by mitomycin C and porfiromycin in hypoxic and aerobic EMT6 and Chinese hamster ovary cells. *Cancer Research* **46**, 3939-3944.

Frankel, A. D., Duncan, B. K. and Hartman, P. E. (1980). Nitrous acid damage to duplex deoxyribonucleic acid: distinction between deamination of cytosine residues and a novel mutational lesion. *Journal of Bacteriology* **142**, 335-338.

Fuller, L. F. and Painter, R. B. (1988). A Chinese hamster ovary cell line hypersensitive to ionizing radiation and deficient in repair replication. *Mutation Research* **193**, 109-121.

Fundia, A., Gorla, N. and Larripa, I. (1994). Spontaneous chromosome aberrations in Fanconi's anaemia patients are located at fragile sites and acute myeloid leukemia breakpoints. *Hereditas* **120**, 47-50.

Futaki, M. and Liu, J. M. (2001). Chromosomal breakage syndromes and the BRCA1 genome surveillance complex. *Trends in Molecular Medicine* **7**, 560-565.

Futaki, M., Watanabe, S., Kajigaya, S. and Liu, J. M. (2001). Fanconi anaemia protein, FANCG, is a phosphoprotein and is upregulated with FANCA after TNF-alpha treatment. *Biochemical and Biophysical Research Communications* **281**, 347-351.

Gabriele, M., Cantemir, C. and Majone, F. (1995). Cytogenetic effects induced by cytochalasin B in Chinese hamster ovary cells. *Journal of Biomedical Science* **2**, 30-35.

Garcia-Higuera, I., Kuang, Y., Naf, D., Wasik, J. and D'Andrea, A. D. (1999). Fanconi anaemia proteins FANCA, FANCC, and FANCG/XRCC9 interact in a functional nuclear complex. *Molecular and Cellular Biology* **19**, 4866-4873.

Garcia-Higuera, I., Kuang, Y., Denham, J. and D'Andrea, A. D. (2000). The Fanconi anaemia proteins FANCA and FANCG stabilize each other and promote the nuclear accumulation of the Fanconi anaemia complex. *Blood* **96**, 3224-3230.

Garcia-Higuera, I., Taniguchi, T., Ganesan, S., Meyn, M. S., Timmers, C., Hejna, J., Grompe, M. and D'Andrea, A. D. (2001). Interaction of the fanconi anaemia proteins and BRCA1 in a common pathway. *Molecular Cell* **7**, 249-262.

Giovanetti, A., Deshpande, T. and Basso, E. (2008). Persistence of genetic damage in mice exposed to low dose of X rays. *International Journal of Radiation Biology* **84**, 227-235.

Godthelp, B. C., van Buul, P. P. W., Jaspers, N. G. J., Elghalbzouri-Maghrani, E., van Duijn-Goedhart, A., Arwert, F., Joenje, H. and Zdzienicka, M. Z. (2006). Cellular characterization of cells from the Fanconi anaemia complementation group, FA-D1/BRCA2. *Mutation Research-Fundamental and Molecular Mechanisms of Mutagenesis* **601**, 191-201.

Golo, V. L. and Volkov, Y. S. (2003). Tunneling of protons and tautomeric transitions in base pairs of DNA. *International Journal of Modern Physics C* **14**, 133-156.

Goodsell, D. S. (2001). The molecular perspective: Ultraviolet light and pyrimidine dimers. *Oncologist* **6**, 298-299.

Goodsell, D. S. (2005). The molecular perspective: RAD51 and BRCA2. *Stem Cells* **23**, 1434-1435.

Gordy, W. (1958). Free Radicals as a Possible Cause of Mutations and Cancer. *Symposium on Information Theory in Biology*, 353-356.

Goth, R. and Rajewsky, M. F. (1974). Persistence of 06-Ethylguanine in Rat-Brain DNA: Correlation with Nervous System-Specific Carcinogenesis by Ethylnitrosourea. *Proceedings of the National Academy of Sciences of the United States of America* **71**, 639-643.

Griffin, C. S., Simpson, P. J., Wilson, C. R. and Thacker, J. (2000). Mammalian recombination-repair genes XRCC2 and XRCC3 promote correct chromosome segregation. *Nature Cell Biology* **2**, 757-761.

Grossmann, K. F., Ward, A. M., Matkovic, M. E., Folias, A. E. and Moses, R. E. (2001). S-cerevisiae has three pathways for DNA interstrand crosslink repair. *Mutation Research-DNA Repair* **487**, 73-83.

Gschwend, M., Levran, O., Kruglyak, L. and other authors (1996). A locus for Fanconi anaemia on 16q determined by homozygosity mapping. *American Journal of Human Genetics* **59**, 377-384.

Hanada, K., Budzowska, M., Modesti, M., Maas, A., Wyman, C., Essers, J. and Kanaar, R. (2006). The structure-specific endonuclease Mus81-Eme1 promotes conversion of interstrand DNA crosslinks into double-strands breaks. *Embo Journal* **25**, 4921-4932.

Hejna, J. A., Timmers, C. D., Reifsteck, C. and other authors (2000). Localization of the fanconi anaemia complementation group D gene to a 200-kb region on chromosome 3p25.3. *American Journal of Human Genetics* **66**, 1540-1551.

Hermine, T., Jones, N. J. and Parry, J. M. (1997). Comparative induction of micronuclei in repair-deficient and -proficient Chinese hamster cell lines following clastogen or aneugen exposures. *Mutation Research-Genetic Toxicology and Environmental Mutagenesis* **392**, 151-163.

Hickson, I. D. and Harris, A. L. (1988). Mammalian DNA repair use of mutants hypersensitive to cytotoxic agents. *Trends in Genetics* **4**, 101-106.

Hinz, J. M., Nham, P. B., Salazar, E. P. and Thompson, L. H. (2006). The Fanconi anaemia pathway limits the severity of mutagenesis. *DNA Repair* **5**, 875-884.

Hirano, S., Yamamoto, K., Ishiai, M. and other authors (2005). Functional relationships of FANCC to homologous recombination, translesion synthesis, and BLM. *Embo Journal* **24**, 418-427.

Ho, G. P. H., Margossian, S., Taniguchi, T. and D'Andrea, A. D. (2006). Phosphorylation of FANCD2 on two novel sites is required for mitomycin C resistance. *Molecular and Cellular Biology* **26**, 7005-7015.

Hoeijmakers, J. H. J. (2001). Genome maintenance mechanisms for preventing cancer. *Nature* **411**, 366-374.

Houghtaling, S., Timmers, C., Noll, M., Finegold, M. J., Jones, S. N., Meyn, M. S. and Grompe, M. (2003). Epithelial cancer in Fanconi anaemia complementation group D2 (Fancd2) knockout mice. *Genes and Development* **17**, 2021-2035.

Howlett, N. G., Taniguchi, T., Olson, S. and other authors (2002). Biallelic inactivation of BRCA2 in Fanconi anaemia. *Science* **297**, 606-609.

Howlett, N. G., Taniguchi, T., Durkin, S. G., D'Andrea, A. D. and Glover, T. W. (2005). The Fanconi anaemia pathway is required for the DNA replication stress response and for the regulation of common fragile site stability. *Human Molecular Genetics* **14**, 693-701.

Huang, M. and D'Andrea, A. D. (2010). A new nuclease member of the FAN club. *Nature Structural and Molecular Biology* **17**, 926-928.

Huang, M., Kim, J. M., Shiotani, B., Yang, K. L., Zou, L. and D'Andrea, A. D. (2010). The FANCM/FAAP24 Complex Is Required for the DNA Interstrand Crosslink-Induced Checkpoint Response. *Molecular Cell* **39**, 259-268.

Hussain, S., Witt, E., Huber, P. A. J., Medhurst, A. L., Ashworth, A. and Mathew, C. G. (2003). Direct interaction of the Fanconi anaemia protein FANCG with BRCA2/FANCD1. *Human Molecular Genetics* **12**, 2503-2510.

Hussain, S., Wilson, J. B., Medhurst, A. L. and other authors (2004). Direct interaction of FANCD2 with BRCA2 in DNA damage response pathways. *Human Molecular Genetics* **13**, 1241-1248.

Hussain, S., Wilson, J. B., Blom, E. and other authors (2006). Tetratricopeptide-motif-mediated interaction of FANCG with recombination proteins XRCC3 and BRCA2. *DNA Repair* **5**, 629-640.

Ishiai, M., Kitao, H., Smogorzewska, A. and other authors (2008). FANCI phosphorylation functions as a molecular switch to turn on the Fanconi anaemia pathway. *Nature Structural and Molecular Biology* **15**, 1138-1146.

Itakura, E., Umeda, K., Sekoguchi, E., Takata, H., Ohsumi, M. and Matsuura, A. (2004). ATR-dependent phosphorylation of ATRIP in response to genotoxic stress. *Biochemical and Biophysical Research Communications* **323**, 1197-1202.

Jablonovich, Z., Liefshitz, B., Steinlauf, R. and Kupiec, M. (1999). Characterization of the role played by the RAD59 gene of Saccharomyces cerevisiae in ectopic recombination. *Current Genetics* **36**, 13-20.

Jackson, J. R., Gilmartin, A., Imburgia, C., Winkler, J. D., Marshall, L. A. and Roshak, A. (2000). An indolocarbazole inhibitor of human checkpoint kinase (Chk1) abrogates cell cycle arrest caused by DNA damage. *Cancer Research* **60**, 566-572.

Jackson, S. P. (2002). Sensing and repairing DNA double-strand breaks - Commentary. *Carcinogenesis* **23**, 687-696.

Jakobs, P. M., Sahaayaruban, P., Saito, H., Reifsteck, C., Olson, S., Joenje, H., Moses, R. E. and Grompe, M. (1996). Immortalization of four new Fanconi anaemia fibroblast cell lines by an improved procedure. *Somatic Cell and Molecular Genetics* **22**, 151-157.

Joenje, H. and Oostra, A. B. (1983). Effect of oxygen-tension on chromosomal-aberrations in Fanconi anaemia. *Human Genetics* **65**, 99-101.

Joenje, H. and Patel, K. J. (2001). The emerging genetic and molecular basis of Fanconi anaemia. *Nature Reviews Genetics* **2**, 446-457.

Johnson, R. D., Liu, N. and Jasin, M. (1999). Mammalian XRCC2 promotes the repair of DNA double-strand breaks by homologous recombination. *Nature* **401**, 397-399.

Jones, N. J., Ellard, S., Waters, R. and Parry, E. M. (1993). Cellular and chromosomal hypersensitivity to DNA cross-linking agents and topoisomerase inhibitors in the radiosensitive Chinese-hamster IRS mutants - Phenotypic similarities to ataxia-telangiectasia and Fanconis anaemia cells. *Carcinogenesis* **14**, 2487-2494.

Joo, W., Xu, G., Persky, N. S., Smogorzewska, A., Rudge, D. G., Buzovetsky, O., Elledge, S. J. and Pavletich, N. P. (2011). Structure of the FANCI-FANCD2 Complex: Insights into the Fanconi Anaemia DNA Repair Pathway. *Science* **333**, 312-316.

Karran, P. (2000). DNA double strand break repair in mammalian cells. *Current Opinion in Genetics and Development* **10**, 144-150.

Keightley, P. D., Davies, E. K., Peters, A. D. and Shaw, R. G. (2000). Properties of ethylmethane sulfonate-induced mutations affecting life-history traits in Caenorhabditis elegans and inferences about bivariate distributions of mutation effects. *Genetics* **156**, 143-154.

Kennedy, R. D. and D'Andrea, A. D. (2005). The Fanconi Anaemia/BRCA pathway: new faces in the crowd. *Genes and Development* **19**, 2925-2940.

Kim, J. M., Parmar, K., Huang, M., Weinstock, D. M., Ruit, C. A., Kutok, J. L. and D'Andrea, A. D. (2009). Inactivation of Murine Usp1 Results in Genomic Instability and a Fanconi Anaemia Phenotype. *Developmental Cell* **16**, 314-320.

Kim, Y., Lach, F. P., Desetty, R., Hanenberg, H., Auerbach, A. D. and Smogorzewska, A. (2011). Mutations of the SLX4 gene in Fanconi anaemia. *Nature Genetics* **43**, 142-U191.

Kirkland (1990). *Basic Mutagenicity tests (UKEMS recommended procedures) - (Book).*

Kitao, H. and Takata, M. (2011). Fanconi anaemia: a disorder defective in the DNA damage response. *International Journal of Hematology* **93**, 417-424.

Knipscheer, P., Raschle, M., Smogorzewska, A., Enoiu, M., Ho, T. V., Scharer, O. D., Elledge, S. J. and Walter, J. C. (2009). The Fanconi Anaemia Pathway Promotes Replication-Dependent DNA Interstrand Cross-Link Repair. *Science* **326**, 1698-1701.

Kramer, B. S., Fenselau, C. C. and Ludlum, D. B. (1974). Reaction of BCNU (1,3-bis (2-chloroethyl)-1-nitrosourea) with polycytidylic acid. Substitution of the cytosine ring. *Biochemical and Biophysical Research Communications* **56**, 783-788.

Kratz, K., Schopf, B., Kaden, S. and other authors (2010). Deficiency of FANCD2-Associated Nuclease KIAA1018/FAN1 Sensitizes Cells to Interstrand Crosslinking Agents. *Cell* **142**, 77-88.

Krishna, G., Kropko, M. L. and Theiss, J. C. (1989). Use of the cytokinesis-block method for the analysis of micronuclei in V79 Chinese-hamster lung-cells - results with mitomycin-C and cyclophosphamide. *Mutation Research* **222**, 63-69.

Kuhn, E. M. and Therman, E. (1982). Origin of symmetrical triradial chromosomes in human cells. *Chromosoma* **86**, 673-681.

Kumaresan, K. R., Sridharan, D. M., McMahon, L. W. and Lambert, M. W. (2007). Deficiency in incisions produced by XPF at the site of a DNA interstrand cross-link in Fanconi anaemia cells. *Biochemistry* **46**, 14359-14368.

Kupfer, G. M., Naf, D., Suliman, A., Pulsipher, M. and Dandrea, A. D. (1997). The Fanconi anaemia proteins, FAA and FAG, interact to form a nuclear complex. *Nature Genetics* **17**, 487-490.

Kupfer, G., Naf, D., Garcia-Higuera, I. and other authors (1999). A patient-derived mutant form of the Fanconi anaemia protein, FANCA, is defective in nuclear accumulation. *Experimental Hematology* **27**, 587-593.

Kutler, D. I. and Auerbach, A. D. (2004). Fanconi anaemia in Ashkenazi Jews. *Fam Cancer* **3**, 241-248.

Lamerdin, J. E., Yamada, N. A., George, J. W., Souza, B., Christian, A. T., Jones, N. J. and Thompson, L. H. (2004). Characterization of the hamster FancG/Xrcc9 gene and mutations in CHOUV40 and NM3. *Mutagenesis* **19**, 237-244.

Lange, S. S., Takata, K. and Wood, R. D. (2011). DNA polymerases and cancer. *Nature Reviews Cancer* **11**, 96-110.

Lasko, D., Cavenee, W. and Nordenskjold, M. (1991). Loss of constitutional heterozygosity in human cancer. *Annual Review of Genetics* **25**, 281-314.

Latt, S. A., Stetten, G., Juergens, L. A., Buchanan, G. R. and Gerald, P. S. (1975). Induction by alkylating agents of sister chromatid exchanges and chromatid breaks in Fanconi's anaemia. *Proceedings of the National Academy of Sciences of the United States of America* **72**, 4066-4070.

Lawley, P. D. and Brookes, P. (1968). Cytotoxicity of alkylating agents towards sensitive and resistant strains of Escherichia coli in relation to extent and mode of alkylation of cellular macromolecules and repair of alkylation lesions in deoxyribonucleic acids. *Biochemical Journal* **109**, 433-and 447.

Lawley, P. D. and Phillips, D. H. (1996). DNA adducts from chemotherapeutic agents. *Mutation Research-Fundamental and Molecular Mechanisms of Mutagenesis* **355**, 13-40.

Lee, S. E., Pulaski, C. R., He, D. M., Benjamin, D. M., Voss, M., Um, J. and Hendrickson, E. A. (1995). Isolation of mammalian cell mutants that are X-ray sensitive, impaired in DNA double-strand break repair and defective for V(D)J recombination. *Mutation Research-DNA Repair* **336**, 279-291.

Lehmann, A. R., Niimi, A., Ogi, T., Brown, S., Sabbioneda, S., Wing, J. F., Kannouche, P. L. and Green, C. M. (2007). Translesion synthesis: Y-farnily polymerases and the polymerase switch. *DNA Repair* **6**, 891-899.

Leveille, F., Blom, E., Medhurst, A. L. and other authors (2004). The Fanconi anaemia gene product FANCF is a flexible adaptor protein. *Journal of Biological Chemistry* **279**, 39421-39430.

Levinson, G. and Gutman, G. A. (1987). Slipped-strand mispairing: a major mechanism for DNA sequence evolution. *Molecular Biology and Evolution* **4**, 203-221.

Levitus, M., Waisfisz, Q., Godthelp, B. C. and other authors (2005). The DNA helicase BRIP1 is defective in Fanconi anaemia complementation group J. *Nature Genetics* **37**, 934-935.

Levitus, M., Joenje, H. and de Winter, J. P. (2006). The Fanconi anaemia pathway of genomic maintenance. *Cellular Oncology* **28**, 3-29.

Levran, O., Erlich, T., Magdalena, N., Gregory, J. J., Batish, S. D., Verlander, P. C. and Auerbach, A. D. (1997). Sequence variation in the Fanconi anaemia gene FAA. *Proceedings of the National Academy of Sciences of the United States of America* **94**, 13051-13056.

Levran, O., Diotti, R., Pujara, K., Batish, S. D., Hanenberg, H. and Auerbach, A. D. (2005a). Spectrum of sequence variations in the FANCA gene: An International Fanconi Anaemia Registry (IFAR) study. *Human Mutation* **25**, 142-149.

Levran, O., Attwooll, C., Henry, R. T. and other authors (2005b). The BRCA1-interacting helicase BRIP1 is deficient in Fanconi anaemia. *Nature Genetics* **37**, 931-933.

Lewis, L. K. and Resnick, M. A. (2000). Tying up loose ends: nonhomologous end-joining in Saccharomyces cerevisiae. *Mutation Research-Fundamental and Molecular Mechanisms of Mutagenesis* **451**, 71-89.

Liao, C., Hu, B., Arno, M. J. and Panaretou, B. (2007). Genomic screening in vivo reveals the role played by vacuolar H+ ATPase and cytosolic acidification in sensitivity to DNA-damaging agents such as cisplatin. *Molecular Pharmacology* **71**, 416-425.

Lindh, A. R., Rafii, S., Schultz, N., Cox, A. and Helleday, T. (2006). Mitotic defects in XRCC3 variants T241M and D213N and their relation to cancer susceptibility. *Human Molecular Genetics* **15**, 1217-1224.

Lingle, W. L., Barrett, S. L., Negron, V. C., D'Assoro, A. B., Boeneman, K., Liu, W. G., Whitehead, C. M., Reynolds, C. and Salisbury, J. L. (2002). Centrosome amplification drives chromosomal instability in breast tumor development. *Proceedings of the National Academy of Sciences of the United States of America* **99**, 1978-1983.

Litman, R., Peng, M., Jin, Z., Zhang, F., Zhang, J. R., Powell, S., Andreassen, P. R. and Cantor, S. B. (2005). BACH1 is critical for homologous recombination and appears to be the Fanconi anaemia gene product FANCJ. *Cancer Cell* **8**, 255-265.

Liu, N., Lamerdin, J. E., Tucker, J. D., Zhou, Z. Q., Walter, C. A., Albala, J. S., Busch, D. B. and Thompson, L. H. (1997). The human XRCC9 gene corrects chromosomal instability and mutagen sensitivities in CHO UV40 cells. *Proceedings of the National Academy of Sciences of the United States of America* **94**, 9232-9237.

Liu, N., Lamerdin, J. E., Tebbs, R. S. and other authors (1998). XRCC2 and XRCC3, new human Rad51-family members, promote chromosome stability and protect against DNA cross-links and other damages. *Molecular Cell* **1**, 783-793.

Liu, T., Ghosal, G., Yuan, J. S., Chen, J. J. and Huang, J. (2010). FAN1 Acts with FANCI-FANCD2 to Promote DNA Interstrand Cross-Link Repair. *Science* **329**, 693-696.

Long, E. C. and Barton, J. K. (1990). On Demonstrating DNA Intercalation. *Accounts of Chemical Research* **23**, 271-273.

Long, D. T., Raschle, M., Joukov, V. and Walter, J. C. (2011). Mechanism of RAD51-Dependent DNA Interstrand Cross-Link Repair. *Science* **333**, 84-87.

LoTenFoe, J. R., Rooimans, M. A., BosnoyanCollins, L. and other authors (1996). Expression cloning of a cDNA for the major Fanconi anaemia gene, FAA. *Nature Genetics* **14**, 320-323.

Lovett, S. T. (2004). Encoded errors: mutations and rearrangements mediated by misalignment at repetitive DNA sequences. *Molecular Microbiology* **52**, 1243-1253.

Lynch, A. M. and Parry, J. M. (1993). The cytochalasin-b micronucleus kinetochore assay invitro - studies with 10 suspected aneugens. *Mutation Research* **287**, 71-86.

Ma, Y. M., Pannicke, U., Schwarz, K. and Lieber, M. R. (2002). Hairpin opening and overhang processing by an Artemis/DNA-dependent protein kinase complex in nonhomologous end joining and V(D)J recombination. *Cell* **108**, 781-794.

Machida, Y. J., Machida, Y., Chen, Y. F., Gurtan, A. M., Kupfer, G. M., D'Andrea, A. D. and Dutta, A. (2006). UBE2T is the E2 in the Fanconi anaemia pathway and undergoes negative autoregulation. *Molecular Cell* **23**, 589-596.

MacKay, C., Declais, A. C., Lundin, C. and other authors (2010). Identification of KIAA1018/FAN1, a DNA Repair Nuclease Recruited to DNA Damage by Monoubiquitinated FANCD2. *Cell* **142**, 65-76.

MacPhail, S. H., Banath, J. P., Yu, T. Y., Chu, E. H. M., Lambur, H. and Olive, P. L. (2003). Expression of phosphorylated histone H2AX in cultured cell lines following exposure to X-rays. *International Journal of Radiation Biology* **79**, 351-358.

Magdalena, N., Pilonetto, D. V., Bitencourt, M. A., Pereira, N. F., Ribeiro, R. C., Jeng, M. and Pasquini, R. (2005). Frequency of Fanconi anaemia in Brazil and efficacy of screening for the FANCA 3788-3790del mutation. *Brazilian Journal of Medical and Biological Research* **38**, 669-673.

Malinge, J. M., Giraud-Panis, M. J. and Leng, M. (1999). Interstrand cross-links of cisplatin induce striking distortions in DNA. *Journal of Inorganic Biochemistry* **77**, 23-29.

Maluf, S. W. and Erdtmann, B. (2001). Genomic instability in Down syndrome and Fanconi anaemia assessed by micronucleus analysis and single-cell gel electrophoresis. *Cancer Genetics and Cytogenetics* **124**, 71-75.

Manderfeld, M. M., Schafer, H. W., Davidson, P. M. and Zottola, E. A. (1997). Isolation and identification of antimicrobial furocoumarins from parsley. *Journal of Food Protection* **60**, 72-77.

Marek, L. R. and Bale, A. E. (2006). Drosophila homologs of FANCD2 and FANCL function in DNA repair. *DNA Repair* **5**, 1317-1326.

Marnett, L. J. and Plastaras, J. P. (2001). Endogenous DNA damage and mutation. *Trends in Genetics* **17**, 214-221.

Marte, B. (2002). A FANCy double life. *Nature Cell Biology* **4**, E151-E151.

Marx, M. P., Smith, S., Heyns, A. D. and Vantonder, I. Z. (1983). Fanconis anaemia: a cytogenetic study on lymphocyte and bone marrow cultures utilizing 1, 2:3, 4-diepoxybutane. *Cancer Genetics and Cytogenetics* **9**, 51-59.

Maser, R. S. and DePinho, R. A. (2003). Take care of your chromosomes lest cancer takes care of you. *Cancer Cell* **3**, 4-6.

Matsushita, N., Kitao, H., Ishiai, M. and other authors (2005). A FancD2-monoubiquitin fusion reveals hidden functions of Fanconi anaemia core complex in DNA repair. *Molecular Cell* **19**, 841-847.

McDonald, J. P., Rapic-Otrin, V., Epstein, J. A., Broughton, B. C., Wang, X. Y., Lehmann, A. R., Wolgemuth, D. J. and Woodgate, R. (1999). Novel human and mouse homologs of Saccharomyces cerevisiae DNA polymerase eta. *Genomics* **60**, 20-30.

McGowan, C. H. and Russell, P. (2004). The DNA damage response: sensing and signaling. *Current Opinion in Cell Biology* **16**, 629-633.

McMahon, L. W., Sangerman, J., Goodman, S. R., Kumaresan, K. and Lambert, M. W. (2001). Human alpha spectrin II and the FANCA, FANCC, and FANCG proteins bind to DNA containing psoralen interstrand cross-links. *Biochemistry* **40**, 7025-7034.

McVey, M. (2010). Strategies for DNA Interstrand Crosslink Repair: Insights From Worms, Flies, Frogs, and Slime Molds. *Environmental and Molecular Mutagenesis* **51**, 646-658.

Mechilli, M., Schinoppi, A., Kobos, K., Natarajan, A. T. and Palitti, F. (2008). DNA repair deficiency and acetaldehyde-induced chromosomal alterations in CHO cells. *Mutagenesis* **23**, 51-56.

Medhurst, A. L., Huber, P. A. J., Waisfisz, Q., de Winter, J. P. and Mathew, C. G. (2001). Direct interactions of the five known Fanconi anaemia proteins suggest a common functional pathway. *Human Molecular Genetics* **10**, 423-429.

Meetei, A. R., de Winter, J. P., Medhurst, A. L. and other authors (2003). A novel ubiquitin ligase is deficient in Fanconi anaemia. *Nature Genetics* **35**, 165-170.

Meetei, A. R., Levitus, M., Xue, Y. T. and other authors (2004a). X-linked inheritance of Fanconi anaemia complementation group B. *Nature Genetics* **36**, 1219-1224.

Meetei, A. R., Yan, Z. J. and Wang, W. (2004b). FANCL replaces BRCA1 as the likely ubiquitin ligase responsible for FANCD2 monoubiquitination. *Cell Cycle* **3**, 179-181.
Meetei, A. R., Medhurst, A. L., Ling, C. and other authors (2005). A human ortholog of archaeal DNA repair protein Hef is defective in Fanconi anaemia complementation group M. *Nature Genetics* **37**, 958-963.

Meyn, R. E., Murray, D., Vanankeren, S. C., Bernard, G. S., Mellard, D. N. and Hobbs, M. L. (1991). Isolation and characterization of nitrogen mustard-sensitive mutants of chinese hamster ovary cells *Mutation Research* **254**, 161-165.

Mi, J., Qiao, F., Wilson, J. B. and other authors (2004). FANCG is phosphorylated at serines 383 and 387 during mitosis. *Molecular and Cellular Biology* **24**, 8576-8585.

Mohseni-Meybodi, A., Mozdarani, H. and Vosough, P. (2007). Cytogenetic sensitivity of G0 lymphocytes of Fanconi anaemia patients and obligate carriers to mitomycin C and ionizing radiation. *Cytogenetic and Genome Research* **119**, 191-195.

Moldovan, G.-L. and D'Andrea, A. D. (2009). How the Fanconi Anaemia Pathway Guards the Genome. In *Annual Review of Genetics*, pp. 223-249.

Moldovan, G. L., Madhavan, M. V., Mirchandani, K. D., McCaffrey, R. M., Vinciguerra, P. and D'Andrea, A. D. (2010). DNA Polymerase POLN Participates in Cross-Link Repair and Homologous Recombination. *Molecular and Cellular Biology* **30**, 1088-1096.

Morgan, N. V., Tipping, A. J., Joenje, H. and Mathew, C. G. (1999). High frequency of large intragenic deletions in the Fanconi anaemia group A gene. *American Journal of Human Genetics* **65**, 1330-1341.

Moynahan, M. E., Chiu, J. W., Koller, B. H. and Jasin, M. (1999). Brca1 controls homology-directed DNA repair. *Molecular Cell* **4**, 511-518.

Moynahan, M. E., Cui, T. Y. and Jasin, M. (2001a). Homology-directed DNA repair, mitomycin-C resistance, and chromosome stability is restored with correction of a Brca1 mutation. *Cancer Research* **61**, 4842-4850.

Moynahan, M. E., Pierce, A. J. and Jasin, M. (2001b). BRCA2 is required for homology-directed repair of chromosomal breaks. *Molecular Cell* **7**, 263-272.

Munoz, I. M., Hain, K., Declais, A. C. and other authors (2009). Coordination of Structure-Specific Nucleases by Human SLX4/BTBD12 Is Required for DNA Repair. *Molecular Cell* **35**, 116-127.

Naf, D., Kupfer, G. M., Suliman, A., Lambert, K. and D'Andrea, A. D. (1998). Functional activity of the Fanconi anaemia protein FAA requires FAC binding and nuclear localization. *Molecular and Cellular Biology* **18**, 5952-5960.

Naim, V. and Rosselli, F. (2009). The FANC pathway and BLM collaborate during mitosis to prevent micro-nucleation and chromosome abnormalities. *Nature Cell Biology* **11**, 761-U127.
Nakanishi, K., Taniguchi, T., Ranganathan, V. and other authors (2002). Interaction of FANCD2 and NBS1 in the DNA damage response. *Nature Cell Biology* **4**, 913-920.

Nakanishi, K., Yang, Y. G., Pierce, A. J., Taniguchi, T., Digweed, M., D'Andrea, A. D., Wang, Z. Q. and Jasin, M. (2005). Human fanconi anaemia monoubiquitination pathway promotes homologous DNA repair. *Proceedings of the National Academy of Sciences of the United States of America* **102**, 1110-1115.

Natarajan, A. T., Berni, A., Marimuthu, K. M. and Palitti, F. (2008). The type and yield of ionising radiation induced chromosomal aberrations depend on the efficiency of different DSB repair pathways in mammalian cells. *Mutation Research-Fundamental and Molecular Mechanisms of Mutagenesis* **642**, 80-85.

Nelson, J. R., Lawrence, C. W. and Hinkle, D. C. (1996). Thymine-thymine dimer bypass by yeast DNA polymerase zeta. *Science* **272**, 1646-1649.

Niedernhofer, L. J., Lalai, A. S. and Hoeijmakers, J. H. J. (2005). Fanconi anaemia (cross)linked to DNA repair. *Cell* **123**, 1191-1198.

Niedzwiedz, W., Mosedale, G., Johnson, M., Ong, C. Y., Pace, P. and Patel, K. J. (2004). The Fanconi anaemia gene FANCC promotes homologous recombination and error-prone DNA repair. *Molecular Cell* **15**, 607-620.

Nussenzweig, A., Chen, C. H., Soares, V. D., Sanchez, M., Sokol, K., Nussenzweig, M. C. and Li, G. C. (1996). Requirement for Ku80 in growth and immunoglobulin V(D)J recombination. *Nature* **382**, 551-555.

Obe, G., Pfeiffer, P., Savage, J. R. K. and other authors (2002). Chromosomal aberrations: formation, identification and distribution. *Mutation Research-Fundamental and Molecular Mechanisms of Mutagenesis* **504**, 17-36.

O'Driscoll, M. and Jeggo, P. A. (2006). The role of double-strand break repair - insights from human genetics. *Nature Reviews Genetics* **7**, 45-54.

Oestergaard, V. H., Langevin, F., Kuiken, H. J. and other authors (2007). Deubiquitination of FANCD2 is required for DNA crosslink repair. *Molecular Cell* **28**, 798-809.

Ogino, H., Fujii, M., Satou, W., Suzuki, T., Michishita, E. and Ayusawa, D. (2002). Binding of 5-bromouracil-containing S/MAR DNA to the nuclear matrix. *DNA Research* **9**, 25-29.

Ohmori, H., Friedberg, E. C., Fuchs, R. P. P. and other authors (2001). The Y-family of DNA polymerases. *Molecular Cell* **8**, 7-8.

Ohshima, S. (2001). Induction of aneuploidy by nickel sulfate in V79 Chinese hamster cells. *Mutation Research-Genetic Toxicology and Environmental Mutagenesis* **492**, 39-50.

Otsuki, T., Kajigaya, S., Ozawa, E. and Liu, J. M. (1999). SNX5, a new member of the sorting nexin family, binds to the Fanconi anaemia complementation group A protein. *Biochemical and Biophysical Research Communications* **265**, 630-635.

Otsuki, T., Young, D. B., Sasaki, D. T. and other authors (2002). Fanconi anaemia protein complex is a novel target of the IKK signalsome. *Journal of Cellular Biochemistry* **86**, 613-623.

Overkamp, W. J. I., Rooimans, M. A., Neuteboom, I., Telleman, P., Arwert, F. and Zdzienicka, M. Z. (1993). Genetic diversity of mitomycin C-hypersensitive Chinese hamster cell mutants: a new complementation group with chromosomal instability. *Somatic Cell and Molecular Genetics* **19**, 431-437.

Pace, P., Johnson, M., Tan, W. M. and other authors (2002). FANCE: the link between Fanconi anaemia complex assembly and activity. *Embo Journal* **21**, 3414-3423.

Pace, P., Mosedale, G., Hodskinson, M. R., Rosado, I. V., Sivasubramaniam, M. and Patel, K. J. (2010). Ku70 Corrupts DNA Repair in the Absence of the Fanconi Anaemia Pathway. *Science* **329**, 219-223.

Pages, V. and Fuchs, R. P. P. (2002). How DNA lesions are turned into mutations within cells? *Oncogene* **21**, 8957-8966.

Palom, Y., Kumar, G. S., Tang, L. Q., Paz, M. M., Musser, S. M., Rockwell, S. and Tomasz, M. (2002). Relative toxicities of DNA cross-links and monoadducts: New insights from studies of decarbamoyl mitomycin C and mitomycin C. *Chemical Research in Toxicology* **15**, 1398-1406.

Pang, Q. and Andreassen, P. R. (2009). Fanconi anaemia proteins and endogenous stresses. *Mutation Research-Fundamental and Molecular Mechanisms of Mutagenesis* **668**, 42-53.

Park, S., Hodge, J., Anderson, C. and Tretyakova, N. (2004). Guanine-adenine DNA cross-linking by 1,2,3,4-diepoxybutane: Potential basis for biological activity. *Chemical Research in Toxicology* **17**, 1638-1651.

Passarge E. (1995). *Color atlas of genetics*, 2nd edn.

Patel, K. J. and Joeje, H. (2007). Fanconi anaemia and DNA replication repair. *DNA Repair* **6**, 885-890.

Pathak, S., Multani, A. S., Furlong, C. L. and Sohn, S. H. (2002). Telomere dynamics, aneuploidy, stem cells, and cancer (Review). *International Journal of Oncology* **20**, 637-641.

Paz, M. M., Ladwa, S., Champeil, E. and other authors (2008). Mapping DNA Adducts of Mitomycin C and Decarbamoyl Mitomycin C in Cell Lines Using Liquid Chromatography/Electrospray Tandem Mass Spectrometry. *Chemical Research in Toxicology* **21**, 2370-2378.

Peng, M., Litman, R., Xie, J., Sharma, S., Brosh, R. M., Jr. and Cantor, S. B. (2007). The FANCJ/MutL alpha interaction is required for correction of the cross-link response in FA-J cells. *Embo Journal* **26**, 3238-3249.

Pichierri, P. and Rosselli, F. (2004). The DNA crosslink-induced S-phase checkpoint depends on ATR-CHK1 and ATR-NBS1-FANCD2 pathways. *Embo Journal* **23**, 1178-1187.

Pierce, B. (2007). Genetics: A Conceptual Approach. **(BOOK).**

Pommier, Y., Leteurtre, F., Fesen, M. R., Fujimori, A., Bertrand, R., Solary, E., Kohlhagen, G. and Kohn, K. W. (1994). Cellular determinants of sensitivity and resistance to DNA topoisomerase inhibitors. *Cancer Investigation* **12**, 530-542.

Porfirio, B., Smeets, D., Beckers, L., Caporossi, D., Tedeschi, B., Vernole, P., Joenje, H., Nicoletti, B. and Dallapiccola, B. (1991). Fragile sites and chromosome instability: the distribution of breaks induced by cis-diamine-dichloro-platinum (II) in Fanconi anaemia lymphocyte cultures. *Human Genetics* **86**, 256-260.

Povirk, L. F., Hogan, M., Dattagupta, N. and Buechner, M. (1981). Copper(II).bleomycin, iron(III).bleomycin, and copper(II).phleomycin: comparative study of deoxyribonucleic acid binding. *Biochemistry* **20**, 665-670.

Povirk, L. F. and Shuker, D. E. (1994). DNA damage and mutagenesis induced by nitrogen mustards. *Mutation Research-Reviews in Genetic Toxicology* **318**, 205-226.

Prakash, A. S., Beall, H., Ross, D. and Gibson, N. W. (1993). Sequence-selective alkylation and cross-linking induced by mitomycin C upon activation by DT-diaphorase. *Biochemistry* **32**, 5518-5525.

Pronk, J. C., Gibson, R. A., Savoia, A. and other authors (1995). Localization of the Fanconi anaemia complementation group A gene to chromosome 16q24.3. *Nature Genetics* **11**, 338-340.

Pulsipher, M., Kupfer, G. M., Naf, D. and other authors (1998). Subtyping analysis of Fanconi anaemia by immunoblotting and retroviral gene transfer. *Molecular Medicine* **4**, 468-479.

Qiao, F. Y., Moss, A. and Kupfer, G. M. (2001). Fanconi anaemia proteins localize to chromatin and the nuclear matrix in a DNA damage- and cell cycle-regulated manner. *Journal of Biological Chemistry* **276**, 23391-23396.

Qiao, F. Y., Mi, J., Wilson, J. B., Zhi, G., Bucheimer, N. R., Jones, N. J. and Kupfer, G. M. (2004). Phosphorylation of Fanconi anaemia (FA) complementation group G protein, FANCG, at serine 7 is important for function of the FA pathway. *Journal of Biological Chemistry* **279**, 46035-46045.

Rahden-Staron, I., Szumilo, M., Grosicka, E., Kraakman-van der Zwet, M. and Zdzienicka, M. Z. (2003). Defective Brca2 influences topoisomerase I activity in mammalian cells. *Acta Biochimica Polonica* **50**, 139-144.

Raschle, M., Knipsheer, P., Enoiu, M., Angelov, T., Sun, J. C., Griffith, J. D., Ellenberger, T. E., Scharer, O. D. and Walter, J. C. (2008). Mechanism of replication-coupled DNA interstrand crosslink repair. *Cell* **134**, 969-980.

Ratnapalan, S., Bentur, Y. and Koren, G. (2008). REVIEW "Doctor, will that x-ray harm my unborn child?". *Canadian Medical Association Journal* **179**, 1293-1296.

Recio, L., Steen, A. M., Pluta, L. J., Meyer, K. G. and Saranko, C. J. (2001). Mutational spectrum of 1,3-butadiene and metabolites 1,2-epoxybutene and 1,2,3,4-diepoxybutane to assess mutagenic mechanisms. *Chemico-Biological Interactions* **135**, 325-341.

Reid, S., Schindler, D., Hanenberg, H. and other authors (2007). Biallelic mutations in PALB2 cause Fanconi anaemia subtype FA-N and predispose to childhood cancer. *Nature Genetics* **39**, 162-164.

Renglin Lindh, A., Schultz, N., Saleh-Gohari, N. and Helleday, T. (2007). RAD51C (RAD51L2) is involved in maintaining centrosome number in mitosis. *Cytogenet Genome Res* **116**, 38-45.

Reuter, T. Y., Medhurst, A. L., Waisfisz, Q. and other authors (2003). Yeast two-hybrid screens imply involvement of Fanconi anaemia proteins in transcription regulation, cell signaling, oxidative metabolism, and cellular transport. *Experimental Cell Research* **289**, 211-221.

Richards, A. D. and Rodger, A. (2007). Synthetic metallomolecules as agents for the control of DNA structure. *Chemical Society Reviews* **36**, 471-483.

Ronen, A., Rahat, A. and Halevy, C. (1976). Marker effects on reversion of T4rII mutants. *Genetics* **84**, 423-436.

Rosendorff, J. and Bernstein, R. (1988). Fanconis anaemia chromosome breakage studies in homozygotes and heterozygotes. *Cancer Genetics and Cytogenetics* **33**, 175-183.

Rothkamm, K., Kruger, I., Thompson, L. H. and Lobrich, M. (2003). Pathways of DNA double-strand break repair during the mammalian cell cycle. *Molecular and Cellular Biology* **23**, 5706-5715.

Rothstein, R., Michel, B. and Gangloff, S. (2000). Replication fork pausing and recombination or "gimme a break". *Genes and Development* **14**, 1-10.

Saito, T. T., Youds, J. L., Boulton, S. J. and Colaiacovo, M. P. (2009). Caenorhabditis elegans HIM-18/SLX-4 Interacts with SLX-1 and XPF-1 and Maintains Genomic Integrity in the Germline by Processing Recombination Intermediates. *Plos Genetics* **5**.

Saleh-Gohari, N. and Helleday, T. (2004). Conservative homologous recombination preferentially repairs DNA double-strand breaks in the S phase of the cell cycle in human cells. *Nucleic Acids Research* **32**, 3683-3688.

Saleh-Gohari, N., Bryant, H. E., Schultz, N., Parker, K. A., Cassel, T. N. and Helleday, T. (2005). Spontaneous homologous recombination is induced by collapsed replication forks that are caused by endogenous DNA single-strand breaks. *Molecular and Cellular Biology* **25**, 7158-7169.

Sasaki, M. S. and Miyata, H. (1968). Biological Dosimetry in Atomic Bomb Survivors. *Nature* **220**, 1189-and 1193

Sasaki, M. S. and Tonomura, A. (1973). High susceptibility of Fanconi anaemia to chromosome breakage by DNA cross-linking agents. *Cancer Research* **33**, 1829-1836.

Savage, J. R. K. (1976). Classification and relationships of induced chromosomal structural-changes. *Journal of Medical Genetics* **13**, 103-122.

Savage, J. R. K. and Simpson, P. J. (1994). FISH painting patterns resulting from complex exchanges. *Mutation Research* **312**, 51-60.

Savage, J. R. K. (2002). Reflections and meditations upon complex chromosomal exchanges. *Mutation Research-Reviews in Mutation Research* **512**, 93-109.

Savery, L. C., Grlickova-Duzevik, E., Wise, S. S., Thompson, W. D., Hinz, J. A., Thompson, L. H. and Wise, J. P., Sr. (2007). Role of the Fancg gene in protecting cells from particulate chromate-induced chromosome instability. *Mutation Research-Genetic Toxicology and Environmental Mutagenesis* **626**, 120-127.

Savino, M., Ianzano, L., Strippoli, P., Ramenghi, U., Arslanian, A., Bagnara, G. P., Joenje, H., Zelante, L. and Savoia, A. (1997). Mutations of the Fanconi anaemia group A gene (FAA) in Italian patients. *American Journal of Human Genetics* **61**, 1246-1253.

Savino, M., Borriello, A., D'Apolito, M. and other authors (2003). Spectrum of FANCA mutations in Italian Fanconi anaemia patients: identification of six novel alleles and phenotypic characterization of the S858R variant. *Human Mutation* **22**, 338-339.

Scharer, O. D. (2005). DNA interstrand crosslinks: Natural and drug-induced DNA adducts that induce unique cellular responses. *Chembiochem* **6**, 27-32.

Schroeder, T. M., Tilgen, D., Kruger, J. and Vogel, F. (1976). Formal genetics of Fanconi's anaemia. *Human Genetics* **32**, 257-288.

Scott, B. R., Pathak, M. A. and Mohn, G. R. (1976). Molecular and genetic basis of furocoumarin reactions. *Mutation Research* **39**, 29-74.

Sharan, S. K. and Kuznetsov, S. G. (2007). Resolving RAD51C function in late stages of homologous recombination. *Cell Div* **2**, 15.

Shiloh, Y. (2001). ATM and ATR: networking cellular responses to DNA damage. *Current Opinion in Genetics and Development* **11**, 71-77.

Shimamura, A. and Alter, B. P. (2010). Pathophysiology and management of inherited bone marrow failure syndromes. *Blood Reviews* **24**, 101-122.

Sidorkina, O., Saparbaev, M. and Laval, J. (1997). Effects of nitrous acid treatment on the survival and mutagenesis of Escherichia coli cells lacking base excision repair (hypoxanthine-DNA glycosylase-ALK A protein) and/or nucleotide excision repair. *Mutagenesis* **12**, 23-27.

Sigma
http://www.sigmaaldrich.com/catalog/ProductDetail.do?N4=M4287|SIGMAandN5=SEARCH_CONCAT_PNO|BRAND_KEYandF=SPEC.

Sijbers, A. M., deLaat, W. L., Ariza, R. R. and other authors (1996). Xeroderma pigmentosum group F caused by a defect in a structure-specific DNA repair endonuclease. *Cell* **86**, 811-822.

Simpson, L. J. and Sale, J. E. (2003). Rev1 is essential for DNA damage tolerance and non-templated immunoglobulin gene mutation in a vertebrate cell line. *Embo Journal* **22**, 1654-1664.

Sims, A. E., Spiteri, E., Sims, R. J. and other authors (2007). FANCI is a second monoubiquitinated member of the Fanconi anaemia pathway. *Nature Structural and Molecular Biology* **14**, 564-567.

Singh, T. R., Bakker, S. T., Agarwal, S. and other authors (2009). Impaired FANCD2 monoubiquitination and hypersensitivity to camptothecin uniquely characterize Fanconi anaemia complementation group M. *Blood* **114**, 174-180.

Sleigh, M. J. (1976). Mechanism of DNA breakage by phleomycin in vitro. *Nucleic Acids Research* **3**, 891-901.

Smogorzewska, A., Matsuoka, S., Vinciguerra, P. and other authors (2007). Identification of the FANCI protein, a monoubiquitinated FANCD2 paralog required for DNA repair. *Cell* **129**, 289-301.

Smogorzewska, A., Desetty, R., Saito, T. T. and other authors (2010). A Genetic Screen Identifies FAN1, a Fanconi Anaemia-Associated Nuclease Necessary for DNA Interstrand Crosslink Repair. *Molecular Cell* **39**, 36-47.

Somyajit, K., Subramanya, S. and Nagaraju, G. (2010). RAD51C: a novel cancer susceptibility gene is linked to Fanconi anaemia and breast cancer. *Carcinogenesis* **31**, 2031-2038.

Sonoda, E., Takata, M., Yamashita, Y. M., Morrison, C. and Takeda, S. (2001). Homologous DNA recombination in vertebrate cells. *Proceedings of the National Academy of Sciences of the United States of America* **98**, 8388-8394.

Soulier, J., Leblanc, T., Larghero, J. and other authors (2005). Detection of somatic mosaicism and classification of Fanconi anaemia patients by analysis of the FA/BRCA pathway. *Blood* **105**, 1329-1336.

Sra, K. K., Babb-Tarbox, M., Aboutalebi, S., Rady, P., Shipley, G. L., Dao, D. D. and Tyring, S. K. (2005). Molecular diagnosis of cutaneous diseases. *Archives of Dermatology* **141**, 225-241.

Sridharan, D., Brown, M., Lambert, W. C., McMahon, L. W. and Lambert, M. W. (2003). Nonerythroid all spectrin is required for recruitment of FANCA and XPF to nuclear foci induced by DNA interstrand cross-links. *Journal of Cell Science* **116**, 823-835.

Stackpole, M. M., Wise, S. S., Goodale, B. C. and other authors (2007). Homologous recombination repair protects against particulate chromate-induced chromosome instability in Chinese hamster cells. *Mutation Research-Fundamental and Molecular Mechanisms of Mutagenesis* **625**, 145-154.

Stoepker, C., Hain, K., Schuster, B. and other authors (2011). SLX4, a coordinator of structure-specific endonucleases, is mutated in a new Fanconi anaemia subtype. *Nature Genetics* **43**, 138-U185.

Stone, S., Sobeck, A., van Kogelenberg, M., de Graaf, B., Joenje, H., Christian, J. and Hoatlin, M. E. (2007). Identification, developmental expression and regulation of the Xenopus ortholog of human FANCG/XRCC9. *Genes to Cells* **12**, 841-851.

Strathdee, C. A., Gavish, H., Shannon, W. R. and Buchwald, M. (1992). Cloning of cDNAs for Fanconi's anaemia by functional complementation. *Nature* **356**, 763-767.

Strauss, B. S. (1995). DNA Repair and Mutagenesis - Friedberg,EC, Walker,GC, Siede,W *Science* **270**, 1511-and.

Streisinger, G. and Owen, J. E. (1985). Mechanisms of spontaneous and induced frameshift mutation in bacteriophage T4. *Genetics* **109**, 633-659.

Sugiura, Y. (1979). Production of hydroxyl radical from copper(I) complex systems of bleomycin and tallysomycin: Comparison with copper(II) and iron(II) systems. *Biochemical and Biophysical Research Communications* **90**, 375-383.

Suzuki, T., Nakagawa, Y., Tayama, S., Yaguchi, K., Suzuki, S. and Suga, T. (2000). Micronucleus test of herbicide terbutol and its metabolites in cultured Chinese hamster lung cells and male CD-1 mice. *Bulletin of Environmental Contamination and Toxicology* **64**, 66-73.

Svendsen, J. M., Smogorzewska, A., Sowa, M. E., O'Connell, B. C., Gygi, S. P., Elledge, S. J. and Harper, J. W. (2009). Mammalian BTBD12/SLX4 Assembles A Holliday Junction Resolvase and Is Required for DNA Repair. *Cell* **138**, 63-77.

Swift, M. (1971). Fanconis anaemia in the genetics of neoplasia. *Nature* **230**, 370-and 373.

Tachibana, A., Kato, T., Ejima, Y., Yamada, T., Shimizu, T., Yang, L. C., Tsunematsu, Y. and Sasaki, M. S. (1999). The FANCA gene in Japanese Fanconi anaemia: Report of eight novel mutations and analysis of sequence variability. *Human Mutation* **13**, 237-244.

Takata, K., Shimizu, T., Iwai, S. and Wood, R. D. (2006). Human DNA polymerase N (POLN) is a low fidelity enzyme capable of error-free bypass of 5S-thymine glycol. *Journal of Biological Chemistry* **281**, 23445-23455.

Takata, M., Kitao, H. and Ishiai, M. (2007). Fanconi anaemia: genetic analysis of a human disease using chicken system. *Cytogenetic and Genome Research* **117**, 346-351.

Talwar, R., Choudhry, V. P. and Kucheria, K. (2004). Differentiation of Fanconi anaemia from idiopathic aplastic anaemia by induced chromosomal breakage study using mitomycin-C (MMC). *Indian Pediatr* **41**, 473-477.

Tamary, H., Bar-Yam, R., Shalmon, L. and other authors (2000). Fanconi anaemia group A (FANCA) mutations in Israeli non-Ashkenazi Jewish patients. *British Journal of Haematology* **111**, 338-343.

Taniguchi, T. and D'Andrea, A. D. (2002). The Fanconi anaemia protein, FANCE, promotes the nuclear accumulation of FANCC. *Blood* **100**, 2457-2462.

Taniguchi, T., Garcia-Higuera, I., Xu, B., Andreassen, P. R., Gregory, R. C., Kim, S. T., Lane, W. S., Kastan, M. B. and D'Andrea, A. D. (2002a). Convergence of the Fanconi anaemia and ataxia telangiectasia signaling pathways. *Cell* **109**, 459-472.

Taniguchi, T., Garcia-Higuera, I., Andreassen, P. R., Gregory, R. C., Grompe, M. and D'Andrea, A. D. (2002b). S-phase-specific interaction of the Fanconi anaemia protein, FANCD2, with BRCA1 and RAD51. *Blood* **100**, 2414-2420.

Taniguchi, T. and D'Andrea, A. D. (2006). Molecular pathogenesis of Fanconi anaemia: recent progress. *Blood* **107**, 4223-4233.

Taylor, A. M. R. (2001). Chromosome instability syndromes. *Best Practice and Research Clinical Haematology* **14**, 631-644.

Tebbs, R. S., Zhao, Y., Tucker, J. D., Scheerer, J. B., Siciliano, M. J., Hwang, M., Liu, N., Legerski, R. J. and Thompson, L. H. (1995). Correction of chromosomal instability and sensitivity to diverse mutagens by a cloned cDNA of the XRCC3 DNA repair gene. *Proceedings of the National Academy of Sciences of the United States of America* **92**, 6354-6358.

Tebbs, R. S., Hinz, J. M., Yamada, N. A., Wilson, J. B., Salazar, E. P., Thomas, C. B., Jones, I. M., Jones, N. J. and Thompson, L. H. (2005). New insights into the Fanconi anaemia pathway from an isogenic FancG hamster CHO mutant. *DNA Repair* **4**, 11-22.

Thacker, J. (2005). The RAD51 gene family, genetic instability and cancer. *Cancer Letters* **219**, 125-135.

Thomas, M. G., Cook, C. E., Miller, K. W. P., Waring, M. J. and Hagelberg, E. (1998). Molecular instability in the COII-tRNA(Lys) intergenic region of the human mitochondrial genome: multiple origins of the 9-bp deletion and heteroplasmy for expanded repeats. *Philosophical Transactions of the Royal Society of London Series B-Biological Sciences* **353**, 955-965.

Thomashevski, A., High, A. A., Drozd, M., Shabanowitz, J., Hunt, D. F., Grant, P. A. and Kupfer, G. M. (2004). The Fanconi anaemia core complex forms four complexes of different sizes in different subcellular compartments. *Journal of Biological Chemistry* **279**, 26201-26209.

Thompson, L. H., Fong, S. and Brookman, K. (1980). Validation of conditions for efficient detection of HPRT and APRT mutations in suspension-cultured Chinese hamster ovary cells. *Mutation Research* **74**, 21-36.

Thompson, L. H., Liu, N., Lamerdin, J. E., Tucker, J. D., Zhou, Z. Q., Walter, C. A. and Busch, D. (1997). Cloning and characterization of the human XRCC9 gene, which corrects chromosomal instability and mutagen sensitivity in CHO UV40. *Environmental and Molecular Mutagenesis* **29**, 50.

Thompson, L. H. (1998). Chinese hamster cells meet DNA repair: an entirely acceptable affair. *Bioessays* **20**, 589-597.

Thompson, L. H., Hinz, J. M., Yamada, N. A. and Jones, N. J. (2005). How Fanconi anaemia proteins promote the four Rs: Replication, recombination, repair, and recovery. *Environmental and Molecular Mutagenesis* **45**, 128-142.

Thompson, L. H. and Hinz, J. M. (2009). Cellular and molecular consequences of defective Fanconi anaemia proteins in replication-coupled DNA repair: Mechanistic insights. *Mutation Research-Fundamental and Molecular Mechanisms of Mutagenesis* **668**, 54-72.

Timmers, C., Taniguchi, T., Hejna, J. and other authors (2001). Positional cloning of a novel fanconi anaemia gene, FANCD2. *Molecular Cell* **7**, 241-248.

Tipping, A. J., Pearson, T., Morgan, N. V. and other authors (2001). Molecular and genealogical evidence for a founder effect in Fanconi anaemia families of the Afrikaner population of South Africa. *Proceedings of the National Academy of Sciences of the United States of America* **98**, 5734-5739.

Tischkowitz, M. D. and Hodgson, S. V. (2003). Fanconi anaemia. *Journal of Medical Genetics* **40**, 1-10.

Titus, T. A., Selvig, D. R., Qin, B. F., Wilson, C., Starks, A. M., Roe, B. A. and Postlethwait, J. H. (2006). The Fanconi anaemia gene network is conserved from zebrafish to human. *Gene* **371**, 211-223.

Titus, T. A., Yan, Y.-L., Wilson, C. and other authors (2009). The Fanconi anaemia/BRCA gene network in zebrafish: Embryonic expression and comparative genomics. *Mutation Research-Fundamental and Molecular Mechanisms of Mutagenesis* **668**, 117-132.

Tomasz, M. and Lipman, R. (1981). Reductive metabolism and alkylating activity of mitomycin C induced by rat liver microsomes. *Biochemistry* **20**, 5056-5061.

Tomasz, M., Chowdary, D., Lipman, R., Shimotakahara, S., Veiro, D., Walker, V. and Verdine, G. L. (1986). Reaction of DNA with chemically or enzymatically activated mitomycin C: isolation and structure of the major covalent adduct. *Proceedings of the National Academy of Sciences of the United States of America* **83**, 6702-6706.

Tomasz, M., Lipman, R., Chowdary, D., Pawlak, J., Verdine, G. L. and Nakanishi, K. (1987). Isolation and structure of a covalent cross-link adduct between mitomycin C and DNA. *Science* **235**, 1204-1208.

Tomasz, M. (1995). Mitomycin C: small, fast and deadly (but very selective). *Chemistry and Biology* **2**, 575-579.

Tomasz, M. and Palom, Y. (1997). The mitomycin bioreductive antitumor agents: Cross-linking and alkylation of DNA as the molecular basis of their activity. *Pharmacology and Therapeutics* **76**, 73-87.

Tomkins, D. J., Care, M., Carreau, M. and Buchwald, M. (1998). Development and characterization of immortalized fibroblastoid cell lines from an FA(C) mouse model. *Mutation Research-DNA Repair* **408**, 27-35.

Tong, W. P. and Ludlum, D. B. (1979). Mechanism of action of the nitrosoureas—III: Reaction of bis-chloroethyl nitrosourea and bis-fluoroethyl nitrosourea with adenosine. *Biochemical Pharmacology* **28**, 1175-1179.

Tonnies, H., Huber, S., Kuhl, J. S., Gerlach, A., Ebell, W. and Neitzel, H. (2003). Clonal chromosomal aberrations in bone marrow cells of Fanconi anaemia patients: gains of the chromosomal segment 3q26q29 as an adverse risk factor. *Blood* **101**, 3872-3874.

Tretyakova, N., Sangaiah, R., Yen, T. Y., Gold, A. and Swenberg, J. A. (1997a). Adenine adducts with diepoxybutane: Isolation and analysis in exposed calf thymus DNA. *Chemical Research in Toxicology* **10**, 1171-1179.

Tretyakova, N. Y., Sangaiah, R., Yen, T. Y. and Swenberg, J. A. (1997b). Synthesis, characterization, and in vitro quantitation of N-7-guanine adducts of diepoxybutane. *Chemical Research in Toxicology* **10**, 779-785.

Tsolakidis, A. and Kaxiras, E. (2005). A TDDFT study of the optical response of DNA bases, base pairs, and their tautomers in the gas phase. *Journal of Physical Chemistry A* **109**, 2373-2380.

van de Vrugt, H. J., Eaton, L., Newell, A. H., Al-Dhalimy, M., Liskay, R. M., Olson, S. B. and Grompe, M. (2009). Embryonic Lethality after Combined Inactivation of Fancd2 and Mlh1 in Mice. *Cancer Research* **69**, 9431-9438.

Van der Heijden, M. S., Brody, J. R., Gallmeier, E., Cunningham, S. C., Dezentje, D. A., Shen, D., Hruban, R. H. and Kern, S. E. (2004). Functional defects in the Fanconi anaemia pathway in pancreatic cancer cells. *American Journal of Pathology* **165**, 651-657.

van Gent, D. C., Hoeijmakers, J. H. J. and Kanaar, R. (2001). Chromosomal stability and the DNA double-stranded break connection. *Nature Reviews Genetics* **2**, 196-206.

van Gent, D. C. and van der Burg, M. (2007). Non-homologous end-joining, a sticky affair. *Oncogene* **26**, 7731-7740.

Van Limbergen, H., Poppe, B., Michaux, L. and other authors (2002). Identification of cytogenetic subclasses and recurring chromosomal aberrations in AML and MDS with complex karyotypes using M-FISH. *Genes Chromosomes and Cancer* **33**, 60-72.

Vaz, F., Hanenberg, H., Schuster, B. and other authors (2010). Mutation of the RAD51C gene in a Fanconi anaemia-like disorder. *Nature Genetics* **42**, 406-U463.

Verma R.S. , B. A. (1994). Human chromosomes principles and techniques.
Vidal, A., Abril, N. and Pueyo, C. (1995). DNA repair by Ogt alkyltransferase influences EMS mutational specificity. *Carcinogenesis* **16**, 817-821.

Volker, M., Mone, M. J., Karmakar, P. and other authors (2001). Sequential assembly of the nucleotide excision repair factors in vivo. *Molecular Cell* **8**, 213-224.

Waisfisz, Q., de Winter, J. P., Kruyt, F. A. E. and other authors (1999). A physical complex of the Fanconi anaemia proteins FANCG/XRCC9 and FANCA. *Proceedings of the National Academy of Sciences of the United States of America* **96**, 10320-10325.

Wang, X. Z., Andreassen, P. R. and D'Andrea, A. D. (2004). Functional interaction of monoubiquitinated FANCD2 and BRCA2/FANCD1 in chromatin. *Molecular and Cellular Biology* **24**, 5850-5862.

Wang, W. D. (2007a). Emergence of a DNA-damage response network consisting of Fanconi anaemia and BRCA proteins. *Nature Reviews Genetics* **8**, 735-748.

Wang, X. Z., Kennedy, R. D., Ray, K., Stuckert, P., Ellenberger, T. and D'Andrea, A. D. (2007b). Chk1-mediated phosphorylation of FANCE is required for the Fanconi anaemia/BRCA pathway. *Molecular and Cellular Biology* **27**, 3098-3108.

Wang, W. (2008). A major switch for the Fanconi anaemia DNA damage-response pathway. *Nature Structural and Molecular Biology* **15**, 1128-1130.

Wang, C. and Lambert, M. W. (2010). The Fanconi Anaemia Protein, FANCG, Binds to the ERCC1-XPF Endonuclease via Its Tetratricopeptide Repeats and the Central Domain of ERCC1. *Biochemistry* **49**, 5560-5569.

Waters, L. S., Minesinger, B. K., Wiltrout, M. E., D'Souza, S., Woodruff, R. V. and Walker, G. C. (2009). Eukaryotic Translesion Polymerases and Their Roles and Regulation in DNA Damage Tolerance. *Microbiology and Molecular Biology Reviews* **73**, 134-+.

Weksberg, R., Buchwald, M., Sargent, P., Thompson, M. W. and Siminovitch, L. (1979). Specific cellular defects in patients with Fanconi anaemia. *Journal of Cellular Physiology* **101**, 311-323.

Whitmore, S. E., Potten, C. S., Chadwick, C. A., Strickland, P. T. and Morison, W. L. (2001). Effect of photoreactivating fight on UV radiation-induced alterations in human skin. *Photodermatology Photoimmunology and Photomedicine* **17**, 213-217.

Whitney, M., Thayer, M., Reifsteck, C. and other authors (1995). Microcell mediated chromosome transfer maps the Fanconi anaemia group D gene to chromosome 3p. *Nature Genetics* **11**, 341-343.

Wiegant, W. W., Overmeer, R. M., Godthelp, B. C., van Buul, P. P. W. and Zdzienicka, M. Z. (2006). Chinese hamster cell mutant, V-C8, a model for analysis of Brca2 function. *Mutation Research-Fundamental and Molecular Mechanisms of Mutagenesis* **600**, 79-88.

Wijker, M., Morgan, N. V., Herterich, S. and other authors (1999). Heterogeneous spectrum of mutations in the Fanconi anaemia group A gene. *European Journal of Human Genetics* **7**, 52-59.

Williams, S. A., Wilson, J. B., Clark, A. P., Mitson-Salazar, A. N., Bale, A. E., Jones, N. J. and Kupfer, G. M. (2010). Functional and Physical Interaction Between the Mismatch Repair and the FA-BRCA Pathways. *Blood* **116**, 1379-1380.

Willingaletheune, J., Schweiger, M., Hirschkauffmann, M., Meek, A. E., Paulinlevasseur, M. and Traub, P. (1989). Ultrastructure of Fanconi anaemia fibroblasts. *Journal of Cell Science* **93**, 651-665.

Wilson, J. B., Johnson, M. A., Stuckert, A. P., Trueman, K. L., May, S., Bryant, P. E., Meyn, R. E., D'Andrea, A. D. and Jones, N. J. (2001). The Chinese hamster FANCG/XRCC9 mutant NM3 fails to express the monoubiquitinated form of the FANCD2 protein, is hypersensitive to a range of DNA damaging agents and exhibits a normal level of spontaneous sister chromatid exchange. *Carcinogenesis* **22**, 1939-1946.

Wilson, J. B., Yamamoto, K., Marriott, A. S. and other authors (2008). FANCG promotes formation of a newly identified protein complex containing BRCA2, FANCD2 and XRCC3. *Oncogene* **27**, 3641-3652.

Wilson, J. B., Blom, E., Cunningham, R., Xiao, Y., Kupfer, G. M. and Jones, N. J. (2010). Several tetratricopeptide repeat (TPR) motifs of FANCG are required for assembly of the BRCA2/D1-D2-G-X3 complex, FANCD2 monoubiquitylation and phleomycin resistance. *Mutation Research-Fundamental and Molecular Mechanisms of Mutagenesis* **689**, 12-20.

Wood, C. M., Timme, T. L., Hurt, M. M., Brinkley, B. R., Ledbetter, D. H. and Moses, R. E. (1987). Transformation of DNA repair-deficient human diploid fibroblasts with a simian virus 40 plasmid. *Experimental Cell Research* **169**, 543-553.

Wyman, C. and Kanaar, R. (2006). DNA double-strand break repair: All's well that ends well. *Annual Review of Genetics* **40**, 363-383.

Wyman, C., Warmerdam, D. O. and Kanaar, R. (2008). From DNA end chemistry to cell-cycle response: The importance of structure, even when it's broken. *Molecular Cell* **30**, 5-6.

Xia, B., Dorsman, J. C., Ameziane, N. and other authors (2007). Fanconi anaemia is associated with a defect in the BRCA2 partner PALB2. *Nature Genetics* **39**, 159-161.

Yajima, E. and Mizunoya, T. (1981). Kinetics of photoinactivation and photooxidation of Mitomycin C in the presence of riboflavin. *Journal of Biochemistry* **89**, 929-936.

Yamashita, T., Barber, D. L., Zhu, Y., Wu, N. and Dandrea, A. D. (1994). The Fanconi anaemia polypeptide FACC is localized to the cytoplasm. *Proceedings of the National Academy of Sciences of the United States of America* **91**, 6712-6716.

Yamashita, T., Kupfer, G. M., Naf, D., Suliman, A., Joenje, H., Asano, S. and D'Andrea, A. D. (1998). The Fanconi anaemia pathway requires FAA phosphorylation and FAA/FAC nuclear accumulation. *Proceedings of the National Academy of Sciences of the United States of America* **95**, 13085-13090.

Yang, Y. G., Herceg, Z., Nakanishi, K. and other authors (2005). The Fanconi anaemia group A protein modulates homologous repair of DNA double-strand breaks in mammalian cells. *Carcinogenesis* **26**, 1731-1740.

Youds, J. L., Barber, L. J. and Boulton, S. J. (2009). C. elegans: A model of Fanconi anaemia and ICL repair. *Mutation Research-Fundamental and Molecular Mechanisms of Mutagenesis* **668**, 103-116.

Zdzienicka, M. Z. (1996). Mammalian X ray sensitive mutants: A tool for the elucidation of the cellular response to ionizing radiation. *Cancer Surveys* **28**, 281-293.

Zhang, Y. B., Yuan, F. H., Wu, X. H. and Wang, Z. G. (2000). Preferential incorporation of G opposite template T by the low-fidelity human DNA polymerase iota. *Molecular and Cellular Biology* **20**, 7099-7108.

Zhang, N., Liu, X., Li, L. and Legerski, R. (2007). Double-strand breaks induce homologous recombinational repair of interstrand cross-links via cooperation of MSH2, ERCC1-XPF, REV3, and the Fanconi anaemia pathway. *DNA Repair* **6**, 1670-1678.

Zheng, H. Y., Wang, X., Warren, A. J., Legerski, R. J., Nairn, R. S., Hamilton, J. W. and Li, L. (2003). Nucleotide excision repair- and polymerase eta-mediated error-prone removal of mitomycin C interstrand cross-links. *Molecular and Cellular Biology* **23**, 754-761.

Zhi, G., Wilson, J. B., Chen, X. Y., Krause, D. S., Xiao, Y. X., Jones, N. J. and Kupfer, G. M. (2009). Fanconi anaemia Complementation Group FANCD2 Protein Serine 331 Phosphorylation Is Important for Fanconi anaemia Pathway Function and BRCA2 Interaction. *Cancer Research* **69**, 8775-8783.

Zietlow, L., Smith, L. A., Bessho, M. and Bessho, T. (2009). Evidence for the Involvement of Human DNA Polymerase N in the Repair of DNA Interstrand Cross-Links. *Biochemistry* **48**, 11817-11824.

Appendix

Appendix-1 **NORMAL METAPHASE SPREAD- NM3-WT**

Appendix-1: presents a CHO metaphase spread with minimal chromosomal overlapping which allow reliable scoring of chromosomal aberrations. It also presents good chromosome morphology and staining.

Appendix-2

(DICENTRICS) IN METAPHASE SPREAD

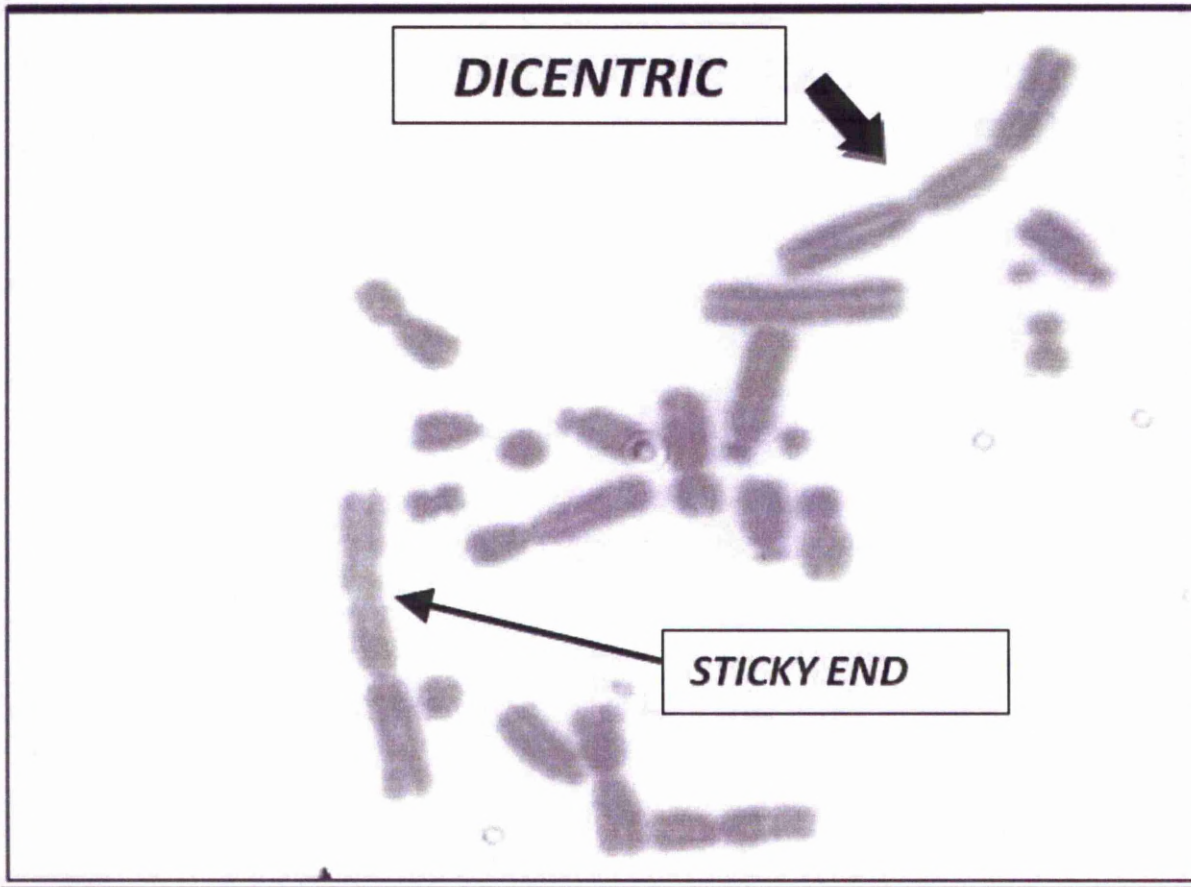

Appendix-2: showing the fusion of two chromosomes forming a dicentric which is a chromosome based aberration.

Appendix-3

RINGS IN METAPHASE SPREAD

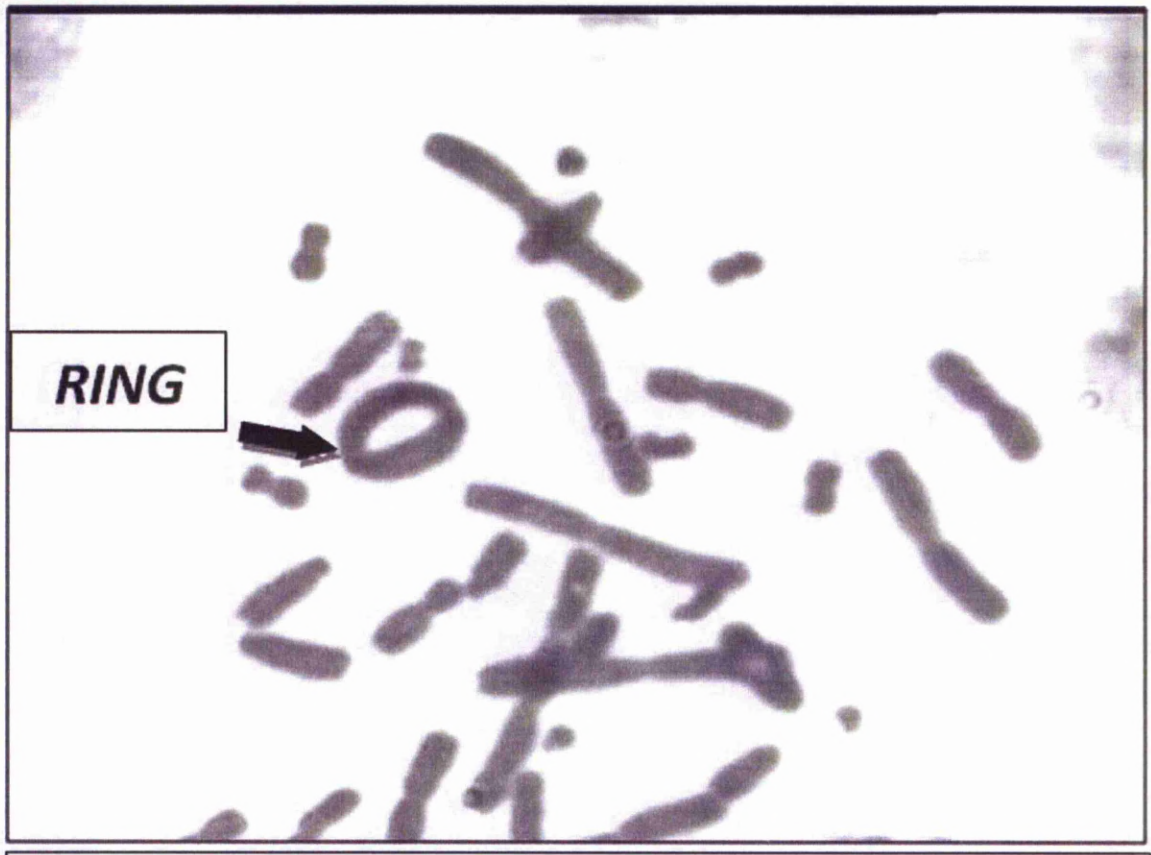

Appendix-3: showing an example of a ring formation which is a chromosome based aberration usually caused by the loss of telomeric integrity of the chromosome which may lead the radical sticky chromosomal ends to form the ring structure.

Appendix-4

TRIRADIALS IN METAPHASE SPREAD

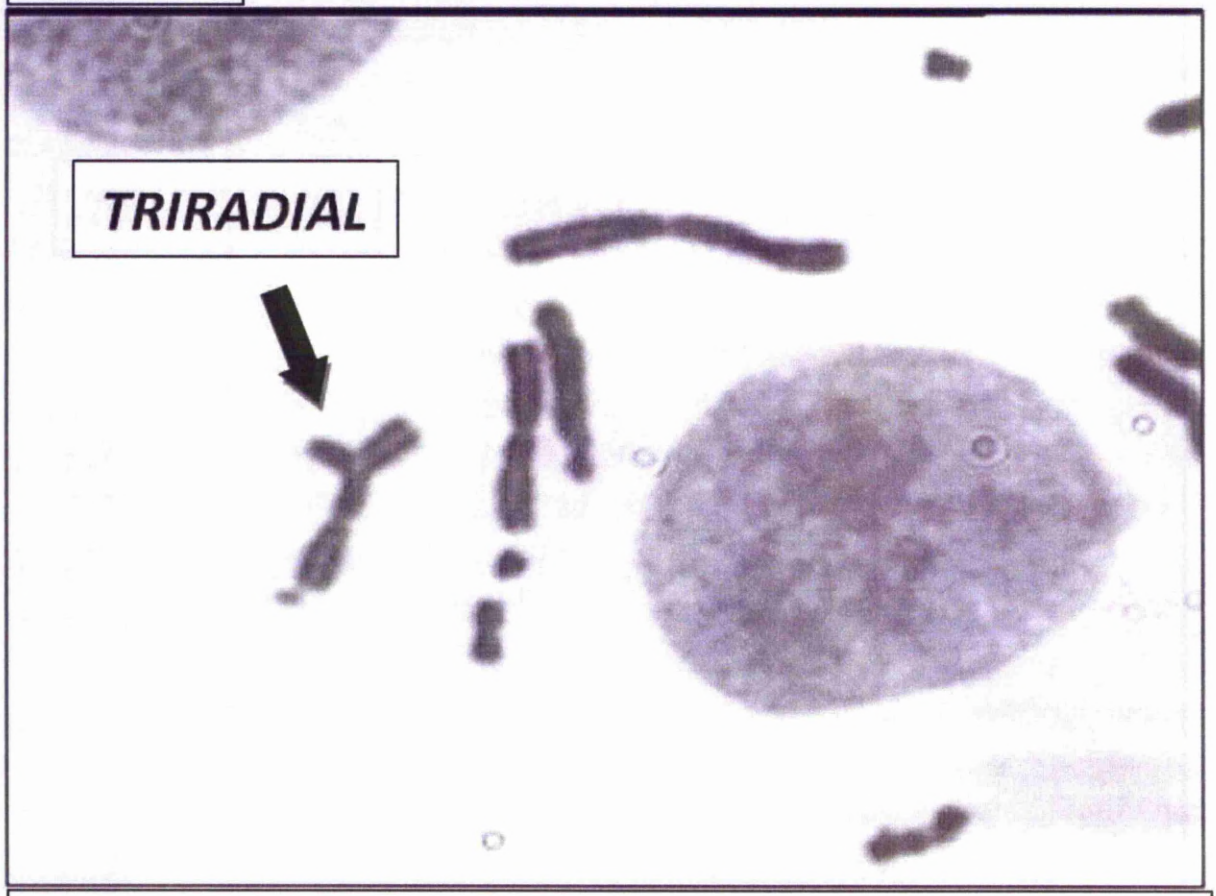

Appendix-4: presenting a triradial structure which is a chromatid based aberration.

Appendix-5

QUADRI-RADIALS IN METAPHASE SPREAD

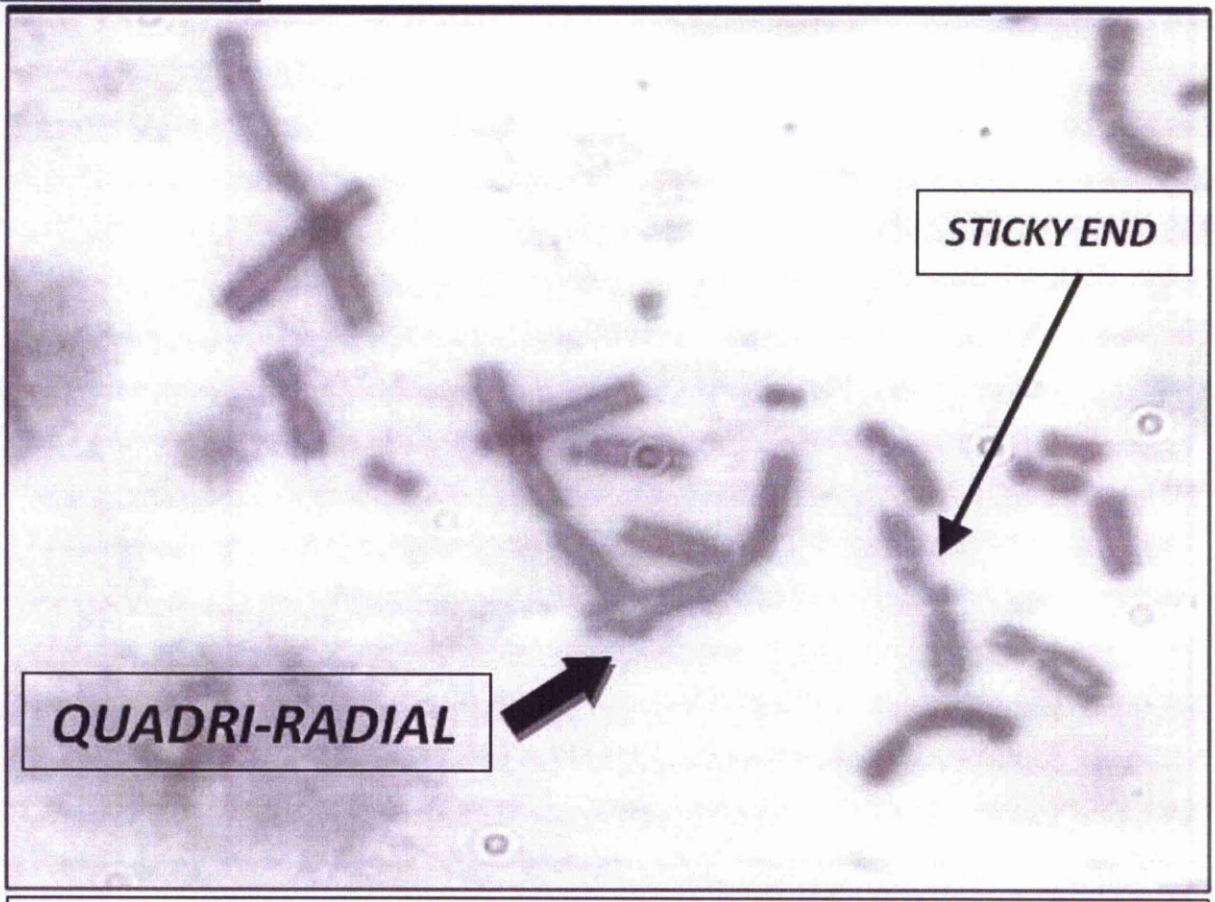

Appendix-5: presenting a quadri-radial structure which is a chromatid based aberration.

Appendix-6

MULTI-COMPLEX ARRANGMENTS IN METAPHASE

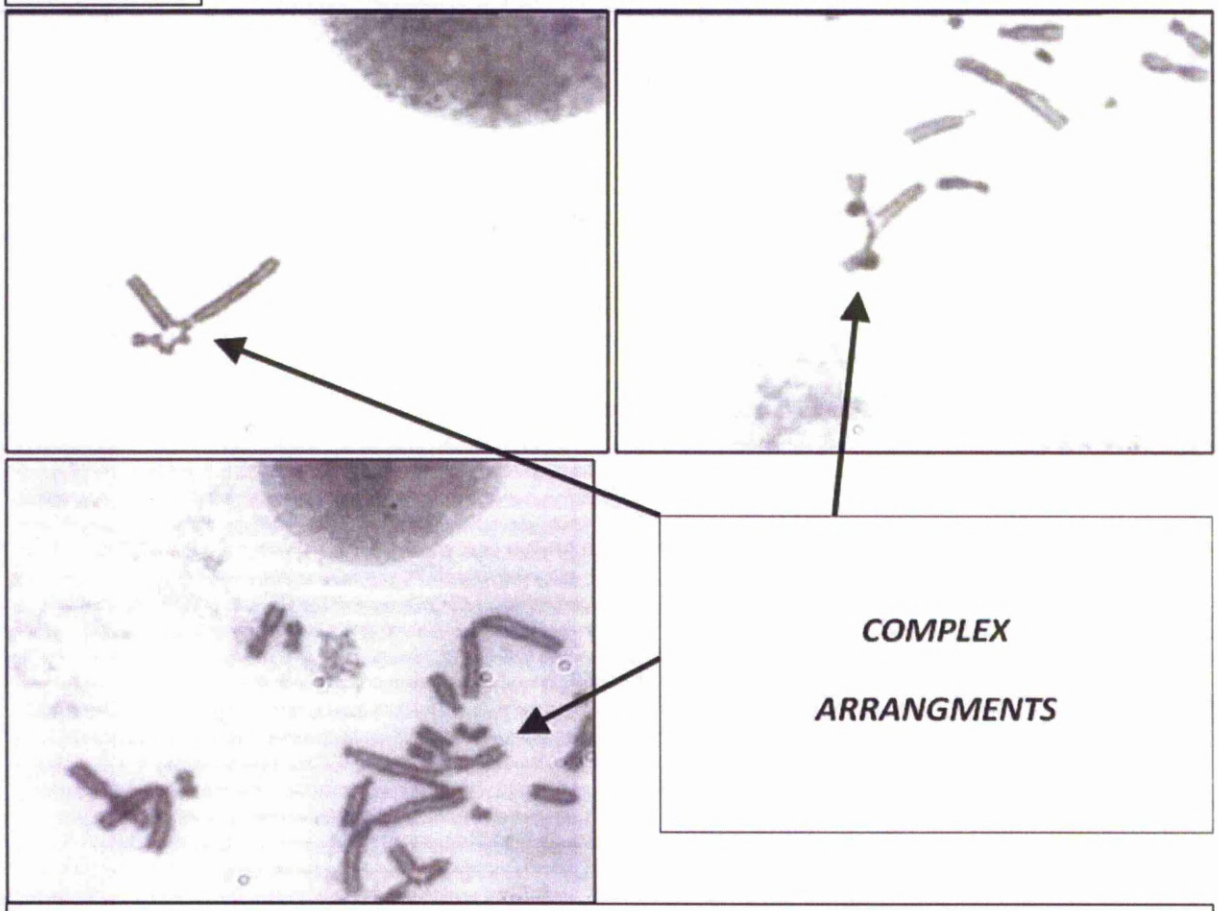

Appendix-6: illustrating some variable complex chromosomal arrangements indicating that a variable number of chromosomes can be involved in any complex arrangement

Appendix-7

Terminal BREAK IN METAPHASE SPREAD

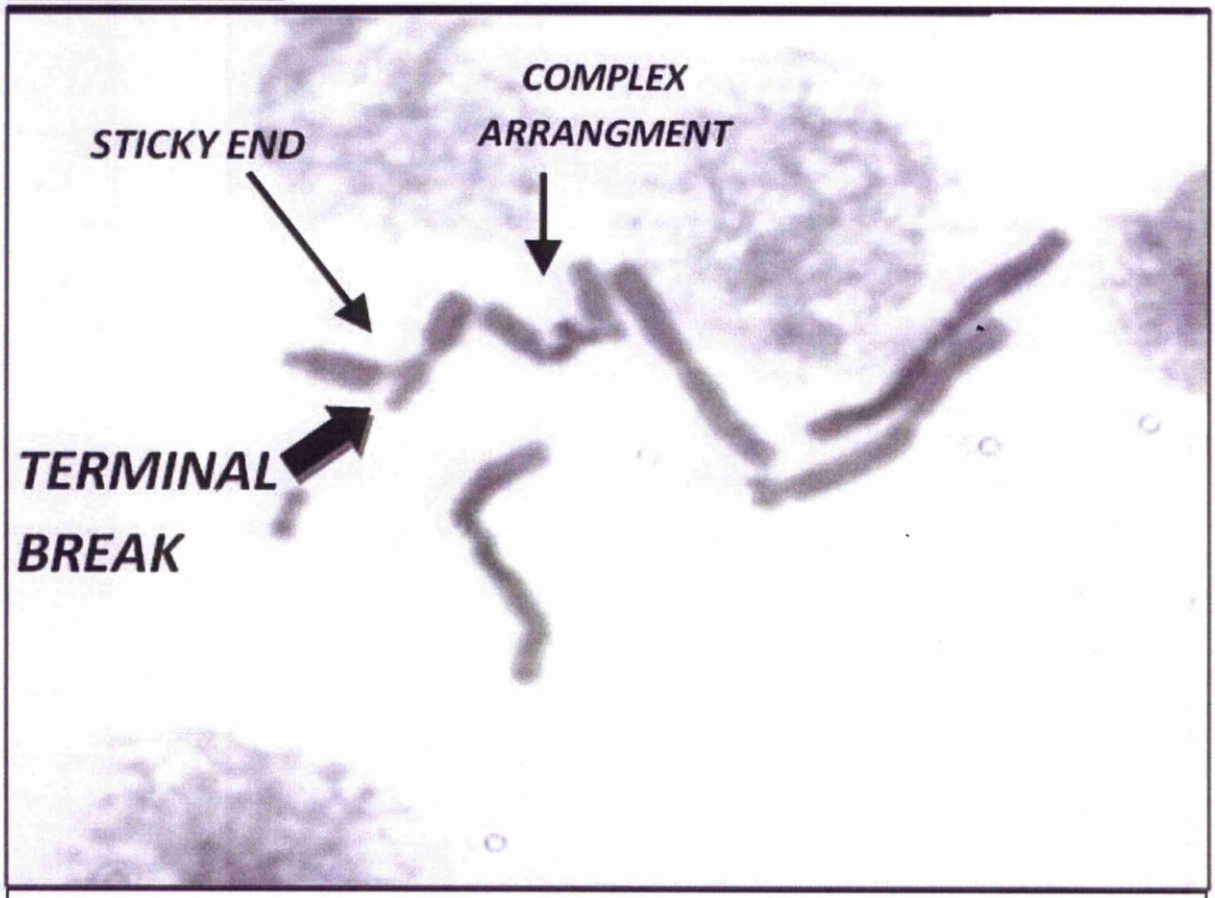

Appendix-7: illustrating how a breakage site such as a terminal break can show stickiness in a step that may develop producing dicentrics, rings, complex or other chromatid based aberrations.

Appendix-8 **MULTI-ABERRATIONS IN METAPHASE SPREAD**

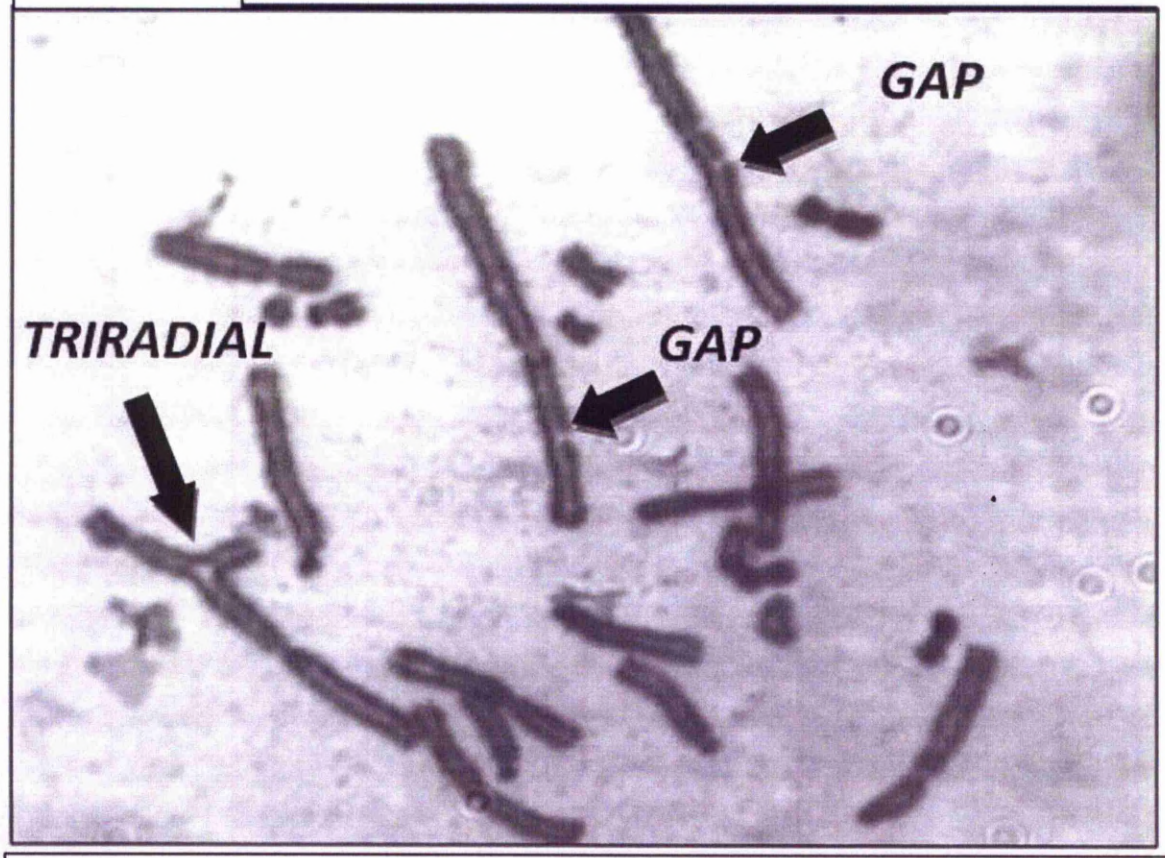

Appendix-8: illustrating the presence of multi chromosomal aberrations in the same metaphase spread. This becomes more frequent as the doses used increase and the cells are more sensitive to the clastogen applied.

Appendix-9-A

Aberration type	Diagrams with symbols[3]	Definitions and comment
A. Chromosome type (*cs*)		Involving both chromatids of a chromosome at identical loci
(1) Chromosome gap	(*csg*, G)	A non-staining region or achromatic lesion at the same locus in both chromatids with minimal misalignment of the chromatids[1]
(2) Chromosome break	(*ace*)	A discontinuity at the same locus in both chromatids giving an acentric fragment (*ace*). The abnormal (shortened) monocentric chromosome may not be identified.[4] Where sister union occurs the aberration should be classified as a chromatid-type 'isochromatid break'[2]
(3) Chromosome exchange (*cse*)		Involving two or more loci in the same or different chromosome(s)
(a) Interchange, between chromosomes (*C/C*)	e.g. Dicentric with associated fragment	The dicentric results from an asymmetrical exchange that also produces a fragment which should not be scored as a separate event.

Appendix 9-A showing structural aberrations classification and definitions

Diagrams and commentary taken from: Kirkland, 1990

Aberration type	Diagrams with symbols[3]	Definitions and comment
A3/ (b) Intrachange, within a chromosome (*C/C*)		
(i) between arms (inter-arm intrachange)	e.g. Centric ring with fragment (*csr + ace*)	The fragment is part of the exchange and should not be scored as a separate event. One fragment should be allocated to each ring (or dicentric)
(ii) within an arm (intra-arm intrachange)	(*cs min*, M)	The centric part of this exchange may not be identified. Acentric rings are formed and are generally small and called minutes (*cs min* or M) or interstitial deletions[5]
B. Chromatid aberrations (*ct*)		Usually involve only one chromatid of a chromosome except for isochromatid breaks
(1) Chromatid gap	(*ctg*, g)	A non-staining region or achromatic lesion in which there is minimal misalignment of the chromatid[1]
(2) Chromatid break		A discontinuity in which there is a clear misalignment of one of the chromatids[1]

Appendix-9-B

Aberration type	Diagrams with symbols[3]	Definitions and comment
B/ (3) Isochromatid break (i)[2,5]	(SU)	Showing complete rejoining or sister union (SU) of broken ends
	(Nud) (Nup)	Incomplete rejoining (non-union, Nu) either proximally (p) or distally (d). Fragments may be aligned or displaced
B/ (4) Chromatid exchange (*cte*)		
(a) Interchange, between chromosomes (c/c)		
(i) Asymmetrical	(*qr*, c/c)	An acentric fragment and a dicentric chromatid are produced if rejoining is complete. Sometimes called a quadriradial (*qr*)
(ii) Symmetrical	(*qr*, c/c)	Does not lead to a dicentric chromatid or to an acentric fragment unless the rejoining is incomplete. Also called a quadriradial (*qr*)
(b) Intrachange, within a chromosome (c/c)		
(i) between arms (inter-arm intrachange)	Asymmetrical	Centric ring formed
	symmetrical	Produces an inversion (*inv*) in a chromatid

Aberration type	Diagrams with symbols[3]	Definitions and comment
(ii) within an arm (intra-arm intrachange)	Minute (*cr min*, m) or interstitial deletion[5]	Often remains associated with the chromosome of origin
(b) Isochromatid/ chromatid interchange (i/c) giving a triradial (*tr*)	Dicentric triradial (*tr (2 cen)*, i/c)	Fragment produced and is not an independent aberration
	Monocentric triradial (*tr (1 cen)*, i/c)	This should be counted as just one aberration as for all exchanges (see text, Section 4.1)

Appendix 9-B showing structural aberrations classification and definitions

Diagrams and commentary taken from: Kirkland, 1990

Appendix-10

NORMAL METAPHASE SPREAD- NM3

Appendix-10: presents a CHO metaphase with optimal chromosomal spreading achieved through hypotonic solution and fixation manipulation. This is ideal for identifying possible chromosomal aberrations.

Appendix-11 NORMAL METAPHASE SPREAD- 6914-FANCA

Appendix-11: presents a 6914 FANCA metaphase spread with minimal chromosomal overlapping, good morphology and staining allowing reliable scoring of chromosomal aberrations.

Appendix-12 **NORMAL METAPHASE SPREAD- 6914-FANCA**

Appendix-12: presents a 6914 FANCA metaphase spread with minimal chromosomal overlapping, good morphology and staining allowing reliable scoring of chromosomal aberrations.

Appendix-13 COMPLEX ARRANGEMENTS IN METAPHASE SPREAD- 6914-FANCA

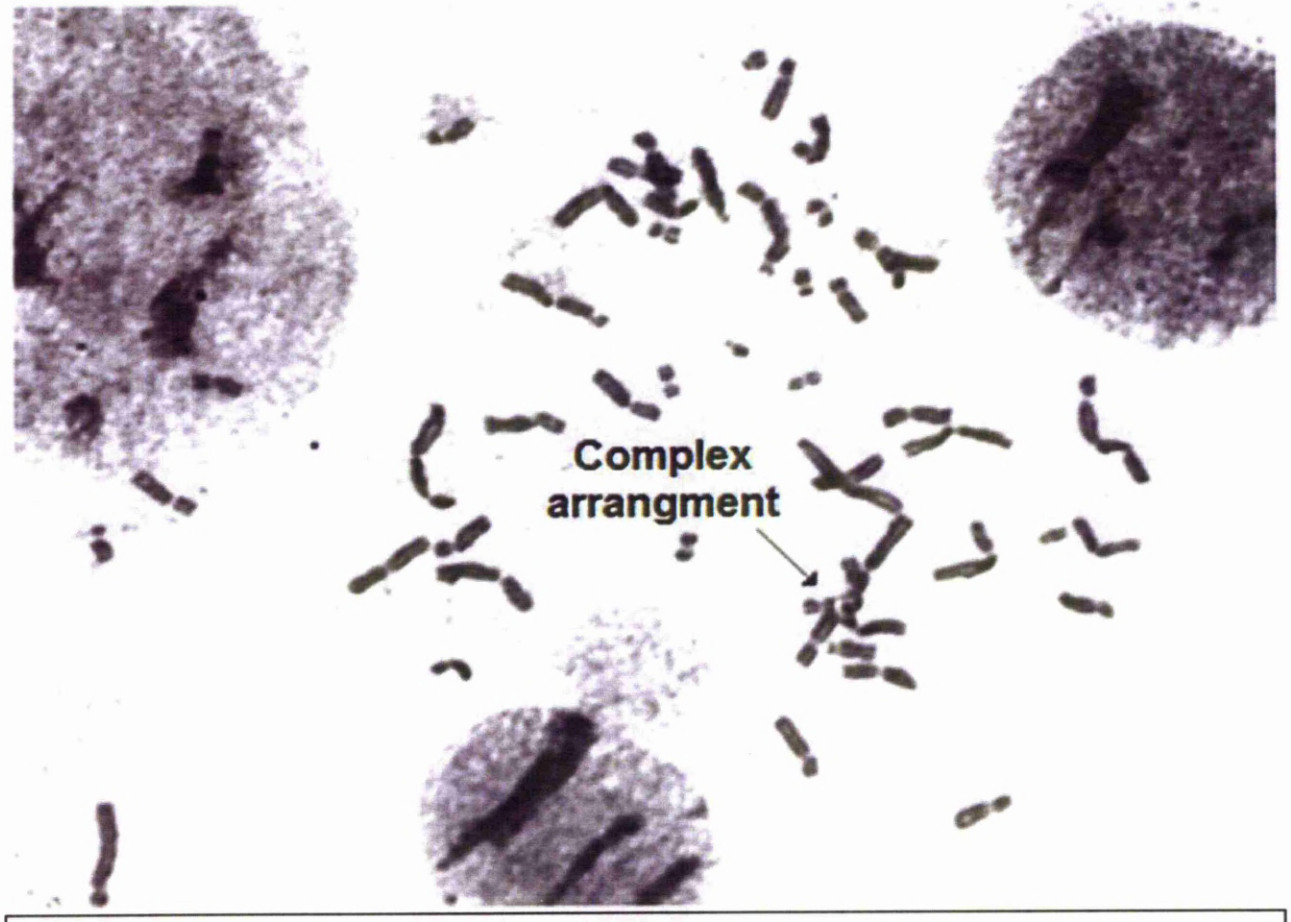

Appendix-13: presents a 6914 FANCA metaphase spread with a complex chromosomal arrangement involving a number of chromosomes.

Appendix-14

Appendix-14: presents a 6914 FANCA metaphase spread showing chromatid based aberrations: breaks exchanges and complex arrangements.

Appendix-15

NORMAL METAPHASE SPREAD- PD20

Appendix-15: presents a PD20 metaphase spread with minimal chromosomal overlapping, good morphology and staining allowing reliable scoring of chromosomal aberrations.

Appendix-16

NORMAL METAPHASE SPREAD- PD20

Appendix-16: presents a PD20 metaphase spread with minimal chromosomal overlapping, good morphology and staining allowing reliable scoring of chromosomal aberrations.

Appendix-17

TRIRADIALS AND QUADRI-RADIALS IN METAPHASE SPREAD- PD20

Appendix-17: presents a PD20 metaphase spread with a triradial and a quadri-radial structures which are chromatid based aberrations.

Appendix-18 MULTI-CHROMATID ABERRATIONS IN METAPHASE SPREAD- PD20

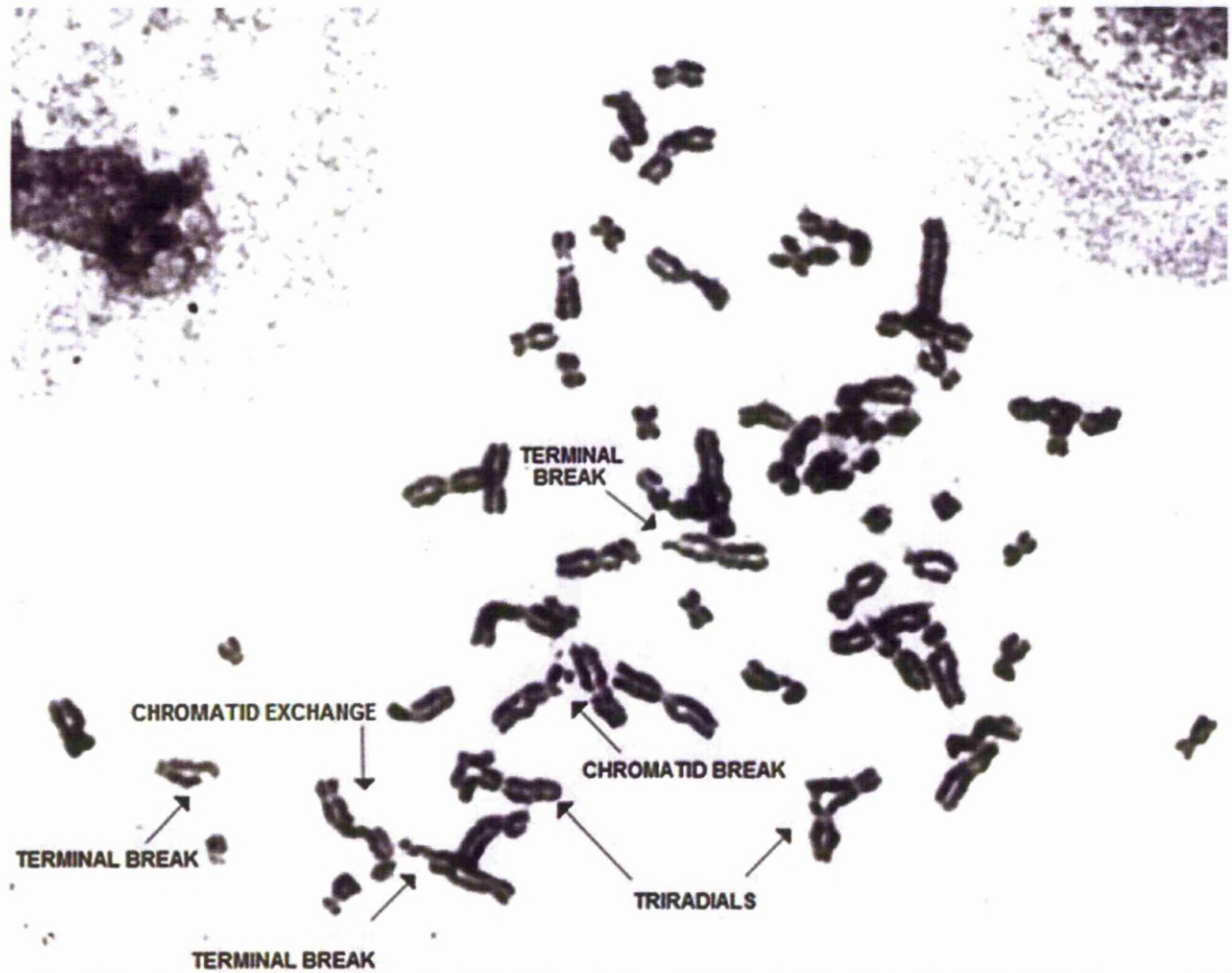

Appendix-18: presents a PD20 metaphase spread showing small triradials and several chromatid breaks.